This is not the end. It is not even the beginning of the end.
But it is, perhaps, the end of the beginning.

Winston Churchill, Mansion House, 10th November 1942
(On the eve of the Battle of Egypt)

To My Mum and Dad

with love

University of Southampton

The Development of Enantioselective Receptors for Amino Acid Derivatives

by

Emma J. Shepherd

Doctor of Philosophy

Faculty of Science

Department of Chemistry

November 2000

UNIVERSITY OF SOUTHAMPTON
FACULTY OF SCIENCE

DEPARTMENT OF CHEMISTRY

Doctor of Philosophy

ABSTRACT

THE DEVELOPMENT OF ENANTIOSELECTIVE RECEPTORS FOR AMINO ACID DERIVATIVES

by Emma Jane Shepherd

This thesis is concerned with the synthesis and investigation of the properties of novel bicyclic receptors for amino acid derivatives. Chapter two describes the synthesis of a previously reported macrocycle, **1**, which had the potential to enhance the rate of intramolecular Diels-Alder cyclisations on substrates such as **26**. Chapter three describes the synthesis of substrates based on the structure of **26** and the experiments carried out to determine whether or not macrocycle **1** could enhance the reaction rate. It was found that macrocycle **1** did not have an effect on the rates of the intramolecular Diels-Alder cyclisations of these substrates. Chapter four describes the synthesis of two novel macrobicycles **59** and **60** which feature novel aromatic spacer units in the macrocycle rim for the purpose of enhancing the binding selectivity over that of macrocycle **1**. Attention is given to the characterisation of the two macrocycles and the investigation of the binding properties of macrocycle **59** with several amino acid guests. The fifth chapter goes on to describe the attempted synthesis of a further two novel macrobicycles, **72** and **77** which incorporate a bis carboxylate binding site for the complexation of glutamate and aspartate derivatives.

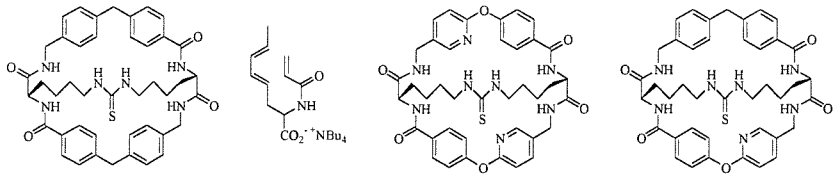

1 **26** **59** **60**

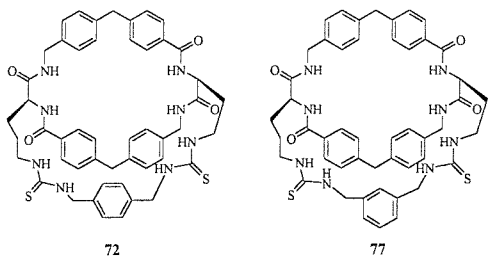

72 **77**

Contents

Preface

The research described in this thesis was carried out under the supervision of Professor Jeremy D. Kilburn at the University of Southampton between October 1997 and October 2000. No part of this thesis has been submitted at this or any other University except where specific acknowledgement has been made.

Acknowledgements

I am indebted to a huge number of people who have lent me their time patience and kindness over the past three years, unfortunately the confines of this page prevent me from mentioning them all individually and I've had to limit my thanks to just a few very special people who really have made a huge difference to me.

Firstly I would like to express my deepest thanks and gratitude to my supervisor Professor Jeremy Kilburn for his enthusiastic encouragement, support and advice as well as for hosting some cracking socials. Thanks also to Dr Andy Thomas and his lab at AstraZeneca who accommodated me so well during my stay there.

I am extremely grateful to Joan Street and Neil Wells for patiently running, re-running and reprocessing NMR spectra for me, often at short notice and on minute quantities of sample! Dr John Langley and Julie Herniman also deserve acknowledgement for help with mass spectrometry.

I owe an enormous amount (probably repayable in pints?!) to the army of proof readers who diligently read this thesis in its crude form, removed my wayward semi-colons and installed some sentence structure to make sense of it all! Thanks then to: Neil Wells, Jon Underwood, Graham Kyne, Faye Watson, Lee Patient and Richard Fitzmaurice.

Huge hugs go out to the Kilburn group – past, present and surrogate members for their friendship and support during my PhD. I would particularly like to thank Graham Kyne for his prompt response to fires and for teaching a complete computer dummy the finer points of molecular modeling and furthermore managing to do it without drawing a diagram! But most of all for 'realising the urgency' when it really mattered. Faye Watson, my partner in crime, for the fireworks in my fumehood, always telling it the way it is and for the very many giggles, chocolate breaks and of course your stores account! Jon Underwood, for his pole dancing, an appreciation of fine perfumes (!) and for bringing back my smile – thank you. Tobias Braxmeier for his fantastic lab humour. Thilo Fessmann, a true gentleman. Ray and Pete for their unfailing sense of humour in spite of my 'oil changes'! Also Fabrice, Glenn, Mr Kitts, Mariangela, Alex, David, Lee, Rossella, Sara, Valerie, Guillaume and Anawat.

In addition thanks to Jon Wilden for all his kindness, Neil Wells, Fred Boardman, Matt Lucas and Nikki Newman.

Finally, I would like to say a special thank you to Mum, Dad and Helen – I would never have got here with out you.

love Em.

Abbreviations

Ac	Acetyl
AIBN	α,α'-azoisobutyronitrile
Ar	Aryl
Boc	*tert*-butyloxycarbonyl
Bu	Butyl
Cat.	Catalyst
CBS	Carboxylate binding site
Cbz	Benzyloxycarbonyl
COSY	Correlated spectroscopy
DCM	Dichloromethane
DIPEA	*N,N'*-Diisopropylcarbodiimide
DMAP	4-Dimethylaminopyridine
DME	1,2-Dimethoxyethane
DMF	*N,N'*-Dimethylformamide
DMSO	Dimethylsulfoxide
Et	Ethyl
ES^+ MS	Positive electrospray mass spectrometry
FAB	Fast atom bombardment
FT-IR	Fourier transform infrared
HOBt	1-Hydroxybenzotriazole
HRMS	High resolution mass spectrometry
IMDA	Intramolecular Diels Alder
Me	Methyl
mp.	Melting point
NMR	Nuclear magnetic resonance
Ph	Phenyl
ppm	parts per million
quant.	Quantitative
TFA	Trifluoroacetic acid
THF	Tetrahydrofuran

Tlc	Thin layer chromatography
TMS	Trimethylsilyl
Ts	Tosyl
UV	Ultra-violet
WSC	1-(3-Dimethylaminopropyl)-3-ethylcarbodiimide hydrochloride

Amino Acids

Ala	Alanine
Asp	Aspartic acid
Gln	Glutamine
Glu	Glutamic acid
Gly	Glycine
His	Histidine
Ile	Isoleucine
Leu	Leucine
Phe	Phenylalanine
Ser	Serine
Thr	Threonine
Trp	Tryptophan
Tyr	Tyrosine
Val	Valine

Chapter One

An Introduction to Host - Guest Chemistry

1.1 Molecular Recognition

The recognition of specific structural motifs by macromolecules is a theme fundamental to all processes that occur in biology. Nucleic acid synthesis, cellular recognition; signal induction by neurotransmitters and immunological antigen-antibody association are just a few examples of biological processes that are entirely dependent on a substrate molecule reversibly binding to a macromolecule capable of eliciting a biological response. Molecular recognition has been defined as a process involving both binding and selection of specific substrates.[1] It is the specific molecular interactions that are involved in such complexation events which are of interest in this field of research.

Macromolecules operating in biological systems are highly selective accepting only compounds which display certain spatial relationships between their constituent atoms; many enzymes can distinguish between enantiomers of a substrate[2] and enzymes utilising the co-enzyme NADPH are even able to distinguish between two prochiral hydrogen atoms. Selectivity of this magnitude is enabled by complex networks of atoms that have evolved to provide optimal interaction with the substrate molecules. The objective of the host-guest chemist is to emulate the binding observed in natural systems, using artificial receptors, to achieve selectivity and strength of binding approaching those found in biological complexation events. The interest in artificial hosts is not only due to their direct relevance to the corresponding biological systems, but also because of their potential to lead to new therapeutics, biosensors and catalysts.[3] A plenitude of sophisticated synthetic receptors now exist for the purpose of binding substrates of great diversity, varying from inorganic anions[4] and cations[5] to common biological substrates including carbohydrates,[5] nucleotides[6] and peptides.[7]

1.2 General Design Features of Synthetic Receptors

Synthetic receptors, whilst less complicated than their biological counterparts, echo the features found in them. Synthetic hosts tend to provide a cavity complementary in size, shape and chemical functionality to the potential guest molecule. The binding site of the host is usually concave and the binding region of the guest convex. Consequently, they usually interact through several different points over the surface of the guest. This is of particular importance because all of the forces involved in host-guest interactions are non-covalent and therefore weak by nature. Thus large areas of complementarity are necessary for the formation of stable host-guest complexes.

The success of a synthetic receptor to bind a specific guest is measured as strength of binding or binding efficiency which is the equilibrium constant, K_a:

$$K_a = \frac{[\text{Host-Guest}]}{[\text{Host}]\,[\text{Guest}]}$$

Obviously, the higher the value of the equilibrium constant the stronger the tendency for the complex to form and, therefore, the stronger the binding between the host and guest. To appreciate how this value is directly linked to the design of the system, it is necessary to consider the binding in terms of the Gibb's free energy. The value of the equilibrium constant is essentially a reflection of the change in Gibb's free energy of the system on complexation. This is related by the following equation:

$$K_a = e^{(-\Delta G/RT)}$$

where R is the gas constant, T is the temperature in Kelvin and ΔG is the free energy change. During a successful complexation event the system will experience a decrease in Gibb's free energy. This energy change is governed by both an enthalpic and entropic term.

$$\Delta G = \Delta H - T\Delta S$$

ΔH refers to the change in enthalpy of the system and ΔS is the change in entropy. The factors contributing to the enthalpic term include, the binding interactions between the host and guest molecules and desolvation, which must take place before complexation can occur. The entropic term is composed of the effects from conformational reorganisation during association and an alteration in translational and rotational degrees of freedom of the host and guest molecules. Desolvation also contributes to this term. For successful complexation, the enthalpic term of the Gibb's free energy must outweigh the entropic term: that is the contribution from binding interactions must offset the energy penalty incurred to organise the host and guest during complexation. When designing a viable synthetic receptor it is, therefore, expedient to maximise the functional group complimentarity between the host and the guest and seek to reduce the conformational flexibility of the host, thereby reducing the reorganisation required upon association.

1.3 Factors Affecting the Association of Host and Guest Molecules

The interactions involved in host-guest complexes are identical to those observed between substrates and receptors in biological systems; they are non-covalent intermolecular interactions. Those commonly employed include: electrostatic interactions (dipole-dipole and dipole-induced dipole interactions); hydrogen bonding; van der Waals interactions or London dispersion forces; π-stacking and charge transfer interactions. Hydrophobic and solvent effects also play a large part in the association of hosts and guests and will also be considered in this section.

1.3.1 Electrostatic Interactions

Electrostatic interactions are conventionally thought of as the attraction between a charged group on one of the components of the complex and an oppositely charged group on the other component of the complex. The force of attraction, F, is given by Coulomb's law:

$$F = \frac{q_1 q_2}{r^2 D}$$

where q_1 and q_2 are the charges on the two groups, r is the distance between them and D is the dielectric constant of the solvent. The optimal distance between the charged groups is 2.8Å.[8] The general term "electrostatic interactions" also applies to the interaction between dipoles and between a dipole on one component, and an induced dipole on the other. The use of electrostatic interactions is best exemplified by the binding displayed by crown ethers and cryptands to cations. One such example is the cyclic polyethers reported by Pedersen (fig. 1).[9] These are derived from aromatic vicinal diols and contain oxygen atoms each separated by two carbon atoms.

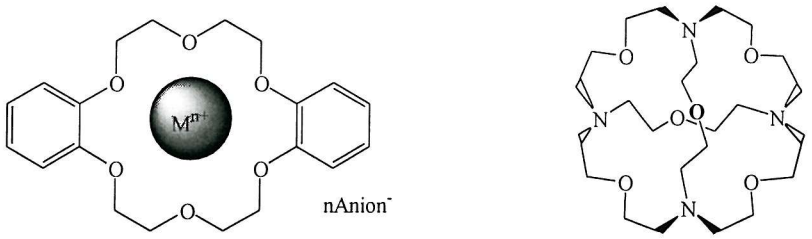

Fig. 1:a) Pedersen's Cyclic Polyether; b) Lehn's Cryptate

The polyether forms stable complexes with ionic compounds of lithium, sodium, potassium, rubidium and cesium. The complex is stabilised by ion-dipole interactions between the cation and the negative dipoles of the oxygen atoms of the polyether ring. A further example of the use of electrostatic interactions in artificial hosts is Lehn's cryptate,[10] composed of ten coordinations sites: four nitrogen atoms linked by bridges containing oxygen sites. The cryptate will form complexes with cations of an appropriate size to fit into the cleft, including potassium, rubidium and cesium ions.

1.3.2 Hydrogen bonds

Hydrogen bonds are generally considered to arise between an atom with an unbonded pair of electrons, the hydrogen acceptor, and a hydrogen atom that has a formal bond to another atom, the hydrogen bond donor. Traditionally the hydrogen bond donor was considered to be an electronegative heteroatom, however C-H groups may also form weak hydrogen bonds.[11] Similarly, the hydrogen bond acceptor is usually an electronegative heteroatom. However,

examples exist where the hydrogen bond acceptor is a transition metal;[12] alkene;[13] or aromatic π-clouds.[14] Hydrogen bonds can be arranged in several different ways (fig. 2): the simplest arrangement involves only one donor and one acceptor, termed "simple", however they may involve two or three acceptor centres, bifurcated and trifurcated respectively.

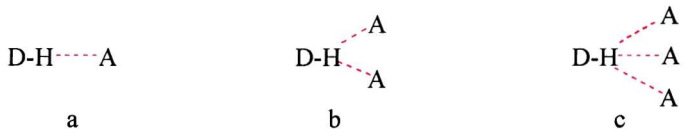

Fig. 2: a) Simple; b) Bifurcated; c) Trifurcated

The length of a hydrogen bond is variable and dependent on the donor and acceptor atoms. The higher the charge on the interacting atoms the shorter and stronger the hydrogen bond. A survey of NH---O=C bonds gave a range of bond lengths from 2.0 to 1.7Å,[15] however, significantly larger distances of 2.9Å have been reported.[16] The shortest values for CH---O bonding observed are approximately 3.0Å.[17] These values represent the distance between the donor and acceptor atoms, it should be noted that that values of bond length and the strength of hydrogen bonds is extremely dependent on solvent. Hydrogen bond strength is maximal when the atoms are colinear,[15] however, the mean distribution of NH---O bond angles is 161.2°, and angles of 180° are rare. This observaton is attributed to the preference of the proton donor to point to the acceptor along the trajectory of the lone pair electron density. In this "simple" hydrogen bond the bond energy can range between 10 and 65 kJ mol^{1} for neutral molecules.[18] The strength of hydrogen bonds is extremely variable and may rise to values of 40 to 190 kJ mol^{-1} for an ionic hydrogen bond. Conversly the CH---O bond energies typically range from 2.1 to 2.5 kJ mol^{1}. In systems where several hydrogen bond donors and acceptors lie in close proximity to one another, the possibility of forming secondary hydrogen bond interactions arises (fig. 3). These may increase the stability of a complex or prove to be a destablising influence.[19] It is possible that they may contribute the equivalent of 0.3 of the strength of a conventional hydrogen bond.

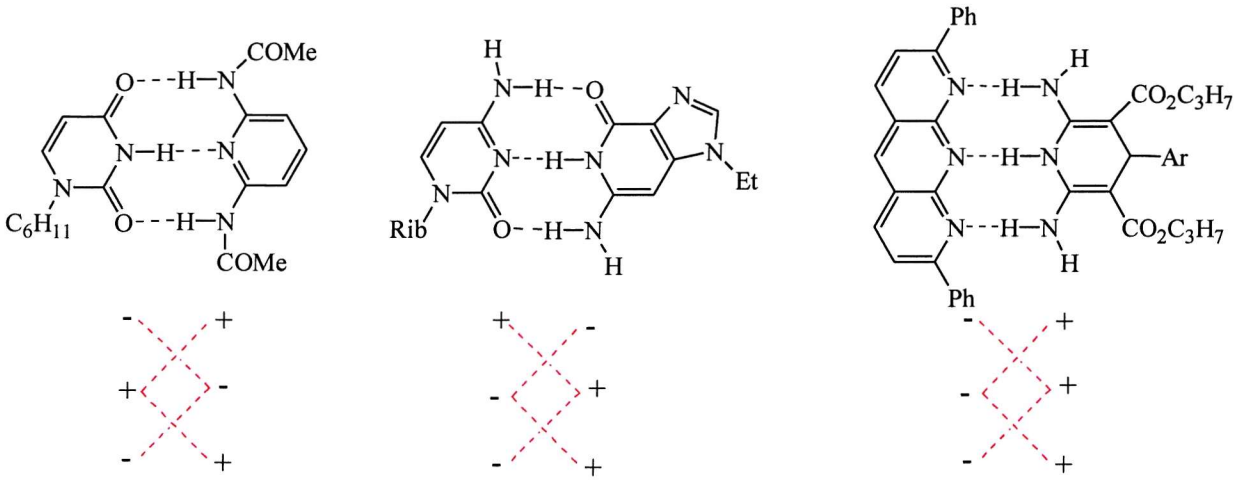

a. 4 repulsive secondary interactions, $K_a = 90$ mol^{-1}dm^3

b. 2 attractive, 2 repulsive $K_a = 1 \times 10^4$ mol^{-1}dm^3

c. 4 attractive $K_a = 1 \times 10^5$ mol^{-1}dm^3

Fig. 3: Secondary Interactions Arising From Multiple Hydrogen Bonds

In this example the outer two complexes have a high level of symmetry allowing association to occur either way around; in the middle complex there is no symmetry so the two components may only associate as shown. This demonstrates how multiple hydrogen bonds can be used to confer a high level of selectivity in the binding of a host to its substrate. The directionality and selectivity of binding that hydrogen bonds confer means that they are fundamental to the stucture and function of most biological macromolecules, in particular the secondary structure of globular proteins. For the same reasons they are no less important to synthetic host molecules and consequently large numbers of synthetic hosts contain some level of hydrogen bonding. The classical example is Hamilton's barbiturate receptor.[20] The receptor shown below (fig. 4) is macrocyclic with six hydrogen bonding groups directed towards the centre of its cavity, these are all ideally positioned for binding to the barbituric acid framework and the complex shown has a binding constant of approximately 10^5 mol^{-1}dm^3. Hamilton demonstrated the importance of hydrogen bonding in this complex by investigating the value of the binding constant with a series of guests which were strategically modified to prevent the exploitation of all of the potential hydrogen bonding sites. As the number of hydrogen bonds formed between host and guest decreased a corresponding drop in the value of the binding constant was observed.

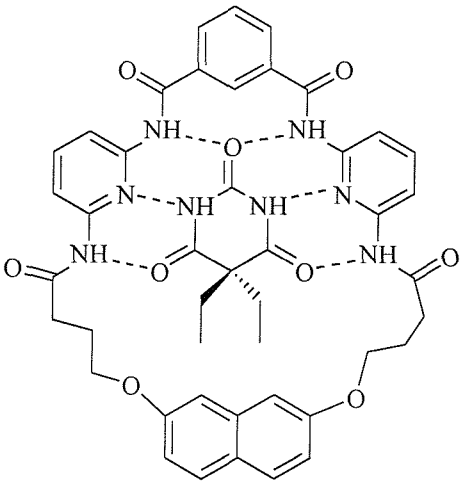

Fig. 4: Hamilton's Barbiturate receptor

1.3.3 Van der Waals Forces

Van der Waals interactions are non-specific forces that arise when any two atoms are 3 to 4Å apart. They are essentially a transient asymmetrical distribution of electron density around one atom forming a dipole that then induces an opposite temporary dipole in the neighbouring atom. The attractive force increases as the distance between the atoms reduces until the point when the electron clouds begin to overlap, the van der Waals contact distance: the force then becomes repulsive. The distance dependence of the van der Waals forces is related to the energy of interaction by the Lennard Jones potential (fig. 5).

$$E_{vdw} = \sum 4\varepsilon \left[\left(\frac{\sigma}{r}\right)^{12} - \left(\frac{\sigma}{r}\right)^{6} \right]$$

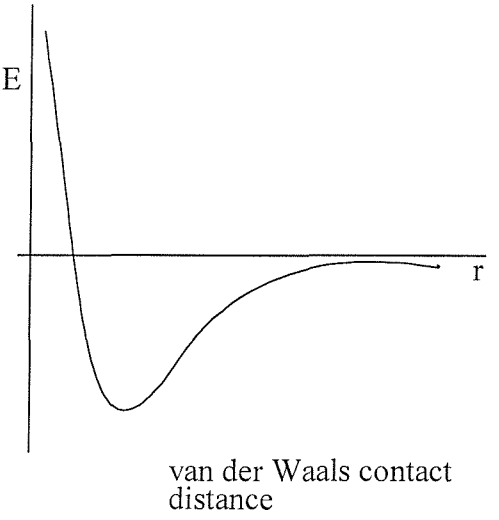

Fig. 5: The Lennard Jones Potential

The energy of these interactions are weak, approximately 4.2 kJ mol^{-1}, however they are additive and represent significant attractive forces over large molecules. Van der Waals forces depend on steric complementarity; in themselves they provide no specificity but specificity may arise when large numbers of interactions can be formed simultaneously. These forces arise between all associated complexes.

1.3.4 π-Stacking Interactions

π-π interactions are non-covalent interactions which arise between delocalised π-systems and include interactions between aromatic molecules.[21] They control a range of molecular recognition events in biological systems, for example the base stacking interactions which determine the structure and properties of the DNA helix, and the recognition of DNA by drugs and regulatory proteins.[22] They therefore represent a significant class of interaction. These interactions arise between aromatic rings that are ~4Å apart, in crystal structures the rings organise themselves in one of two ways: the parallel stacked array or the herring bone array (fig. 6).

Parallel stacked array Herring bone array

Fig. 6: The Stacking Organisation of Aromatic Rings

Hunter proposed a model to account for these observations where the interacting molecule is considered in terms of its charge distribution; the positive σ-framework is taken to be sandwiched between two regions of negatively charged π-electron density (fig. 7). The positively polarised hydrogen atoms attached to the aromatic ring will be directed towards the regions of high electron density, namely the π-electron cloud, of another ring, leading to the off-set stacking geometries observed. A special case of these stacking arrangements is the "T-stacking" geometry where the interplanar angle is 90°. For benzene rings, this "edge-to-face" geometry has been calculated to be a global energy minimum; this is more stable than the "face-to-face" geometry by approximately 6.3 kJ mol^{-1}.[23]

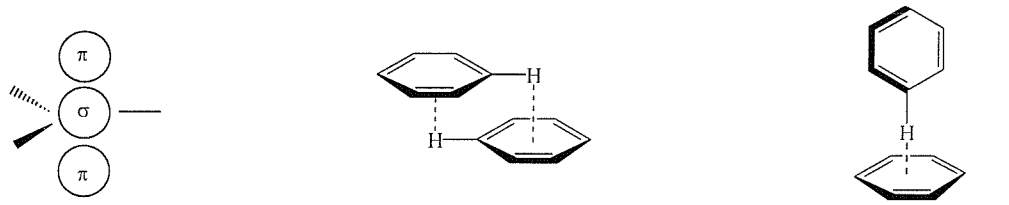

An sp^2 hybridised atom in a π system

'face-to-face' stacking

'edge-to-face' stacking

Fig. 7: Hunter's Model for the Stacking of Aromatic Rings

The magnitude of the π-π stacking interaction was investigated by Wilcox *et al*[24] using a molecular torsion balance to measure an intramolecular 'edge-to-face' π-π interaction: this value was reported as 1 kJ mol^{-1}. More recently Hunter *et al*[25] have employed a double mutant approach to estimate the value of an 'edge-to-face' π-π interaction to be -1.4 kJ mol^{-1} although the validity of this measurement has been questioned by Schneider.[26] The use of π-π interactions in artificial receptors is exemplified by Kelly's tweezer receptor (fig. 8).[27] The peptide host contains a dibenzofuran moiety designed to bind to the *C*-terminal benzamide unit of the guest *via* aromatic π-π stacking interactions thereby initiating the binding of the host and guest to form an antiparallel β-sheet structure (fig. 8).

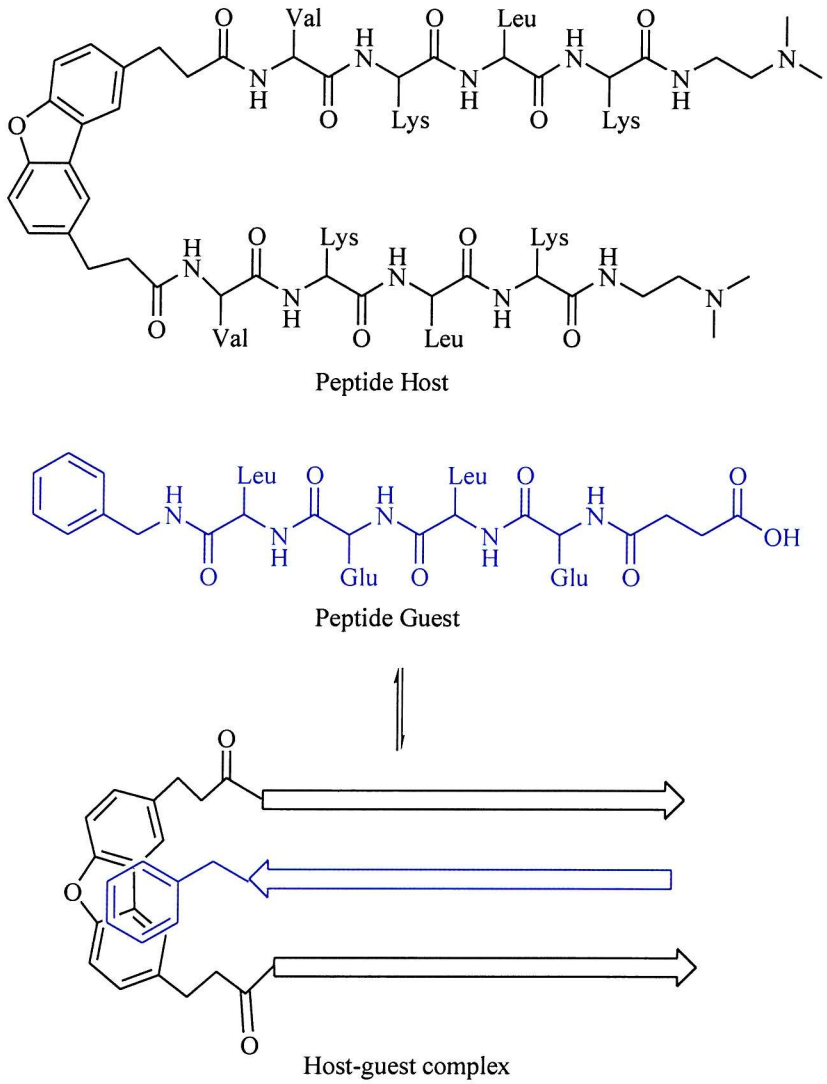

Fig. 8: Kelly's Tweezer Receptor

1.3.5 Solvent Effects

Solvent is extremely important to the thermodynamic stability of molecular complexes and, therefore, exerts a great deal of influence over the complexation event. Association is favoured by solvents which either weakly solvate the uncomplexed components of the system or strongly solvate the molecular complex. Diederich *et al*[28] used the binding of aromatic guest molecules to water-soluble cyclophanes with hydrophobic cavities to demonstrate the relationship between binding strength and the solvent polarity parameter $E_T(30)$, which in turn is dependent upon the

solvent's dipole moment, cohesion and polarisability. Diederich's studies revealed that the binding constants decrease for this system when moving from polar protic solvents through to non-polar solvents, which is directly due to solvation.

For hosts and guests with non-polar cavities and molecular surfaces, solvation in polar solvents, for example aqueous media, is enthalpically unfavourable, since the solvent molecules surrounding the solutes can form fewer hydrogen bonds than would be possible in the bulk solution and are therefore higher in energy. On complexation these solvent molecules are released into the bulk solution becoming higher in energy. There is also an entropic contribution to the hydrophobic effect: the solvent molecules surrounding the host and guest are organised in a highly ordered clathrate structure which, maximises the hydrogen bonding within the system.[29] When this cage-like formation is disrupted the molecules of solvent returning to the bulk solution adopt a less ordered state.

When non-polar hosts and guests are dissolved in non polar solvents the interactions between the host, guest and solvent - usually dipole interactions and van der Waals forces - are commonly of similar magnitude, hence the enthalpic drive for complexation is low.[30] Similarly, for polar host and guest molecules in polar solvents, the uncomplexed components are well solvated; the interactions present between the host, guest and solvent are similar in nature so the drive for complexation is low.

1.3.6 Loss of Translational and Rotational Freedom

During the complexation event, the degrees of freedom experienced by the host and guest decrease. If we consider the host and guest molecules moving freely in space, their gross motion can be broken down into three translational and three rotational components along the *x*, *y* and *z* axes (fig. 9). They have six degrees of freedom each, twelve in total. When complexation occurs, the host and guest molecules move as one: they have a total of six degrees of freedom, forming a more ordered system. Bond rotation becomes more restricted for host and guest on complexation, incurring a further entropy loss. The contribution from the translational entropy is of the order of 40 kJ mol^{-1} for a 1M solution at 298K,[31] although this value is dependant on

concentration; rotational entropy accounts for approximately 35 kJ mol^{-1}. The contribution from vibrational entropy is insignificant compared to that of rotational and vibrational entropy.

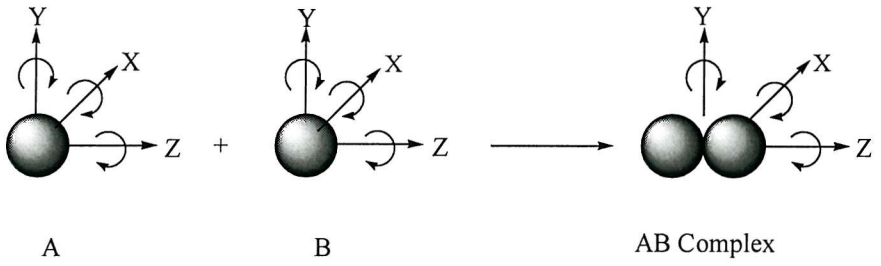

Fig. 9: The Loss of Rotational and Translational Freedom Experienced During Complexation

.

1.3.7 Preorganisation and Cooperativity

During the complexation event there is a loss of entropy due to conformational reorganisation of the host molecule. This can be alleviated by constraining the molecular flexibility of the host during synthesis, effectively "preorganising" it. The reorganisation that occurs during complexation is illustrated by the crystal structures of the complexed and uncomplexed forms of the18-crown-6 host. This is represented below (fig. 10).[32]

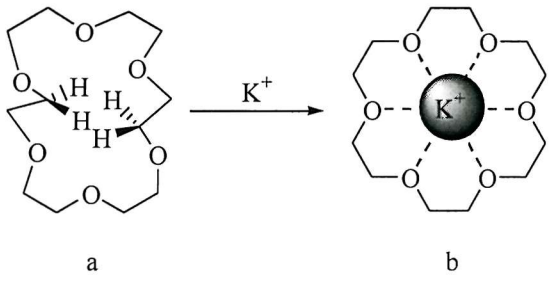

Fig. 10: a) 18-Crown-6 Prior to complexation. b) 18-Crown-6 upon Binding Potassium

In the uncomplexed form two of the ethylene bridges are turned inwards filling the potential cavity. The potassium ion re-organises the structure during complexation enabling it to bind within the cavity incurring an entropic and enthalpic penalty. Cram developed spherand molecules which were designed to have the orbitals of unshared electron pairs of the binding

sites orientated in a spherical cavity; these were held in place by a surrounding covalent structure (fig. 11). This preorganised host was found to have strong binding to lithium ions. A further demonstration of the value of preorganisation of a host during the synthesis is given below in the comparison of the binding of four hosts to potassium ions. Table 1 illustrates that the more highly organised the host molecule is for binding, prior to complexation, the more stable the complex. These values were recorded in methanol.

Host	Log K_a
Podand 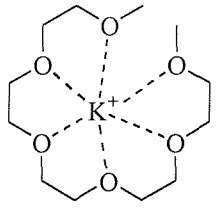	2.3
Crown 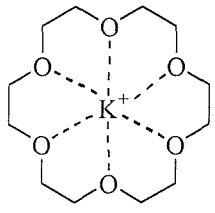	6.08
Lariat Ether 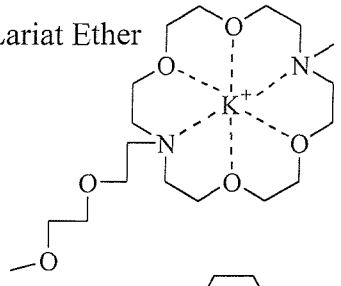	4.8
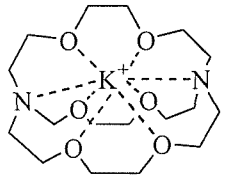	9.75

Table 1

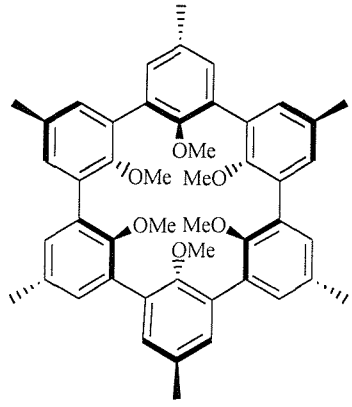

Fig. 11: Cram's Spherand

Complex stability can be further enhanced by the incorporation of many potential sites of interaction between the host and guest. It has been noted that many weak non-covalent interactions can act together on binding to generate a net release of free energy that is greater

than the sum of the individual intermolecular interactions.[33] This concept of cooperativity is exemplified below (fig. 12). The binding of the covalently linked molecule AB is more entropically favourable than the complexation of the separate components, A and B. The importance of cooperativity has been demonstrated by Hunter[34] using molecular zipper molecules. It was observed that a non-linear relationship between the stability of his complexes and their length existed indicating that cooperativity between sites is increased with the length of the zipper.

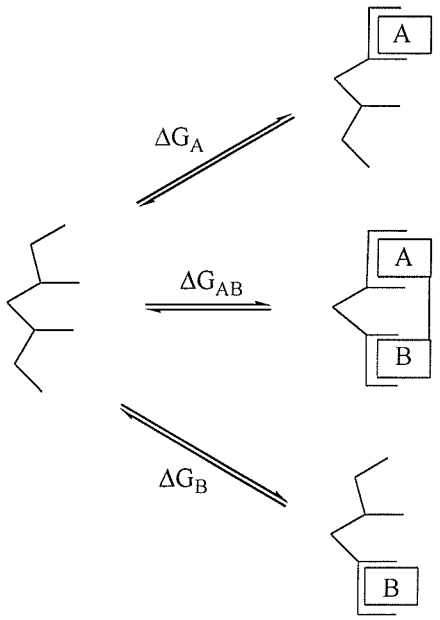

Fig. 12: $\Delta G_{AB} > (\Delta G_A + \Delta G_B)$

Williams has also reported evidence of cooperativity in the binding of two molecules of vancomycin to two molecules of *N*-Ac-D-Ala-D-Ala.[35] The incorporation of numerous binding sites into host molecules is also important for enantioselective recognition. In order to achieve chiral recognition it is essential to have three simultaneous interactions,[36] this is exemplified by Mendoza's receptor for aromatic amino acids (fig. 13).[37]

The aromatic amino acids associate to the receptor *via* a guanadinium-carboxylate interaction; the ammonium moiety is bound to the crown ether and the naphthalene ring provides a planar surface to facilitate π-π stacking interactions. The molecule has a chiral structure and demonstrates a high degree of chiral recognition. To conclude, many factors influence the stability of host-guest complexes and must, therefore, be taken into account when designing such a system.

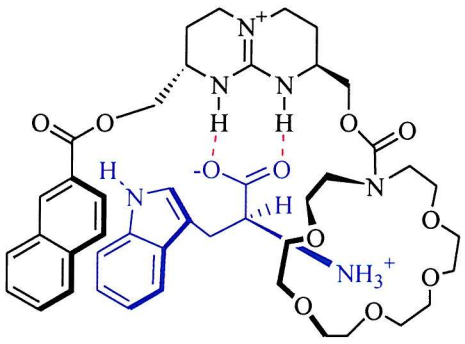

Fig. 13: de Mendoza's Receptor binding L-tryptophan

1.4 Artificial Receptors for Amino Acids and Their Derivatives

The area of supramolecular chemistry is extensive and a phenomenal number of sophisticated host-guest systems have been developed and investigated. The design strategies and interactions underlying the complexes they form are diverse and it would be impossible to cover all of them here, instead I have limited the following review to artificial receptors that complex amino acids and their derivatives. The hosts falling into this category are diverse in themselves and will serve to illustrate the theoretical principals of receptor design outlined above, in addition to giving an insight into the progress that has been made in this field to date.

1.4.1 Receptors Operating in Aqueous Systems

Binding α-amino acids and peptides in water is an attractive goal in host-guest chemistry. Receptors capable of complexing peptide sequences have the potential to mimic the natural

antibiotic vancomycin, commonly used as a last line of defence against serious bacterial diseases and, unfortunately, becoming increasingly less effective against the growing number of resistant strains.[38] The task of complexing small polar molecules such as α-amino acids and peptides in aqueous media is a challenging one because the hydrophobic desolvation and dispersion forces that usually provide the driving force for binding are limited by the small size of their apolar surface area. Selective peptide complexation in polar solutions has been addressed only recently and there are comparatively few examples of systems operating in aqueous media.

Diederich *et al*[39] have produced polyammonium cyclophane receptors (fig. 14), which partially mimic the vancomycin carboxylate binding site complexing aromatic and aliphatic carboxylates as well as *N*-protected α-amino acids and dipeptides.

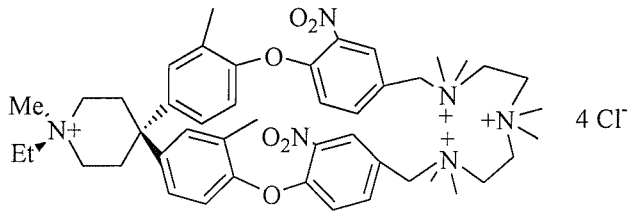

Fig. 14: Diederich's Receptor

The cyclophane structure provides a degree of preorganisation for the carboxylate binding site. However, titration binding experiments indicated that it did not provide a cavity for inclusion of the guests and instead binding occurs exclusively on the external surface. The driving force for binding is the ion-pairing interactions between the adjacent quaternary ammonium ions of the host and the carboxylate anion. It should also be noted that although the sodium salts of Ac-D-Ala, Ac-D-Val and Ac-D-Ala-D-Ala were bound with association constants of 74 dm^3mol^{-1}; 36 dm^3mol^{-1} and 51 dm^3mol^{-1} respectively, the unprotected zwitterionic α-amino acids were found not to bind.

Stoddart demonstrated that cyclobis(paraquat-*p*-phenylene) (fig. 15), forms stable inclusion charge-transfer complexes with amino acids possessing electron rich aromatic side chains.[40] The receptor has a box-like structure with a very well defined cavity lined by the two paraquat acceptor subunits. Titration studies revealed binding to tryptophan, tyrosine and phenylalanine

with strengths of 1022 dm^3mol^{-1}; 571 dm^3mol^{-1} and 7 dm^3mol^{-1} respectively, in each case addition of the guest produced a visible charge transfer band. The receptor showed no interaction with alanine and histidine, supporting the notion that association arises from an interaction with the electron rich aromatic rings of the guests.

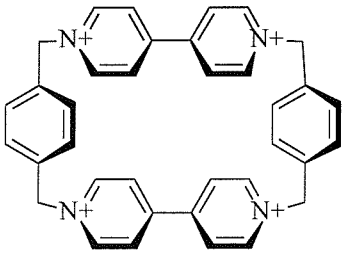

Fig. 15: Stoddart's Receptor

Organometallic hosts were reported by Fish[41] consisting of a triangular dome-shaped structure featuring three cyclopentadiene groups, three methyl groups, three adenine planes and three rhodium atoms (fig. 16). The host was shown to bind aromatic and aliphatic amino acids including L-Trp, L-Phe and L-Val within the cavity, probably *via* π-π stacking and hydrophobic interactions.

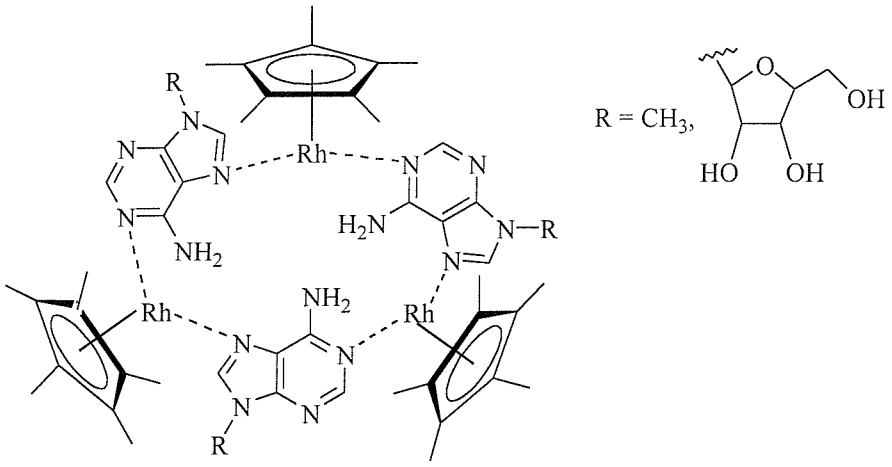

Fig. 16: Fish's Organometallic Receptor

A series of zinc porphyrins, soluble in water and featuring a hydrophobic binding pocket and polar recognition groups were developed by Mitzutari and co-workers.[42] The receptors were composed of a rigid and hydrophobic binding pocket provided by the porphyrin framework; a

Lewis acid site derived from the zinc moiety and a salt bridge site (fig. 17). The receptors were found to bind a range of guests forming tightly bound complexes to cationic amino esters, such as the methyl esters of lysine and arginine. The tripeptide Gly-His-Lys was bound with a binding constant of 2850 - 22300 dm^3mol^{-1} in 0.01 M Borax at pH 8. Studies revealed the association constant was dependent upon pH and ionic strength indicating that the driving force for complexation was the interaction between the *N*-terminal amino group of the guest and the carboxylate group of the receptors. For the hydrophobic guests studied, for example the methyl esters of leucine and phenylalanine,the largest binding constants were observed with receptor **3** which has a hydrophobic binding pocket. Here the receptor-guest complex formation is driven by hydrophobic interactions.

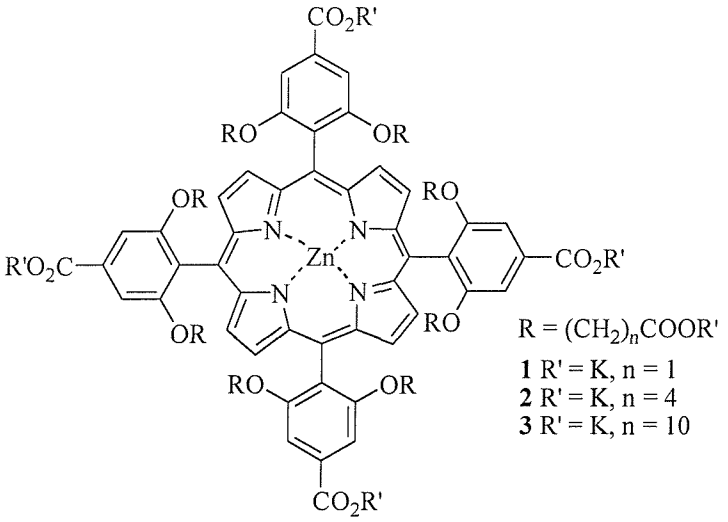

Fig. 17: Mitzutari's Receptor

Schneider *et al*[43] have also used porphyrin derivatives to complex amino acid derivatives and peptides in aqueous solutions. The incorporation of a crown ether unit onto the porphyrin framework provided a binding site for primary ammonium moieties thus facilitating the complexation of unprotected di-and tri-peptides (fig. 18). The binding constants observed are some of the highest reported for unprotected peptides in aqueous solutions. The binding strength was shown to increase as a function of peptide length and with the number of aromatic rings on the amino acid side chain, suggesting contributions from stacking interactions. The strongest binding observed was for tetraglycine which bound with an association constant of 10^5 dm^3mol^{-1}.

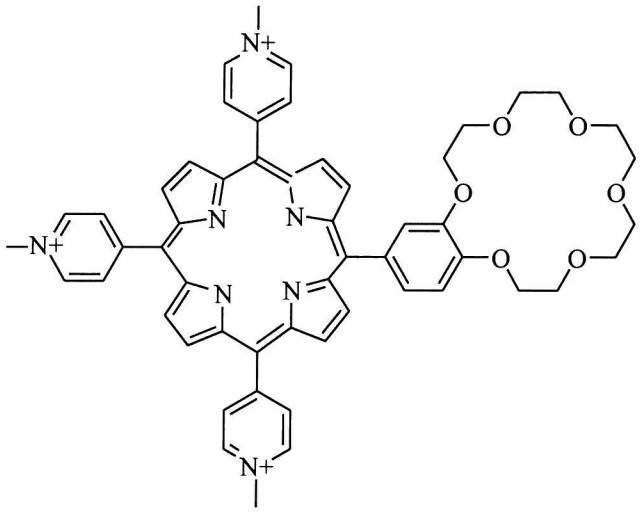

Fig. 18: Schneider's Porphyrin Receptor

Schneider has also developed receptors which recognise natural peptides in water. They have length and sequence selectivity also allowing for the directional alignment of the peptide chain in space.[44] The receptor was designed to exert primary binding at the terminal ionic groups whilst ensuring that these did not interact with each other to self-associate. Secondary interactions along the peptide chain would provide amino acid and sequence selectivity (fig. 19).

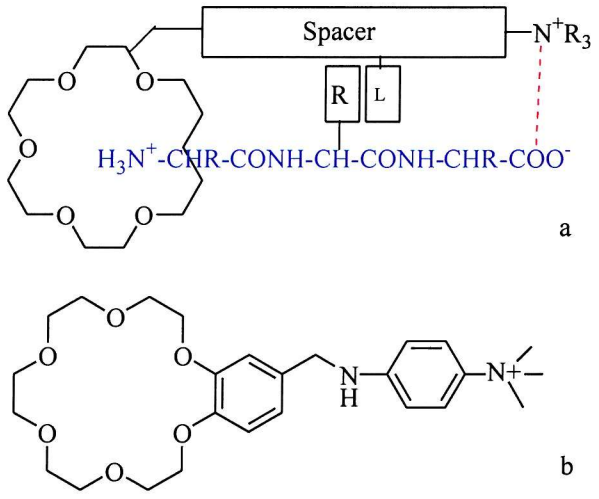

Fig. 19: a) The design concept for Schneider's receptor
b) Schneider's receptor

An 18-crown-6 ether was employed for recognition of the *N*-terminus and a perallyl ammonium group positioned for carboxylate binding. The values of association constants observed for various di- and tripeptides indicated a moderate selectivity for amino acid nature and sequence; length selectivity was demonstrated along with the bidentate binding mechanism.

Breslow has used cyclodextrin dimers to bind peptides in aqueous solutions; the receptors produced showed cooperative chelate binding to some peptides.[45] The largest association constants were achieved between the two guests shown (fig. 20) giving values of 2590 dm^3mol^{-1} and 1100 dm^3mol^{-1} for the cyclic peptide and linear peptide respectively; this is the first example in which the double binding of hydrophobic side chains is used to chelate a receptor to a peptide.

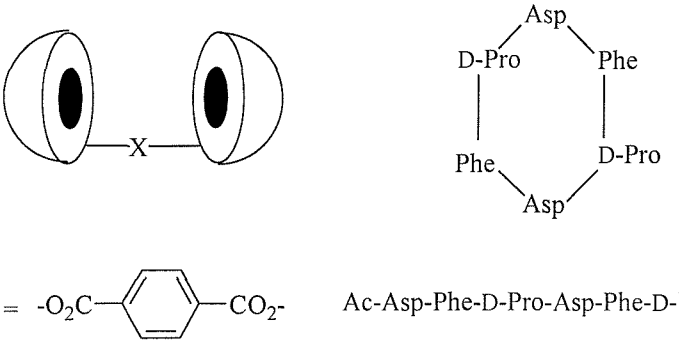

Fig. 20: Breslow's Cyclodextrin Receptor and Guests

Aromatic and aliphatic amino acids have been bound in hosts composed of electron-rich aromatic cavities of water soluble pyrogallol and resorcinol (fig. 21).[46] Hydrophilic amino acids such as alanine, serine and glycine were not bound. However, the aliphatic amino acids were complexed with binding strengths which increased with increasing length of side chain. This indicates that the alkyl side chain provides the primary site of interaction. The amino acids are thought to be bound with the alkyl chain embedded in the aromatic cavity of the host and the polar head groups exposed to the bulk solvent.

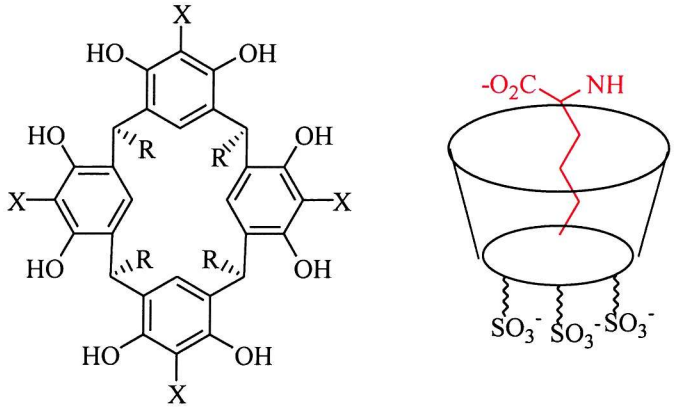

$R = (CH_2)_2SO_3Na$, X = OH
$R = (CH_2)_2SO_3Na$, X = H

Fig. 21: Kobayashi's Receptor

Guanidinocarbonyl pyrrole receptors were recently employed by Schmuck[47] to bind carboxylates in aqueous media. The most effective receptor is shown below (fig. 22) and found to bind the tetramethyl ammonium salts of *N*-acetyl alanine, phenylalanine and tryptophan with binding constants in the range of 585 dm^3mol^{-1} to 1610 dm^3mol^{-1}. The major contribution to binding strength arises from an ion pairing interaction between the carboxylate of the guest and the amide NH adjacent to the pyrrole ring. Hydrogen bonding to the pyrrole NH and the terminal carbamoyl group further contribute to the stability of the complex, and with phenylalanine and tryptophan, π-stacking occurs between the aromatic system and the guanidinocarbonyl pyrrole moiety. Interactions between the bulky amino acid side chains and the isopropyl group of the receptor leads to binding enatioselectivity; the association constants for the enantiomers of phenylalanine and tryptophan differ by a factor of 1.2 and by a factor of 1.6 for alanine, with a preference for the L-enatiomer of alanine and tryptophan. In the case of phenylalanine stronger binding is observed with the D-enantiomer.

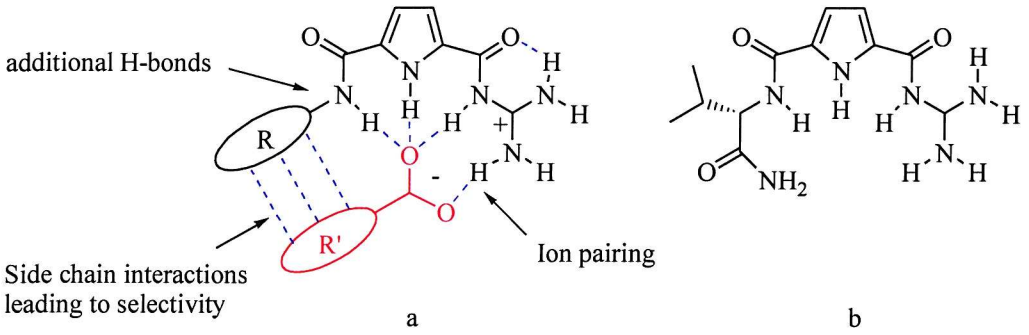

Fig. 22: a) General design of guanidiniocarbonyl pyrrole receptor
b) The structure of the most effective receptor.

A tweezer receptor designed to bind to tripeptides was developed by Kilburn and Bradley,[48] the stucture features a guanidinium moiety which binds, *via* a strong interaction, to the carboxylate terminus of the guest peptide (fig. 23). The tweezer arms are peptidic and provided the potential to form both hydrophobic and β-sheetlike hydrogen bonding interactions with the peptide substrate. Screening of the tweezer receptor against a 1000-member library of tripeptides attatched to TentaGel resin *via* the amino terminus in water followed by appropriate sequencing of bound library members, revealed a 95% selectivity for Val at the carboxy terminus of the tripeptide and a 40% selectivity for Glu (O^tBu) at the amino terminus. When the tweezer receptor was subjected to microcalorimetry with one of the tripeptides selected from the screening studies, Z-Glu (O^tBu)-Ser (O^tBu)-Val-OH, the binding constant K_a was found to be 4 x $10^5 \pm 5$ x 10^5 mol dm^{-3} in sodium borate buffer containing 16.7% DMSO.

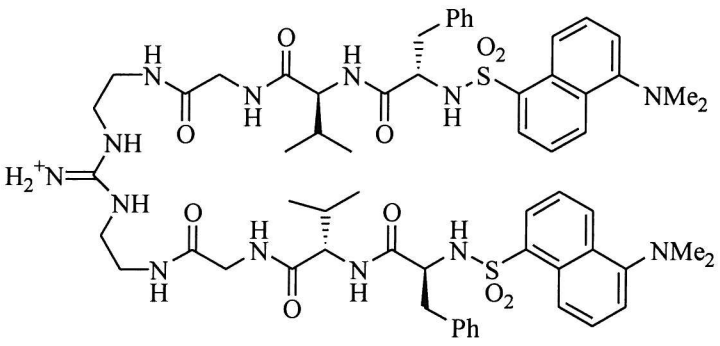

Fig. 23: Kilburn and Bradley's Tweezer Receptor

Still has produced water-soluble analogues of his original receptors;[49] these feature a non-polar conformationally rigidified binding cavity surrounded by polar functionality for association with substrate functionality. A water-soluble dye was also incorporated allowing for screening of the receptor against peptide libraries (fig. 24). The receptor was found to have a strong preference for binding protected tripeptides with hydrophobic amino acids of a similar size adjacent to an amide substituted amino acid of the opposite chirality. The driving force for association was thought to be hydrophobic.

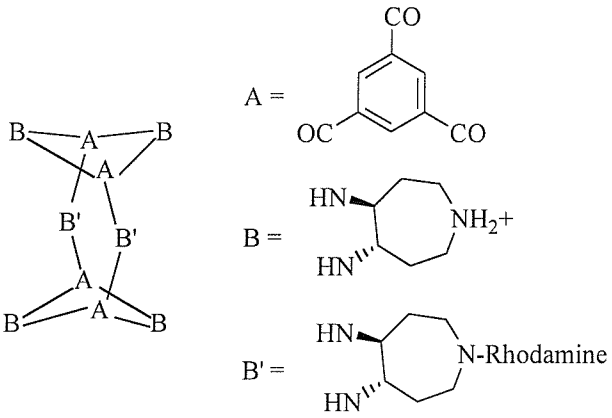

Fig. 24: Still's water soluble polycyclic receptor

Still has modified another of his receptors to produce an HPLC chiral stationary phase by covalently attaching a synthetic C_3-symmetric receptor to silica gel microparticals.[50] The chiral stationary phase showed strong affinities for the L-enantiomers of *N*-Boc amino acid methylamides and operated in both organic solvents and aqueous media.

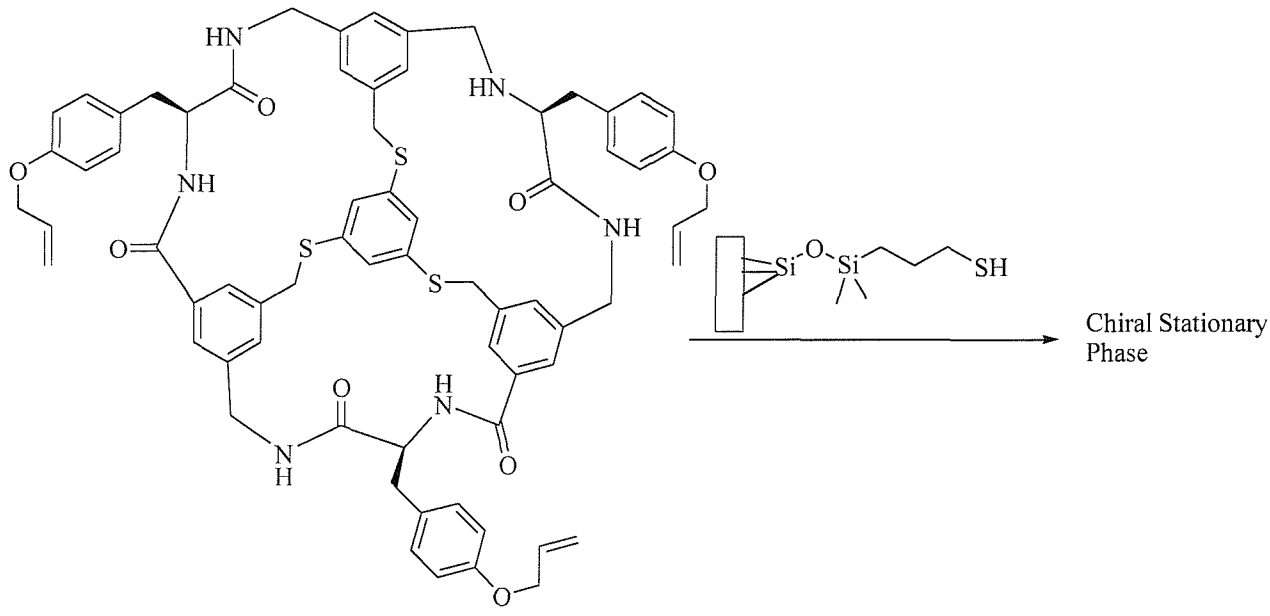

Fig. 25: The Modification of Still's receptor to produce a chiral stationary phase

Davis[51] has produced steroidal based guanidinium receptors which are based on a cholic acid scaffold with the secondary hydroxy groups modified to generate receptors based on the general structure shown below fig. 26 a. The receptors shown (fig. 26 b and c) were designed to achieve the extraction of carboxylates from neutral or basic aqueous solutions, a guanidinium moiety was included as one of the substituents on the cholic acid skeleton for the purpose of complexing the carboxylate functionality of the guests. The extraction efficiencies for both of the receptors was found to be moderate to good for substrates with non-polar side chains. Receptor 26 b was consistently effective in its differentiation between the enantiomers of its guests extracting *N*-Ac L-phenylalanine and *N*-Ac D-phenylalanine in a ratio of 7:1 with an efficiency of 87 mol% and extracting *N*-Ac L-tryptophan and *N*-Ac D-tryptophan also in a ratio of 7:1 with a slightly lower efficiency of 83 mol%. Receptor 26 c generally had a higher capacity to extract the guests but was more variable in its ability to distinguish between the enantiomers, *N*-Ac L-phenylalanine and *N*-Ac D-phenylalanine were extracted in a ratio of 9:1 with an efficiency of 93 mol% whereas *N*-Ac L-tryptophan and *N*-Ac D-tryptophan were extracted in a ratio of 6:1 in a 92 mol% efficiency. Neither receptor was effective with the polar asparagine derivatives.

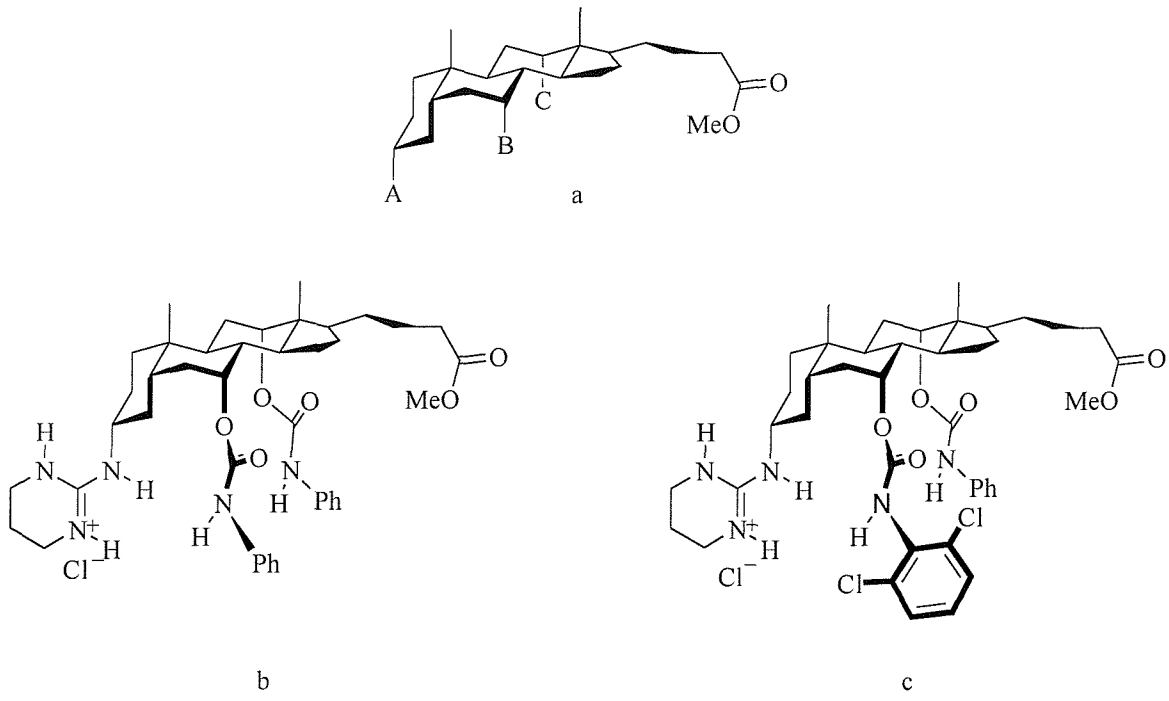

Fig. 26: Davis' Cholic Acid Receptors

1.4.2 Receptors Operating in Non-polar Solvents

For receptors that bind to target molecules in non-polar solvents the contribution to binding from solvent energies is much less significant than in aqueous media, the interactions between host and guest dominate and therefore design of such receptors is less complicated. For this reason a large number of receptors have been developed which operate to bind amino acids and their derivatives in non-polar solvents.

Porphyrin units have been used extensively to form the basis of artificial receptors for binding amino acid derivatives. They provide a relatively rigid framework from which various functional groups can be attached allowing for flexibility in design and synthesis. Mitzutani and Ogoshi have used a trifunctional chiral porphyrin to complex amino acid esters.[52] A zinc ion was employed to provide the primary recognition element for the amino group of the guest; *o*-hydroxyphenyl groups act as hydrogen bond donor sites which further stabilise the host-guest complex. The third recognition element, 2,6-bis((methoxycarbonyl)methyl)phenyl groups, were found to act as sites of steric repulsion for D-amino esters and as an attractive site for D-Ser-

OBzl. The host, therefore, exhibited enantioselective binding of L-amino esters above the D forms with the exception of D-Ser-OBzl. The strength of binding ranged from 48100 dm^3mol^{-1} for L-Pro-OMe to 1340 dm^3mol^{-1} for L-serine-OMe; the enantioselectivity observed is attributed to the convergent binding of the guest *via* two points of attachment.

Ogoshi has modified this host molecule to produce a double bridged porphyrin based host which also binds amino esters.[53] The host, again, utilised a zinc ion to provide the primary interaction with the guest, the bridging reagents gave rise to chiral binding sites which formed a hydrogen bonding interaction between the amide NH of the bridge and the carboxymethyl group of the guest. Evidence from binding experiments indicated that the hydrogen bonding ability of the NH group is enhanced by the electronic effect from the nitro group leading to chiral recognition of the amino acid methyl esters.

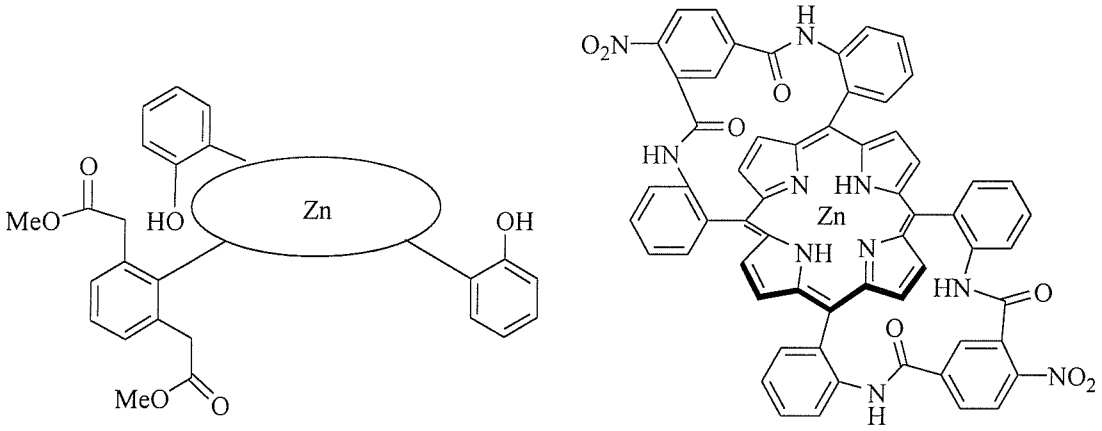

a b

Fig. 27: a. Schematic Representation of Mizutani and Ogoshi's o-hydroxyphenyl Porphyrin Receptor. b. Ogoshi's modifided Porphyrin Receptor

Ogoshi used the same recognition pattern of simultaneous metal co-ordination and hydrogen bonding interaction with a rhodium based metalloporphyrin to achieve the 1:1 binding of L-leucine methyl ester with binding constant of 5 x 10^6 dm^3mol^{-1}.[54] This host has also demonstrated amino acid extraction from neutral aqueous solutions.

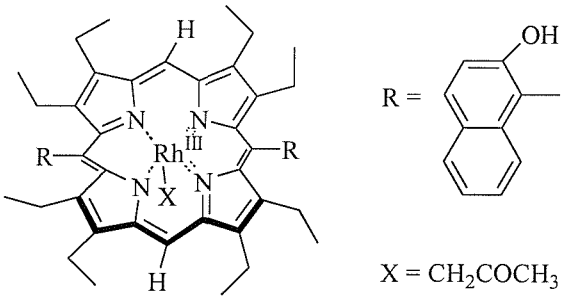

Fig. 28: Ogoshi's Rhodium Based Metalloporphyrin Receptor

Crossley *et al* used zinc porphyrin units to construct chiral clefts[55] which bind histidine esters within the cavity with high enantioselectivity. L-His-benzyl ester was found to bind to the (+) enantiomer of the host (fig. 29) more tightly than to its (-) counterpart by a factor of 9.2. The magnitude of the binding constant for complexation between the benzyl ester of L-His and the (+)-zinc porphyrin was 1.1 x 10^8 dm^3mol^{-1}. L-lysine benzyl ester was found to bind less tightly than L-His-benzyl ester to both enantiomers of the host; the observed enantioselectivity was also less well pronounced and this was attributed to the increased conformational flexibility between the two nitrogen binding sites in this guest compared to the histidine benzyl ester. The strong binding is thought to be the result of a ditopic interaction between the two basic nitrogen sites of the guest molecules with the two zinc centres, the enantioselectivity arising from further steric interactions between the guest and the walls of the helical cavity.

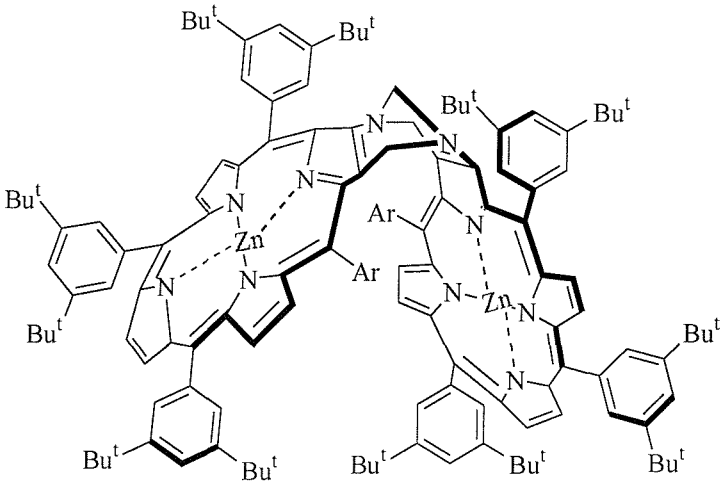

Fig. 29: Crossley's Porphyrin Chiral Cleft Receptor

A range of sapphyrin based receptors have been reported by Sessler *et al*[56] which form strong complexes with *N*-benzyloxy protected aspartate and glutamate anions (fig. 30). The structure of the receptors was based on open chain sapphyrin-sapphyrin dimers. The pentapyrrolic units protonate at neutral pH and therefore serve as carboxylate binding sites allowing for both coulombic and hydrogen bonding attractions to arise. Further hydrogen bonding interactions are derived from the chiral diamino-functionalised spacer units, employed to link the sapphyrin units. It is the variation in this portion of the molecule which provides the diversity in the series of receptors. The receptor pictured (fig. 30) displayed binding strengths of 324500 dm^3mol^{-1} and 20600 dm^3mol^{-1} for *N*-Cbz-L-Glutamate and *N*-Cbz-L-Aspartate respectively, clearly showing a preference for the glutamate derivatives over the aspartate. Enantioselectivity in the binding of these two guests was also observed for this receptor.

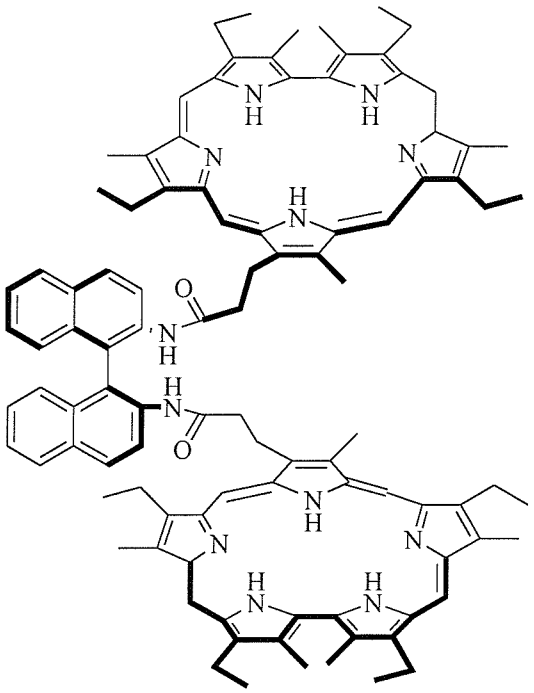

Fig. 30: Sessler's Sapphyrin Dimer Receptor

1,1-Binaphthalene-8,8-diol has been shown to enantioselectively bind derivatives of valine and phenylalanine.[57] The enantioselectivity observed was greatest with the valine derivatives, particularly the derivative shown (fig. 31c); the strength of binding was found to be 80 mol^{-1} dm^3 for the *R* enantiomer of the host and 11 mol^{-1} dm^3 with the *S* enantiomer. The chiral recognition is attributed to the three interactions between host and guest: a hydrogen bonding interaction

between the carboxylate moiety of the guest and the phenolic hydroxyls; an ammonium - π interaction between the guest and the naphthalene ring and a CH - π interaction arising between the isopropyl group of the guest and the naphthalene ring. These sites of interaction are all located in a highly asymmetic micro environment.

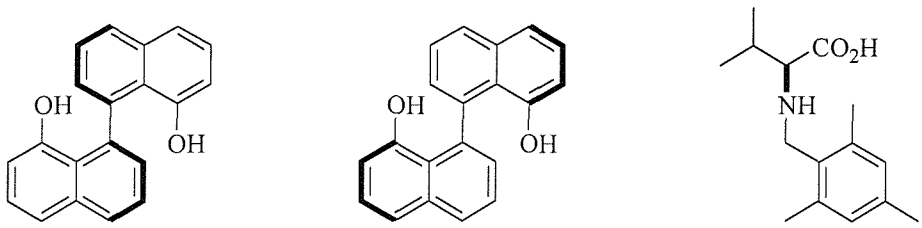

a b c

Fig. 31: a. (R)-1,1'-binaphthalene-8,8'-diol. b. (S)-1,1'-binaphthalene-8,8'-diol. c. Enantioselectivity is most pronounced with this valine derivative.

Morán *et al* have produced receptors which bind *N*-benzoylamino acid derivatives.[58] The receptors are based on xanthone units and complex the carboxy terminus of the amino acid derivatives *via* three hydrogen bonds and a simple π-stacking surface. Studies of the guest *N*-(3,5 dinitro benzoyl) isoleucine with a series of related hosts demonstrated that a combination of π-stacking and charge transfer effects increased the strength of binding. The association constants recorded were 1.1 x 10^3 mol^{-1} dm^3, 4.9 x 10^3 mol^{-1} dm^3 and 5.5 x 10^3 mol^{-1} dm^3 for hosts **a**, **b** and **c** (fig. 32) respectively. These hosts were further developed to allow for chiral recognition with the *N*-benzoylamino acid derivatives.[59]

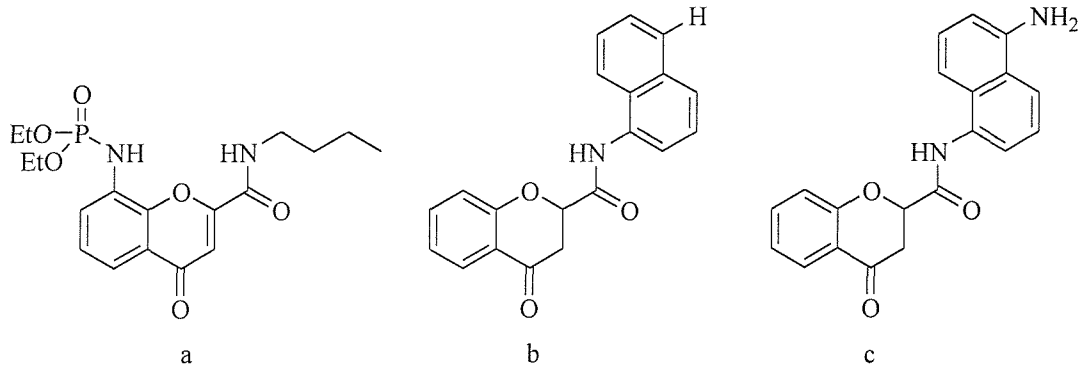

a b c

Fig. 32: Morán's Receptors

Wills and co-workers have developed chiral diazaphospholidine oxide cleft receptors for the purposes of binding *N*-Boc protected amino acids.[60] The structure of these receptors was closely related to cleft receptors developed by Morán[61] which were unable to completely bind the amino acids within the cleft owing to a narrow bite angle. Wills *et al* employed a different rigid aromatic spacer to increase the cleft size and incorporated a chiral diazaphospholidine oxide moiety to encourage enatioselective binding (fig. 33). Complex formation between the successful receptors and the amino acid derivatives was thought to be due to two hydrogen bonding interactions. These are between the acid of the guest and the carbamate of the host and between the carbamate NH of the amino acid derivative and the phosphoamide portion of the guest. The most successful receptor (fig. 33) was found to bind *N*-Boc glycine with a binding constant of 930 mol^{-1} and was capable of enantioselective binding of *N*-Boc alanine derivatives binding *N*-Boc-D-alanine and *N*-Boc-L-alanine with binding constants of 1030 dm^3mol^{-1} and 440 dm^3mol^{-1} respectively.

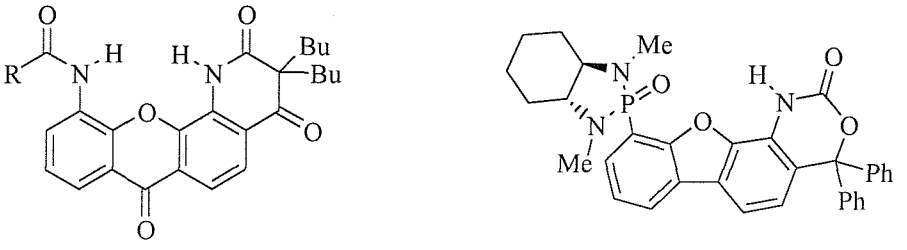

a b

Fig. 33: a. Morán's Cleft Receptor. b. Wills' Diazaphospholidine Receptor

Kemp's triacid forms the basis of a series of cleft receptors designed by Rebek.[62] The receptors consist of two triacid units linked with spacer units (fig. 34). The structure of the triacid moiety is such that three carboxyl groups are constrained to a triaxial conformation so that they protrude from a single face of the molecule creating chiral cavities. Receptor **a** (fig. 34) features three convergent binding domains: a carboxylic acid moiety, an acridine unit which provides a surface on which π-π stacking interactions may occur, and a phenylalanine derivative. The receptor recognises a derivative of phenylalanine, although no enantiomeric discrimination occurred with phenylalanine methyl ester as the guest. When the phenyl ring of the guest was substituted in the *para* position with either a nitro group or a hydroxyl functionality, asymmetric recognition was observed to take place. The dipole in the aromatic ring appears to enhance the interactions

between aryl subunits in the receptor and substrate. Modification of receptor **a** to include a 2,6-disubstituted naphthalene as the spacer unit produced receptor **b** (fig. 34); the new receptor was found to complex cyclo L-leu-gly and cyclo L-leu-L-leu with binding constants of 50,000 and 12,000 mol^{-1} respectively.[63]

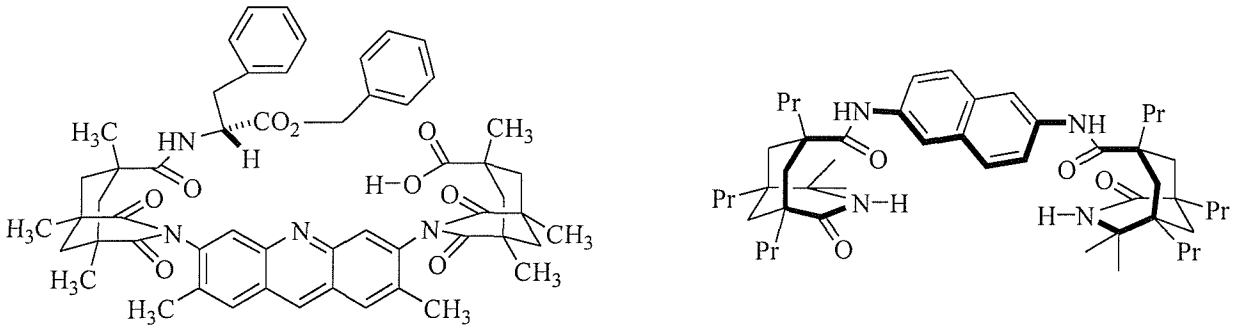

a b

Fig. 34: a. Rebek's Acridine Receptor. b. Rebek's Naphthalene Receptor

de Mendoza *et al* employed a rigid bicyclicguanidinium subunit as a carboxylate binding site attached to two naphthoyl derivatives in receptors designed to complex amino acid derivatives (fig. 35).[64] The driving force for complexation arose from the formation of hydrogen bonds between the guanidinium unit of the host and the carboxylate functionality of the amino acid derivative with additional π-π stacking interactions from the naphthoyl moiety. The bis-naphthoyl receptor demonstrated a clear preference for the L enantiomer of *N*-acetyl tryptophan, binding with a binding strength of 1051 mol^{-1} as compared to a binding strength of 534 mol^{-1} for the D form. The receptor was modified to feature not only the guanidinium unit and naphthalene ring but also a crown ether enabling interaction to take place between the receptor and the ammonium portion of the guest molecule (fig. 35 b).[37] Competition experiments carried out with this receptor indicated a preference for aromatic amino acids, for example derivatives of tryptophan and phenylalanine and displayed a high degree of chiral recognition.

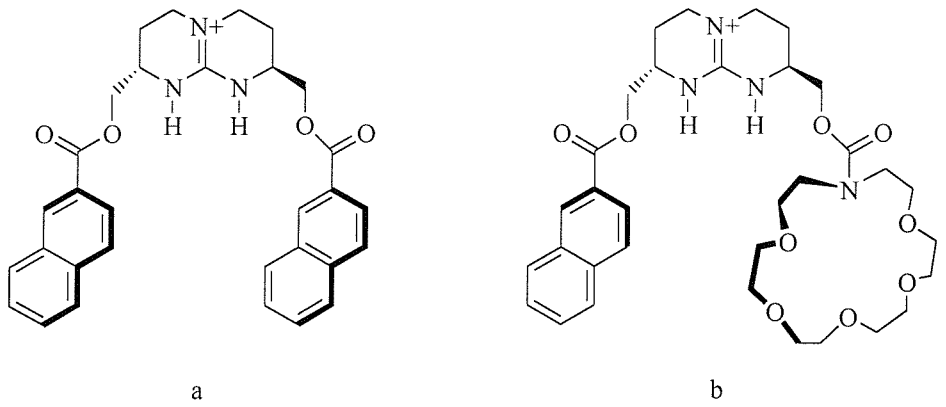

a b

Fig. 35: a. de Mendoza's bisnaphthoyl receptor. b. The crown ether receptor

Cristofaro and Chamberlin[65] produced a C_2-symmetric macrolactam host for the purposes of complexing peptide derivatives. The design of the structure was aided by molecular modelling calculations and features two short peptide strands linked with two rigid aromatic spacers to form macrocyclic lactams (fig. 36). The amide functionalities of the peptide strands provide the potential for the formation of hydrogen bonding interactions with guest peptides; these interactions are the driving force for complexation. The two receptors shown below (fig. 36) bound to cyclo gly-leu and cyclo leu-leu with binding constants ranging between 74 mol^{-1} and 2260 mol^{-1} showing a preference for the former guest. When the peptide strands of the receptor were composed entirely of L-amino acids (fig. 36a) enantioselective binding was observed, the cyclo leu-leu substrate being preferred over the cyclo D-leu-D-leu guest; in the case of the second receptor where the peptide strands featured D and L amino acids no enantioselectivity was found.

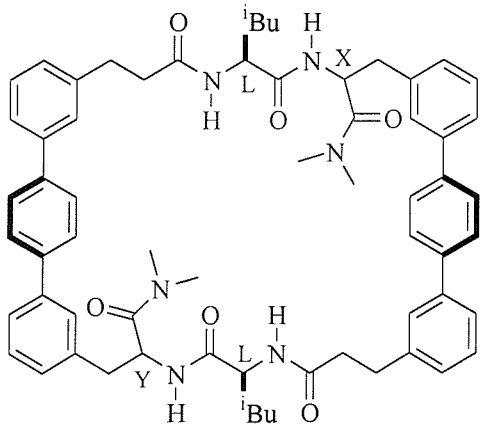

Fig. 36: a. Peptide receptor LLLL (X = Y = L)
b. Peptide receptor LDLD (X = Y = D)

Kilburn and co-workers have also produced macrocyclic receptors for the purpose of binding small peptides and amino acid derivatives.[66] The host molecules feature a binding site for a carboxylate or carboxylic acid terminus of a peptide; amide functionality to provide potential hydrogen bonding sites and a rigid spacer unit to maintain the open conformation of the macrocycle. The receptor given below (fig. 37) was found to complex several *N*-benzyloxy carbonyl amino acids with values of K_a ranging from 308 to 588 mol^{-1} dm^3.[67] The host was produced in racemic form but titration with homochiral guests gave diastereomeric complexes with differing values of K_a. The most pronounced difference was observed with *N*-benzyloxycarbonyl β-alanyl-L-alanine: when titrated with the monocyclic receptor two diastereomeric complexes were produced with K_a = 2515mol^{-1} dm^3 and 691 mol^{-1} dm^3.

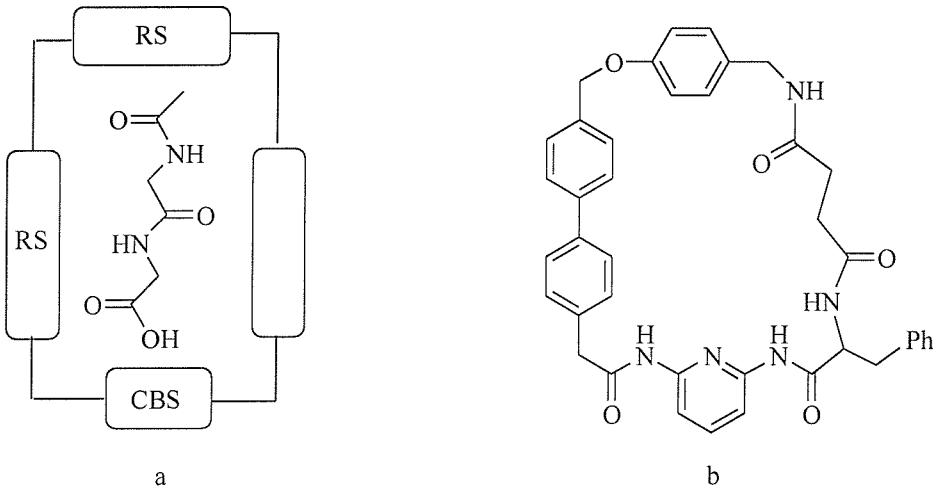

Fig. 37: a. Schematic view of Kilburn's monocycle.
b. Kilburn's monocycle

The design of these macrocyclic receptors was modified to produce a series of receptors with a macrobicyclic structure featuring a specific carboxylate binding site located at the base of a C_2-symmetric cavity.[68] A thiourea moiety was utilised as a carboxylate binding site and biarylmethane units acted as rigid spacers to hold the conformation of the macrocycle open. The desired chirality and amide funcitonality were introduced *via* two lysine derivatives. The receptor was found to bind to a range of *N*-acetyl amino acid derivatives with little selectivity. However, NMR experiments revealed that the D-amino acid guests were bound on the external face of the macrocycle cavity whereas the L-amino acid deriviatives were bound within the

cavity *via* a strong carboxylate-thiourea interaction. The L-amino acid guests internalised in the macrocycle were also shown to adopt a *cis* configuration around the *N*-acetyl amide bond; this higher energy conformation is thought to be stabilised by two hydrogen bonds between the *cis* amide and the rim of the macrobicycle.[69] The strength of binding ranged from $K_a = 5.8 \times 10^3$ dm^3mol^{-1} for N^{α}-Ac-L-histidine to 130×10^3 dm^3mol^{-1} for N^{α}-Ac-L-lysine.

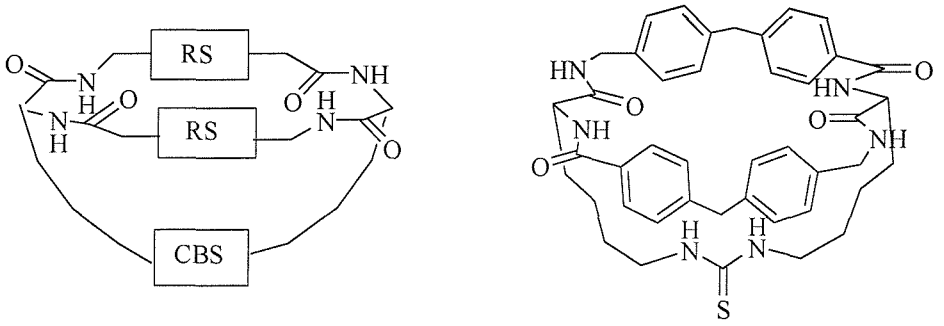

a b

Fig. 38: a. A schematic representation of Kilburns Macrobicycles
b. Kilburn's Thiourea Macrobicyclic Receptor

Variations on the macrobicyclic structure included the use of a diamidopyridine unit as the carboxylic acid binding site.[70, 71] The modified receptor featured the carboxylate binding site located at the base of a deepened cavity with amide functionality, again used to provide a site for additional hydrogen bonding. A phenylalanine unit was incorporated to increase the chiral information within the receptor framework and to enhance the solubility of the host in non-polar solvents (fig. 39).[72] The diamidopyridine receptor was found to be a strong, selective receptor for peptides with a carboxylic acid terminus; the strongest interaction observed was with Cbz-β-Ala-D-Ala-OH which was bound with a binding constant of $K_a = 12200$ dm^3mol^{-1}. A further modification was made to the diamidopyridine receptor to reduce its flexibility and produce a more preorganised host.[73] The new receptor was found not only to strongly bind the dipeptide Cbz-L-Ala-L-AlaOH, $K_a = 33000$ dm^3mol^{-1}, but also to do so selectively. A result such as this is of particular interest due to the relevance to binding L-lys-D-Ala-D-AlaOH, the bacterial cell wall precursor peptide.

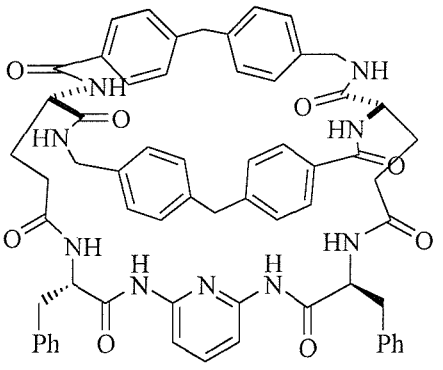

Fig. 39: Kilburn's Diamidopyridine Receptor

Pieters and Diederich have achieved the enantioselective complexation of amino acid derivatives with a C_3-symmetrical receptor (fig. 40).[74] The host structure is cage like, composed of two 1,3,5-triarylbenzene units linked by three amino acid spacers. The spacer units provide chirality as well as sites for hydrogen bonding with *N-Z* amino acids. The driving force for complexation was attributed to the formation of hydrogen bonds between one of the spacer arms and the carboxylate group of the amino acid derivative. NMR studies indicated that complexation occurs within the cavity and that further contributions to complex stability arise from interactions between the receptor and the carbamate moiety of the guests. The host bound to a range of amino acid derivatives but the most stable complexes were formed between the receptor and *N-Z* protected amino acids. A preference was demonstrated for forming complexes with *N-Z*-L-Glu over *N-Z*-D-Glu and the difference in stability between the two diastereomeric complexes was observed to be $\Delta(\Delta G) = 4.2$ kJ mol^{-1}.

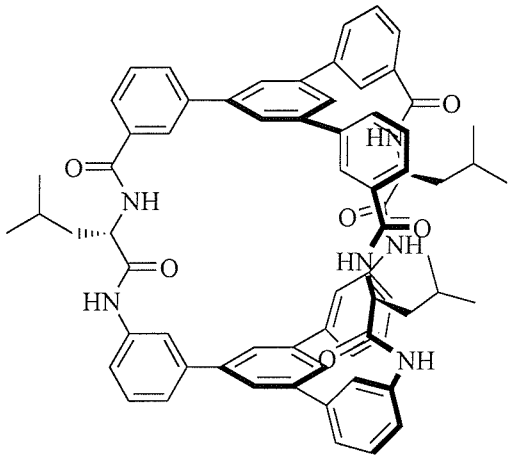

Fig. 40: The C_3 - Symmetrical Receptor devised by Pieters and Diederich

Kohmoto *et al* have produced a steroidal triply bridged cyclophane capable of binding to *N-Z* protected amino acids.[75] The receptor was designed to have a hydrophilic cavity containing six hydroxyl groups directed towards the centre of the cavity. Kohmoto's host was shown to form 1:1 complexes with *N-Z*-ala and *N-Z*-Phe as guest molecules, displaying enantioselective binding with the phenylalanine derivaties. *N-Z*-L-phenylalanine and *N-Z*-D-phenylalanine were bound with binding constants of $K_a = 268 \pm 22$ $mol^{-1}dm^3$ and $K_a = 40 \pm 6$ mol^{-1} dm^3 respectively.

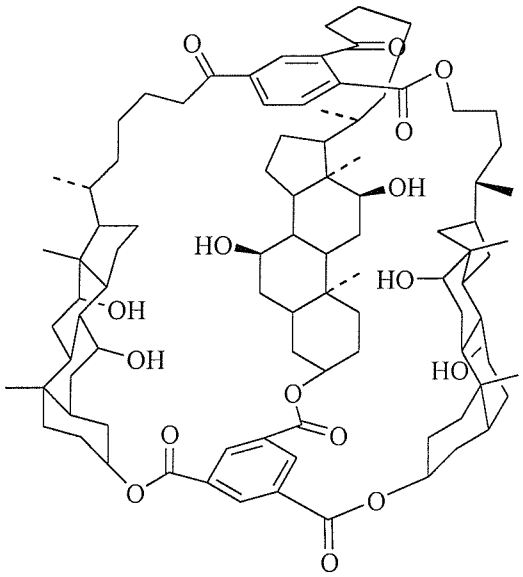

Fig. 41: Kohmoto's Triply-bridged Cyclophane

A homooxacalix[3]arene was used by Shinkai to form the basis of a pseudo-C_2-symmetrical macrocycle.[76] The host binds to the primary ammonium ion of amino acid hydrochloride and picrate salts *via* hydrogen bonding interactions with the three oxygen atoms of the guest. The (-) enantiomer of the host formed more stable complexes with the L-amino acid derivatives than the (+) enatiomer. The largest chiral discrimination was observed for the picrate salt of L-Phenylalanine ethyl ester which was bound to the (-) enantiomer of the receptor with an association constant, $K_a = 1200\ mol^{-1}\ dm^3$ and to (+) receptor with an association constant, $K_a = 180\ mol^{-1}\ dm^3$.

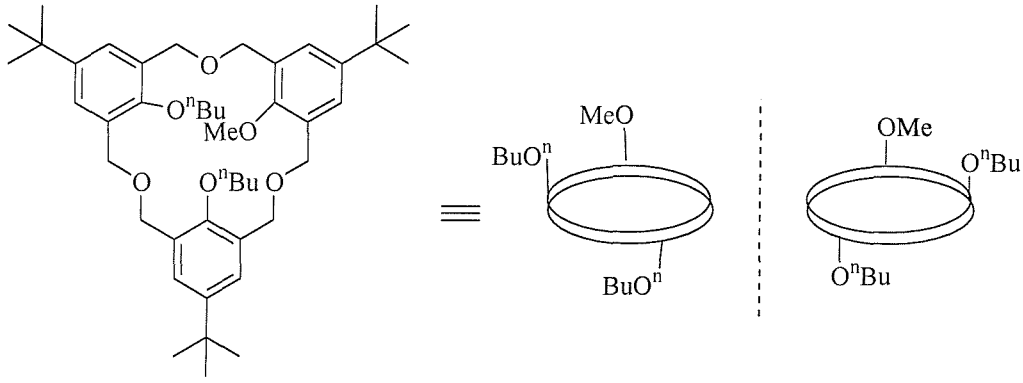

Fig. 42: Shinkai's Pseudo-C_2-Symmetrical Macrocycle

Still produced receptors with high binding selectivities for peptide derivatives. The receptor is an A_4B_6 cyclooligomer of trimesic acid (A) and (R, R) - diaminocyclohexane (B) which forms a deep binding cavity with minimal conformational flexibility (fig. 43).[77] The cavity was found to fully encapsulate the side chains of bound L-peptides. Peptide derivatives were found to be bound with high selectivity for the L-configuration except when the side chains were particularly large. The amino acid side chains for the D-amino acids were thought to project away from the binding site and into the solvent. A series of receptors based on the A_4B_6 design, where A = trimesic acid and B = 1,2 - diamines have been produced and reported to bind peptides containing L-valine or L-phenylalanine residues with high enantioselectivities.[78, 79] Fragments of this type of receptor were also screened against peptide substrate libraries to determine binding selectivities; the smallest effective fragment (fig. 43) was shown to bind with substantially more selectively than the parent receptor.[80]

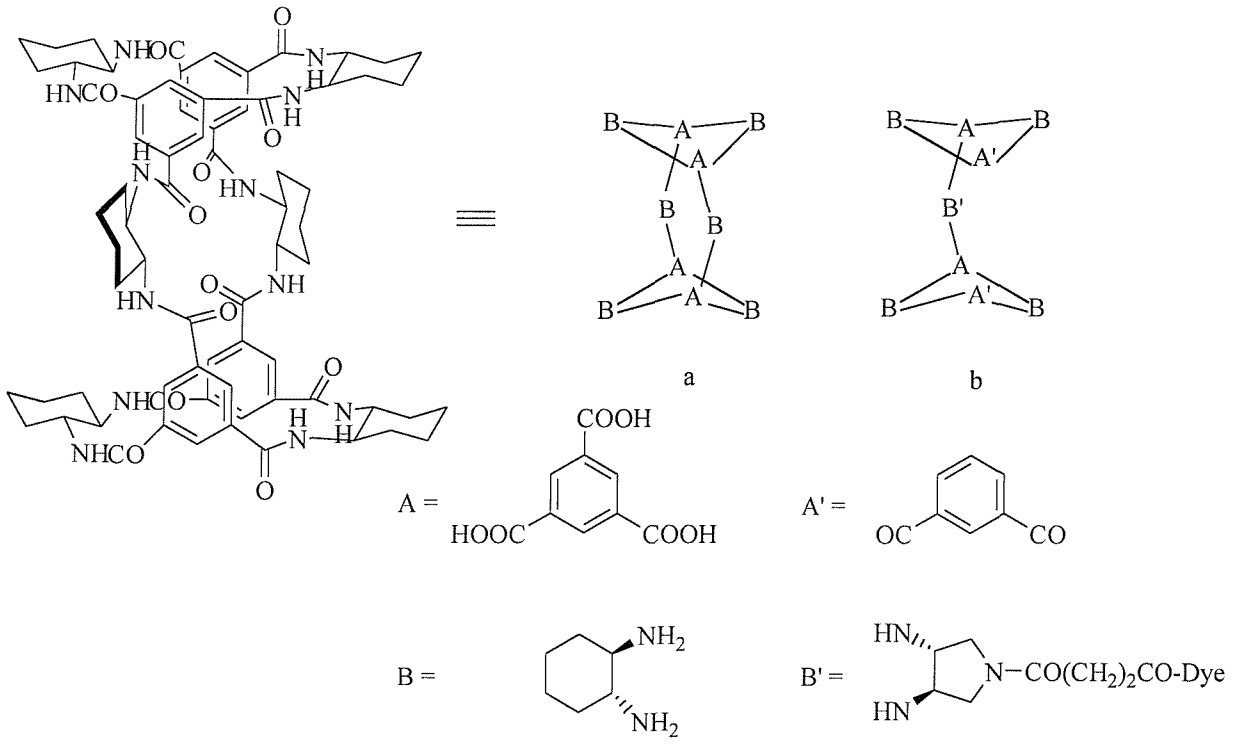

Fig. 43: a. An example of Still's A_4B_6 Receptors. b. The smallest Effective Fragment of Receptor

Still has also produced a series of C_3-symmetric receptors with a deep binding cavity featuring alternating hydrogen bond donor and acceptor sites around the rim of the cavity (fig. 44).[81] The receptors themselves are inflexible and bind amino acid derivatives with high selectivity displaying a preference for the L isomer. It was also observed that in the case of Boc protected *N*-methylamides of α-amino acids, the receptor showed a selectivity for amino acids featuring hydroxyl groups on their side chain. Serine and threonine were found to be preferentially bound over amino acids such as alanine, valine and leucine. The binding strengths for the *N*-methylamide amino acid derivatives ranged between 7.1 kJ dm^3mol^{-1} and 12.6 kJ dm^3mol^{-1}. NMR and molecular modelling studies indicated that the Boc L-amino acid *N*-methyl amides were bound within the cavity by three hydrogen bonds such that the methylamide terminus projected into the cavity. However, when *N*-methoxycarbonyl amino acid esters were complexed the opposite, *N*-terminus of the amino acid substrate was directed towards the centre of the cavity; again a preference for the L-configuration was observed (fig. 44).[82]

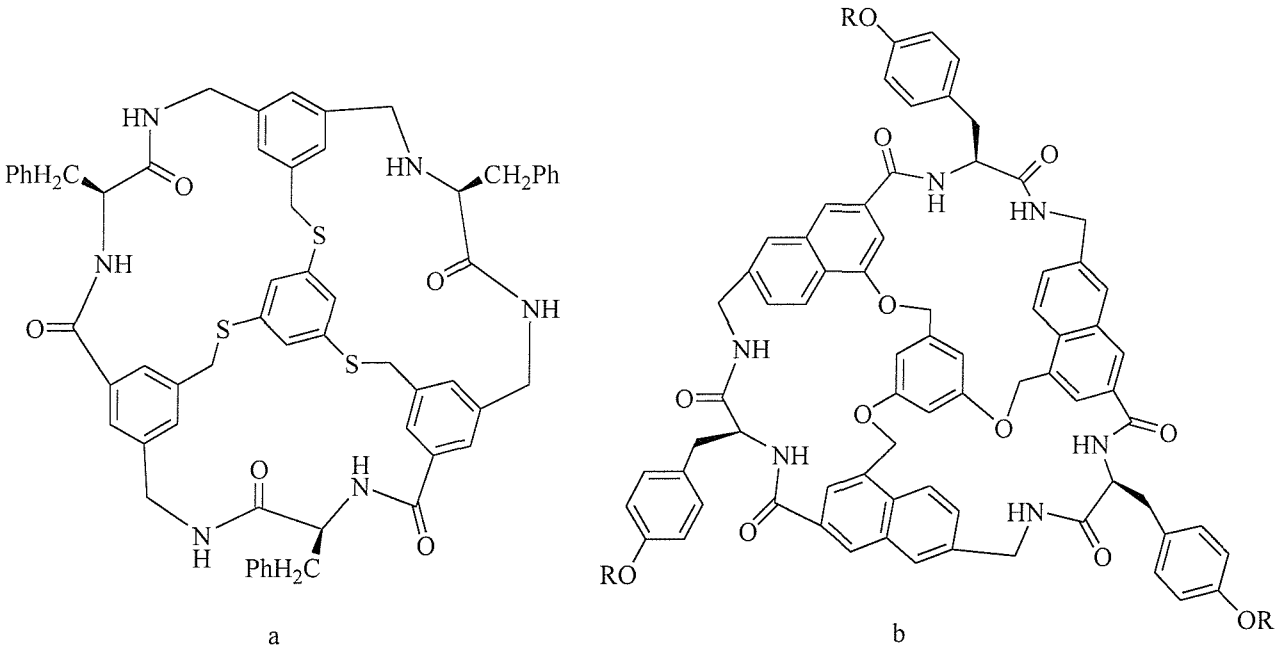

Fig. 44: a. Still's C_3-Symmetric Receptor. b. Still's Naphthalene Based C_3 - Symmetric Receptor

Analogues of the C_3-symmetric receptor have been produced. The initial modifications involved the incorporation of additional methylene units between the sulfur atoms and the benzene ring at the base of the cavity which served to increase the conformational flexibility of the binding cavity. The new receptor bound substrates with significantly less enantioselectivity than the original host **a** (fig. 45), illustrating the importance of preorganisation in the selective complexation of guest molecules.[83] Later modifications to the structure involved replacing the benzene rings with naphthalene rings and employing oxygen atoms within the cavity in place of sulfur (fig. 45b).[84] The resulting host molecule had a similar conformation to that of the original host, **a**. However, the binding cavity was substantially widened, consequently the mode of binding of the peptidic guests was found to be altered. Instead of selection for small terminal substituents the new host molecule, **b** (fig. 45), demonstrated an ability to select tripeptides with an L-proline derivative in the second position, and amino acids with an L-configuration in flanking positions.

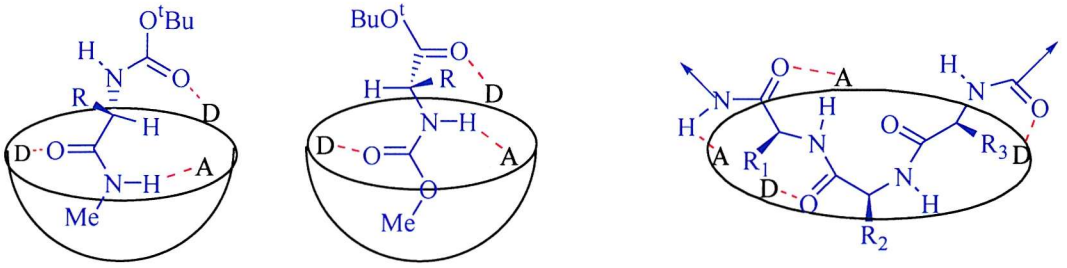

Fig. 45: a. Binding mode for the Boc Methylamides in Still's original receptor.
b. Binding mode for the Methoxycarbonyl Ester Complexes in Still's original Receptor.
c. Binding mode for the Peptidic Guests in Still's modified Receptor

Still has also produced tweezer receptors to bind peptidic guests (fig. 46).[85] The tweezer was composed of a linker, formed from trimesic acid and two sulfonyl peptide binding arms. The receptor was shown to successfully complex oligopeptides, the strength of binding was low but the selectivity was good for tripeptides which featured L-Gln in the first amino acid position, D-Asn or D-Gln in the central position and D-Proline in the third amino acid position. The nature of the *N*-terminal acyl group was found not to effect binding. Still and co-workers have synthesised a series of tweezer receptors which differ only in the hinge portion of the molecule, in an effort to determine the effect of incorporating less flexible hinges into the tweezer structure.[86]

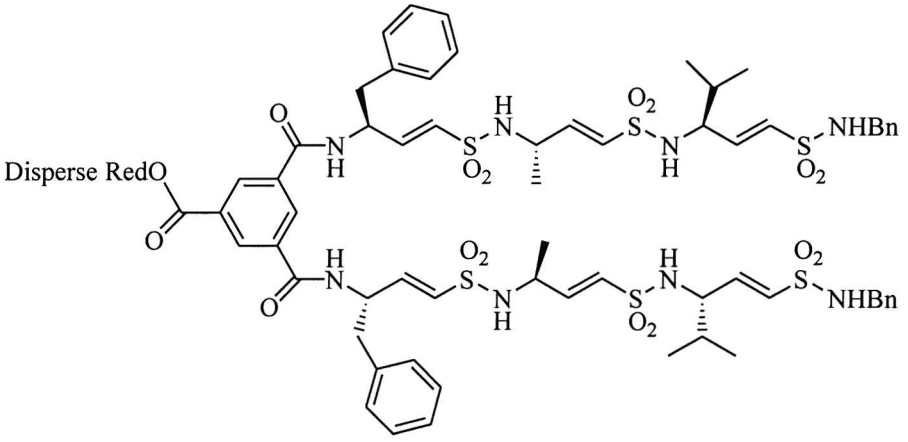

Fig. 46: Still's Tweezer Receptor

Kilburn *et al* have also designed and synthesised tweezer receptors for the purposes of binding the carboxylate terminus of peptides.[87] A diamidopyridine unit was used as the tweezer head group which provides a specific recognition site for the terminal carboxylate group of a peptide. The side arms were composed of simple tripeptides which have the potential to interact with the back bone of the peptide guests.[88] A library of resin bound tweezer receptors was produced using the 'split and mix' strategy.[89] The library was screened against a danzyl labelled tripeptide DNS-L-Glu(O^{t}Bu)-L-Ser(O^{t}Bu)-L-Val-OH. Sequencing of the receptors that were successful in binding the guest were sequenced by Edman degradation, revealing that the consensus sequence for the peptide side arms was Val-Leu-Trp. A tweezer receptor was synthesised to confirm that the observed binding with the resin bound tweezers was also operating in free solution (fig. 47). However the receptor, once synthesised, was found to be insoluble in $CDCl_3$ or CD_3CN and therefore the binding studies were carried out in a solution of DMSO:$CDCl_3$ (2:98). The strength of binding was observed to be $K_a = 2.6 \times 10^5$ dm^3mol^{-1} by fluorescence spectroscopy.

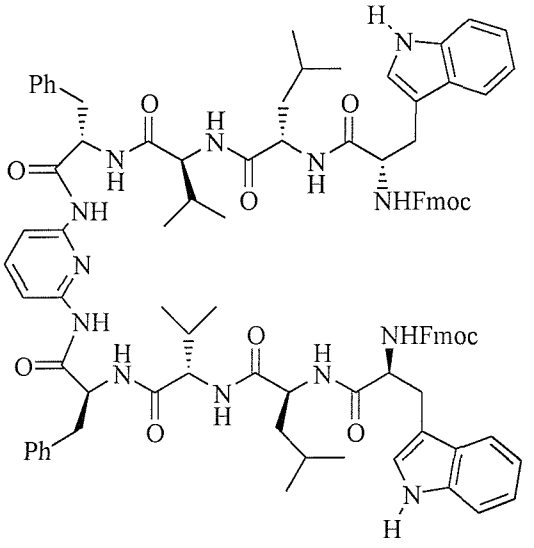

Fig. 47: Kilburn's Tweezer Receptor

1.5 Programme of Work

Previous work within the Kilburn group established that macrocycle **1** (fig. 38) binds to a range of *N*-acetyl amino acids in the form of their tetrabutylammonium salts.[90] An initial control experiment was carried out to establish that macrocycle **1** did interact with the carboxylate of its

guests. The methyl ester of *N*-acetyl-L-phenylalanine and macrocycle **1** were mixed together in a 1:1 ratio and the spectrum of this mixture compared to the spectra of the uncomplexed materials. There was no evidence of a binding interaction between the host and guest components.

NMR titration experiments of macrocycle **1** with *N*-acetyl amino acids in deuterochloroform did not provide classical saturation curves for a 1:1 host-guest complex, instead binding plots with a sigmoidal curve were observed. This type of behaviour was described by Wilcox[120] for systems where two competing guests are present, the stronger binding guest displacing the poorer substrate. However, the systems under scrutiny did not contain two different guests and postulations of either competition between macrocycle **1** and the tetrabutylammonium counter ion for the guest, or a higher binding stoichiometry were disproved by Job plots.[121, 122] The majority of binding data was obtained by extraction experiments[117] and initially seemed to indicate that macrocycle **1** bound to simple *N*-acetyl amino acids, with the association being dominated by the strong interaction between the guest carboxylate moiety and the thiourea of the host. There was no apparent contribution to the binding energy from secondary interactions between the host and guests compared to simple carboxylates such as benzoate and hexanoate. Furthermore no selectivity in binding between enantiomers of the same substrate were observed. However, detailed NMR studies elucidated a far more complicated binding scenario.

Further examination of the data revealed that although there was little selectiviy for amino acid configuration (*R* or *S*), the ^{1}H NMR spectra of 1:1 mixtures of macrobicycle **1** with the tetrabutylammonium salts of D- or L-*N*-acetyl alanine and D- or L-*N*-acetyl phenylalanine had markedly different chemical shifts for the L-amino acid derivatives compared to the D-amino acid derivatives. This would suggest very different modes of binding for the two enantiomers. In all cases the spectrum of the complex showed the signal for the thiourea NH to be substantially shifted downfield by between 2 and 3 ppm, relative to the uncomplexed macrocycle, indicating hydrogen bonding interactions formed between the carboxylate and thiourea. The chemical shifts for the aliphatic resonances of the D-alanine derivative in the 1:1 complex were not significantly different to those observed in the spectrum of the uncomplexed amino acid. However, in the 1:1 complex of macrocycle **1** with the L-alanine derivative all four

of the alanine resonances were significantly shifted upfield (fig. 48). Similarly, the D-phenylalanine derivative, when complexed displayed only minor differences in chemical shifts compared to the free amino acid. However, the acetyl methyl, NH, $C^{\alpha}H$ and $C^{\beta}H$ resonances were shifted by a large amount in the complexed form of the L-phenylalanine derivative (fig. 48).

The aromatic resonances for the guest and the macrocycle were not dramatically shifted suggesting that any π-π interactions do not significantly contribute to the association. The observations are consistent with binding of the D-amino acid derivatives to the thiourea moiety on the external face of the cavity, while the L-amino acid derivatives are bound within the macrocycle cavity.

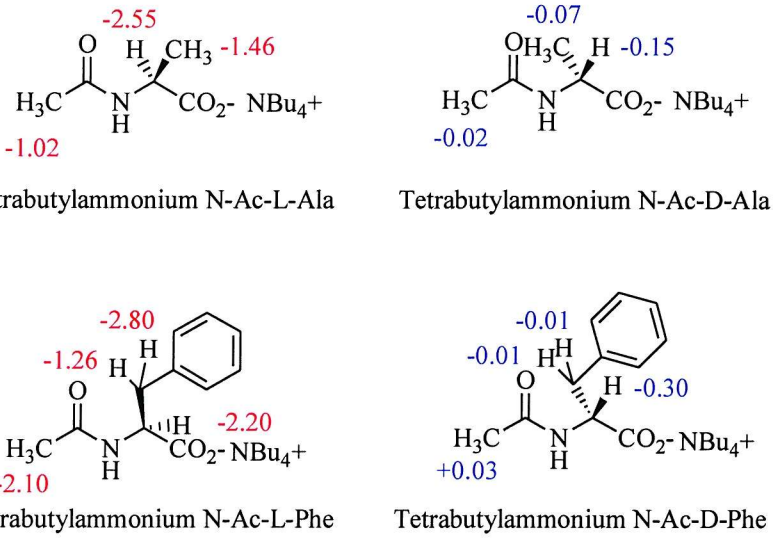

Fig. 48: Upfield Shifts (ppm) for the Indicated Protons Relative to the Uncomplexed Signals

Rigorous NMR studies of the macrocycle **1** and *N*-Ac-L-Phe-NBu_4 complex were carried out and the complex assigned using 500MHz DQF-COSY and TOCSY experiments. NOESY experiments did not provide any useful information whereas ROSEY spectra obtained at 283 K gave a multitude of cross-peaks representing either inter- or intramolecular NOE contacts. A series of NOE contacts between the acetyl methyl **a** of the guest and the protons on the phenylalanine ring (**e**, **f**, **g**) and the α-proton, **c** were observed. Only a weak cross-peak was present corresponding to **a** and the NH proton **b**. This did not correspond to the ROSEY

spectrum of the free guest which features none of the cross-peaks with the exception of the correlation between **a** and **b**.

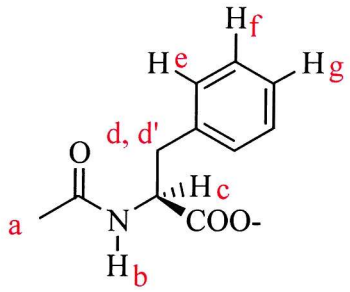

Fig. 49: N-Ac-L-Phenylalanine

From this data the structures of the bound and unbound guest were determined and revealed that a *trans* amide bond exists in the unbound state and a *cis* amide configuration is present in the complexed form. Thus, it would appear that in order to be accommodated in the cavity of macrocycle **1**, the guest undergoes an isomerisation of the acetyl amide from the favoured *trans* conformation to the *cis* geometry. The energetic preference of a secondary amide to adopt a *trans* conformation over a *cis* conformation is estimated to be 8-10 kJ mol^{-1}.[128, 129] Similarly the NOE cross-peaks in the ROSEY spectrum of the *N*-Ac-L-alanine complex with macrocycle **1** showed the amide bond of the guest to be in the *cis* configuration when complexed. Molecular dynamics calculations indicated that the *cis* amide configuration is stabilised by two hydrogen bonding interactions between the amide carbonyl of the guest and the side wall of the host.[69]

The aliphatic resonances of the guest were found to account for only 70% of the required intensity when compared to that of the tetrabutylammonium group. It was observed that in the 2D spectra of the complex between macrocycle **1** and *N*-Ac-L-phenylalanine that protons from the aromatic spacer of macrocycle **1** are in exchange with another set of resonances representing approximately 30% of guest and the second set of signals did not display the intermolecular NOE cross-peaks associated with the first, and also showed chemical shifts similar to those of the free macrocycle. This phenomenon was attributed to the substrate molecule being associated with the macrocycle both inside the cavity (70%) and on the external face (30%) utilising just a carboxylate-thiourea interaction (cf. binding the D enantiomer), with a rapid exchange occuring between the internal and external forms, the guest possibly rearranging from the *cis* amide

configuration to the *trans*. The existence of different modes of binding in the complex is likely to be reflected in the sigmoidal shape of the original NMR titration studies carried out. A representation of the modes of binding is given below (fig. 50) along with the estimates of the free energy values associated with each process.

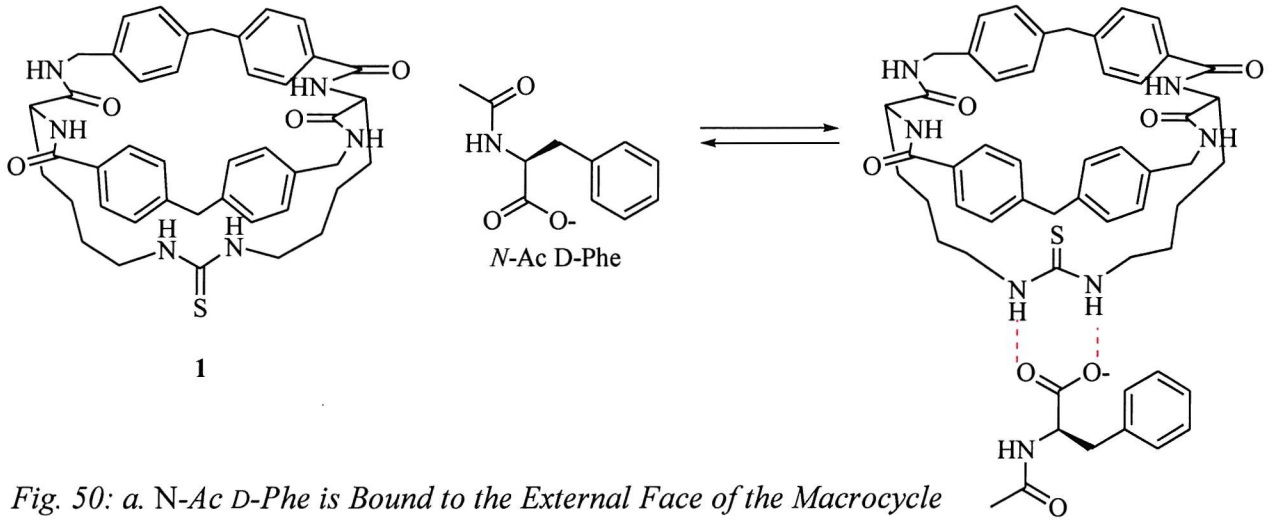

Fig. 50: a. N-*Ac* D-*Phe is Bound to the External Face of the Macrocycle*

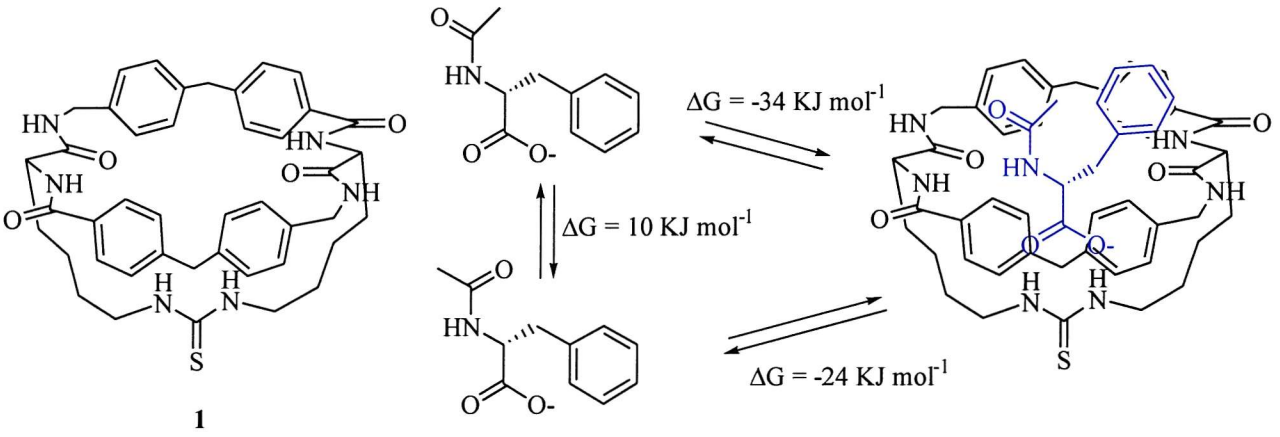

Fig. 50: b. N-*Ac* L-*Phe is Bound within the Cavity of the Macrocycle*

It was therefore, concluded that receptor **1** binds *N*-Ac D-amino acid substrates *via* a strong carboxylate - thiourea interaction on the external face of the cavity, while *N*-Ac L-amino acid substrates are bound within the cavity of the receptor. It is of particular note that the *N*-Ac unit of the internalised L-amino acid derivatives is bound in a *cis* amide configuration, stabilised by two hydrogen bonds.

The initial aim of this project was to explore the possibility of using macrocycle **1** as an enantioselective catalyst to enhance the rate of intramolecular reactions where achieving *cis* geometry around an amide bond is essential if a reaction is to take place. One such example is the intramolecular Diels-Alder (IMDA) reaction of dienylacrylamides such as **2** (fig. 51).

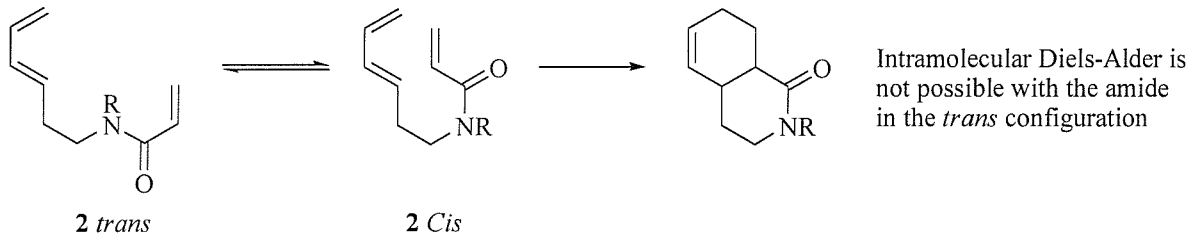

2 *trans* **2** *Cis*

R = Me *conditions:* 25°C, toluene, 20h, 77% yield
R = H *conditions:* 85°C, toluene, 10h, 63% yield

*Fig. 51: Dienylacrylamides, potential Substrates for Macrocycle **1***

The Diels-Alder cyclisation of **2**, R = H, proceeds in toluene at 85°C over ten hours. The methylated material cyclises in two hours at the same temperature or in twenty hours at 25°C;[91] the difference in conditions required to effect cyclisation in the two substrates is attributed to the methylated material adopting the necessary *cis* configuration more readily. It was anticipated that macrocycle **1** would, therefore, be an effective catalyst for substrates based on this structure, with a further enhancement to the rate from hydrogen bonding to the carbonyl group serving to increase the reactivity of the dienophile moiety. The effect of macrocycle **1** on the cyclisation of a range of substrates based on the general dieneylacrylamide structure **3** (fig. 52) was to be investigated.

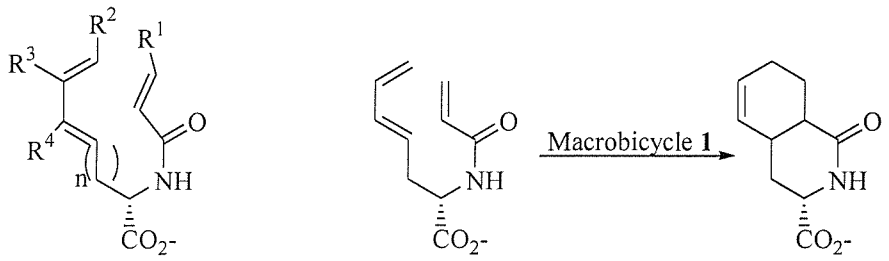

3

Fig. 52: Substrates Initially of Interest in the IMDA Studies

In order to enhance the binding strengths, and therefore the catalytic activity of macrocycle **1** modified macrocycles were prepared containing pyridine units in the biaryl spacer and replacing the methylene moiety of the biaryl spacer with an oxygen atom (fig. 53). The binding behaviour of these second generation macrocycles with various amino acid derivatives is also an area of interest and one that we sought to study during the course of this project. The structural design of the original macrocycle **1** was further altered to enhance its selectivity for certain amino acid guests. The synthesis of related macrocycles containing bisthiourea units, with the potential to complex dicarboxylates, was a further extension that was considered.

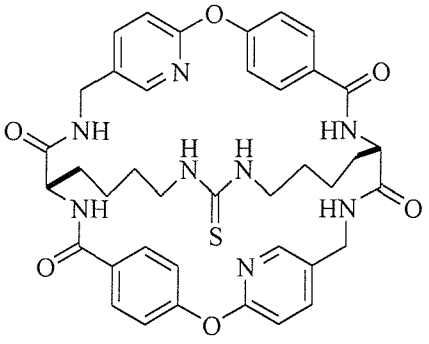

59

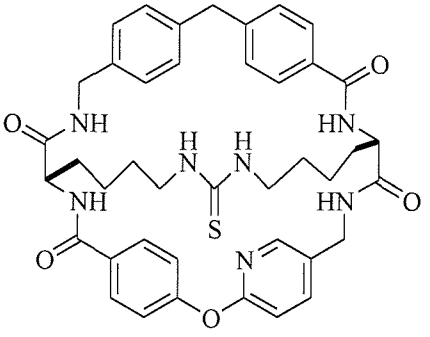

60

Fig. 53: The Two Modified Macrocycles

Chapter Two

Synthesis of Macrocycle 1

2.1 Introduction

The initial target for this project was to establish whether macrocycle **1** (scheme 1) had the potential to enhance the rates of IMDA reactions. Thus it was necessary to synthesise sufficient quantities of the macrocycle and of the Diels - Alder precursors to enable these investigations to take place.

2.2 Overview of the Synthetic Pathway

Macrocycle **1** can be produced *via* a relatively straightforward and efficient pathway, previously investigated and optimised by G. J. Pernia.[90] The disconnection of the macrocycle (scheme 1) illustrates the key intermediates produced during the synthesis. Initially, the rigid aromatic spacer is built up and then coupled to an orthogonally protected lysine derivative, which forms the remainder of the macrocycle rim and sidewalls. The ε-amine of the lysine is selectively converted to the isothiocyanate functionality and combined with one equivalent of the corresponding amine **5**, thus forming the linear, symmetric macrocycle precursor bearing the appropriate protecting groups **4**. The formation of two amide bonds can then be effected to furnish the desired macrocycle. The synthetic strategy allows for alterations to the macrocycle structure to be easily accommodated, for example, different amino acids can be incorporated to provide varying cavity sizes and properties; modification of the aromatic spacer is also a possibility.

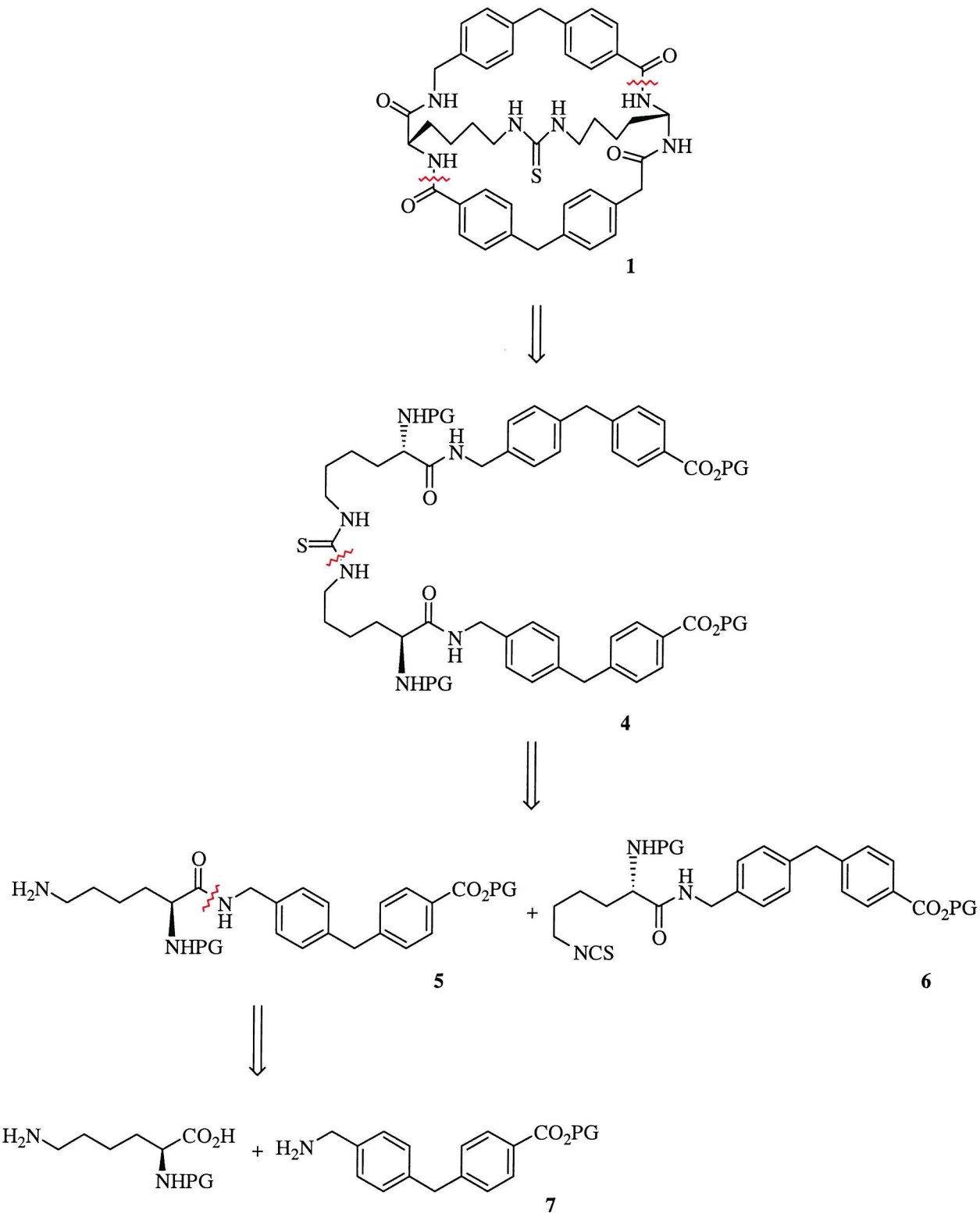

*Scheme 1: The Retrosynthetic Analysis of Macrocycle **1***

2.3 Synthesis of Macrocycle 1

The route followed to produce macrocycle **1** was essentially the same as that developed by G. J. Pernia. However, attempts were made to improve the strategy of synthesis and yields of the reactions employed and alterations to the original route are discussed where appropriate.

The first component of the rigid aromatic spacer was produced *via* a radical bromination of commercially available methyl 4-methylbenzoate, **8** (scheme 2).[92] The reaction was amenable to large scale preparation and the mono brominated product **9** was generally achieved in good yields (53%), provided the addition of bromine was carried out in a dropwise fashion over several hours. The second component of the rigid biaryl methane unit, boronic acid **11**, was derived from the corresponding bromide **10** in excellent yields (93%). This was achieved by treatment of 4-bromobenzonitrile with *n*-butyllithium to effect a halogen - metal exchange, followed by quenching of the anion with trimethyl borate.[93] The carbanion formed during the reaction is extremely sensitive to temperature and it was found to be critical that the temperature of the reaction mixture was maintained below -95°C. If the reaction temperature rose above this level, the carbanion was found to undergo side reactions and product yield and purity suffered.

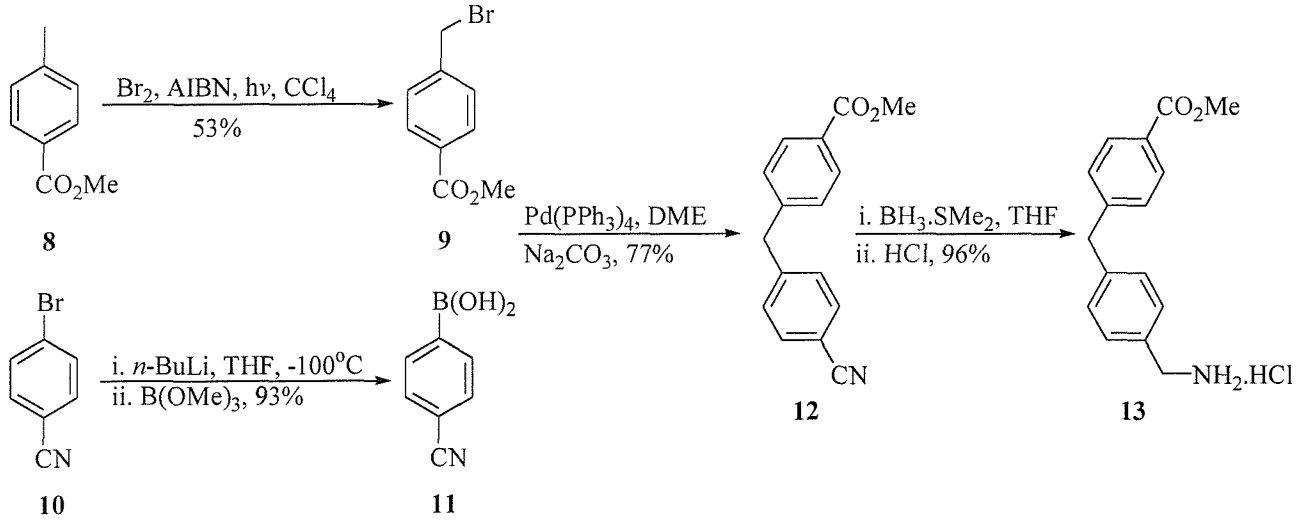

Scheme 2: Synthesis of the Aromatic Spacer Unit

The constituents of the rigid aromatic spacer were then joined using a palladium mediated Suzuki coupling reaction.[94] The desired nitrile **12** was consistently produced in very good yields

(77%) when the reaction was conducted in thoroughly degassed 1,2-dimethoxyethane and in the absence of light. The selective reduction of the nitrile functionality in the presence of the methyl ester was then carried out using borane dimethylsulfide complex.[95, 96] The free amine product rapidly degraded by reacting with itself; it was therefore necessary to isolate amine **13** as the hydrochloride salt. In this form the intermediate may be purified by recrystallisation from water and stored for several months. Again the reaction gave excellent yields of desired product (96%) completing the formation of the rigid aromatic spacer.

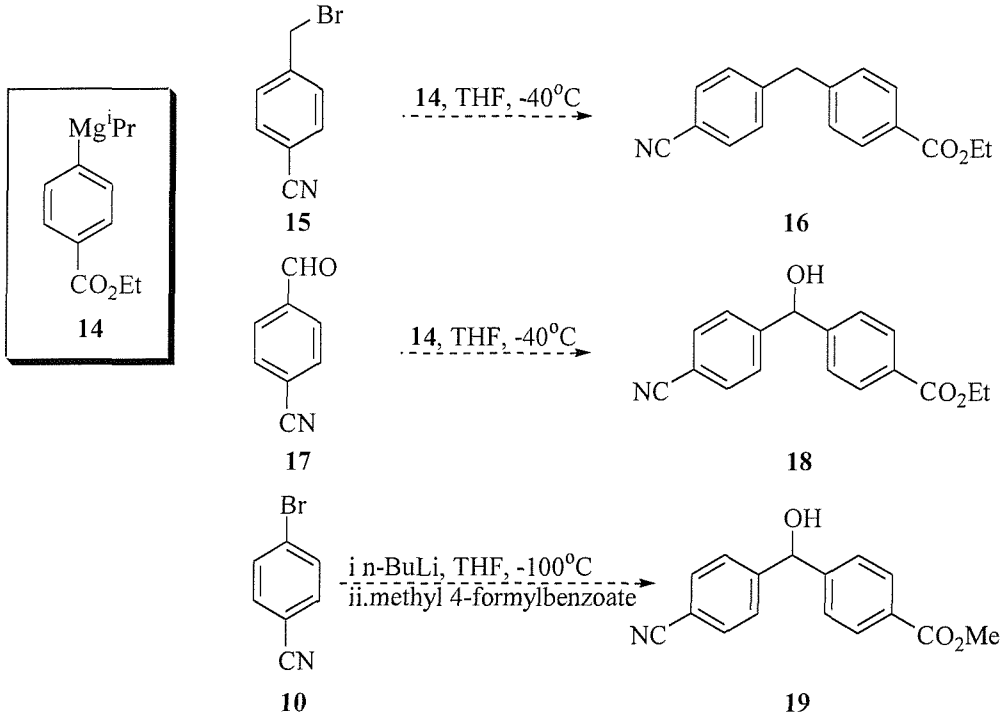

Scheme 3: Alternative Routes to the Aromatic Spacer

Alternative routes to the aromatic spacer **13** were investigated with the aim of reducing the number of steps required to reach this intermediate and therefore increasing the efficiency of the synthesis (scheme 3). The Grignard reagent of ethyl 4-iodobenzoate was generated using isopropyl magnesium chloride.[97] The reagent, **14**, was then added to 4-bromomethyl nitrile but the biarylnitrile **16** was not formed. Addition of the Grignard reagent **14** to 4-cyanobenzaldehyde, **17** was also carried out. The product of this reaction **18** would contain a hydroxyl group in the benzylic position, however it was anticipated that this would be removed during the subsequent reduction of the nitrile group to furnish the desired biaryl spacer. The

number of steps to reach the biaryl spacer **13** would therefore, be reduced to two, compared to the four required in the Pernia route. Unfortunately the desired product could not be obtained using this route. Attention then turned to producing the carbanion of 4-bromobenzonitrile, as previously carried out in the original synthesis of the aromatic spacer when forming boronic acid **11**. However, instead of quenching with trimethyl borate to give **11**, the anion was treated with methyl 4-formylbenzoate. This would lead to biaryl component **19**, containing the benzylic hydroxyl group. Despite repeated attempts we were unable to maintain the temperature below -95°C: a factor doubtless contributory to the failure of this reaction. It was concluded that these alternative routes to the aromatic spacer were not viable and therefore, we reverted to the original pathway.

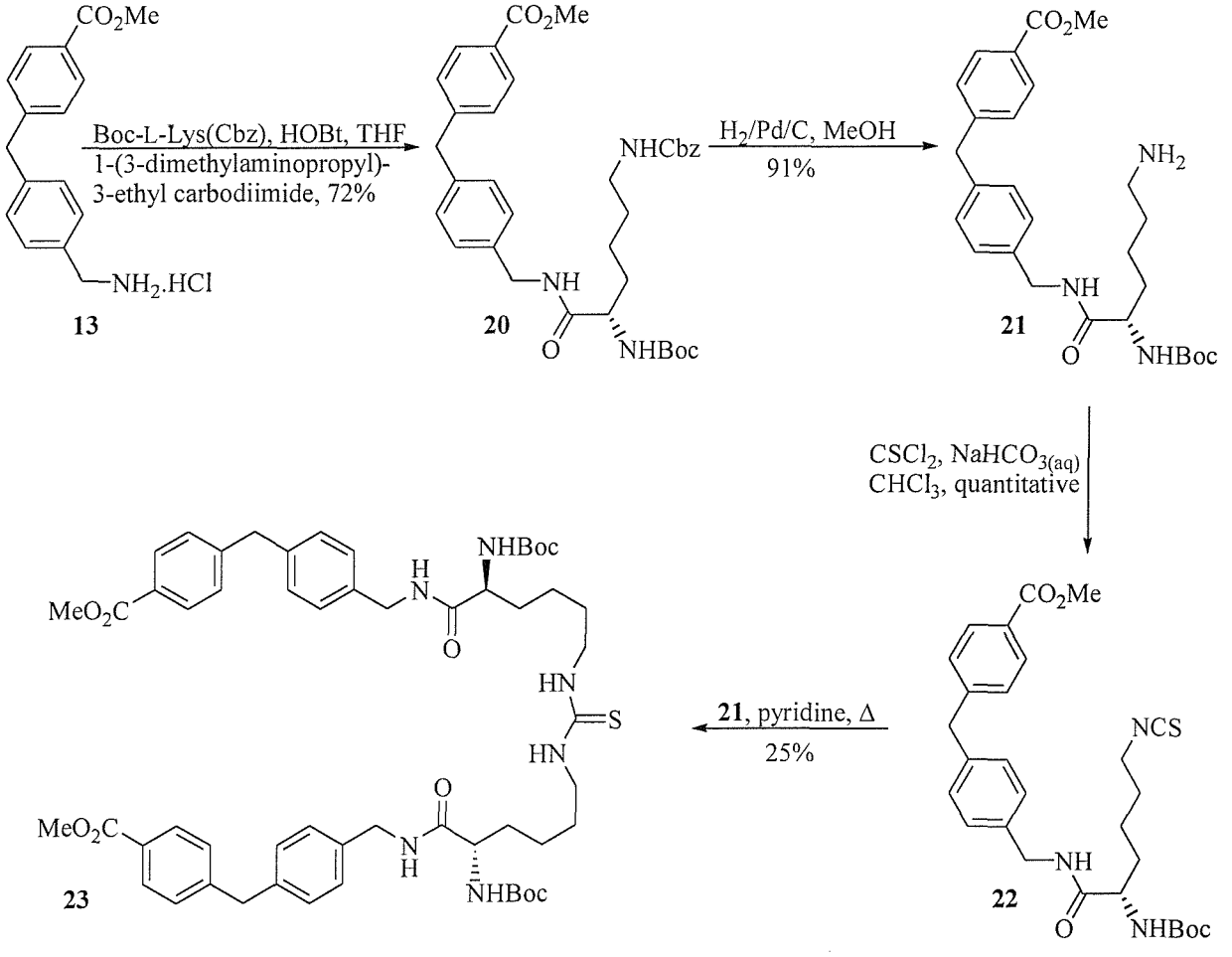

*Scheme 4: Synthesis of Macrocycle **1***

With the aromatic spacer **13** in hand, the synthesis of macrocycle **1** was continued. To this end, N_{ε}-benzyloxycarbonyl-N_{α}-*t*-butyloxycarbonyl-L-lysine was coupled to intermediate **13**, using 1-(3-dimethylaminopropyl)-3-ethyl carbodiimide hydrochloride and HOBt to provide amide **20** in good yields (72%), (scheme 4). The Cbz group of **20** was removed using gaseous hydrogen and 10% palladium on charcoal[98] to afford the free amine in excellent yields (91%). Thiophosgene was subsequently employed to effect the transformation of **21** to isothiocyanate **22** as detailed in the Pernia synthesis. Good yields (55%) were observed when the free amine was refluxed with thiophosgene in the presence of aqueous potassium carbonate,[99] however, it was found that the use of aqueous sodium bicarbonate at room temperature enabled the conversion to the desired intermediate to proceed quantitatively.

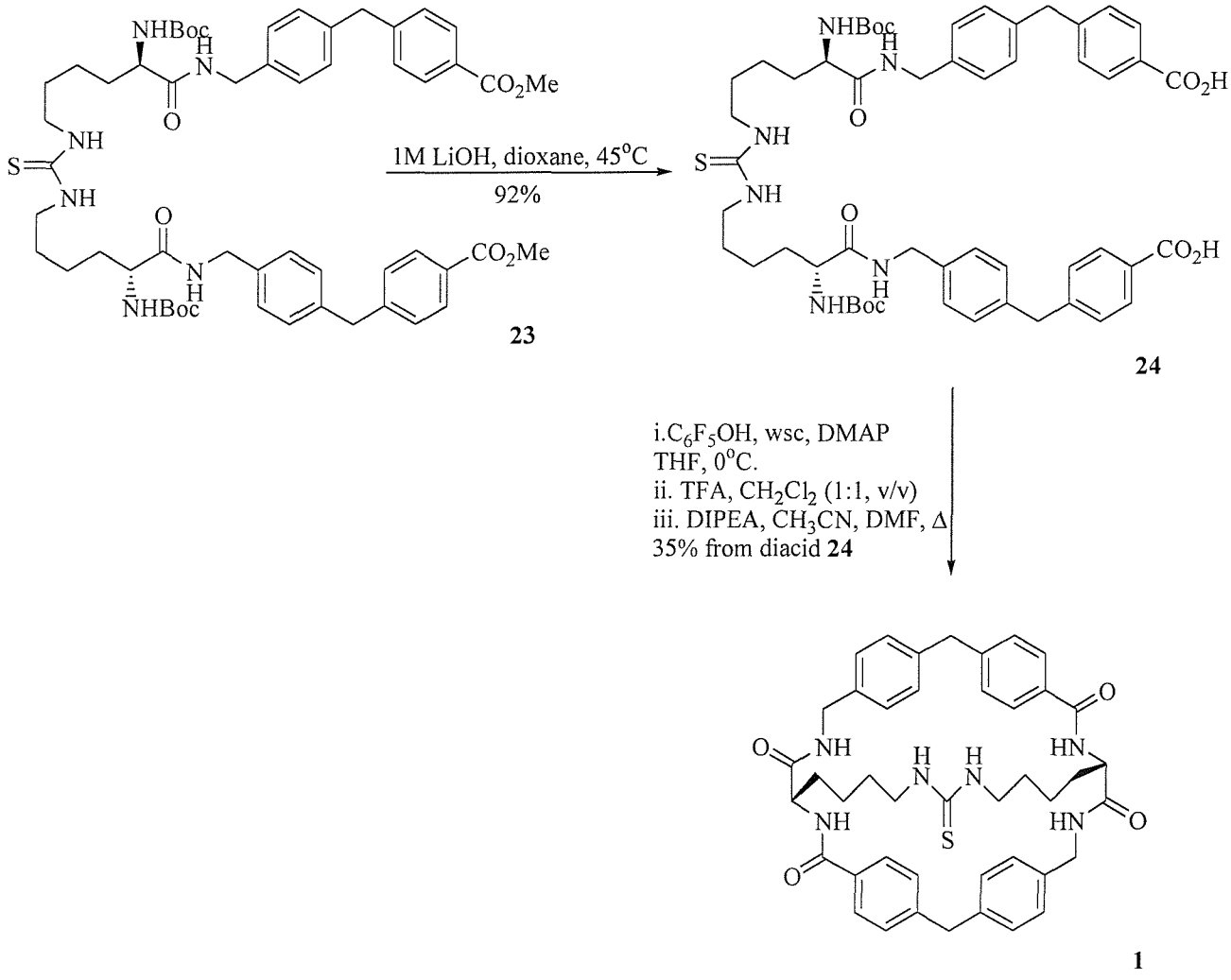

23 **24** **1**

Scheme 5: Synthesis of Macrocycle 1

The remainder of the synthesis was carried out in accordance with the Pernia route and similar yields were obtained for each transformation. Isothiocyanate **22** was combined with one equivalent of amine **21** generated in the previous step, in refluxing pyridine, to furnish the fully protected, linear macrocycle precursor **23** in fair yields (25%).

To complete the synthesis of macrocycle **1** the methyl esters of the thiourea **23** were hydrolysed using aqueous lithium hydroxide at 45°C to generate the corresponding diacid **24** in excellent yields (92%), (scheme 5). Diacid **24** was subsequently activated using pentafluorophenol under standard coupling conditions.[100] The Boc groups were then removed using trifluoroacetic acid to provide the ditrifluoroacetic acid salt[101] and cyclisation was effected using diisopropylethyl amine in refluxing acetonitrile under conditions of high dilution. The final three steps were carried out without purification of the intermediates due to their sensitivity to flash column chromatography; the transformation to macrocycle **1** was achieved in yields of around 35% from the diacid **24**.

In conclusion, macrocycle **1** was synthesised on numerous occasions to afford several hundred milligram quantities of **1** which was a sufficient quantity to allow studies with the intramolecular Diels-Alder precursors to proceed, as outlined in the following chapter.

Chapter Three

Synthesis and Cyclisation of the IMDA Precursors

3.1 Introduction

With macrocycle **1** in hand our attention then turned to producing the Diels-Alder precursors – the guest component of our host-guest system. Initially we planned to produce a range of guest molecules based on a generalised structure **3** (fig. 54) They would have differing substituents on the diene and dienophile portion of the molecule and variations in the length of the chain tethering the functional moieties together. In reality three specific substrates, precursors **25**, **26**, **27**, were targeted.

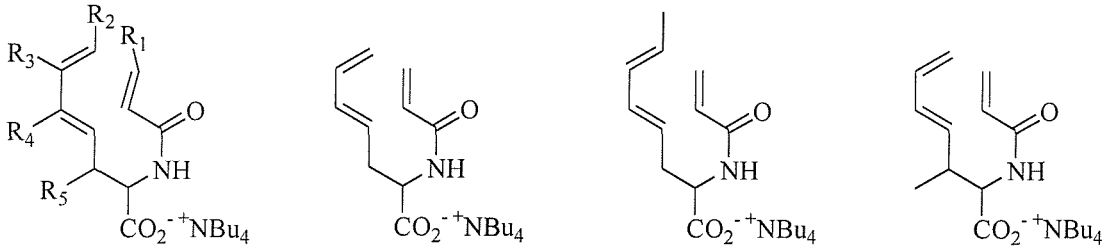

3 **25** **26** **27**

Fig. 54: The IMDA Substrate Structures Targetted

3.2 Synthesis of the Diels-Alder Precursors

Attempts to produce dienylacrylamide **25** began with the use of allyl glycine **30** as a starting point to access aldehyde **33**, previously employed by Baldwin[102] in the production of similar dienylacrylamides. The synthetic strategy, based on Baldwin's synthesis, relied on two successive Wittig reactions to furnish the desired diene in the required *trans* geometry. This work was undertaken in collaboration with the Universiteit van Amsterdam and DSM research who have developed the synthesis of enantiomerically pure, unnatural amino acids by employing an aminopeptidase[103] to resolve amino amides. The protocol for the synthesis of allyl glycine was well established within this group and enabled access to the unnatural amino acid in enantiomerically pure form.

Racemic allyl glycine **30** was readily prepared in two steps from commercially available diethyl acetamidomalonate **28** (scheme 6). Alkylation of **28** with allyl bromide furnished the malonate derivative **29** in good yields (60%). Conversion of **29** to allyl glycine **30** occurred quantitatively on exposure of **29** to a refluxing solution of 2M hydrochloric acid. Treatment of allyl glycine with two equivalents of thionyl chloride in refluxing methanol gave methyl ester **31** in quantitative yield, which was then reacted with di-*tert*-butyl dicarbonate and sodium hydrogen carbonate in dioxane and water to produce the protected allyl glycine derivative **32** in excellent yields (81%).

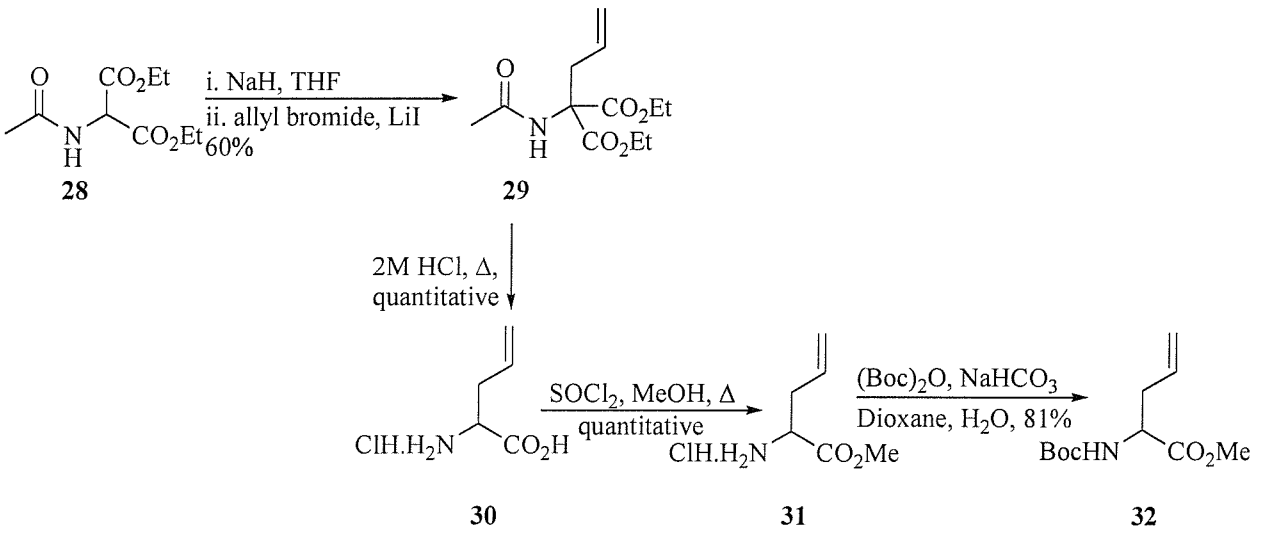

Scheme 6: Synthesis of Allyl Glycine

With the amine and acid moieties protected attention was then turned to functionalising the side chain of allyl glycine. Ozonolysis of derivative **32** effected the formation of aldehyde **33** in excellent yields (85%). The production of amino acid **38** was initially attempted using stabilised phosphorane **34** to install the first alkene as the *trans* isomer, followed by a further Wittig reaction with methylene phosphorane **36** to generate the second olefin without disrupting the existing stereochemical integrity (scheme 7). Phosphorane **34** is commercially available but expensive so its synthesis was attempted from triphenyl phosphine and chloroacetaldehyde following published procedures.[104, 105] Anhydrous conditions are critical for the successful formation of phosphorane **34**. A solution of choloroacetaldehyde-water azeotrope in chloroform was distilled to produce a water free solution, however, refluxing this solution for five hours with triphenyl phosphine failed to produce the desired product. Further attempts to synthesise phosphorane **34** included passing the choloroform-

chloroacetaldehyde solution through a silica column to remove the water. Despite our efforts none of the required phosphorane could be isolated. The Wittig reaction was eventually attempted with commercial phosphorane **34**: crude aldehyde **33** was initially treated with three equivalents of phosphorane **34** in dichloromethane, however the desired product was not formed. Similar treatment with purified aldehyde **33** also failed to yield intermediate **35** and consequently this approach was abandoned.

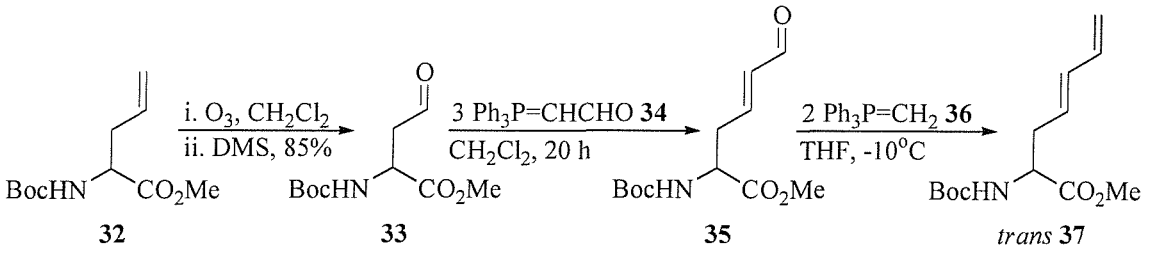

Scheme 7: The Double Wittig Route to the Diene

Allyl dienetriphenyl phosphorane **38**, an unstabilised ylid was then considered as a means of forming the diene in one step as a mixture of the *cis* and *trans* isomers. It was anticipated that the mixture could be isomerised to the desired *trans* geometry using either iodine or mercaptan[106] (scheme 8). Allyl dienetriphenyl phosphonium bromide was obtained in excellent yields (97%) by refluxing triphenyl phosphine in allyl bromide. Methyl lithium was initially employed to generate the ylid to which aldehyde **33** was added The resulting products were a mixture of many by-products and the desired diene could not be obtained. Further attempts were made to obtain dieneamino ester **37** using phosphorane **38** by generating the corresponding ylid using *n*-butyllithium. Again, many by-products were produced and the required product could not be isolated.

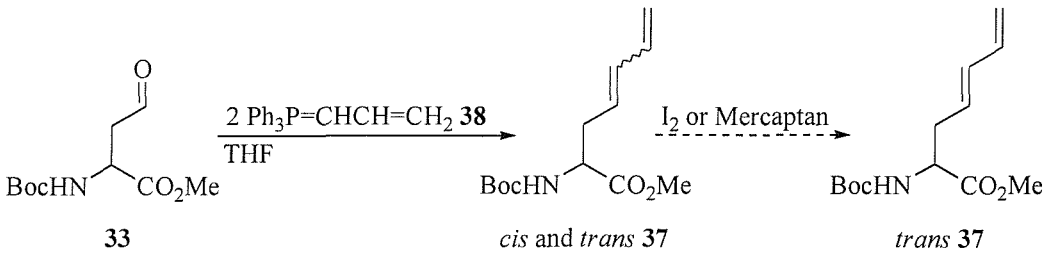

Scheme 8: The Single Wittig Route to the Diene

The failure of the Wittig reactions was attributed to the basic nature of the phosphonium ylids, which may remove a proton adjacent to the carbonyl functionality of aldehyde **33** leading to the occurrence of a multitude of side reactions. At this stage an alternative approach was sought.

The synthetic route next employed was based on Schöllkopf's method for the synthesis of amino esters.[107, 108] In this strategy the non-proteinogenic side chain of the amino ester being synthesised is introduced as an appropriate electrophile in the alkylation of ethylated glycine anhydride **47**. (2*E*, 4*E*)-1-bromo-2,4-hexadiene **42** is not commercially available; the synthesis of *trans*-2,4-pentadienoic acid **39** from malonic acid and acrolein was thus attempted with the notion of reducing the acid to the corresponding alcohol which could then be converted to bromide **42** (scheme 9). The Knoevenagel reaction with malonic acid and acrolein[109] was carried out in pyridine at 70°C. However, the product acid **39** appeared to be particularly susceptible to polymerisation and repeated synthesis failed to elevate the yield above 14%. *Trans*-2,4-pentadienoic acid **39** was converted to the corresponding methyl ester **40** in good yields (48%) by treatment with methanol and concentrated sulfuric acid.[110] The crude methyl ester was reacted directly with lithium aluminium hydride due to concerns regarding its stability. Unfortunately, the reaction failed to give the desired alcohol and direct reduction of the acid **39** to alcohol **41** also failed. Thus, the pursuit of bromide **42** was abandoned at this point and the synthesis of an alternative IMDA substrate commenced.

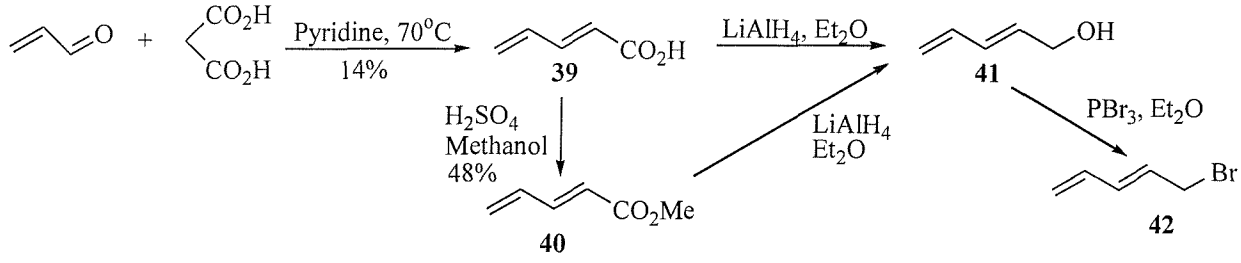

Scheme 9: The Synthesis of (2E,4E)-1-Bromo-2,4-Hexadiene

The substrate chosen featured a methyl group on the terminus of the diene, substrate **26** (fig. 54). It was anticipated that the additional steric hindrance would make the bromide and subsequent intermediates less susceptible to polymerisation and therefore easier to synthesise. It should be noted that the Diels-Alder cyclisation also had the potential to be effected by the methyl group.

Trans, *trans*-2,4-hexadien-1-ol **43** is commercially available. Conversion to the corresponding bromide **44** was initially attempted using phosphorous tribromide in dry diethyl ether according to the methods employed by Mori.[111] However, acquiring the pure product proved to be difficult. Purification by flash column chromatography was unsuccessful leading to polymerisation of the product. Distillation of the crude material in both a classical and Kugelrohr apparatus was also employed but, in both cases, although some of the desired bromide was obtained, the majority of the crude material polymerised. Carbon tetrabromide with triphenyl phosphine in dichloromethane[112] was also used as a potential means to gain the bromide. However, it was found that either the product decomposed in the reaction mixture or it was impossible to isolate the bromide from the contaminants.

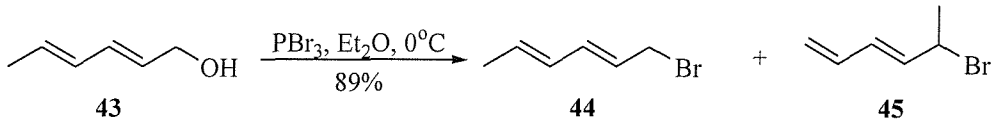

43 **44** **45**

*Scheme 10: Synthesis of Bromide **44***

An alternative bromination using *N*-bromosuccinamide and anhydrous dimethyl sulfide in dichloromethane according to the methods of Meyers[113] was attempted, but the crude reaction mixture proved to contain mainly the starting alcohol along with numerous by-products. Attempts were made to tosylate *trans,trans*-2,4-hexadiene-1-ol but this approach was unsuccessful. Bromide **44** was eventually obtained by reverting to the use of phosphorous tribromide in diethyl ether[114] but altering the procedure to that of Jacobsen so that the aqueous work up was omitted and instead the reaction mixture was distilled directly (scheme 10).

The bromide was found to be more stable using this method and was obtained in an apparent yield of 89%. It should be noted that the product contained contaminants, one of which was bromide **45**, a fact which is reflected in the poor yields obtained from the subsequent alkylation step (scheme 11).

Commercially available Meerwein salt was used to alkylate the carbonyl oxygen of glycine anhydride **46** to form the ethylated intermediate **47**:[115] excellent yields (86%) were routinely

obtained provided four equivalents of reagent were added as two separate portions, the second after twelve hours. The reaction was always found to proceed cleanly and purification of this product was unnecessary. The ethylated glycine anhydride **47** was then alkylated using *n*-butyllithium and bromide **44**. The reaction produced many side products and the desired monoalkylated product **48** was isolated in disappointing yields (15%). Compound **49**, the product of ring alkylation with one of the contaminants of bromide **44**, was also isolated in 10% yield. Although unexpected, this by-product gave us access to a second IMDA precursor, **27**.

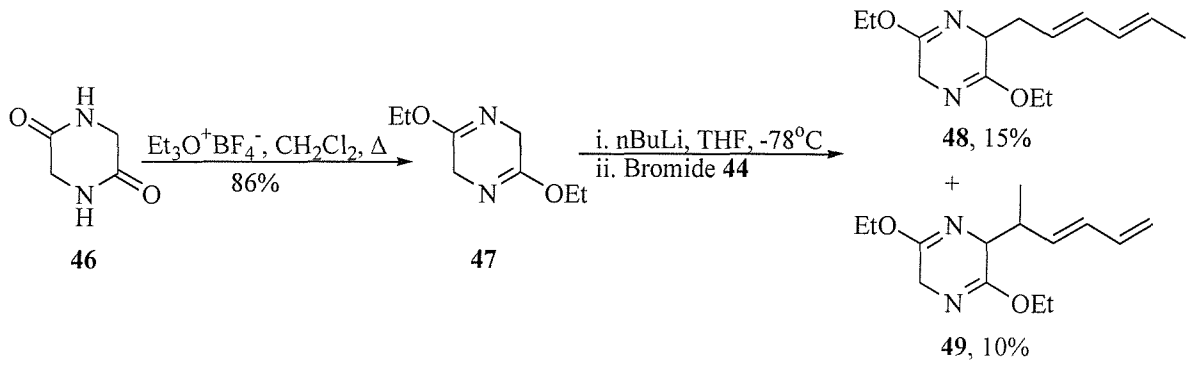

46 47

*Scheme 11: Synthesis Towards IMDA Precursor **26***

The next step in the pathway was to cleave the heterocycle **48** to liberate the new amino ester **50** (scheme 12). Hydrolysis of **48** with 15% hydrochloric acid in dioxane at room temperature afforded the ethyl ester **50** quantitatively. The dieneophile portion of the IMDA precursor was then added using acryloyl chloride in the presence of triethylamine in dichloromethane at -78°C. Following purification by flash column chromatography the desired ethyl ester **51** was obtained in 72%. The ester was hydrolysed in excellent yields (95%) using 1M aqueous lithium hydroxide solution in dioxane, however, concerns about the stability of the acid prompted us to react it immediately to produce the corresponding tetrabutylammonium salt **26**.

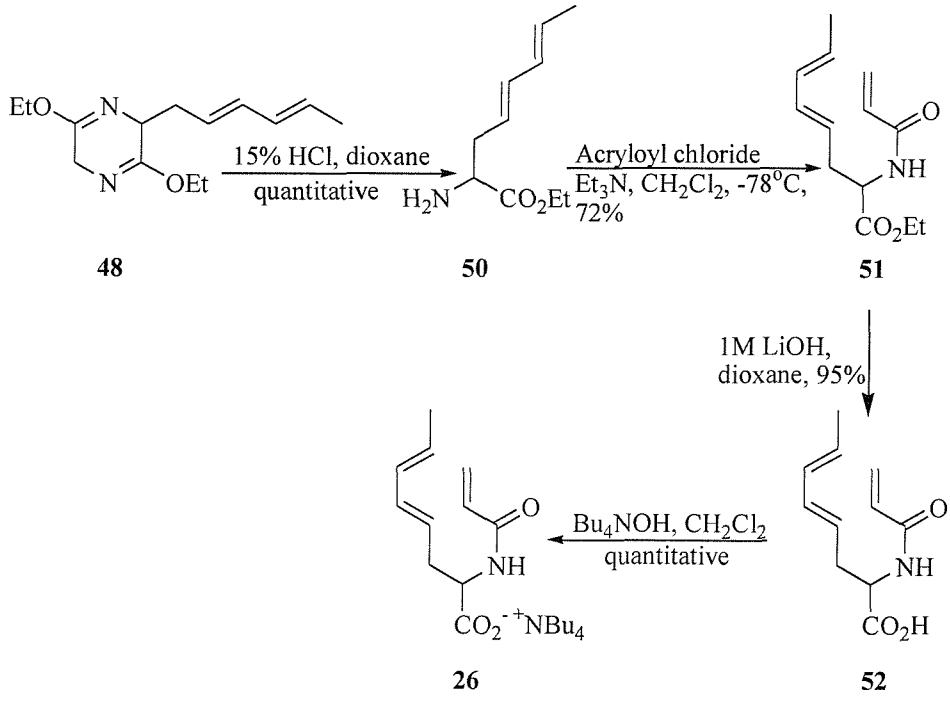

Scheme 12: Synthesis of IMDA Precursor ***26***

The conversion of intermediate **49** to the IMDA precursor **27** was carried out in an identical manner: hydrolysis of the heterocycle **49** with 15% hydrochloric acid to amino ester **53** occurred quantitatively. The amino ester was then exposed to acryloyl chloride and triethylamine as described above to afford precursor **54** in satisfactory yields (40%). Treatment of **54** with 1M lithium hydroxide solution followed by tetra *n*-butylammonium hydroxide furnished the racemic IMDA substrate **27** as the tetrabutylammonium salt.

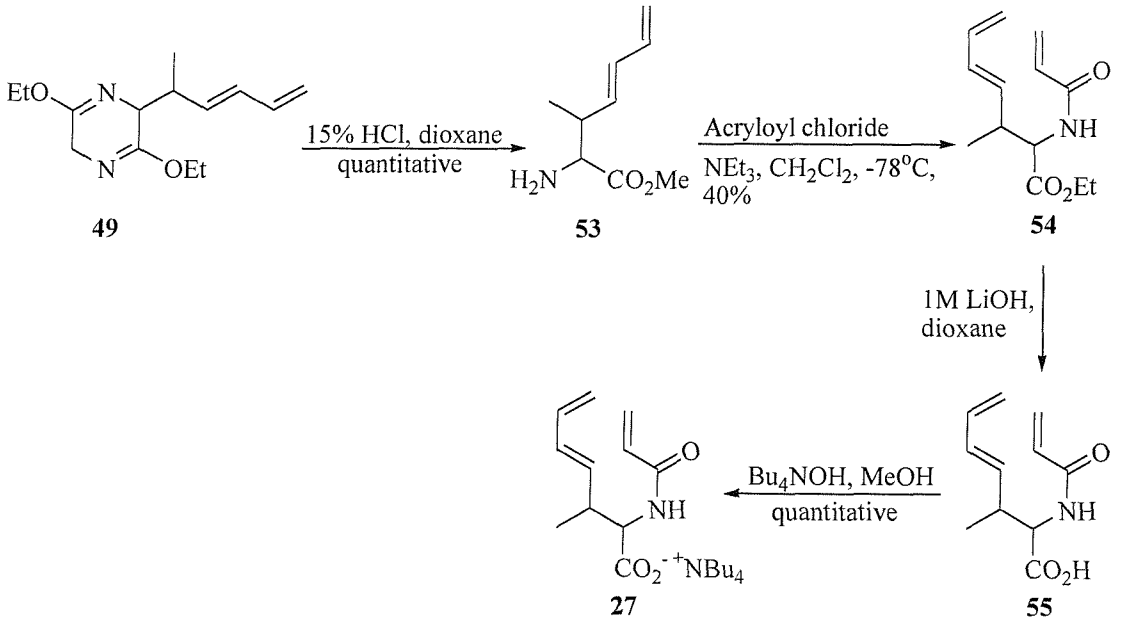

Scheme 13: The Synthesis of IMDA Precursor 27

Portions of the IMDA precursors in the form of the ethyl esters **51** and **54** were submitted for enantiomeric separation on a chiral column at AstraZeneca. However, intermediate **54** polymerised before the separation could be carried out. The enantiomers of **51** were obtained and treated in the same way as their racemic counterparts to produce the enantiomeric tetrabutylammonium salts of **26** (scheme 14).

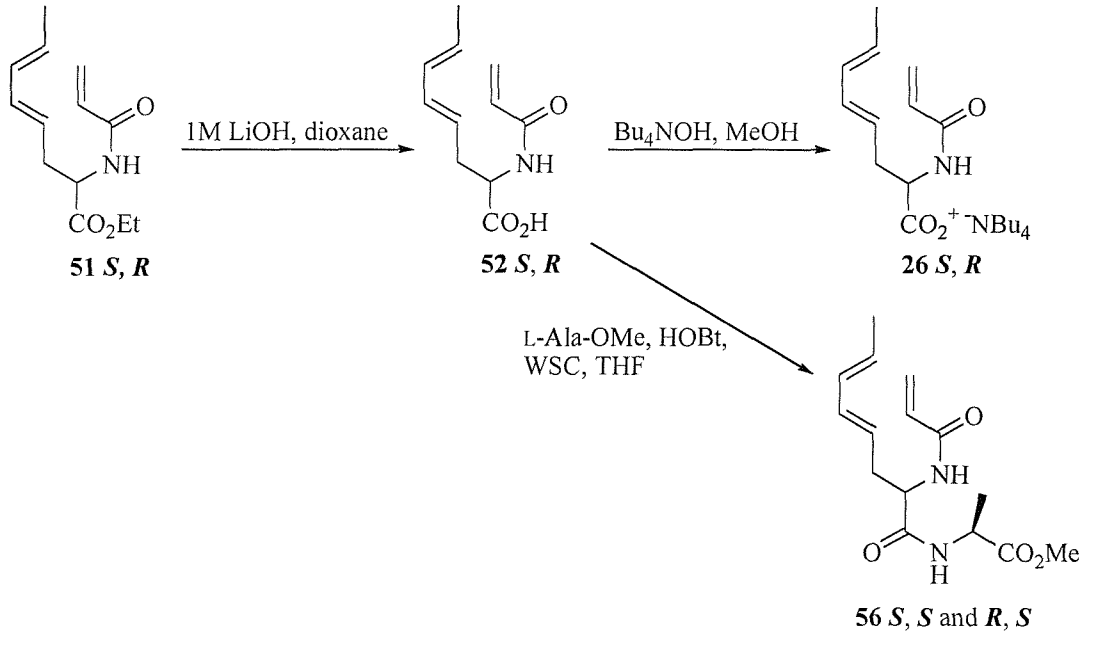

Scheme 14: Synthesis of the Enantiomeric Salts

It should be noted that the IMDA substrates do degrade over time; the acids obtained from the hydrolysis were not pure. The acids themselves were also known to be unstable and were therefore, carried directly through to the tetrabutylammonium salts. Although clearly impure the relevant peaks could be identified to see if any changes occurred. The degree of racemisation sustained during the hydrolysis step was assessed by coupling 10 mg of the enantiomeric acids **52** with L-alanine-OMe to produce dipeptide **56** the same reaction was also carried out with the racemate. The ^{13}C NMR spectra of the products were then compared (fig.55).

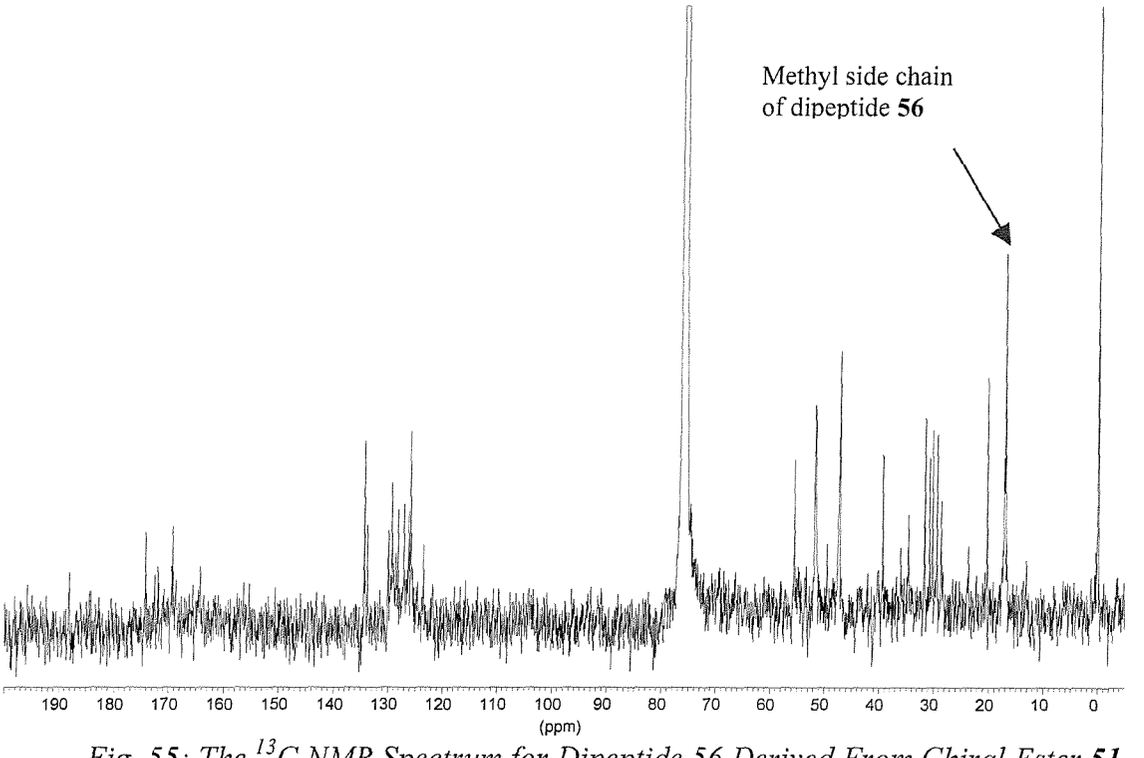

*Fig. 55: The ^{13}C NMR Spectrum for Dipeptide 56 Derived From Chiral Ester **51***

The spectrum of the coupled product **56** derived from the chiral acid revealed some degree of racemisation had taken place; the relative heights of the peaks corresponding to the methyl side chain of alanine are in a ratio of 2.4:1, in the racemic sample the relative heights of the methyl side chain occur in a ratio of 1.3:1. Although the chiral acid **26** has not remained as a single isomer it has not completely racemised either and can be considered to be enantiomerically enriched. Similar results were assumed for the other isomer.

3.3 Cyclisation of the IMDA Substrates

3.3.1 Thermal Cyclisations

In order to draw meaningful conclusions regarding the effect macrocycle **1** has on the Diels-Alder cyclisations of the substrates, thermal cyclisations of the racemic compound **51** was carried out.

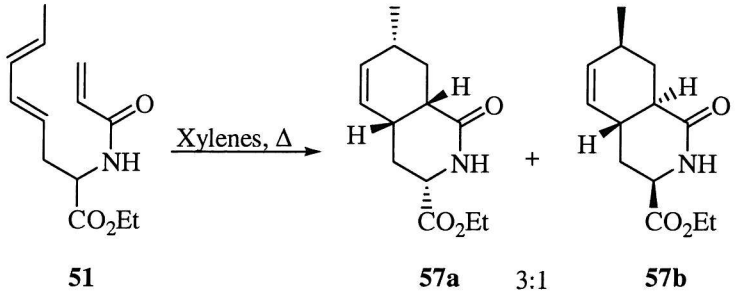

51 **57a** **57b**

Scheme 15: The Thermal Cyclisation of the IMDA Precursors

Ester **51** was refluxed in xylenes in the presence of a trace of hydroquinone for eight hours. The products from the cyclisation were a mixture of the *cis* and *trans* fused rings, these were easily separated using flash column chromatography and their stereochemistries determined by a careful consultation of the ^{1}H NMR spectra and infra red spectra. The major product from the thermal Diels-Alder cyclisations was the *cis* fused ring product (fig. 56).

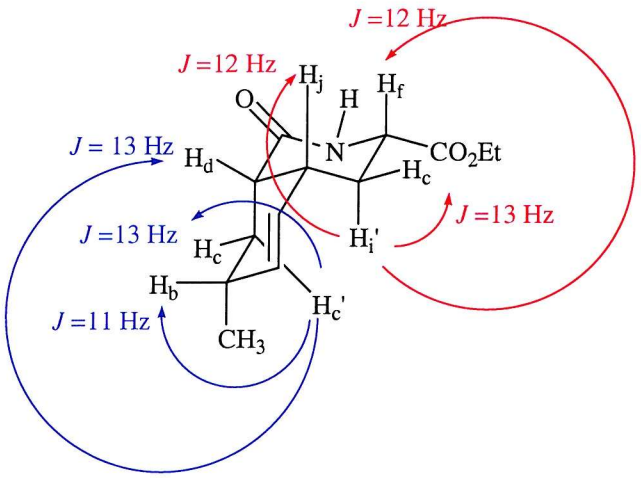

Fig. 56: Stucture Elucidation ***57a*** *by examination of coupling constants*

The ^{1}H NMR spectrum for **57a** shows the signal for H_i' to be a ddd with coupling constants of 13, 12 and 12 Hz. This is consistent with a geminal coupling and two axial-axial couplings placing H_i' and both the α-proton H_f and the proton sited at the ring junction H_j, in the axial positions. The signal for the α-proton H_f, is clearly a dd exhibiting coupling constants of 12 and 4 Hz which corroborate its assignment to the axial position. Unfortunately the signal for H_j is unresolved. H_c' shows a signal in the pattern of a ddd, the coupling constants of which are 13, 13 and 11 Hz; from these it is clear that H_c' is in the axial position and experiences a geminal coupling and two axial-axial couplings. The proton at the ring junction H_d is therefore, in the axial position and on the same side as H_j. The second axial-axial coupling of H_c' is to H_b, the proton adjacent to the methyl group, thus the methyl group is in the equatorial position.

The minor cyclisation product was the *trans* fused adduct (fig. 57). The ^{1}H NMR spectrum of **57b** exhibits a ddd at 1.84 ppm with coupling constants of 13, 13 and 6 Hz. This corresponds to H_i', an axial proton which is experiencing a geminal coupling and an axial-axial coupling. The value of the last coupling constant corresponds to the coupling constant arising from the dt at 4.15 ppm associate with the α-proton H_f. Assigning the orientation of this proton is difficult, intuitively we expect the ethyl ester to lie in the equatorial position, however, the value of the coupling constant is lower than usually observed for an axial-axial interaction. Electron withdrawing groups such as the ethyl ester and the amide nitrogen can have the effect of lowering coupling constants, but it should be noted that although this may account for the observations no such lowering in coupling constant was found in the ^{1}H NMR spectrum of **57a**. The signal for H_i' indicates that proton H_j at the ring junction is orientated in the axial position. The signal arising from the second proton at the ring junction H_d, a ddd at 2.00 ppm with coupling constants of 12, 12 and 2 Hz, indicates that this proton is involved with two axial-axial interactions and one axial-equatorial interaction. From this we can conclude that H_d is located in an axial position and involved in an axial-axial interaction with H_j – the two rings are, therefore, *trans* fused. Further evidence for this conformation is provided by the signal at 1.63 ppm, arising from H_c', the splitting pattern is a ddd with coupling constants of 13, 13 and 6 Hz. These values correspond to a geminal coupling an axial-axial coupling and an axial-equatorial coupling. This signal establishes not only the axial orientation of H_d but shows the orientation of H_b to be equatorial placing the methyl

group in the axial position. The stereochemistry of the diene is such that H_j and H_b are forced to be *cis* to one another in the product.

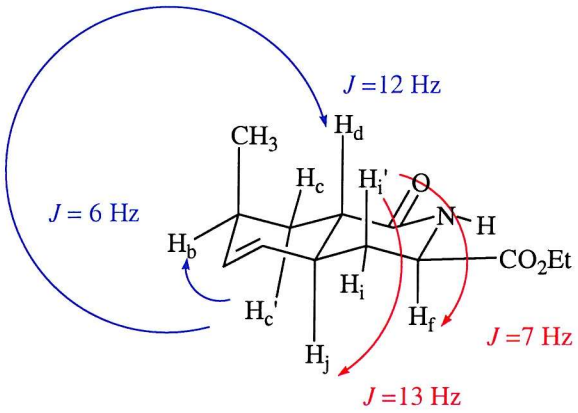

*Fig. 57: Elucidation of the Stereochemistry of **57b** by examination of coupling constants*

Supporting evidence for these assignments of **57a** and **57b** was obtained from the IR spectum; *trans* fused lactams are more strained and rigid than their *cis* fused counterparts, a phenomenon that manifests itself as a lactam stretch that is 5-10 cm^{-1} higher in the case of the *trans* fused lactam. In the cyclised products obtained the frequencies observed were 1657.4 and 1663.0 cm^{-1} for **57a** and **b** respectively.

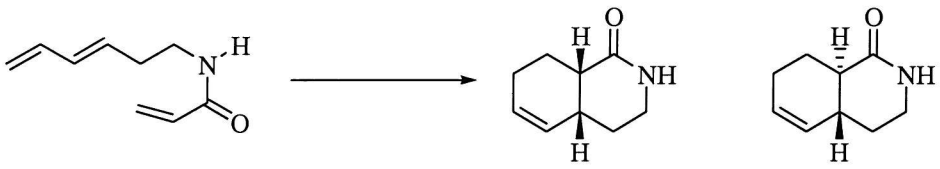

58 7:1

*Scheme 16: The Cyclisation of Triene **58***

The *cis* and *trans* fused rings were isolated in a ratio of 3:1, this is consistent with work carried out by Martin *et al*[91] during the synthesis of hydroisoquinolines (scheme 16). Triene **58** was found to cyclise to give the *cis* and *trans* adducts in the ratio of 7:1. The stereoselectivity is observed because in substrates with four atoms between the diene and the dieneophile portion of the molecule, a strain free syn transition state with a coplanar acrylyl-amide system can be achieved enabling secondary orbital overlap of the carbonyl with the diene (fig. 58).

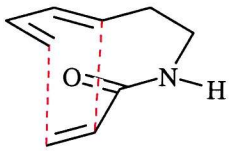

Fig. 58: The Syn Transition State for Martin's Triene

Similarly, triene **51** could adopt a strain free transition state during cyclisation leading to a preference for one product over the other. The purpose of carrying out the thermal cyclisation of **51** was to provide products which would act as standards against which any reactions occurring in the presence of macrocycle **1** could be compared. The cyclised esters were therefore, duly converted to the corresponding acids using 1M aqueous lithium hydroxide solution in dioxane.

3.3.2 Cyclisations of the IMDA Substrates in the Presence of Macrocycle 1

The IMDA precursors, racemate **27**; racemate **26** and both enantiomers of **26** were incubated with macrocycle **1** to investigate its effect on the rate of the intramolecular Diels-Alder cyclisations. The experiments were carried out in an identical manner: stoichiometric quantities of macrocycle **1** and the IMDA precursor were dissolved in deuterochloroform at room temperature and monitored daily by ^{1}H NMR. Alongside this a control experiment was run. The IMDA substrates were dissolved in deuterochloroform and also monitored by ^{1}H NMR to ensure that any cyclisation occurring was a true effect of macrocycle **1** and not due to a background rate or due to catalysis by any residual acidity in the deuterochloroform. Addition of the IMDA substrates led to some changes in the spectrum of macrocycle **1**. Firstly the spectra taken were all badly resolved. Previous work carried out by G. Pernia[90] established that the substrates can be bound in several ways and this may account for the poor resolution seen. Secondly, the NH protons of the thiourea were seen to shift downfield by approximately 2 ppm and slight alterations in the aromatic region of the spectrum were observed. This is indicative of binding of the guest to the thiourea protons.

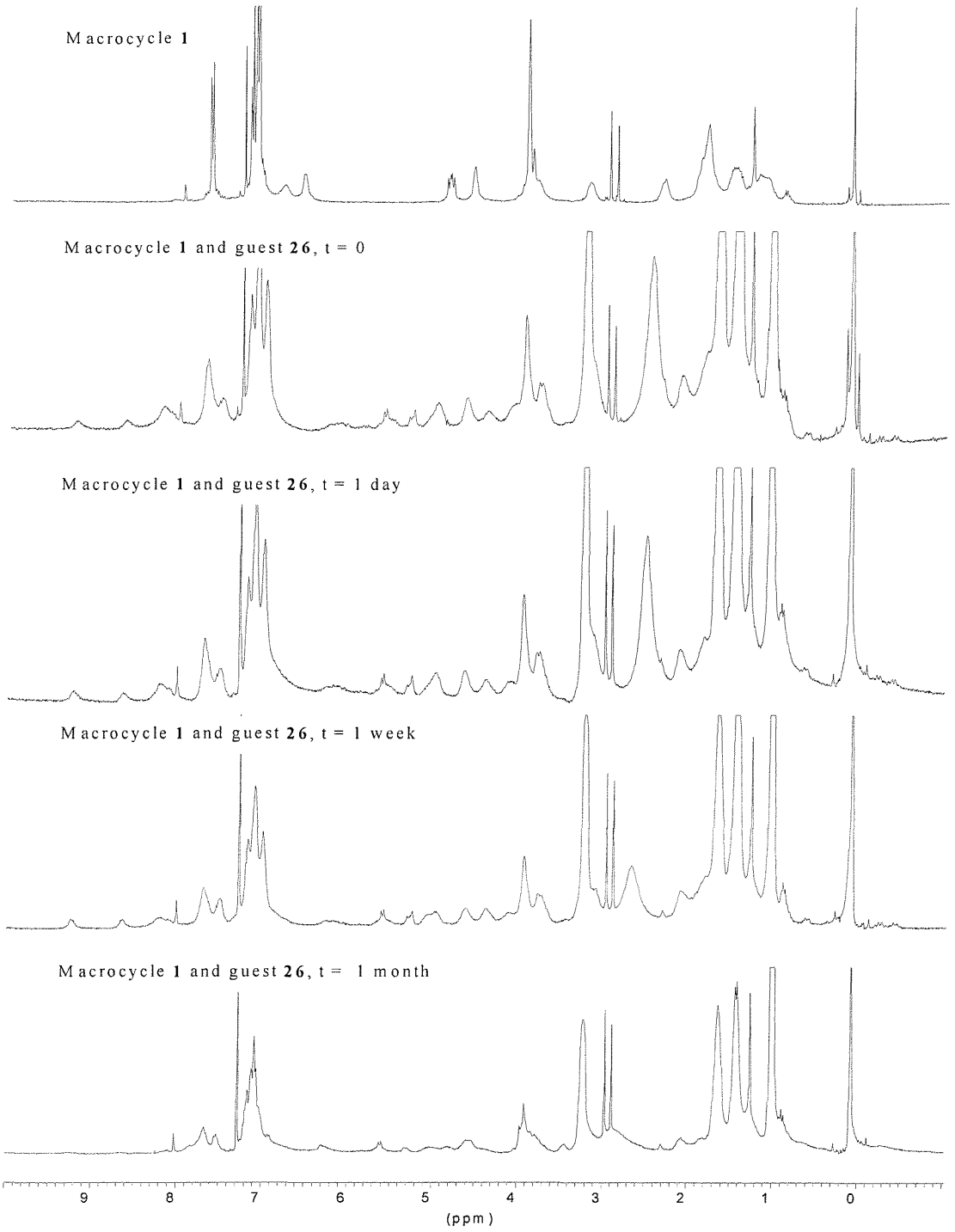

*Fig. 59: ^{1}H NMR spectra of enantiomeric **26** with Macrocycle **1** over time.*

The samples were monitored by ^{1}H NMR however, no significant changes in the spectra were observed for any of the experiments over the period of one week (fig. 59). After one month, a general degradation of the spectrum was observed in each sample and from these there was no conclusive evidence that any changes had taken place.

For substrate **26** futher experiments were carried out with the enantiomers to probe the nature of the complexes formed with macrocycle **1**. Aliquots of each enantiomer of guest **26** were added to macrocycle **1** dissolved in deuterochloroform and the ^{1}H NMR spectrum aquired. The thiourea protons of macrocycle **1** were seen to move sharply downfield by approximately 2 ppm and small changes in the relative positions of the aromatic protons were observed for each enantiomer. These findings are consistent with a carboxylate-thiourea interaction taking place between the host and guest. The reverse experiment was also carried out in order to determine if the mode of binding of the two enantiomers was different. Addition of aliquots of host to the diene enantiomers dissolved in deuteriochloroform did not lead to any discernable changes in the ^{1}H NMR signals attributable to the diene.

Previous binding results obtained by G. Pernia[69] have shown that substrates binding inside the cavity of macrocycle **1** experience a significant shift in the aliphatic proton signals relative to the uncomplexed guests. Whereas substrates bound externally undergo no such perturbation in the chemical shifts of their aliphatic proton resonances, this was exemplified with the enantiomers of *N*-Ac phenylalanine and *N*-Ac-alanine (see chapter one, section 1.5 for a detailed discussion). The lack of change in the chemical shift on addition of aliquots of macrocycle **1** to a solution of our diene guests in deuterochloroform is therefore highly indicative that the guests were not binding inside the cavity but were instead binding to the external face *via* a thiourea-carboxylate interaction as observed in the binding of N-acetyl D-phenylalanine and N-acetyl L-alanine.[69, 90] The absence of any increase in rate of the intramolecular Diels-Alder cyclisation for either substrate is attributable to this binding mode. The substrates are not bound within the cavity and so not constrained to a conformation with a *cis* geometry around the amide bond, hence the rate of cyclisation is unaffected. The synthesis and investigation of alternative guests was not pursued any further.

Chapter Four

The Properties of Modified Macrocycles

4.1 Introduction

Macrocycle **1** was found to bind to a range of *N*-acetyl amino acids and displayed the unusual property of binding *N*-acetyl L-amino acid carboxylate salts, in particular alanine and phenyl alanine, with the acetyl amide in the *cis* configuration. One of the key features of macrocycle **1** was the biarylmethylene unit which functions as a rigid spacer to provide a well defined, open rim to the bowl shaped cavity. Interest in increasing the selectivity of this macrocycle led to the production of two modified macrocycles based on the structure of macrocycle **1**[116] but with one or both of the biaryl methanes replaced with a pyridyl aryl ether.

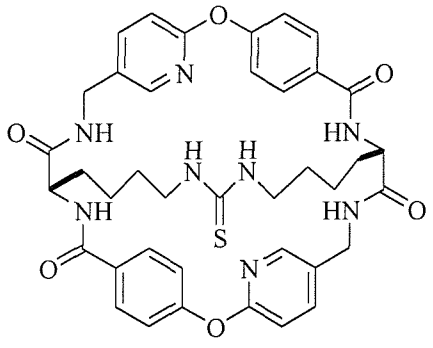

59

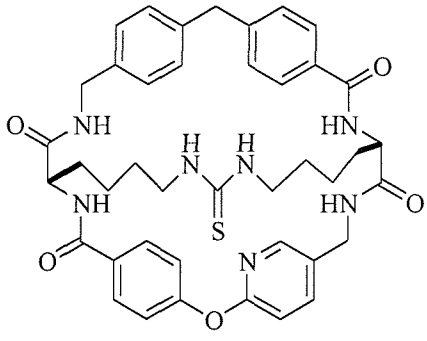

60

Fig. 60: The Two Modified Macrocycles

Receptors **59** and **60** (fig. 60) incorporate additional hydrogen bonding functionality without dramatically altering the gross structure of the receptor design. The synthesis of the new receptors was carried out in collaboration with V. Jullian. Receptors **59** and **60** were produced broadly following the strategy employed to produce macrocycle **1** (chapter two). Thus the cyclisation precursors were designed to undergo a double macrocyclisation and prepared by coupling the modified biaryl portion to a suitably protected lysine derivative which was also used to form the thiourea on the ε-amino group of the lysine.

4.2 Synthesis of Macrocycles 59 and 60

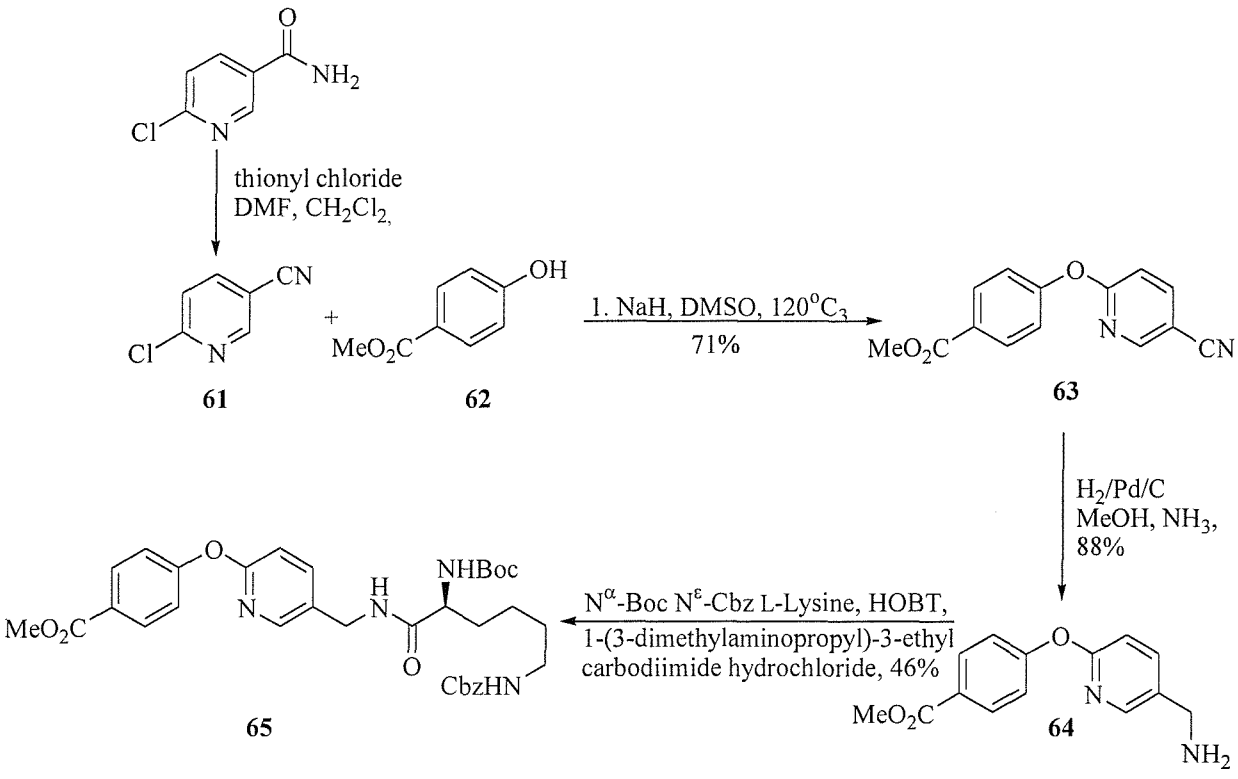

Scheme 17: The Synthesis of the Modified Aromatic Spacer

The synthesis of the aromatic spacer commenced with the production of one of the components of the biaryl unit (scheme 17). 6-Chloronicotinamide was quantitatively converted to 6-chloronicotinonitrile **61**, by treatment with thionyl chloride in dimethylformamide and dicholoromethane at 0°C. Nitrile **61** was then joined with methyl 4-hydroxybenzoate, the second constituent of the aromatic spacer using sodium hydride and dimethyl sulfoxide at 120°C, to provide the biaryl unit **63** in very good yields (71%). Reduction of the nitrile functionality in the presence of methyl ester was best achieved using gaseous hydrogen and 10% palladium on activated charcoal in methanol saturated with ammonia, to furnish the desired free amine in excellent yields (88%). Amine **64** was found to be stable provided it was stored in a freezer, this is in contrast to the analogous amine **13** in the macrocycle **1** pathway which rapidly degraded and had to be isolated in the form of the hydrochloride salt. The free amine was then coupled to N_{ε}-benzyloxycarbonyl-N_{α}-t-butyloxycarbonyl-L-lysine using TBTU and diisopropylethyl amine in dichloromethane to afford amide **65** in reasonable yields (46%).

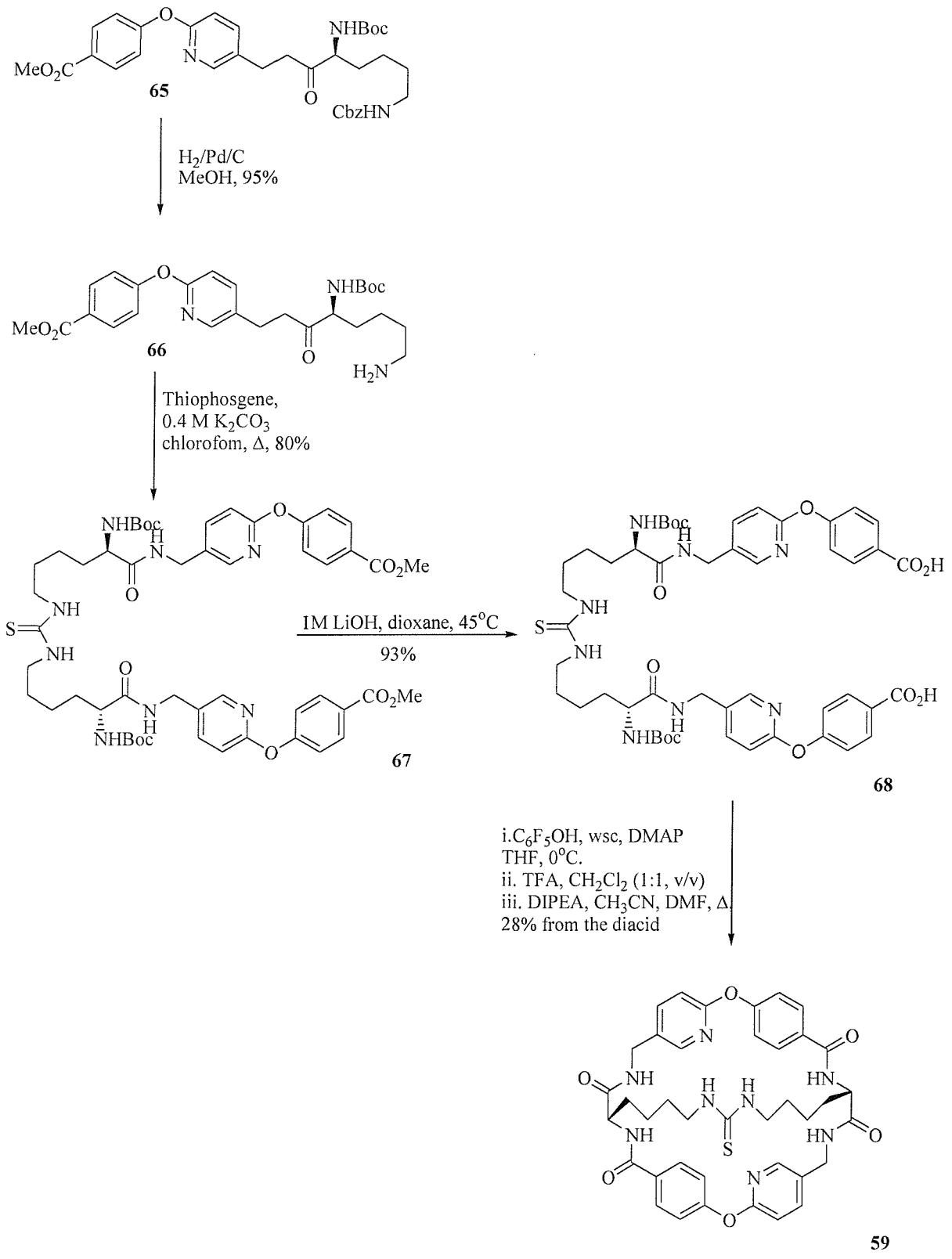

*Scheme 18: Synthesis of Macrocycle **59***

From this point the remainder of the synthesis was performed solely by V. Jullian. Thus the next step in the synthesis was the removal of the Cbz group of **65**. This transformation was achieved using hydrogen gas with 10% palladium on charcoal to provide the free amine **66** in

excellent yields (95%). The symmetrical macrocycle **59** was produced as follows: amine **66** was refluxed with thiophosgene and a 0.4M aqueous solution of potassium carbonate in chloroform to produce the fully protected macrocycle precursor, dimethyl ester **67** in very good yields (80%). The methyl esters were then hydrolysed using a 1M aqueous lithium hydroxide solution in dioxane to give the corresponding diacid **68** (93%). The final three steps of the synthesis were carried out without purification of the intermediates; pentafluorophenol, WSC and DMAP were employed to form an activated diester, followed by the removal of the two Boc protecting groups using anhydrous trifluoroacetic acid in dichloromethane. The double macrocyclisation was carried out with diisopropylethyl amine in acetonitrile under conditions of high dilution to give macrocycle **59** in yields of approximately 28% from diacid **68**.

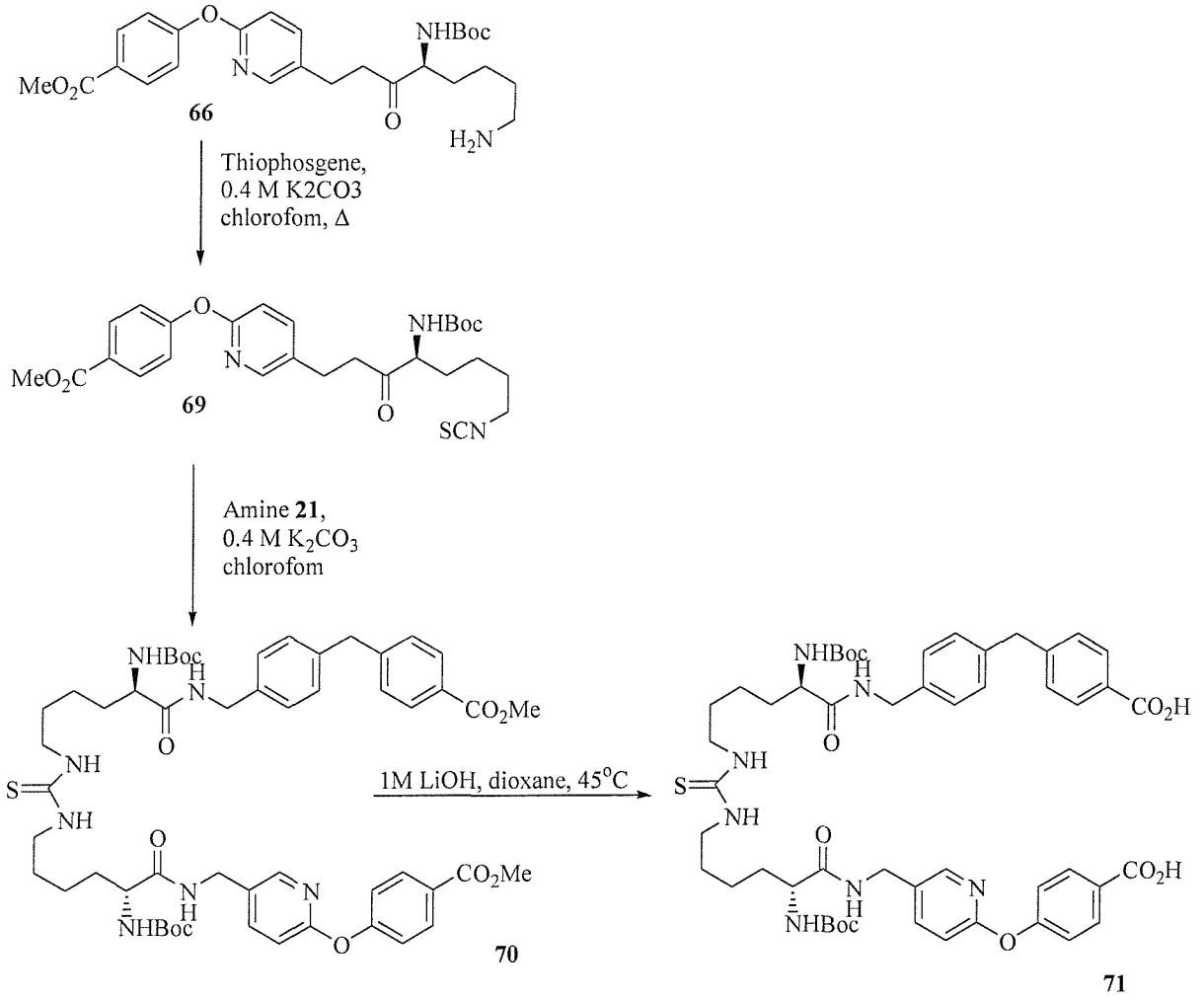

*Scheme 19: The Synthesis of the Precursor for Macrocycle **60***

The unsymmetrical macrocycle **60** containing one pyridyl spacer and one biaryl methylene spacer unit was synthesised in a similar way except that amine **66** was converted to the corresponding isothiocyanate **69** with thiophosgene and aqueous potassium carbonate solution in refluxing chloroform. One equivalent of isothiocyanate **69** and one equivalent of amine **21** were then combined using 0.4M aqueous potassium carbonate solution in chloroform to afford the non-symmetrical dimethyl ester **70**. The non-symmetrical precursor was treated in an identical way to its symmetrical counterpart to produce receptor **60** in slightly higher yields (54% from the diacid) than macrocycle **59**.

4.2 The Properties of Macrocycle 59 and 60

4.2.1 NMR Characterisation

With the synthesis of macrocycle **59** and **60** completed by V. Jullian, I then continued with the investigation into the properties of the novel macrocycles. Macrocycles **59** and **60** proved to be insoluble in chloroform and only partially soluble in dichloromethane to the extent that dissolving sufficient quantities for ^{1}H NMR analysis was difficult. Spectra of the two macrocycles were obtained using Brüker DPX400 spectrometer and are displayed below with the spectrum of macrocycle **1** (fig. 61) for comparison.

It is evident that the lower region of the three spectra are, broadly speaking, the same featuring signals that correspond to the lysine side chain moiety which makes up part of the rim and sidewall of each of the macrocycles. The spectrum of macrocycle **1** features a singlet at 3.90 ppm, the signal for the methylene unit separating the two aromatic rings of the rigid spacer unit. As would be expected this signal is also observed in the spectrum for the non-symmetric macrocycle **60** which contains one of these spacer units but is absent in the spectrum of symmetric macrocycle **59**; this contains two novel spacer units where the aromatic rings are separated by an ether linkage. Similarly the aromatic regions of the spectra differ in all three. Macrocycle **1** shows splitting patterns consistent with the presence of two *para*-substituted benzene rings. The signals found in the spectrum of macrocycle **59** are more complex since the aromatic spacer group is composed of one *para*-substituted benzene ring and a 2,5-substituted pyridine ring separated by an oxygen atom. The aromatic region for macrocycle **59** thus features four doublets and a singlet. Comparison of the

spectrum obtained for macrocycle **60** (fig. 61c) with the other two spectra clearly shows that the aromatic region of the spectra for macrocycle **60** is an amalgamation of the spectra for **1** and **59**, indicating the presence of one of the original biarylmethylene spacer units and one of the pyridine ether spacer units. The NH signals for each macrocycle fall between 6 and 8 ppm making their assignment difficult, the positioning of the NH signals is broadly the same in each spectrum indicating that there is no additional hydrogen bonding occurring in the modified macrocycles **59** and **60** compared to the original macrocycle **1**. Overall it appears that all three macrocycles are likely to have similar conformations in solution.

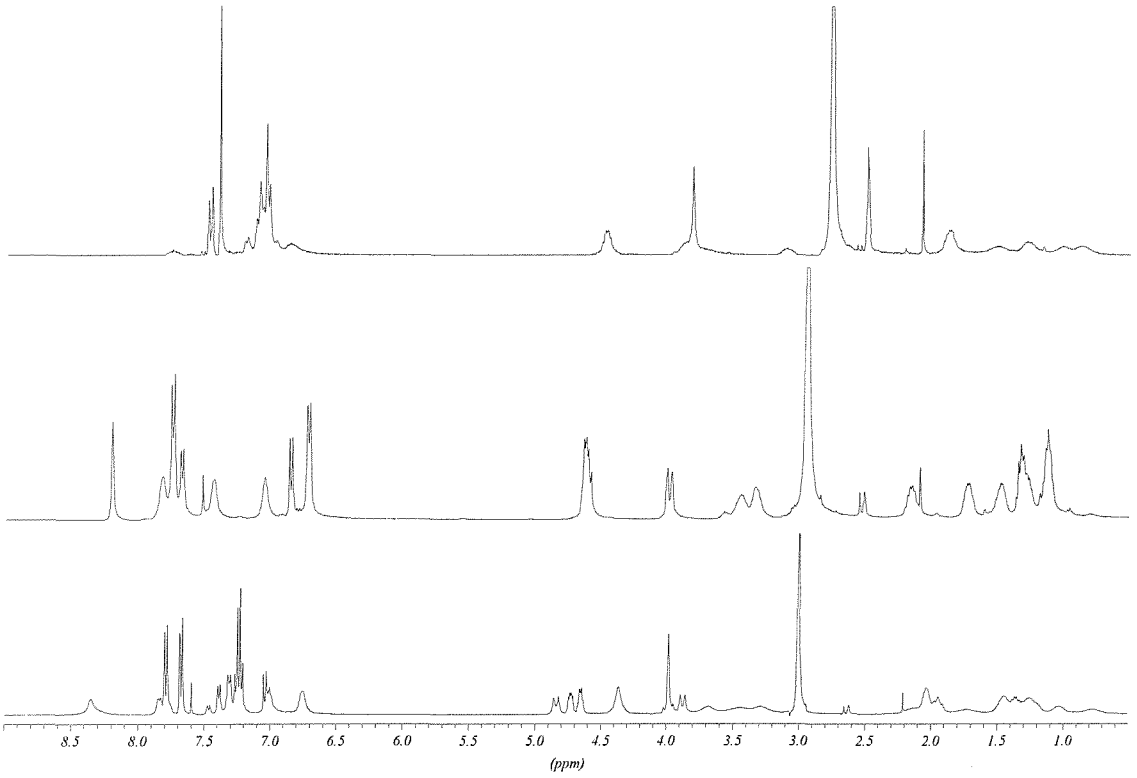

*Fig. 61: ^1H NMR spectra of, a. Macrocycle **1** b. Symmetric Macrocycle **59** c. Macrocycle **60***

4.2.2 X-Ray Crystallography

The C_2 symmetric macrocycle **59** was recrystallised from methanol and the non-symmetric macrocycle **60** from DMSO/H_2O to provide crystals for X-ray analysis. The structures of both **59** and **60** feature a large open cavity but differ in the orientations of the aromatic rings in the spacer units (fig. 62). The pyridyl ether unit of **59** has a more twisted conformation than the biarylmethane unit of **60** and consequently the rim of **60** is more open. The

orientation of the thiourea in macrocycle **59** is stabilised by a pair of hydrogen bonds from both NH's of the thiourea to the benzamide $C=O^3$ of an adjacent molecule of **59**. The configuration of macrocycle **60** is stabilised by an intramolecular hydrogen bond from the thiourea sulfur to N^4-H to the benzamide $C=O^3$ of an adjacent molecule of **60**. Modelling carried out on macrocycle **1**[69] indicates that the thiourea and side wall, derived from the lysine chain, which connects the carboxylate binding site to the macrocycle rim is very flexible, enabling the thiourea to orientate both into or out of the cavity with little enthalpic penalty when in solution. Therefore, binding of these new receptors to amino acid derivatives is still to be expected.

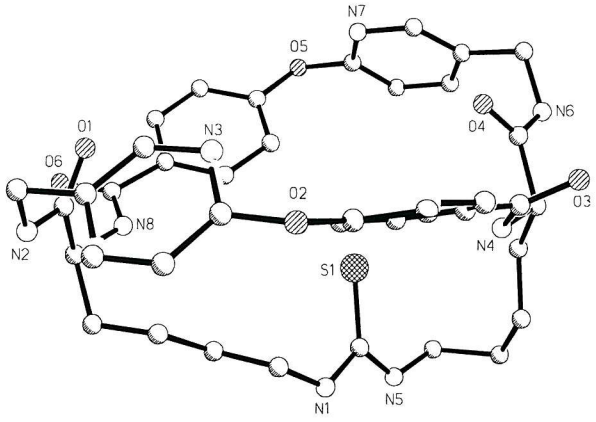

Macrocycle **59**

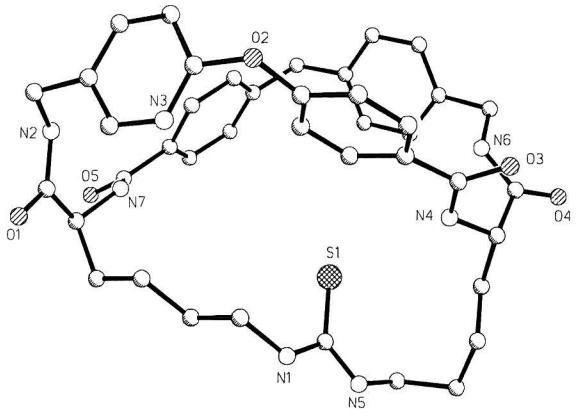

Macrocycle **60**

*Fig. 62: The X-Ray Crystal Structures of Macrocycles **59** and **60***

4.2.3 Binding Studies

The strength of binding of a host to its guest can be assessed by numerous methods including extraction experiments,[117] dilution studies[118] and titration methods.[119] During a titration experiment to determine association constant, successive aliquots of guest are added to a solution of receptor and the alteration of a physical parameter on complexation measured. A plot of the change in physical parameter against increasing concentration of the host can then be produced using curve-fitting software, which will also determine the association constant.

A very common tool employed to measure changes in a host-guest complex is ^{1}H NMR, where the movement of the chemical shift of signals from the host are recorded. The insoluble nature of the macrocycles in chloroform and dichloromethane, meant that sufficient quantities of receptor could not be dissolved in the volumes of solvent appropriate to NMR study. The binding studies were instead carried out with macrocycle **59** using UV titration experiments. UV spectroscopy is an extremely sensitive technique requiring solutions in the order of 10^{-5} mol dm^{-3} to gain adequate data.

UV experiments were performed by adding 0.2 equivalents of guests in a solution of host at concentration 2.6×10^{-5} mol dm^{-3} to a solution of host at a concentration of 2.6×10^{-5} mol dm^{-3}. This ensured that the addition of successive portions of guests did not dilute the solution of host to which they were being added. The change in absorbance was monitored at 249.5 nm.

With the tetrabutylammonium salts of *N*-acetylated L- and D-glutamine; *N*-acetylated L- and D-asparagine and *N*-acetylated L- and D-alanine as guests. Titration of **59** in dichloromethane with the glutamine and asparagine derivatives gave saturation curves with a good fit to the presumed 1:1 binding,[120] (see table 2 for association constants). The binding constants for *N*-acetyl L-asparagine suggest that the additional hydrogen bonding potential of the host enables a stabilising interaction with the CONH side chain functionality of this guest leading to predominantly one mode of binding. Titration with the alanine derivatives, however, gave a complicated titration curve, which indicated multiple binding equilibria consistent with the findings from G. Pernia.

Guest Molecules (as NBu_4^+ Salts)	K_a / mol^{-1} dm^{-3}	ΔG_{ass} / kJ mol^{-1}
N-Ac L-Asparagine	$5.5 \times 10^4 \pm 15\%$	27 + 1.3,-1.5%
N-Ac D-Asparagine	$4.3 \times 10^4 \pm 15\%$	26 + 1.3,-1.5%
N-Ac L-Glutamine	$8.7 \times 10^4 \pm 20\%$	28 + 1.6,-2.0%
N-Ac D-Glutamine	$1.8 \times 10^4 \pm 20\%$	24 + 1.9,-2.3%

Table 2

Job plots[121, 122] were carried out with each guest to ascertain that the binding was indeed that of 1:1 stoichiometry. Thus solutions were prepared which contained different mole fractions of host and guest but with total molar concentrations that were the same. The difference in absorbance in the UV specta at 249.5 nm between these and solutions containing the same mole fraction of host but with the remainder of the solution composed of solvent instead of guest, were recorded. The data was used to produce graphs of the difference in absorbance against mole fraction which indicate the stoichiometry of the complex measured. The curve obtained is an inverted parabola with a maximum which will occur at a mole fraction of 0.5 for binding with a 1:1 stoichiometry, and strongly bound complexes tend to produce curves with sharp maxima whereas weaker bound complexes will give results leading to flatter curved plots. The experiments carried out with the L and D glutamine and asparagine derivatives confirmed that the complexes formed were of a 1:1 stoichiometry whereas the Job plots taken for the alanine derivatives indicated that this was not the case. A possible explanation for these preliminary observations is that a number of modes of binding are possible for the *N*-acetyl alanines, a feature previously observed by G. Pernia[69, 90] with macrocycle **1** (for a detailed discussion see chapter one, section 1.5). It is likely that macrocycle **59** can bind *N*-acetyl alanine both internally and externally as observed with macrocycle **1**. With *N*-acetyl asparagine and glutamine, however, we postulate that additional hydrogen bonds between the side-chain of the guest and the pyridyl of the spacer unit exists, which would serve to favour a single mode of binding within the macrocycle cavity. Thus, we have successfully modified the design of macrocycle **1** to produce a receptor with a more selective binding profile.

Chapter Five

The Synthesis of Glutamate and Aspartate Receptors

5.1 Introduction

Receptors for biologically relevant substrates pose interesting and challenging targets for synthetic chemists. An enormous variety of synthetic receptors now exist which bind to substrates of biological relevance.[123] Of particular interest are aspartate and glutamate, that function as excitory neurotransmitters.[124] Development of enantioselective receptors for these substrates has the potential to lead to important new biosensors. Macrocycle **1** incorporates a thiourea moiety at the base of its cavity which functions as the carboxylate binding site; alteration of the cavity base to incorporate to carboxylate binding sites would lead to a novel macrocycle which could potentially bind to either glutamate or aspartate derivatives. The dicarboxylate binding site first chosen was one first reported by Hamilton.[125] It is composed of two thiourea moieties separated by a *para*-substituted arylmethylene unit. The advantages of utilising Hamilton's dicarboxylate binding site were two-fold: firstly, the dithiourea motif enabled the majority of the synthesis to proceed according to the established protocols for macrocycle **1**; secondly the strength of any binding of glutamate derivatives to novel macrocycle **72** (fig. 63) could be compared to the values obtained by Hamilton.

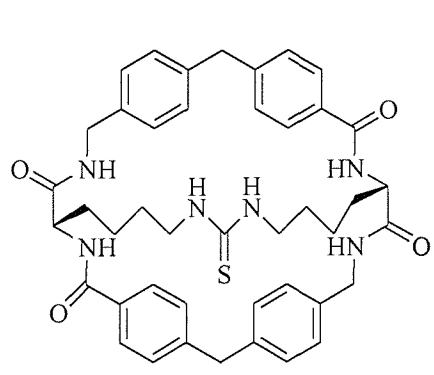

1

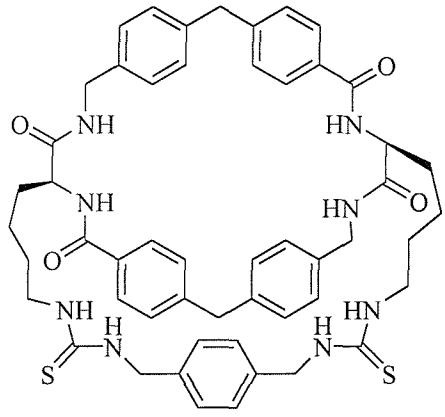

72

Fig. 63: The Proposed Bisthiourea Macrocycle

Receptor **72** displays the functionality to chemically complement a dicarboxylate guest. However, as with the previous two modified macrocycles **59** and **60**, the modifications have been selected such that the gross structure of the receptor remains broadly unchanged. Thus, the rim and side walls of the cavity still have features found in macrocycle **1**. It was anticipated that the amide functionality present around the rim of macrocycle **72** would interact with the amino moiety of glutamate and therefore **72** would be more selective for guests such as derivatives of glutamate and aspartate over simple dicarboxylates.

5.2 Retrosynthesis of Macrocycle 72

The strategy employed for the synthesis of macrocycle **1** was closely adhered to until the point of formation of the carboxylate binding sites. The disconnection of macrocycle **72** is given for comparison to that of macrocycle **1** (scheme 1 and 20 respectively). Thus, disconnection across the two amide bonds in the cavity rim leads to a linear symmetric macrocycle precursor which, after suitable activation can undergo a double macrocyclisation reaction in an analogous way to precursor **4** in the macrocycle **1** scheme. The linear precursor **73** can be disconnected back to *p*-xylene diamine **74** and isothiocyanate **6**, an intermediate common to the synthesis of both macrocycle **1** and **72**. Much of the early synthesis would be identical to that of macrocycle **1** and similarly the protecting group strategy adopted for the synthesis of **1** could also be applied to macrocycle **72**.

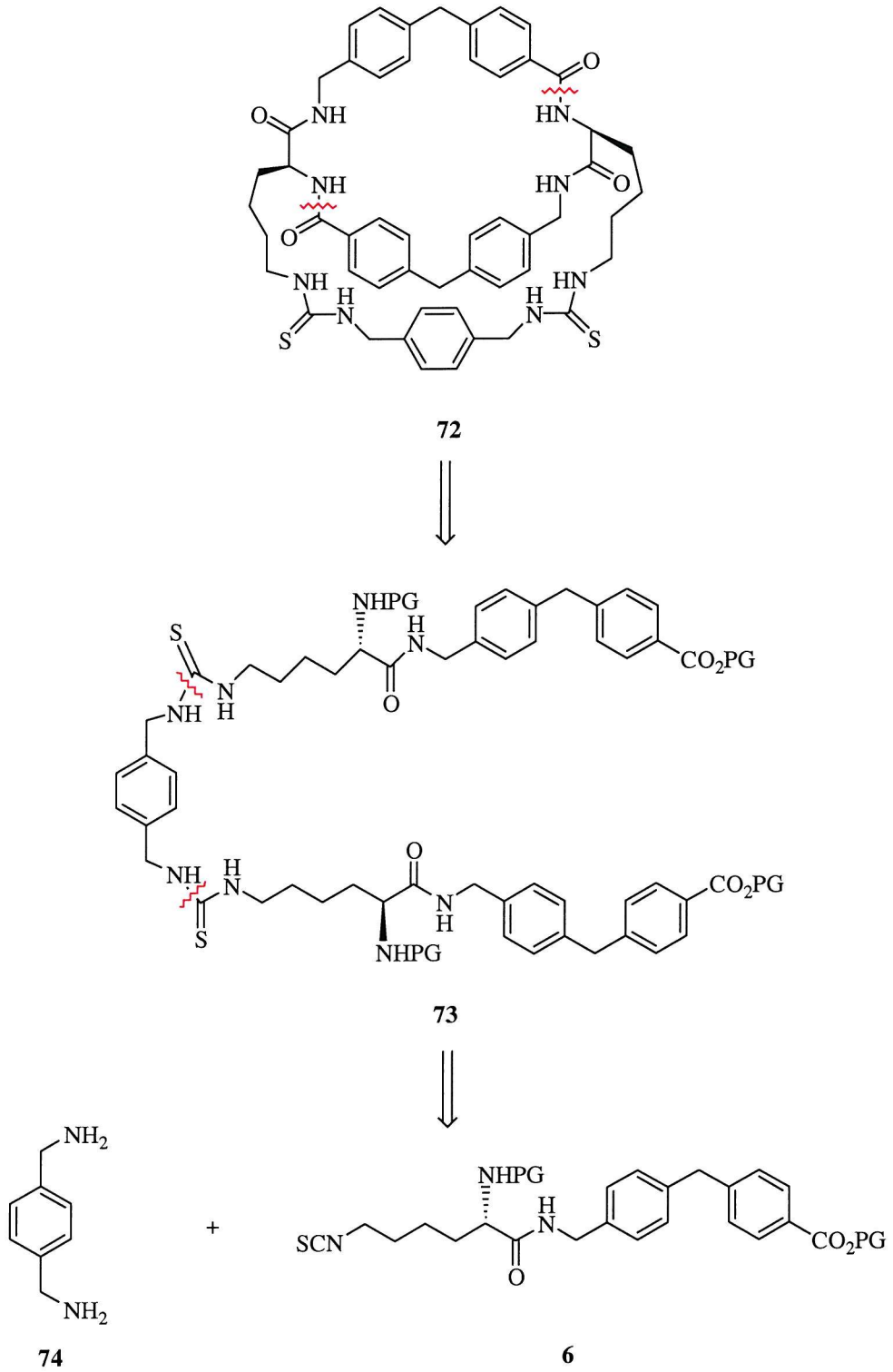

Scheme 20: The Retrosynthetic Analysis of Macrocycle **72**

5.3 The Synthesis of Macrocycle 72

The synthetic procedures employed to form isothiocyanate **22** were identical to those described in chapter 2 (schemes 2 and 4). The next step in the synthesis of macrocycle **72** was the coupling of two equivalents of **22** with one equivalent of *p*-xylenediamine **74** to produce the linear, fully protected macrocycle precursor **75** with the bisthiourea moiety in place (scheme 69). Initially attempts involved carrying out the reaction in refluxing pyridine. However, all attempts to couple the amine and isothiocyanate under these conditions failed. The coupling was eventually achieved in good yields (59%) by refluxing isothiocyanate **22** and *p*-xylenediamine **74** in chloroform with a 0.4M aqueous solution of potassium carbonate. The resulting dimethyl ester **75** was hydrolysed to diacid **76** in very good yields (86%) using a 1M aqueous solution of lithium hydroxide in dioxane at 45°C.

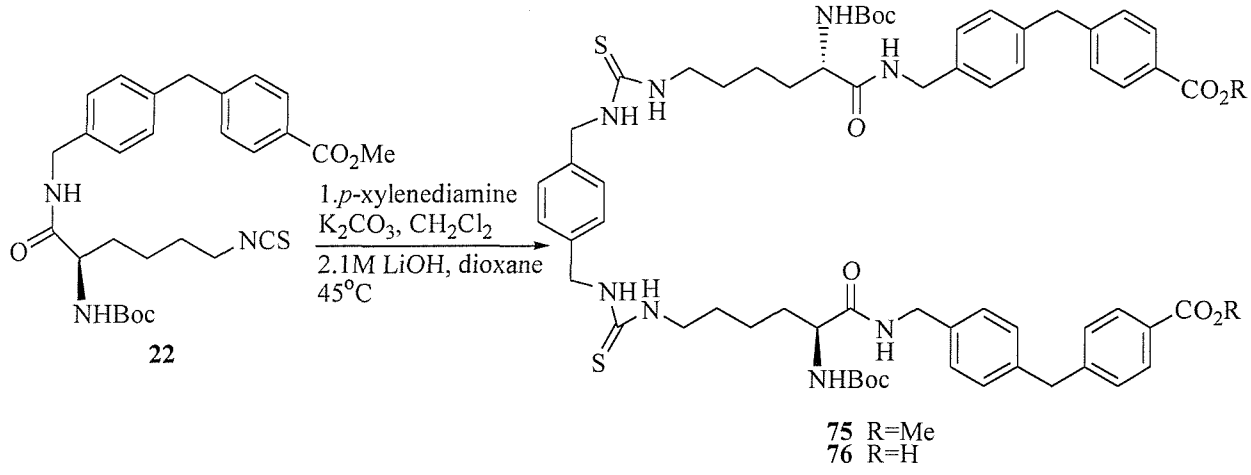

Scheme 21: Synthesis of Macrocycle 72

The final three steps of the synthesis: production of the activated bispentafluorophenyl ester; removal of the Boc protecting groups and cyclisation under conditions of high dilution were carried out without purification. The intermediates were isolated and crude ^{1}H NMR taken to confirm that they had formed. The final three steps were attempted on numerous occasions employing a variety of methods (table 3) but in each case, although activation of the ester and deprotection to remove the Boc groups was successful, the subsequent double macrocyclisation could not be effected.

Formation of the Activated Ester	Boc deprotection	Cyclisation Conditions
C_6H_5OH, DMAP, WSC, THF	TFA, CH_2Cl_2, 0°C	MeCN, DIPEA, DMF, Δ
C_6H_5OH, DMAP, WSC, THF	TFA, CH_2Cl_2, 0°C	THF, DIPEA, DMF, Δ
C_6H_5OH, DMAP, WSC, THF	4M HCl, dioxane	MeCN, DIPEA, DMF, Δ
C_6H_5OH, DMAP, WSC, THF	4M HCl, dioxane	THF, DIPEA, DMF, Δ
C_6H_5OH, DMAP, WSC, THF	TFA, CH_2Cl_2, 0°C	Dioxane, DMAP, DMF, Δ
C_6H_5OH, DMAP, WSC, THF	TFA, CH_2Cl_2, 0°C	MeCN, DMAP, DMF, Δ
C_6H_5OH, DMAP, WSC, THF	4M HCl, dioxane	DCM, DMAP, DMF, Δ

Table 3: Conditions Employed in the Attempts to form Macrocycle ***72***

The failure to form macrocycle **72** was attributed to the cyclisation of the precursor being harder to achieve in this case than with the original macrocycle **1** due to the presence of the *para*-substituted aromatic ring. This may serve to increase the rigidity of the precursor in such a way that achieving a conformation where the reacting species were in close proximity to one another would be difficult. Despite many attempts, the macrocycle precursor could not be prevailed upon to cyclise thus macrocycle **72** remained elusive. We therefore sought to alter the nature of our modification to macrocycle **1** in our quest to obtain a novel dicarboxylate receptor.

An alternative to the *para*-substituted bisthiourea was therefore sought. It was desirable to maintain the thiourea entities as the primary binding sites of interaction with the guest, in order to enable the synthesis of the new macrocycle to proceed along an analogous route to that of macrocycle **1**. The dicarboxylate binding site design was altered to feature a *meta*-substituted aromatic ring in place of the *para*-substituted ring. This spacer motif was also

used by Hamilton[126] between guanidiunium moieties in receptors designed to accelerate the rate of phosphate diester transesterification. It was anticipated that this slight modification to the spacer unit between the thioureas would increase the potential for the free amine and activated ester portions of the macrocycle precursor to unite during the cyclisation reaction thereby elevating the chances of obtaining a cyclised product.

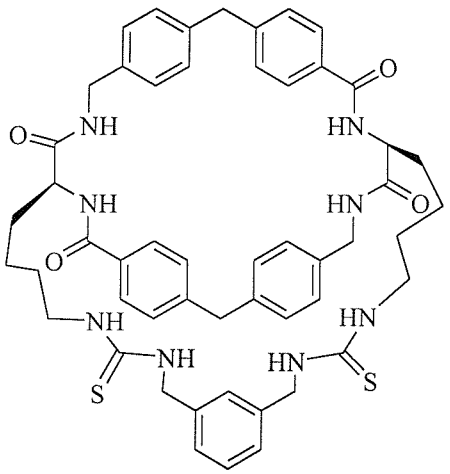

77

Fig.64: Proposed Structure of Modified Macrocycle

The new macrocycle **77** would have a slightly smaller distance between the two carboxylate binding sites. This may make it more suitable as a receptor for aspartate derivatives over glutamate derivatives.

5.4 Synthesis of Macrocycle 77

The synthetic route applied to the formation of macrocycle **77** is essentially identical to the proposed route for macrocycle **72**, since the retrosynthetic analysis of macrocycle **1** has been discussed in some detail and the analysis of macrocycle **72** considered in comparison, I find it unnecessary to also consider macrocycle **77** in this way.

The synthesis of intermediates to the point of isothiocyanate **22** is common to macrocycle **1**, **72** and **74** and covered above (chapter two). Two equivalents of isothiocyanate **22** and *m*-xylenediamine were refluxed in chloroform with 0.4M aqueous potassium carbonate solution, the desired macrocycle precursor in the form of the dimethyl ester **78** was consistently

isolated in good yields (65%). The two methyl esters were successfully hydrolysed to form the corresponding acids **79** in excellent yields (80%).

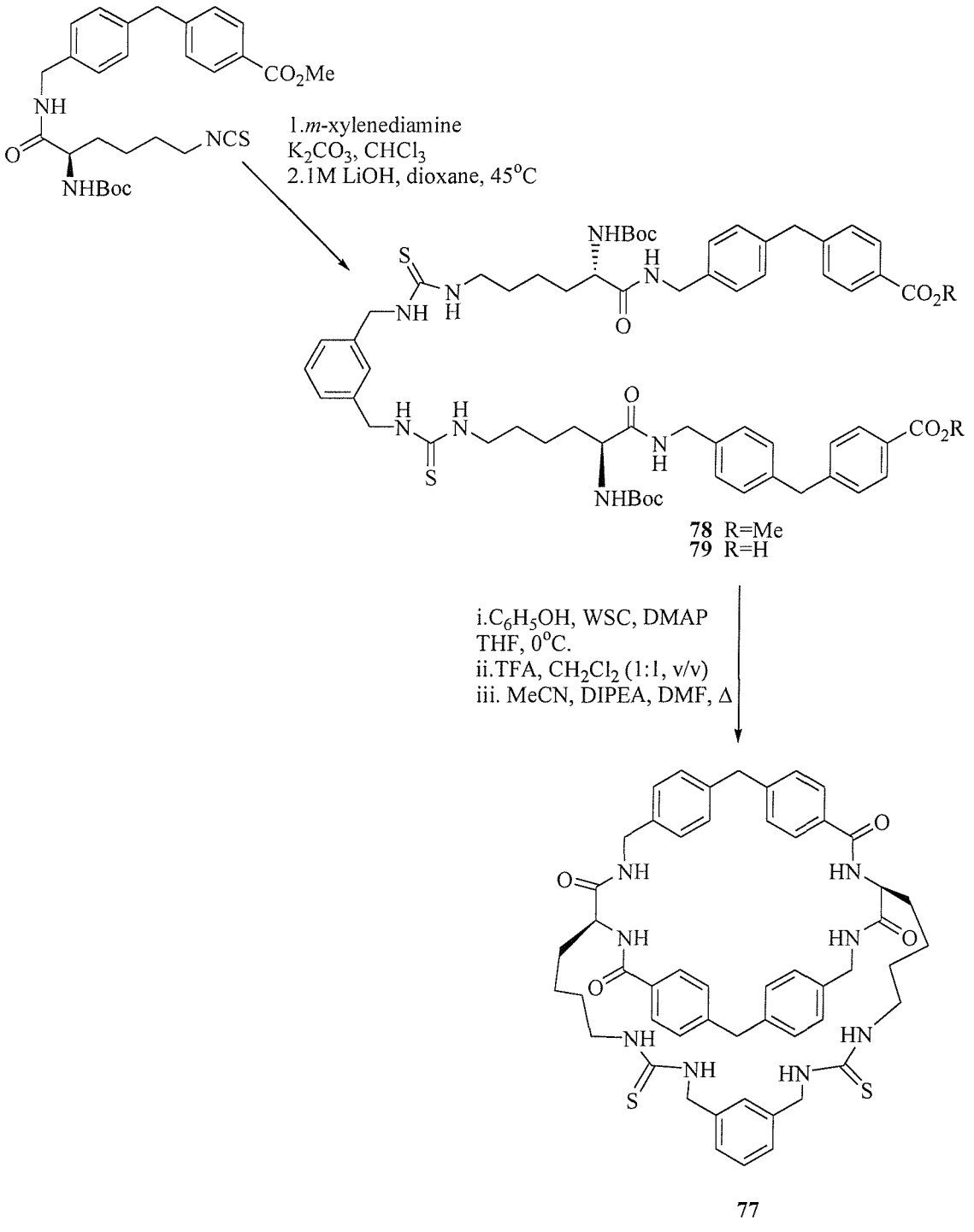

Scheme 20: The Synthesis of Macrocycle 77

Diacid **79** was activated using pentafluorophenol, 1-(3-dimethylaminopropyl)-3-carbodiimide hydrochloride and DMAP in tetrahydrofuran. The removal of the Boc protecting group was

carried out in trifluoroacetic acid and chloroform, and the resulting salt cyclised using diisopropylethyl amine in refluxing acetonitrile under conditions of high dilution. As with the previous two macrocycle syntheses described, no purification was carried out during the final three steps and ^{1}H NMR was employed to ascertain that the transformations had occurred. Macrocycle **77** was synthesised on a small scale; the isolated compound was correct according to the low resolution mass spectrum which gave the mass ion at 923.5. Other characteristics of the compound were also consistent with the properties displayed by macrocycle **1**. All attempts to purify the crude cyclisation product were unsuccessful, even the application of HPLC failed to provide adequately clean material. Thus the binding properties of the cyclisation product could not be investigated.

To conclude the synthesis of macrocycles **72** and **77** were carried through to the final stages of the route. In the case of the macrocycle **72** the final cyclisation could not be accomplished despite the use of different conditions. The synthesis of macrocycle **77** was carried out but difficulties in purification have prevented its investigation and to date the only proof that the synthesis was successful is a low resolution mass spectrum.

Chapter Six

Experimental

6.1.1 General Experimental

Reactions which required a dry atmosphere were conducted in flame dried glassware under an atmosphere of nitrogen. Reactions were carried out in solvents of commercial grade and where necessary were distilled prior to use (for solvent distilling procedures see Purification of Laboratory Chemical by Perrin and Armarego). THF was distilled under nitrogen from benzophenone and sodium and CH_2Cl_2 was distilled from calcium hydride, as was petroleum ethereum ether where the fraction boiling between 40 and 60°C was used. TLC was done on foil backed sheets coated with silica gel (0.25 mm) which contained the fluorescent indicator UV_{254}. Flash column chromatography was performed on Sorbsil C60, 40-60 mesh silica.

6.1.2 Instrumentation

^{1}H NMR spectra were obtained at 300 MHz on Brüker AC300 and Brüker AM 300 spectrometers, at 360 MHz on a Brüker AM360 spectrometer and at 400 MHz on a Brüker DPX400 spectrometer, a Gemini300 was also used. ^{13}C NMR spectra were obtained at 75.5 MHz on Brüker AC300 and Brüker AM 300 spectrometers and at 100 MHz on a Brüker DPX400 spectrometer. Spectra were referenced with respect to the residual solvent peak for the deuterated solvent. Infrared spectra were obtained on Perkin-Elmer 1600 series and Golden Gate FT-IR machines. Spectra were obtained either from KBr disks or as neat films supported on sodium chloride plates on the Perkin-Elmer machine and as solids on the Golden Gate machine. All melting points were measured in open capillary tubes using a Gallenkamp Electrothermal Melting Point Apparatus and are uncorrected. Electrospray mass spectra were obtained on a Micromass platform with a quadrupole mass analyser. FAB spectra were obtained on a VG Analytical 70-250-SE normal geometry double focusing mass spectrometer. High resolution accurate mass measurements were carried out at 10, 000 resolution using mixtures of polyethylene glycols and/or poylethylene glycol methyl ethers as mass calibrants for FAB.

6.2 Experimental Details

Methyl 4-bromomethylbenzoate 9[69]

A solution of bromine (13.3 ml, 258 mmol) in degassed carbon tetrachloride (100 ml) was added dropwise to a solution of methyl 4-methylbenzoate (40 g, 266 mmol) and AIBN (200 mg) in degassed carbon tetrachloride (200 ml) over two hours whilst irradiating with a 150 W tungsten lamp. Irradiation and stirring was continued for 24 h and the exhaust gasses passed through sodium hydrogen carbonate solution. The solvent was removed *in vacuo* to afford a cloudy orange liquid which, was filtered and the residue washed with dichloromethane, the filtrate was concentrated to an orange liquid that solidified on standing. The crude material was purified by recrystallisation from petroleum ether to afford the desired product as an orange solid (32.2 g, 53%); mp 51-53°C, lit.[69] mp 50-53°C; ν_{max}/cm^{-1} 3455.1, 1719.3, 1280.8, 857.7, 703.7; δ_H(300 MHz, $CDCl_3$) 8.2 (d, *J* 8.3 Hz, 2 H, Ar*H ortho* to CO_2CH_3), 7.7 (d, *J* 8.3 Hz, 2 H, Ar*H meta* to CO_2CH_3), 4.5 (s, 2 H, ArCH_2Br), 3.9 (s, 3 H, CO_2CH_3); δ_C(75.5 MHz, $CDCl_3$) 166.7 (C), 142.8 (C), 130.2 (CH), 129.2 (CH), 52.4 (CH_3), 32.4 (CH_2).

4-Cyanophenylboronic acid 11[69]

n-Butyllithium (42.3 ml of a 2 M solution in hexanes) was added over 1.5 h to a stirred solution of 4-bromobenzonitrile (15 g, 82.3 mmol) in tetrahydrofuran (190 ml) at -100°C under argon. The mixture was stirred for 15 min and then trimethylborate (13.8 ml, 103.4 mmol) added dropwise at -100°C and the solution allowed to warm to room temperature overnight. Work up consisited of acidifying the reaction mixture to pH 2 using 15% hydrochloric acid, the aqueous layer was separated and extracted with dichloromethane, the organic layers washed with water until acid free and dried ($MgSO_4$) and concentrated to a yellow solid which was triturated with petroleum ether and dried to afford the title compound as a yellow solid (11.2 g, 93%); mp > 250 °, lit.[69] mp > 300°C; ν_{max}/cm^{-1} 2222.6. 1417.6, 1345.9, 1067.5, 1008.2, 824.6, 540.2; δ_H(300 MHz, DMSO) 8.45 (br s, 2 H, BO*H*), 7.93 (d, *J* 8.1 Hz, 2 H, Ar*H meta* to CN), 7.79 (d, *J* 8.1, 2 H, Ar*H ortho* to CN); δ_C(75.5 MHz, DMSO) 134.7 (CH), 131.1 (CH), 119.1 (C) 112.4 (C).

Methyl 4-(4'-cyanophenylmethyl)benzoate 12[69]

An aqueous solution of sodium carbonate (50 ml of a 2 M solution) was added to a solution of bromide **9** (11.4 g, 49.9 mmol); boronic acid **11** (7.3 g, 49.9 mmol) and tetrakis(triphenyl phosphine) palladium (0) (100 mg) in degassed 1,2-dimethoxyethane (115 ml) and the mixture refluxed for 24 h under a nitrogen atmosphere. The reaction was cooled to room temperature, water added and the aqueous layer extracted with dichloromethane. The organic layer was dried ($MgSO_4$) and concentrated to a solid which was recrystallised from ethyl acetate-petroleum ether to furnish the product as yellow crystals (9.68 g, 77%); mp 117-120°C, lit.[69] mp 125-127°C; ν_{max}/cm^{-1} 2224.7, 1712.9, 1289.0, 736; δ_H(300 MHz, $CDCl_3$) 8.00 (d, *J* 8.0 Hz, 2 H, Ar*H ortho* to CO_2CH_3), 7.60 (d, *J* 7.9 Hz, 2 H, Ar*H meta* to CO_2CH_3), 7.48 (d, *J* 7.2 Hz, 2 H, Ar*H meta* to CN), 7.24 (d, *J* 7.9 Hz, 2 H, Ar*H ortho* to CN), 4.09 (s, 2 H, ArCH_2Ar), 3.91 (s, 3 H, CO_2CH_3); δ_C(75.5 MHz, $CDCl_3$) 167.0 (C), 145.8 (C), 144.7 (C), 132.6 (CH), 130.2 (CH), 129.8 (CH), 129.1(CH), 119.0 (C), 110.6 (C), 52.3 (CH_3), 42.0 (CH_2).

Methyl 4-(4'-aminomethylphenylmethyl)benzoate hydrochloride 13[69]

Borane-dimethylsulfide complex (8.8 ml of a 2.8 M solution in tetrahydrofuran) was added to a refluxing solution of nitrile **12** (4.1 g, 16.5 mmol) in tetrahydrofuran (75 ml) under a static argon atmosphere. The solution was refluxed for 16 h. The reaction mixture was cooled to 0°C, hydrochloric acid solution added (8.2 ml of a 6 M aqueous solution) and the mixture refluxed for a further hour. The reaction mixture was re-cooled to 0°C and soduim hydroxide added (27.5 ml of a 3 M aqueous solution); the solution was extracted with diethyl ether, the organic layer dried ($MgSO_4$) and gaseous hydrochloric acid bubbled through the solution for 15 min to afford the product as a white solid (4.6 g, 96%); mp 225-230°C, lit.[69] mp 241-243°C; ν_{max}/cm^{-1} 3424.9, 3001.9, 1723.8, 1609.8, 1484.3, 1438.7, 1279.5, 1098.1, 875.9; δ_H (400 MHz, d_6-DMSO) 8.62 (bs, 2 H, CH_2NH_2), 8.00 (d, *J* 8.0 Hz, 2 H, Ar*H ortho* to CO_2CH_3), 7.53 (d, *J* 8.0 Hz, 2 H, Ar*H meta* to CO_2CH_3), 7.48 (d, *J* 8.0 Hz, 2 H, Ar*H meta* to CH_2NH_2), 7.40 (d, J 8.0 Hz, 2 H, Ar*H ortho* to CH_2NH_2), 4.15 (s, 2 H, ArCH_2NH_2), 4.06 (s, 2 H, ArCH_2Ar), 3.94 (s, 3 H, CO_2CH_3); δ_C (100 MHz, DMSO) 166.6 (C), 147.3 (C), 141.2 (C), 132.5 (C), 129.8 (CH), 129.7 (CH), 129.5

(CH), 129.4 (CH), 128.8 (CH), 128.0 (C), 52.5 (CH_3), 42.3 (CH_2), 41.0 (CH_2); LRMS (ES^+) *m/z* 511.1 (2 M + H, 5%), 338.1 (M + H + 2 MeCN, 5%), 297.1 (M + H + MeCN, 100%), 256.0 (M + H, 15%).

(8s)-methyl 12-benzyloxycarbonylamino-8-t-butyloxycarbonylamino-7-oxo-6-aza-2(1,4), 4 (1,4)-dibenzenadodecaphanoate 20[69]

1-(3-dimethylaminopropyl)-3-ethyl carbodiimide hydrochloride (7.89 g, 41.17 mmol) was added to a solution of amine salt **13** (10.05 g, 34.30 mmol), N_ε-benzyloxycarbonyl-N_α-*t*-butyloxycarbonyl-L-lysine (16.95 g, 44.6 mmol), HOBt (5.59 g, 41.17 mmol), diisopropylethyl amine (11.95 ml, 68.60 mmol) in dimethylformamide (20 ml) and tetrahydrofuran (101 ml) at 0°C under a nitrogen atmosphere and the mixture stirred overnight. The reaction mixture was diluted with dichloromethane, washed with 1 M hydrochloric acid, a saturated aqueous solution of sodium hydrogen carbonate and the organic layer dried ($MgSO_4$) and purified by flash column chromatography with ethyl acetate-dichloromethane (20-40%) to afford the title compound as a white solid (15.19 g, 72%); mp 120-122°C, lit.[69] mp 125-127°C; ν_{max}/cm^{-1} 3315.6, 2933.9, 1717.7, 1684.1, 1644.8, 1277.4, 1168.9, 740.9; δ_H (300 MHz, $CDCl_3$) 7.95 (d, *J* 8.1 Hz, 2 H, Ar*H ortho* to CO_2CH_3), 7.33 (s, 5 H, OC_6H_5), 7.23 (d, *J* 8.6 Hz, 2 H, Ar*H meta* to CO_2CH_3), 7.19 (d, *J* 8.1 Hz, 2 H, Ar*H meta* to CH_2NH), 7.12 (d, *J* 7.9 H, 2 H, Ar*H ortho* to CH_2NH), 6.59 (bs, 1 H, CH_2CONH), 5.20 (bs, 1 H, $NHCO_2$), 5.10 (s, 2 H, $COCH_2Ar$), 4.89 (bs, 1 H, $ArCH_2NHCO$), 4.40 (bd, *J* 4.8 Hz, 2 H, $ArCH_2NH$), 4.09 (bs, 1 H, $CHCH_2CH_2$), 4.00 (s, 2 H, $ArCH_2Ar$), 3.90 (s, 3 H, CO_2CH_3), 3.18 (bd, J 5.7 Hz, 2 H, CH_2CH_2NH), 1.95-1.31 (m, 6 H, $CHCH_2CH_2CH_2CH_2NH$), 1.40 (s, 9 H, $C(CH_3)_3$; δ_C (75.5 MHz, $CDCl_3$) 172.4 (C), 167.2 (C), 156.8 (C), 156.0 (C), 146.6 (C), 139.5 (C), 136.7 (C), 136.4 (C), 130.0(CH), 129.3(CH), 129.0(CH), 128.6(CH), 128.2(CH), 128.0 (CH), 80.1 (C), 66.7 (CH_2), 54.6 (CH), 52.2 (CH_3), 43.2 (CH_2), 41.7 (CH_2), 40.5 (CH_2), 32.0 (CH_2), 29.6 (CH_2), 28.4 (CH_3), 22.7 (CH_2); LRMS (ES^+) *m/z* 640.0 (M + Na^+, 100%), 618.0 (M + H, 70%).

(8s)-Methyl 12 amino-8-*t*-butyloxycarbonylamino-7-oxo-6-aza-2(1,4), 4 (1,4)-dibenzenadodecaphanoate 21[69]

A solution of **20** (4.56 g, 7.39 mmol) and 10% palladium on activated charcoal in dimethylformamide (6.70 ml) and methanol (50 ml) was stirred under a static hydrogen atmosphere for 24 h. The reaction mixture was filtred through celite and the residue washed with methanol; the filtrate was concentrated *in vacuo* and ethyl acetate (50 ml) added to the residue. The organic layer was washed thoroughly with water and dried ($MgSO_4$), the solvent was then removed to afford a colourless oil which solidified on standing (3.23 g, 90%); mp 80-85°C; ν_{max}/cm^{-1} 3325.8, 2933.0, 2363.2, 1722.9, 1641.5, 1521.1, 1285.2, 867.3, 738.8; δ_H (300 MHz, $CDCl_3$) 7.95 (d, *J* 8.2 Hz, 2 H, Ar*H ortho* to CO_2CH_3), 7.24 (d, *J* 8.2 Hz, 2 H, Ar*H meta* to CO_2CH_3), 7.20 (d, *J* 7.8 Hz, 2 H, Ar*H meta* to CH_2NH), 7.13 (d, *J* 7.9 Hz, 2 H, Ar*H ortho* to CH_2NH), 6.68 (bs, 1 H, CH_2NHCO), 5.11 (bd, *J* 7.4 Hz, 1 H, $CHNHCO$), 4.40 (bs, 2 H, $ArCH_2NH$), 4.07 (bs, 1 H, $CHNHCO$), 4.00 (s, 2 H, $ArCH_2Ar$), 3.90 (s, 3 H, CO_2CH_2), 2.74-2.66 (m, 2 H, $CH_2CH_2NH_2$), 1.93-1.30 (m, 6 H, $NHCHCH_2CH_2CH_2$), 1.46 (s, 9 H, $CO_2C(CH_3)_3$); δ_C (75.7 MHz, $CDCl_3$) 172.3 (C), 167.2 (C), 156.0 (C), 146.5 (C), 139.5 (C), 136.4 (C), 130.0 (CH), 129.3 (CH), 129.0 (CH), 128.1 (CH), 80.2 (C), 54.6 (CH), 52.2 (CH_3), 43.2 (CH_2), 41.7 (CH_2), 32.9 (CH_2), 32.4 (CH_2), 28.4 (CH_3), 22.9 (CH_2); LRMS (ES^+) *m/z* 966.9 (2 M + H, 5%), 484.1 (M + H, 100%).

(8s)-Methyl 12-isothicyanato-8-t-butyloxycarbonylamino-7-oxo-6-aza-2(1,4),4(1,4)-dibenzenadodecaphanoate 22[69]

Thiophosgene (0.24 ml, 3.1 mmol) was added to a solution of amine **21** (1.50 g, 3.1 mmol) and sodium hydrogen carbonate (1.17 g, 13.9 mmol) in water (74 ml) and chloroform (178 ml) at 0°C; the reaction was stirred for 20 h. The layers of the reaction mixture were separated and the aqueous layer extracted with chloroform, the combined organic layers were dried ($MgSO_4$) and concentrated to a yellow solid (1.68 g, quantitative yield); mp 80-83°C, lit.[69] mp 104-106°C; υ_{max}/cm^{-1} 3317.7, 2928.3, 2342.7, 2107.6, 1717.5, 1683.9, 1645.9, 1521.0, 1281.3, 738.4; δ_H (400 MHz, $CDCl_3$) 7.86 (d, *J* 10.3 Hz, 2 H, Ar*H ortho* to CO_2CH_3), 7.15 (d, *J* 8.5 Hz, 2 H, Ar*H*

meta to CO_2CH_3), 7.10 (d, *J* 8.3 Hz, 2 H, Ar*H ortho* to CH_2NH), 7.04 (d, *J* 8.0 Hz, 2 H, Ar*H meta* to CH_2NH), 6.56 (bs, 1 H, CH_2NHCO), 5.04 (bd, *J* 7.8 Hz, 1 H, $CHNHCO$), 4.31 (d, *J* 5.8 Hz, 2 H, $ArCH_2NH$), 4.03 (bs, 1 H, $CHNHCO$), 3.91 (s, 2 H, $ArCH_2Ar$), 3.81 (s, 3 H, CO_2CH_3), 3.47-3.33 (m, 2 H, CH_2CH_2NCS), 1.85-1.25 (m, 6 H, $NHCHCH_2CH_2CH_2$), 1.32 (s, 9 H, $CO_2C(CH_3)_3$); δ_C (100 MHz, $CDCl_3$) 172.4 (C), 167.7 (C), 156.5 (C), 147.1 (C), 140.2 (C), 136.8 (C), 131.1 (C), 130.3 (CH), 129.7 (CH), 129.3 (CH), 128.4 (CH), 128.7 (CH), 81.0 (C), 54.6 (CH), 52.4 (CH_3), 45.2 (CH_2), 43.6 (CH_2), 42.0 (CH_2), 32.1 (CH_2), 30.0 (CH_2), 28.7 (CH_3), 23.2 (CH_2); LRMS (ES^+) *m/z* 1051.4 (2 M + H, 20%), 526.1 (M + H, 90%).

(8s, 20s)-Methyl 8,20-bis(t-butyloxycarbonylamino)-7,21-dioxo-14-thioxo-6, 13, 15, 22-tetraaza-2(1, 4), 4 (1,4), 24 (1,4), 26 (1,4) – tetrabenzaheptacosaphanediazte 23[69]

A solution of amine **21** (1.60 g, 3.30 mmol) and isothiocyanate **22** (1.07 g, 2.03 mmol) in pyridine (15 ml) was refluxed for 16 h. The reaction mixture was cooled to room temperature and diluted with dichloromethane, washed with 1 M hydrochloric acid solution and dried ($MgSO_4$). The solvent was then removed *in vacuo* to afford the crude product as a yellow oil which was purified by flash column chromatography with methanol-dichloromethane (10%) to afford the desired compound as a yellow solid (1.87 g, 91%); mp 117-118°C, lit.[69] mp 128-129°C; ν_{max}/cm^{-1} 3316.8, 2928.3, 1715.9, 1682.5, 1635.6, 1521.7, 1273.9, 1166.7, 738.0; δ_H (300 MHz, $CDCl_3$) 7.94 (d, *J* 8.1 Hz, 4 H, Ar*H ortho* to CO_2CH_3), 7.24 (d, *J* 8.1 Hz, 4 H, Ar*H meta* to CO_2CH_3), 7.19 (d, *J* 7.9 Hz, 4 H, Ar*H meta* to CH_2NHCO), 7.11 (d, *J* 8.1 Hz, 4 H, Ar*H ortho* to CH_2NHCO), 6.58 (bs, 2 H, CH_2NHCS), 5.20 (bs, 2 H, $CHNHCO_2$), 4.90 (bs, 2 H, $ArCH_2NHCO$), 4.40 (bd, *J* 4.8, 4 H, $ArCH_2NHCO$), 4.14 (bs, 2 H, $CHNHCO_2$), 4.00 (s, 4 H, $ArCH_2Ar$), 3.90 (s, 6 H, CO_2CH_3), 3.17 (bd, J 5.5, CH_2CH_2NHCS), 2.00-1.3 (m, 12 H, $CHCH_2CH_2CH_2CH_2NHCS$), 1.40 (s, 18 H, $NHCO_2C(CH_3)_3$.

(8s, 20s)-Methyl 8, 20-bis(t-butyloxycarbonylamino)7, 21-dioxo-14thiooxo-6, 13, 15, 22-tetraaza-2(1, 4), 4(1, 4), 24(1, 4), 26(1, 4)-tetrabenzeneaheptacosaphanedioic acid 24[69]

An aqueous solution of lithium hydroxide (19.9 ml of a 1 M solution) was added to a solution of thiourea **23** (1.43 g, 1.42 mmol) in dioxane (20 ml) and the mixture stirred at 45°C for 3 h. After cooling to room temperature, a 1 M aqueous solution of hydrochloric acid was added until a permanent white precipitate was observed. The reaction mixture was extracted with ethyl acetate, dried ($MgSO_4$) and the solvent removed *in vacuo* to produce an off-white foam which was then triturated with ether to give the title compound as a white powder (1.29 g, 92%); mp 134-136°C, lit.[69] 145-146°C; ν_{max}/cm^{-1} 3343.6, 1695.8, 1655.7, 1548.5, 1508.3, 1247.1, 1166.7, 738.0; δ_H (300 MHz, $CDCl_3$) 7.82 (d, *J* 8.1 Hz, 4 H, Ar*H ortho* to CO_2H), 7.79 (bs, 2 H, CON*H*CH_2), 7.19 (d, *J* 8.3 Hz, 4 H, Ar*H meta* to CO_2H), 7.11 (d, *J* 7.9 Hz, 4 H, Ar*H meta* to CH_2NH), 7.05 (d, *J* 7.9 Hz, 4 H, Ar*H ortho* to CH_2NH), 6.90 (bs, 2 H, CHN*H*CS), 5.99 (bd, J 8.1 Hz, 2 H, N*H*$CO_2C(CH_3)_3$), 4.25 (bd, *J* 4.6 Hz, 4 H, ArCH_2NH), 4.00 (bs, 2 H, C*H*$NHCO_2$), 3.92 (s, 4 H, ArCH_2Ar), 1.80-1.20 (m, 16 H, CH$CH_2CH_2CH_2CH_2$NHCS), 1.33 (s, 18 H, $C(CH_3)_3$); δ_C (100 MHz, $CDCl_3$) 172.7 (C), 167.7 (C), 155.8 (C), 147.0 (C), 139.4 (C), 137.7 (C), 129.9 (CH), 129.2 (CH), 129.2 (CH), 129.1 (CH), 128.9 (CH), 127.7 (CH), 78.4 (C), 54.9 (CH), 42.1 (CH_2), 41.0 (CH_2), 32.1 (CH_2), 31.7 (CH_2), 28.9 (CH_2), 28.6 (CH_3), 23.5 (CH_2).

(1s, 12s)-7-thioxo-6, 8, 13, 19, 21, 27-hexaaza-15(1, 4), 17(1, 4), 25(1, 4)-tetrabenzenabicyclo[10.8.8]octacosaphane14, 20, 22, 28-tetraone 1[69]

1-(3-dimethylaminopropyl)-3-ethylcarbodiimide hydrochloride (0.10 g, 0.71 mmol) was added to a solution of diacid **24** (0.30 g, 0.31 mmol), DMAP (cat.) and pentafluorophenol (0.14 g, 0.77 mmol) in tetrahydrofuran (10 ml) at 0°C and the mixture stirred for 24 h. A solution of 1 M aqueous hydrochloric acid was added and the mixture extracted with dichloromethane. The combined organics were washed with 1 M hydrochloric acid and then dried ($MgSO_4$) and the filtrate concentrated to an off-white foam. A solution of trifluoroacetic acid/dichloromethane (5.00 ml of a 1:1 v/v solution) was added to a solution of the crude bispentafluorophenyl ester in dichloromethane (5.00 ml) at 0°C and the mixture stirred for 3 h. The solvent was removed in

vacuo, and the resultant oil triturated with ether. The crude bistrifluoroacetic acid salt was then dissolved in DMF (0.60 ml) and acetonitrile (9.40 ml) and the solution added dropwise over 6 h to a refluxing solution of diisopropylethyl amine (0.54 ml) in acetonitrile (150 ml) and the mixture refluxed for a further 20 h. After cooling to room temperature the reaction mixture was filtered and the filtrate concentrated *in vacuo*, the residue was diluted with dichloromethane and washed with a 1 M solution of hydrochloric acid, dried ($MgSO_4$) and the solvent removed *in vacuo* to afford the crude product as a yellow oil which was purified by flash column chromatography with methanol-ethyl acetate-dichloromethane (0-12% in a 1:1 mixture) to furnish the title compound as a white solid (76.4 mg, 34%); mp >230°C, lit.[69] mp > 230°C; ν_{max}/cm^{-1} 3317, 2930.1, 1649.1, 1642.8, 1519.4, 1490.1, 1303.2, 731.6; δ_H (300 MHz, $CDCl_3$) 7.50 (d, *J* 8.0 Hz, 4 H, Ar*H meta* to CONH), 7.37 (bs, 2 H, CON*H*CH_2), 7.12 (d, *J* 7.5 Hz, Ar*H meta* to CONH), 7.09-7.00 (m, 8 H, Ar*H meta* and *ortho* to CH_2NHCO), 4.60 (bs, 2 H, C*H*NHCOAr), 4.50-4.40 (m, 2 H, NHCH_AH_BAr), 4.00-3.80 (bs, 8 H, ArCH_2Ar, NHCH_AH_B, $CH_2CH_AH_BNHCS$), 3.19 (bs, 2 H, $CH_2CH_AH_BNHCS$), 1.90 (bs, 4 H, $CH_AH_B(CH_2)_3NHCS$), 1.60 (bs, C$H_AH_BCH_2NHCS$), 1.32 (bs, $CH_AH_BCH_2NHCS$), 1.05 (bs, $CHCH_2CH_2$); LRMS (ES^+) *m/z* 744.8 (M + H, 20%), 766.9 (M + Na, 20%).

Diethyl 2-(acetylamino)-2-allylmalonate 29[103]

Diethyl acetamido malonate (5.00 g, 23.02 mmol) was added to a stirred suspension of sodium hydride (1.29 g, 32.26 mmol) in tetrahydrofuran (200 ml) under a nitrogen atmosphere, the mixture was allowed to stir for five minutes and then allyl bromide (1.99 ml, 27.62 mmol) and lithium iodide (cat.) were added. The reaction mixture was brought to reflux and heating continued for a futher 3 h. The mixture was allowed to cool to room temperature and ammonium chloride (150 ml) added, when effervescence had ceased the aqueous layer was extracted with dichloromethane and the organic layer dried ($MgSO_4$), the solvent was removed *in vacuo* to afford the crude product as a yellow oil which was purified by flash column chromatography using diethyl ether-petroleum ether (7:3) as eluent to afford the title product as an oil (3.56 g, 60%); δ_H(300 MHz, $CDCl_3$) 5.60 (m, 1 H, $CCH_2CH{=}CH_2$), 5.12 (d, *J* 12.7 Hz, 2

H, $CCH_2CH{=}CH_2$), 4.47 (q, *J* 8.1 Hz, 4 H, $CO_2CH_2CH_3$), 3.10 (d, *J* 8.6 Hz, 2 H, $CCH_2CH{=}CH_2$), 2.00 (s, 3 H, CH_3CONH), 1.50 (t, *J* 8.1 Hz, 6 H, $CO_2CH_2CH_3$).

2-Amino-4-pentenoic acid 30[103]

A solution of malonate derivative **29** was refluxed in a 2 M aqueous solution of hydrochloric acid for 18 h, the water was removed by freeze drying to afford the title compound as an off-white solid (2.14 g, quantitative yield); mp 168-170°C; ν_{max}/cm^{-1} 3441.39, 2998.52, 2356.54, 2342.77, 2252.79, 1748.44, 1706.13, 1581.27, 1407.97, 1330.01, 1250.4, 1162.23, 988.24, 911.68, 734.56; δ_H (300 MHz, CD_3OD) 5.80 (ddt, *J* 17.2, 9.9, 7.3, 1 H, $CH_2CH{=}CH_2$) 5.25 (bs, apparent dd, *J* 10.2, 10.2 Hz, 2 H, $CH_2CH{=}CH_2$) 4.06 (dd, *J* 6.5, 6.5 Hz, 1 H, $NHCHCH_AH_B$) 2.78-2.61 (m, 2 H, $NHCHCH_AH_B$) ; δ_C(75.5 MHz, CD_3OD) 171.4 (C), 131.7 (CH), 121.7 (CH_2), 53.4 (CH), 35.6 (CH_2).

Methyl 2-amino-4-pentenoate 31[103]

Thionyl chloride (2.06 ml, 28.25 mmol) was added to a solution of allyl glycine **30** (2.14 g, 14.13 mmol) in methanol (100 ml) at 0°C, the mixture brought to room temperature and refluxed for 4 h. The reaction mixture was cooled to room temperature and the solvent then removed *in vacuo* to afford the desired compound as a yellow oil, used directly in the next reaction (2.30 g, quantitative yield); ν_{max}/cm^{-1} 2881.6, 2342.71, 1740.31, 1507.95, 1439.61, 1229.50, 911.33, 733.22; δ_H(300 MHz, $CDCl_3$) 5.66 (ddt, *J* 17.1, 9.6, 7.2 Hz, 1 H, $CH_2CH{=}CH_2$); 4.40 (bs, 1 H, NHCH); 4.34 (bs 1 H, $CHCH_AH_B$); 3.70 (s, 3 H, CO_2CH_3); 2.47 (m, 2 H, $CHCH_AH_B$); δ_C(75.5 MHz, $CDCl_3$) 169.5 (C), 130.4 (CH), 121.3 (CH_2), 53.2 (CH_3), 34.5 (CH_2); LRMS (ES^+) *m/z* 171.1 (M + H + MeCN, 50%), 130.0 (M + H, 100%).

Methyl 2-[(*tert*-butoxycarbonyl)amino]-4-pentenoate 32[103]

A solution of methyl ester **32** (1.82 g, 13.96 mmol) and sodium hydrogen carbonate (2.35 g, 27.92 mmol) in dioxane (100 ml) and water (100 ml) was cooled to 0°C and di-*tert*-dibutyl

dicarbonate (4.57 g, 20.94 mmol) added, the reaction mixture was allowed to warm to room temperature and stirred for 5 h. The reaction mixture was extracted with dichloromethane, dried ($MgSO_4$) and concentrated *in vacuo* to give a yellow oil which was purified by flash column chromatography with methanol-dichloromethane (3%) to afford the desired compound as a yellow oil (2.60 g, 81%); ν_{max}/cm^{-1} 3440.6, 2977.0, 2336.8, 1744.9, 1709.6, 1507.2, 1437.8, 1366.5, 1159.9, 912.8, 734.5; δ_H (300 MHz, $CDCl_3$) 5.66 (ddt, *J* 17.1, 9.6, 7.2 Hz, 1 H, $CH_2CH{=}CH_2$), 5.12 (bd, *J* 3.9 Hz, 2 H, $CH{=}CH_2$), 4.34 (dd, *J* 13.2, 6.3, 1 H, $CHCH_AH_B$), 3.70 (s, 3 H, CO_2CH_3), 2.47 (m, 2 H, $CHCH_AH_B$), 1.40 (s, 9 H, $(CH_3)_3CO$); δ_C (75.5 MHz, $CDCl_3$) 172.7 (C), 155.3 (C), 132.4 (CH), 119.1 (CH_2), 80.0 (C), 53.0 (CH), 52.3 (CH_3), 36.9 (CH_2), 28.4 (CH_3); LRMS (ES^+) *m/z* 230.1 (M + H, 30%).

Methyl 2-[(tert-butoxycarbonyl)amino]-4-oxobutanoate 33

A solution of allyl glycine derivative **32** (0.30 g, 1.31 mmol) in chloroform (18 ml) was cooled to -70°C and ozone bubbled through the mixture for 30 min. Dimethyl sulfide (1 ml, 13.1 mmol) was added to the reaction mixture and the solution allowed to warm to room temperature. The solvent was removed *in vacuo* to give a colourless oil which was purified by flash column chromatography using methanol-dichloromethane (8%) to afford the title compound as a clear oil (0.26 g, 85%); δ_H (300 MHz, $CDCl_3$) 9.70 (s, 1 H, CH_2CHO), 5.40 (bs, 1 H, $NHCHCO_2$), 3.68 (s, 3 H, CO_2CH_3), 2.92 (m, 2 H, $CHCH_AH_B$), 1.46 (s, 9 H, $(CH_3)_3CO$).

(2E)-2,4-pentadienoic acid 39[109]

Acrolein (4.00 ml, 60.00 mmol) was added to a stirred solution of malonic acid (5.00 g, 48.04 mmol) in pyridine (7 ml) at 75-80°C and the mixture stirred for 4 h until evolution of carbon-dioxide had ceased. A 1 M aqueous sodium hydroxide solution was added and the mixture extracted with ethyl acetate, the aqueous layer was then acidified to pH 2 with 15% hydrochloric acid and re-extracted with ethyl acetate. The organic layer was dried and the solvent removed *in vacuo* to produce a yellow oil, which was purified by flash column chromatography with methanol-dichloromethane (3%) to afford the title compound as a white solid (0.67 g, 14%); ν

$_{max}$/cm^{-1} 3440.6, 2927.3, 1702.1, 1600.4, 1506.9, 1265.8, 1163.4, 910.3, 735.3; δ_H (300 MHz, $CDCl_3$) 11.60 (bs, 1 H, CO_2H), 7.37 (dd, *J* 15.4, 11.0 Hz, 1 H, CH_2=CHC*H*=CH), 6.50 (ddd, *J* 16.9, 10.5, 10.5 Hz, 1 H, CH_2=C*H*CH), 5.93 (d, *J* 15.3 Hz, 1 H, CH=C*H*CO_2H), 5.67 (d, *J* 16.9 Hz, 1 H, CH_TH$_C$=CHCH), 5.57 (d, J 9.9 Hz, 1 H, CH$_T$$H_C$=CHCH).

Methyl (2E)-2,4-pentadienoate 40[109]

A solution of (2E)-2,4-pentadienoate **39** (0.67 g, 6.80 mmol) and concentrated sulfuric acid (0.12 ml) in methanol (16 ml) was refluxed for 19 h. The reaction mixture was cooled to room temperature and a saturated aqueous solution of sodium bicarbonate added (8 ml). The mixture was extracted with diethyl ether, the organic layer washed with water, dried ($MgSO_4$) and the solvent removed *in vacuo* to afford a yellow oil which was used directly in the following reaction (0.37 g, 48%); δ_H (300 MHz, $CDCl_3$) 7.29 (dd, *J* 14.2, 11.0 Hz, 1 H, CH_2=CHC*H*=CH), 6.46 (ddd, *J* 17.1, 10.5, 10.5 Hz, 1 H, CH_2=C*H*CH), 5.93 (d, *J* 15.5 Hz, 1 H, CH=C*H*CO_2H), 5.62 (d, *J* 16.9 Hz, 1 H, CH_TH$_C$=CHCH), 5.50 (d, J 9.9 Hz, 1 H, CH$_T$$H_C$=CHCH), 3.76 (s, 3 H, CO_2CH_3).

(2E, 4E)-1-bromo-2,4-hexadiene 44[114]

A solution of *trans-trans*-2,4-hexadiene-1-ol (11.96 g, 121.85 mmol) in diethyl ether (100 ml) was added dropwise to phosphorous tribromide (6.37 ml, 67.02 mmol) at 0°C under a nitrogen atmosphere; the mixture was stirred for 2.5 h. The liquid was decanted off and the residue washed with two portions of diethyl ether, the solvent was removed *in vacuo* and the resulting orange liquid distilled to afford the desired compound as a clear liquid contaminated with 17% of bromide **45**; bp 58-62°C at 15 mm Hg, lit.[114] bp 59-62°C at 14 mm Hg; ν_{max}/cm^{-1} 3420.1, 2113.5, 1652.7, 1439.6, 1376.8, 1200.6, 989.1; δ_H (300 MHz, $CDCl_3$) 6.30 (dd, *J* 14.0, 10.7 Hz, 1 H, C*H*=CHCH_2), 6.09 (d, *J* 10.7 Hz, 1 H, CH_3CH=C*H*), 5.90-5.71 (m, 2 H, CH_3C*H*=CHCH=C*H*), 4.10 (d, *J* 7.9 Hz, 2 H, CHCH_2Br), 1.81 (d, J 6.6 Hz, 3 H, CH_3CH=CH); δ_C(75.5 MHz, $CDCl_3$) 135.4 (CH), 132.4 (CH), 130.3 (CH), 126.1 (CH), 34.0 (CH_2), 18.4 (CH_3).

2,5-Diethoxy-3,6-dihydropyrazine 47[127]

Triethyloxonium tetrafluoroborate (25.00 g, 131.50 mmol) in dichloromethane (35 ml) was added to a stirred refluxing solution of glycine anhydride (7.51 g, 65.82 mmol) in dichloromethane (69 ml) after 15 h a further two equivalents of triethyloxonium tetrafluoroborate (25.00 g, 131.50 mmol) in dichloromethane (35 ml) was added and the mixture refluxed for a further 18 h. The reaction mixture was cooled to room temperature and then added to a vigorously stirred saturated aqueous solution of sodium bicarbonate, when effervescence had ceased the solution was extracted with dichloromethane and the combined organics dried ($MgSO_4$) and concentrated *in vacuo* to give the desired product as a white solid (10.58 g, 95%); mp 82-84°C, lit.[127] mp 84°C; ν_{max}/cm^{-1}2979.8, 2905.3, 1709.9, 1684.1, 1481.0, 1364.7, 1349.8, 1254.5, 1132.5, 1076.1, 1028.3, 919.7, 781.9; δ_H (300 MHz, $CDCl_3$) 4.05 (q, *J* 7.7 Hz, 4 H, OCH_2CH_3), 3.48 (s, 4 H, NCH_2), 1.21 (t, *J* 7.7 Hz, 6 H, OCH_2CH_3); δ_C(75.5 MHz, $CDCl_3$) 162.3 (C), 61.0 (CH_2), 46.6 (CH_2), 14.4 (CH_3); LRMS (ES^+) *m/z* 171.1 (M + H, 100%).

3,6-di(ethyloxy)-2-[(2E, 4E)-2,4-hexadienyl] 48 and 3,6-diethyoxy-2-[(2E)-1-methyl-2,4-pentadienyl]-2,5-dihydropyrazine 49

A solution of *n*butyllithium (40.94 ml of a 1.6 M solution in hexanes) was added dropwise of **47** (9.28 g, 54.59 mmol) in tetrahydrofuran (450 ml) at -70°C under a nitrogen atmosphere, the mixture was stirred for 15 min and a solution of bromide **44** (12.30 g, 76.42 mmol) in tetrahydrofuran (50 ml) was added dropwise. The mixture was allowed to warm to room temperature over 12 h. The reaction mixture was then diluted with dichloromethane, washed with brine and the organic layers dried ($MgSO_4$) and the solvent removed *in vacuo* to afford the crude product as a brown oil which was purified by flash column chromatography using ethyl acetate-petroleum ether (0-20%) to afford the two products **48** and **49** as yellow oils, **48**: (2.03 g, 15%), ν_{max}/cm^{-1} 2977.0, 2899.9, 1744.9, 1690.4, 1369.1, 1235.7, 1031.0, 986.8, 910.9, 732.4; δ_H (300 MHz, $CDCl_3$) 6.03-5.83 (m, 2 H, CH=C*H*CH=CHCH$_3$), 5.52 (dq, *J* 13.4, 6.6 Hz, 1 H, CH=C*H*CH$_3$) 5.34 (dt, J 13.6, 7.2 Hz, 2 H, CHCH_2CH=CH), 4.20-3.98 (m, 5 H, C*H*CH$_2$CH=CH and OCH_2CH$_3$), 3.89 (d, J 3.5 Hz, 1 H, CH_AH$_B$N), 3.85 (d, J 3.5 Hz, 1 H, CH$_A$$H_B$N), 2.54-2.38

(m, 2 H, CHCH_2CH=CH), 1.64 (d, J 6.4 Hz, 3 H, CH=CHCH_3), 1.23 (t, J 7.0 Hz, 3 H, OCH$_2$CH_3); δ_C(75.5 MHz, $CDCl_3$) 164.1 (C), 162.5 (C), 134.1 (CH), 131.6 (CH), 128.2 (CH), 125.7 (CH), 61.1 (CH_2), 61.0 (CH_2), 56.2 (CH), 46.9 (CH_2), 37.5 (CH_2), 18.2 (CH_3), 14.5 (CH_3); LRMS (ES^+) *m/z* 292.3 (M + H + MeCN, 5%), 251.3 (M + H, 100%). [Found (EI) M^+, 250.1351 $C_{14}H_{22}N_2O_2$ requires M^+, 250.1681]. **49**: (1.40 g, 10%); ν_{max}/cm^{-1} 2975.6, 2928.6, 2897.9, 1690.4, 1367.7, 1230.6, 1030.5, 1002.76, 899.5; δ_H (300 MHz, $CDCl_3$) 6.24 (ddd, *J* 16.5, 9.9, 9.9 Hz, 1 H, CHC*H*=CH$_2$), 5.99 (ddd, *J* 15.6, 11.4, 0.6 Hz, 1 H, CH=C*H*CH=CH$_2$), 5.48 (dd, *J* 14.7, 8.1 Hz, 1 H, CH(CH$_3$)C*H*=CH), 5.08 (dd, *J* 16.8, 1.2 Hz, 1 H, CH=CH_TH$_C$), 4.96 (dd, *J* 9.9, 1.5 Hz, 1 H, CH=CH$_T$$H_C$), 4.26-3.96 (m, 4 H, OC$H_2CH_3$, N*H*C(CH$_3$)CH), 3.91 (d, *J* 3.7 Hz, 1 H, CCH_AH$_B$N), 3.87 (d, J 3.7 Hz, CCH$_A$$H_B$N), 2.84 (dqd, *J* 7.3, 7.3, 3.3 Hz, CH(CH$_3$)C*H*CH=CH, 1.28 (t, *J* 7.0, 6 H, OCH$_2$CH_3), 1.16 (d, J 7.0 Hz, 3 H, CH(CH_3)CH); δ_C(75.5 MHz, $CDCl_3$) 163.9 (CH), 162.4 (CH), 137.2 (CH), 135.2 (CH), 131.9, (CH), 116.0 (CH_2), 61.2 (CH_2), 61.1 (CH_2), 61.0 (CH), 46.7 (CH_2), 41.1 (CH), 16.7 (CH_3), 14.5 (CH_3), 14.4 (CH_3); LRMS (ES^+) *m/z* 251.0 (M + H, 60%). [Found 251.1773, $C_{14}H_{23}N_2O_2$ requires 251.1759].

Ethyl (4E)-2-amino-4,6-octadienoate 50

A 15% solution of hydrochloric acid (14.22 ml) was added to a solution of **48** (1.42 g, 5.69 mmol) in 1,4-dioxane (197 ml) at room temperature and the mixture stirred for 3 h. The solvent was removed *in vauo* at 40°C, the residual hydrochloride salt was dissolved in water (100 ml), 30% ammonia solution was added (14.22 ml) and the mixture extracted with diethyl ether. The organic layer was dried ($MgSO_4$) and concentrated to afford the title compound as a yellow oil (1.68 g, quantitative); ν_{max}/cm^{-1} 3017.5, 2980.0, 2934.8, 1735.7, 1188.3, 989.3; δ_H (300 MHz, $CDCl_3$) 6.18-5.93 (m, 6 H, CH=C*H*C*H*=CHCH$_3$), 5.64 (dq, *J* 13.4, 6.6 Hz, 1 H, CH=C*H*CH$_3$), 5.47 (dt, *J* 14.5, 7.4 Hz, 1 H, CH$_2$C*H*=CH), 4.19 (q, *J* 7.3 Hz, OCH_2CH$_3$), 3.51 (dd, *J* 7.3, 5.1 Hz, 1 H, CH$_2$C*H*NH$_2$), 2.60-2.13 (m, 2 H, C$H_A$$H_B$CHNH$_2$), 1.75 (d, *J* 6.6 Hz, CH=CHCH_3), 1.61 (bs, 2 H, CHNH_2), 1.30 (t, J 7.0 Hz, 3 H, CH$_2$CH_3); δ_C(75.5 MHz, $CDCl_3$) 175.4 (CO), 134.4 (CH), 131.2 (CH), 128.8 (CH), 125.5 (CH), 61.1 (CH_2), 54.4 (CH), 38.2 (CH_2), 18.2 (CH_3), 14.4 (CH_3); LRMS (CI) *m/z* 184 (M + H, 100%), 367 (2 M + H, 10%). [Found 184.1341 $C_{10}H_{18}NO_2$ requires 184.1337].

Ethyl (4E,6E)-2-(acryloylamino)-4,6-octadienoate 51

Acryloyl chloride (0.43 ml, 5.40 mmol) was added to a stirred solution of amino ester **50** (0.76 g, 4.15 mmol) and triethylamine (0.87 ml, 6.20 mmol) in dry dichloromethane (76 ml) at -78°C under a nitrogen atmosphere. The mixture was allowed to warm to room temperature over 18 h and then a saturated aqueous solution of sodium hydrogen carbonate was added. The aqueous layer was extracted with dichloromethane and the organics dried ($MgSO_4$) and concentrated to a yellow oil which was then purified by flash column chromatography eluting with ethyl acetate-dichloromethane (5%) to afford the product as a yellow oil (0.88 g, 89%); mp 56-58°C; ν_{max}/cm^{-1} 3278.8, 2982.7, 2359.2, 1739.9, 1660.3, 1629.7, 1538.0, 1206.0, 988.0; δ_H (300 MHz, $CDCl_3$) 6.32 (d, *J* 16.9 Hz, 1 H, COCH=CH_TH_C), 6.17 (dd, *J* 16.7, 10.1 Hz, 1 H, COC*H*=CH_TH_C), 6.13-5.91 (m, 2 H, CH=C*H*C*H*=CHCH$_3$), 5.69 (d, *J* 9.9 Hz, 1 H, COCH=CH_TH_C), 5.63 (m, 1 H, CH=C*H*CH$_3$), 5.38 (dt, *J* 21.7, 7.4 Hz, 1 H, CH_2C*H*=CHCH), 4.71 (dt, *J* 7.53, 5.3 Hz, CH_2C*H*NH), 4.23 (q, *J* 3.3 Hz, OCH_2CH$_3$), 2.62 (dd, *J* 12.5, 5.9 Hz, 2 H, CHCH_2CH=CH), 1.74 (d, J 6.6 Hz, 3 H, CH=CHCH_3), 1.29 (t, *J* 7.2 Hz, 3 H, OCH_2CH_3); δ_C(75.5 MHz, $CDCl_3$) 171.9 (C), 165.1 (C), 134.8 (CH), 131.0 (CH), 130.5 (CH), 129.3 (CH), 127.2 (CH_2), 124.0 (CH), 61.7 (CH_2), 52.2 (CH), 35.5 (CH_2), 18.2 (CH_3), 14.4 (CH_3); LRMS (ES^+) *m/z* 238.3 (M + H, 80%), 475.6 (2 M + H, 10%). [Found 238.1441 $C_{13}H_{20}NO_3$ requires 238.1443].

(4E, 6E)-2-(acryloylamino)-4,6-octadienoic acid 52

Lithium hydroxide (1.69 ml of a 1 M aqueous solution) was added to a solution of amino ester **51** (0.10 g, 0.42 mmol) in 1,4-dioxane (10.6 ml) and the mixture stirred at room temperature for 2 h. The solvent was removed *in vacuo* and the residue diluted with water, the aqueous was washed with ethyl acetate and then acidified to pH 2 using a 15% solution of hydrochloric acid. The solution was then re-extracted with ethyl acetate, the organic layers dried ($MgSO_4$) and concentrated to a white solid (83.0 mg, 95%) which was immediately reacted on.

Tributyl(propyl)ammonium (4E, 6E)-2-(acryloylamino)-4,6-octadienoate 26

Acid **52** was dissolved in methanol (5 ml) and *n*-tetrabutylammonium hydroxide (14.0 µl of a 1 M aqueous solution) was added the mixture was stirred for 10 min, the solvent evapourated *in vacuo* and the residual water removed by freeze drying to afford the desired compound as a yellow oil (13.3 mg, quantitative); ν_{max}/cm^{-1} 2958.5, 2342.6, 2252.6, 1747.1, 1701.8, 1605.4, 1377.5, 1258.5, 911.2, 733.3; δ_H (300 MHz, $CDCl_3$) 6.18-6.06 (m, 2 H, COC*H*=CH_TH_C, COCH=CH_TH_C), 5.98-5.85 (m, 2 H, CH=C*H*C*H*=$CHCH_3$), 5.04-5.41 (m, 3 H, CH_2CH=CHCH, CH=C*H*CH_3, COCH=CH_TH_C), 4.28 (dd, *J* 12.8, 6.8 Hz, CH_2CHNH), 3.20 (bs, 8 H, $NCH_2CH_2CH_2CH_2CH_3$), 2.62 (bs, 2 H, $CHCH_2CH$=CH), 1.66-1.50 (m, 11 H, CH=$CHCH_3$, $NCH_2CH_2CH_2CH_2CH_3$), 1.38 (bs, 8 H, $NCH_2CH_2CH_2CH_2CH_2CH_3$), 0.93 (t, *J* 7.7 Hz, 12 H,$NCH_2CH_2CH_2CH_2CH_3$).

Ethyl (4E)-2-amino-3-methyl-4,6-heptadienoate 53

15% Hydrochloric acid (8.81 ml, 17.70 mmol) was added to a solution of **49** (0.88 g, 3.54 mmol) in dioxane (121 ml) and the mixture stirred at room temperature for 3 h. The dioxane was removed *in vacuo* at 40°C, the residue taken up in water (100 ml), 30% ammonia solution added (8.81 ml) and the mixture extracted with diethyl ether. The organic layers were combined, dried ($MgSO_4$) and concentrated to a brown oil which was used directly in the subsequent reaction (0.64 g, quantitative yield); δ_H (300 MHz, $CDCl_3$) 6.32 (ddd, *J* 16.9, 10.1, 10.1 Hz, 1 H, CH=CHC*H*=CH_2), 6.10 (dd, *J* 14.9, 10.1, 1 H, CH=C*H*CH=CH_2), 5.60 (dd, *J* 15.1, 7.9 Hz, 1 H, C*H*=CHCH=CH_2), 5.16 (d, *J* 16.9 Hz, 1 H, CH=CH_TH_C), 5.03 (d, *J* 9.9 Hz, 1 H, CH=CH_TH_C), 4.29-4.10 (m, 2 H, OCH_2CH_3), 2.65 (dqd, *J* 6.81, 6.81, 6.81 Hz, 1 H, C*H*(CH_3)$CHNH_2$), 1.30 (t, *J* 7.2, 3 H, OCH_2CH_3), 1.13 (d, *J* 6.8 Hz, 3 H, CH(CH_3)$CHNH_2$); LRMS (CI) *m/z* 184.0 M + H, 100%). [Found 184.1335 $C_{10}H_{18}NO_2$ requires 184.1337].

Ethyl (4E)-2-(acryloylamino)-3-methyl-4,6-heptadienoate 54

A solution of amino ester **53** (0.48 g, 2.60 mmol) and triethylamine (0.54 ml, 3.90 mmol) in dry dichloromethane (48 ml) was cooled to -78°C under nitrogen. Acryloyl chloride (0.20 ml, 3.40 mmol) was added and the mixture allowed to come to room temperature over 18 h. A saturated aqueous solution of sodium hydrogen carbonate was added and the aqueous layers extracted with dichloromethane, the organic layer was dried ($MgSO_4$) and concentrated to a brown oil which was purified by flash column chromatography using ethyl acetate-petroleum ether (15-20%) to afford the title compound as a brown oil (0.24 g, 40%); δ_H (300 MHz, $CDCl_3$) 6.37-6.03 (m, 4 H, CH=C*H*C*H*=CH_2, COC*H*=CH_TH$_C$), 5.96 (bs, 1 H, N*H*CO), 5.68 (dd, *J* 9.9, 1.5 Hz, 1 H, COCH=CH$_T$*H*$_C$), 5.56 (dd, *J* 15.0, 7.3 Hz, C*H*=CHCH=CH_2), 5.16 (d, *J* 16.5 Hz, 1 H, CH=CHCH=CH_TH$_C$), 5.06 (d, *J* 9.9 Hz, 1 H, CH=CH$_T$*H*$_C$), 4.72 (dd, *J* 8.4, 4.7 Hz, 1 H, C*H*NHCO), 4.30-4.25 (m, 2 H, OCH_2CH$_3$), 2.88 (dqd, *J* 7.7, 7.7, 7.7 Hz, C*H*(CH$_3$)CHNH$_2$), 1.28 (t, J 7.3 Hz, 3 H, , OCH$_2$CH_3), 1.10 (d, *J* 7.0 Hz, 3 H, CH(CH_3)CHNH$_2$); LRMS (ES$^+$) *m/z* 260 (M + Na, 10%), 238 (M + H, 100%). [Found 238.1440 $C_{13}H_{20}NO_3$ requires 238.1443].

(4E)-2-(acryloylamino)-3-methyl-4,6-heptadienoic acid 55

Lithium hydroxide (3.97 ml of a 1 M aqueous solution) was added to a solution of amino ester **54** (0.23 g, 0.99 mmol) in 1,4-dioxane (25 ml), the mixture stirred at room temperature for 2 h and the solvent then removed *in vacuo*. The residue was diluted with water, the aqueous washed with ethyl acetate and then acidified to pH 2 using a 15% solution of hydrochloric acid. The solution was then re-extracted with ethyl acetate, the organic layers dried ($MgSO_4$) and concentrated to a white solid (0.17 g, 81%) which was reacted on immediately.

Tributyl(propyl)ammonium (4E)-2-(acyloylamino)-3-methyl-4,6-heptadienoate 27

Acid **55** was dissolved in methanol (5 ml) and *n*-tetrabutylammonium hydroxide (0.72 ml of a 1 M aqueous solution) was added the mixture was stirred for 10 min, the solvent evapourated *in vacuo* and the residual water removed by freeze drying to afford the desired compound as a

yellow oil (0.32 g, quantitative yield); δ_H (300 MHz, $CDCl_3$) 6.37-6.03 (m, 4 H, CH=C*H*CH=CH_2, COC*H*=C$H_T$$H_C$), 5.60 (dd, *J* 8.7, 4.3 Hz, C*H*=CHCH=CH_2), 5.09 (d, *J* 17.1 Hz, 1 H, CH=CHCH=C$H_T$$H_C$), 4.92 (d, *J* 9.4 Hz, 1 H, CH=C$H_T$$H_C$), 4.30 (dd, *J* 18.4, 8.1 Hz, 1 H, C*H*NHCO), 3.29 (bs, 8 H, C$H_2$$CH_2$$CH_2$$CH_3$), 2.93 (bs, C*H*($CH_3$)$CHNH_2$), 1.62 (bs, 8 H, CH_2C$H_2$$CH_2$$CH_3$), 1.45 (dq, *J* 8.1 Hz, 8 H, $CH_2$$CH_2CH_2$$CH_3$), 1.01 (t, *J* 8.5 Hz, 12 H, $CH_2$$CH_2$$CH_2CH_3$).

Methyl (2R)-2-{[(4E, 6E)-2-(acryloylamino)-4,6-octadienoyl]amino}-propanoate 56

1-(3-dimethylaminopropyl)-3-ethylcarbodiimide hydrochloride (91.90 mg, 0.48 mmol) was added to a stirred solution of racemic acid **52** (83.50 mg, 0.4 mmol), L-alanine methyl ester hydrochloride (55.70 mg, 0.40 mmol), HOBt (65.10 mg, 0.48 mmol) and diisopropylethyl amine (0.14 ml, 0.80 mmol) in dimethyl formamide (0.24 ml) and tetrahydrofuran (1.17 ml) at 0°C under a nitrogen atmosphere, the reaction mixture was allowed to warm to room temperature over 19 h. The reaction mixture was diluted with dichloromethane and washed with a 1 M solution of hydrochloric acid, a saturated aqueous solution of sodium hydrogen carbonate and then dried ($MgSO_4$), the solvent was removed *in vacuo* to afford a yellow oil which was purified by flash column chromatography using methanol-dichloromethane (1%) to give the pure product as a pair of diastereoisomers (37.00 mg, 30%);ν_{max}/cm^{-1} 3263.54, 2933.24, 2351.19, 1734.76, 1646.15, 1616.54, 1542.61, 1202.38, 1162.89, 1059.35, 990.24; δ_H (300 MHz, $CDCl_3$) 6.80 (bs, 1 H, CN*H*CH), 6.41 (bs, 1 H, CHN*H*C(CH_3)CO), 6.22 (d, *J* 16.8 Hz, 1 H, COC*H*=$CH_T$$H_C$), 6.00-5.91 (m, 2 H, CH=C*H*C*H*=$CHCH_3$), 5.62 (d, J 10.3 Hz, 1 H, COCH=$CH_T$$H_C$), 5.56 (m, 1 H, CH=C*H*$CH_3$), 5.40 (dt, J 18.6, 1.9 Hz, 1 H, $CHCH_2$C*H*=CH), 4.59-4.39 (m, 2 H, CH_2C*H*NHCO, NHC*H*(CH_3)CO_2), 3.57 (s x 2, 3 H, CO_2CH_3), 2.50 (bs, 2 H, NHCHCH_2CH=CH), 1.65 (d, *J* 5.6 Hz, 3 H, CH=CHCH_3), 1.31 (d x 2, *J* 7.5 Hz, NHCH(CH_3)CO_2); δ_C(75.5 MHz, $CDCl_3$) 173.4 (C), 173.3 (C), 171.0 (C), 170.8 (C), 165.8 (C), 165.7 (C), 135.1 (CH), 131.5 (CH), 131.3 (CH), 130.8 (CH), 130.7 (CH), 130.0 (CH), 129.5 (CH), 129.4 (CH), 127.6 (CH_2), 127.5 (CH_2), 127.3 (CH), 125.0 (CH), 53.2 (CH), 53.1(CH), 53.0 (CH), 48.6 (CH_3), 48.5 (CH_3), 36.1 (CH_2), 36.1 (CH_2), 18.6 (CH_3), 18.5 (CH_3), 18.4 (CH_3);

LRMS (ES^+) *m/z* 295.3 (M + H, 20%), 317.4 (M + Na, 20%). [Found 294.1581 $C_{15}H_{22}N_2O_4$ requires 294.1579].

Ethyl 7-methyl-1-methylene-1, 2, 3, 4, 4a, 7, 8, 8a-octahydro-3-isoquinoline carboxylate 57a and 57b

Using the method employed by Mellor,[130] a solution of triene **51** (0.20 g, 0.84 mmol) in xylenes (10 ml) with a trace of hyroquinone was refluxed for 8 h. The reaction mixture was cooled to room temperature and then concentrated to a brown liquid which was then purified by flash column chromatography using ether-petroleum (50%) to afford the two products **57a (*cis*)**: (96.50 mg, 48%); mp 88-92°C; ν_{max}/cm^{-1} 3074.9, 2959.9, 2951.0, 2843.9, 2361.0, 1739.1, 1657.4, 1479.9, 1404.9, 1259.7, 1223.1, 1157.8, 1034.2, 799.8, 744.6; δ_H (300 MHz, $CDCl_3$) 6.48 (bs, 1 H, CHN*H*), 5.60-5.49 (m, 2 H, CH=C*H*CHCH$_3$), 4.21 (dq, *J* 7.2, 2.4 Hz, 2 H, OC*H*$_2$CH$_3$), 4.06 (dd, *J* 12.0, 4.0 Hz, 1 H, CH$_A$H$_B$C*H*NH), 2.58 (dddd, *J* 13.1, 6.3, 3.0, 1.0 Hz, 1 H, CH$_A$H$_B$C*H*CONH), 2.47 (m, 1 H, C*H*CH$_A$H$_B$CHNH), 2.25 (bs, 1 H, CH=CHC*H*CH$_3$), 2.22 (bs, 1 H, CHC*H*$_A$H$_B$CHNH), 2.15 (m, 1 H, C*H*$_A$H$_B$CHCONH), 1.53 (ddd, *J* 13.4, 12.0, 12.0 Hz, 1 H, CHCH$_A$*H*$_B$CHNH), 1.28 (t, J 7.2 Hz, 3 H, OCH$_2$C*H*$_3$), 1.15 (ddd, *J* 13.0, 13.0, 11.0 Hz, 1 H, CH$_A$*H*$_B$CHCONH), 0.97 (d, J 7.0 Hz, 3 H, CH=CHCHC*H*$_3$); δ_C(75.5 MHz, $CDCl_3$) 174.6 (C), 170.6 (C), 135.4 (CH), 127.2 (CH), 62.1 (CH_2), 54.6 (CH), 40.2 (CH), 32.9 (CH), 31.9 (CH_2), 31.4 (CH), 29.4 (CH_2), 21.4 (CH_3), 14.3 (CH_3); LRMS (ES^+) m/z 238.3 (M + H, 60%), 475.6 (2 M + H, 100%). **57b (*trans*)**: (28.40 mg, 14%); ν_{max}/cm^{-1} 2963, 2150, 1754, 1663, 1362, 1202; δ_H (300 MHz, $CDCl_3$) 6.07 (bs, 1 H, CHN*H*), 5.69 (bs, 1 H, CH=C*H*CHCH$_3$), 5.48 (d, *J* 9.9 Hz, CHC*H*=CHCHCH$_3$), 4.21 (q, *J* 7.2 Hz, 2 H, OC*H*$_2$CH$_3$), 4.15 (dt, *J* 7.4, 2.0 Hz, 1 H, CH$_A$H$_B$C*H*NH), 2.40 (bs, 1 H, CH=CHC*H*CH$_3$), 2.35 (bs, 1 H, C*H*$_A$H$_B$CHNH), 2.20 (bs, 1 H, C*H*$_A$H$_B$CHCONH), 2.15 (bs, 1 H, C*H*CH$_A$H$_B$CHNH), 2.01 (td, J 12.5, 2.0 Hz, 1 H, CH$_A$H$_B$C*H*CONH), 1.85 (ddd, *J* 13.2, 13.2, 7.4 Hz, 1 H, CH$_A$*H*$_B$CHNH), 1.63 (ddd, J 13.1, 13.1, 6.6 Hz, 1 H, CH$_A$*H*$_B$CHCONH), 1.29 (t, *J* 7.2 Hz, 3 H, OCH$_2$C*H*$_3$), 1.03 (d, *J* 7.2 Hz, 3 H, CH=CHCHC*H*$_3$); δ_C(75.5 MHz, $CDCl_3$) 174.2 (C), 172.0 (C), 134.9 (CH), 128.0 (CH), 62.1 (CH_2), 53.6 (CH), 39.6 (CH), 33.8 (CH), 31.1 (CH_2), 29.7 (CH), 28.8 (CH_2), 21.4 (CH_3), 14.3 (CH_3);

6-Chloro-3-pyridyl cyanide 61

A solution of 6-chloronicotinamide (1.00 g, 6.38 mmol), thionyl chloride (1.40 ml, 19.16 mmol) and DMF (0.92 ml) in dichloromethane (5 ml) was stirred at room temperature under nitrogen for 5 h. Water was added and the mixture extracted with dichloromethane, the organics were then washed with water, dried ($MgSO_4$) and the solvent removed *in vacuo* to afford the title compound as a white solid (0.75 g, 85%); ν_{max}/cm^{-1} 3087.1, 3046.9, 2233.7, 1579.6, 1545.9, 1370.0, 1108.0, 855.3; δ_H (300 MHz, $CDCl_3$) 8.71 (s with fine splitting, 1 H, NC*H*CCN), 7.96 (d with fine splitting, *J* 8.6 Hz, 1 H, CHC*H*CCN), 7.52 (d, *J* 8.6 Hz, 1 H, ClCC*H*CHCN); δ_C(75.5 MHz, $CDCl_3$) 155.8 (C), 152.8 (CH), 141.5 (CH), 125.1 (CH), 115.8 (C), 109.0 (C).

Methyl 4-[(5-cyano-2-pyridyl)oxy] benzoate 63

Methyl 4-hydroxybenzoate (0.58 g, 3.84 mmol) was dissolved in distilled dimethyl sulfoxide (6.60 ml) and sodium hydride (0.17 g, 4.23 mmol) added carefully, after stirring at room temperature under a nitrogen atmosphere for 10 min, **61** (0.53 g, 3.84 mmol) was added and the solutin heated at 120°C for 15 h. The mixture was allowed to cool to room temperature and then poured onto brine and dichloromethane, the layers were separated and the aqueous extracted with dichloromethane, the organic layers were then washed with water, dried ($MgSO_4$) and concentrated to a brown solid which was recrystallised from ethanol to afford the title compound as a fluffy light brown solid (0.39 g, 40%); mp. 90-91°C; ν_{max}/cm^{-1} 3425.5, 2956.5, 2365.0, 2231.1, 1714.9, 1589.8, 1476.7, 1432.2, 1378.3, 1272.6, 911.3, 735.3; δ_H (300 MHz, $CDCl_3$) 8.52 (s with fine splitting, J 1.83, 1 H, CC*H*N), 8.14 (d, *J* 8.6 Hz, 1 H, Ar*H meta* to CO_2CH_3), 7.97 (d with fine splitting, *J* 8.6, 2.4 Hz, 1 H, Ar*H ortho* to CN), 7.23 (d, *J* 8.6 Hz, 2 H, Ar*H ortho* to CO_2CH_3), 7.09 (d, *J* 8.5 Hz, 1 H, Ar*H meta* to CN), 3.93 (s, 3 H, CO_2CH_3); δ_C(75.5 MHz, $CDCl_3$) 166.4 (C), 165.1 (C), 156.5 (CH), 152.2 (CH), 142.6 (CH), 131.7 (CH), 127.7 (C), 121.5 (CH), 116.7 (C), 112.5 (CH), 104.9 (C), 52.4 (CH_3).

Methyl 4-[4-(aminomethyl) phenoxy] benzoate 64

10% Palladium on charcoal (78 mg) was added to a solution of nitrile **63** (0.36 g, 1.42 mmol) in methanol saturated with ammonia (8 ml) was stirred under a static hydrogen atmosphere for 8 h. The reaction mixture was then filtered through celite and the residue washed with methanol, the solvent was removed *in vacuo* to furnish the title compound as a clear oil (0.32 g, 88%); mp 260-262°C; ν_{max}/cm^{-1} 3426.8, 2988.3, 2361.68, 1713.9, 1668.5, 1597.0, 1480.8, 1397.4, 1274.5, 1256.5, 1112.0, 911.6, 735.3; δ_H (300 MHz, $CDCl_3$) 8.10 (s, 1 H, Ar*H ortho* to N), 8.05 (d, *J* 8.5 Hz, 2 H, Ar*H ortho* to CO_2CH_3), 7.72 (d, *J* 6.1 Hz, 1 H, Ar*H ortho* to CH_2NH_3Cl), 7.10 (d, *J* 8.5 Hz, 2 H, Ar*H meta* to CO_2CH_3), 6.90 (d, *J* 8.3 Hz, 1 H, Ar*H meta* to CH_2NH_3Cl), 3.90 (s, 3 H, CO_2CH_3), 3.79 (s, 2 H, $ArCH_2NH_3Cl$); δ_C(75.5 MHz, $CDCl_3$) 166.1 (C), 149.8 (CH), 143.0 (CH), 131.6 (CH), 121.3 (CH), 121.2 (CH), 112.4 (CH), 52.6 (CH_3), 47.1 (CH).

Methyl 4-(4 [[1-[5-amino-1-[(tert-butoxycarbonyl) amino] pentyl) vinyl) amino] methyl] phenoxy] benzoate 65

A solution of amine **64** (0.32 g, 1.24 mmol) in dichloromethane (4 ml) was cooled to 0°C TBTU (0.44 g, 1.36 mmol), Boc-lys(Z)OH (0.52 g, 1.36 mmol) and diisopropylethyl amine (0.65 ml, 3.72 mmol) were added and the mixture stirred at room temperature for 3 h. The reaction mixture was diluted with dichloromethane, and washed with a saturated aqueous solution of sodium hydrogen carbonate, a 1 M solution of $KHSO_4$ and then washed again with saturated sodium hydrogen carbonate solution. The organics were dried ($MgSO_4$) and concentrated to a yellow oil, purified by flash column chromatography using ethyl acetate-petrol (50%) to afford the desired product as a yellow oil (0.19 g, 24%); ν_{max}/cm^{-1} 2967.9, 2364.5, 2252.7, 1669.8, 1596.2, 1507.3, 1476.8, 1278.8, 1245.8, 1162.3, 906.0, 725.6; δ_H (300 MHz, $CDCl_3$) 7.97 (s, 1 H, Ar*H ortho* to N), 7.87 (d, *J* 8.5 Hz, 2 H, Ar*H ortho* to CO_2CH_3), 7.59 (d, *J* 8.5 Hz, 1 H, Ar*H meta* to N), 7.07 (d, *J* 8.8 Hz, 1 H, Ar*H para* to N), 6.83 (d, *J* 8.5 Hz, 2 H, Ar*H meta* toCO_2CH_3), 6.73 (bs, 1 H, $CH_2NHCOCH$), 5.14 (bd, *J* 7.0 Hz, 1 H, $CHNHCO_2$), 5.00 (bs, 2 H, OCH_2CH_3), 4.85 (bs, 1 H, CH_2NHCO),4.31 (bs, 2 H, $ArCH_2NH$), 3.97 (bs, 1 H, NHCOC*H*), 3.83 (s, 3 H, OCH_2CH_3), 3.10 (bs, 2 H, CH_2CH_2NHCO), 1.40-1.59 (m, 6 H, $CHCH_2CH_2CH_2CH_2NH$), 1.33

(s, 9 H, C(CH_3)$_3$); δ_C(75.5 MHz, $CDCl_3$) 172.7 (C), 166.9 (C), 162.6 (C), 158.7 (C), 157.1 (C), 156.4 (C), 147.2 (CH), 140.0 (CH), 136.9 (C), 131.9 (CH), 130.0 (C), 128.9 (CH), 128.6 (CH), 128.5 (CH), 120.7 (CH), 112.7 (CH), 80.7 (C), 67.1 (CH_2), 54.9 (CH), 52.5 (CH_3), 40.6 (CH_2), 31.8 (CH_2), 29.9 (CH_2), 28.7 (CH_3), 22.9 (CH_2); LRMS (ES^+) *m/z* 621.4 (M + H, 60%).

Methyl 4-[4-({[1-[(tert-butoxycarbonyl)amino]-5-({[(4-{[({[5-[(tert-butyoxycarbonyl)amino-5-({4-[4-(methyoxycarbonyl)benzyl]benzyl}amino)pentyl]amino}carbothioyl)amino]methyl}benzyl)amino]carbothioyl}amino)pentyl]amino}methyl)benzyl]benzoate 75

Following a modified method of Pernia,[69] potassium carbonate (0.43 ml of a 0.4 M aqueous solution) was added to a solution of isothiocyanate **22** (0.20 g, 0.38 mmol) and *p*-xylenediamine (25.90 mg, 0.19 mmol) in chloroform (1.2 ml) and the solution refluxed for 20 h. The reaction mixture was allowed to cool to room temperature and a saturated solution of sodium hydrogen carbonate added, the aqueous layer was extracted with chloroform and the organic layer dried ($MgSO_4$) and concentrated to a yellow oil which solidified overnight. The solid was recrystallised from ethyl acetate-dichloromethane (75%) to afford a fluffy pale yellow solid (0.13 g, 59%); mp 118-120°C; ν_{max}/cm^{-1} 1720, 1642, 1559, 1509, 1456, 1365, 1280, 1166, 1110, 1095, 748; δ_H (300 MHz, $CDCl_3$) 8.26 (bt, *J* 5.7 Hz, 2 H, CON*H*CH_2Ar), 7.86 (d, *J* 8.3 Hz, 4 H, Ar*H* *ortho* to CO_2CH_3), 7.73 (bs, 2 H, ArCH_2N*H*CS), 7.46 (bs, 2 H, ArCH_2NHCSN*H*), 7.37 (d, *J* 8.3 Hz, 4 H, Ar*H* *meta* to CO_2CH_3), 7.17 (s, 12 H, Ar*H*CH_2Ar, Ar*H*CH_2NHCS), 6.85 (bd, *J* 7.9 Hz, 2 H, CHN*H*CO_2), 4.60 (bs, 2 H, ArCH_2NHCS), 4.23 (bd, J 7.9 Hz, 4 H, CONHCH_2Ar), 3.99 (s, 4 H, ArCH_2Ar), 3.89 (bs, 2 H, C*H*NHCO_2), 3.82 (s, 6 H, CO_2CH_3), 1.65-1.20 (m, 8 H, CHCH_2CH_2CH_2CH_2), 1.37 (s, 18 H, C(CH_3)$_3$); δ_C(75.5 MHz, $CDCl_3$) 172.7 (C), 166.6 (C), 155.8 (C), 147.6 (C), 139.2 (C), 137.8 (C), 129.8 (CH), 129.4 (CH), 128.9 (CH), 128.8 (CH), 127.7 (CH), 127.6 (CH), 78.4 (C), 55.4 (C), 54.9 (CH), 52.4 (CH_3), 42.1 (CH_2), 41.0 (CH_2), 32.1 (CH_2), 28.9 (CH_3), 23.5 (CH_2); LRMS (ES^+) *m/z* 1188.7 (M + H, 20%), 1211.2 (M + Na, 10%). [Found: C, 64.09; H, 6.97; N, 9.26; S, 5.37. $C_{62}H_{76}N_8O_{10}S_2$ requires C, 64.73; H, 6.96; N, 9.44; S, 5.40%].

4-[4-({[1-[(tert-butoxycarbonyl)amino]-5-({[(4-{[({[5-[(tert-butyoxycarbonyl)amino-5-(4-[4-(carboxybenzyl)benzyl]amino)pentyl]amino}carbothioyl)amino]methyl}benzyl)amino] carbothioyl}amino)pentyl]amino}methyl)benzyl]benzoic acid 76

Following the methods described by Pernia,[69] lithium hydroxide (0.34 ml of a 1 M aqueous solution) was added to a solution of dimethyl ester **75** (0.14 g, 0.12 mmol) in dioxane (1.72 ml) was stirred at 55°C for 24 h. The reaction mixture was allowed to cool to room temperature and then a 1 M solution of hydrochloric acid added until a permanent white precipitate was observed, the solution was extracted with ethyl acetate and then dried ($MgSO_4$), the filtrate was concentrated *in vacuo* to a crispy solid (0.12 g, 86%); δ_H (300 MHz, $CDCl_3$) 7.86 (d, *J* 8.1 Hz, 4 H, Ar*H ortho* to CO_2CH_3), 7.55 (bs, 2 H, $ArCH_2NHCS$), 7.30 (bs, 2 H, $ArCH_2NHCSNH$),), 7.19 (s, 4 H, $ArHCH_2NHCS$), 7.18 (d, *J* 8.3 Hz, 4 H, Ar*H meta* to CO_2CH_3), 7.11 (d, *J* 8.1 Hz, 4 H, Ar*H ortho* to CH_2Ar), 7.04 (d, *J* 8.1 Hz, 4 H, Ar*H meta* to CH_2Ar), 6.99 (bs, 2 H, $CONHCH_2Ar$), 6.79 (bs, 2 H, $CHNHCO_2$), 4.61 (bs, 2 H, $ArCH_2NHCS$), 4.24 (bs, 4 H, $CONHCH_2Ar$), 4.00 (bs, 2 H, $CHNHCO_2$), 3.90 (s, 4 H, $ArCH_2Ar$), 3.82 (bs, 4 H, $CSNHCH_2CH_2$), 1.78-1.40 (m, 12 H, $CHCH_2CH_2CH_2CH_2$), 1.32 (s, 18 H, $C(CH_3)_3$. [Found: C, 62.01; H, 6.96; N, 9.05; S, 5.30. $C_{62}H_{76}N_8O_{10}S_2$ requires C, 64.42; H, 6.78; N, 9.66; S, 5.53%].

Methyl 4-[4-({[1-[(tert-butoxycarbonyl)amino]-5-({[(3-{[({[5-[(tert-butyoxycarbonyl)amino-5-({4-[4-(methyoxycarbonyl)benzyl]benzyl}amino)pentyl]amino}carbothioyl)amino] methyl}benzyl)amino]carbothioyl}amino)pentyl]amino}methyl)benzyl]benzoate 78

Following a modified procedure of Pernia,[69] potassium carbonate (1.47 ml of a 0.4 M aqueous solution) was added to a solution of isothiocyanate **22** (0.62 g, 1.17 mmol) and *m*-xylenediamine (77.40 µl, 0.59 mmol) in chloroform (5.86 ml) and the solution refluxed for 16 h. The reaction mixture was allowed to cool to room temperature; a saturated aqueous solution of sodium hydrogen carbonate was added, the mixture extracted with dichloromethane and the organics dried ($MgSO_4$). The solvent was removed *in vacuo* to afford a yellow foam which was purified by flash column chromatography using methanol-dichloromethane (1%) to afford the desired compound as a white solid (0.45 g, 65%);mp 110-112°C; δ_H (300 MHz, $CDCl_3$) 8.26 (bs, 2 H,

CON*H*CH_2Ar), 7.87 (d, J 8.1 Hz, 4 H, Ar*H ortho* to CO_2CH_3), 7.77 (bs, 2 H, CH_2N*H*CS), 7.49 (bs, 2 H, CH_2NHCSN*H*), 7.35 (d, *J* 8.0 Hz, 4 H, Ar*H meta* to CO_2CH_3), 7.17 (s, 12 H, Ar*H*CH_2Ar, Ar*H*CH_2NHCS), 6.89 (bd, *J* 7.5 Hz, 2 H, CHN*H*CO), 4.67 (bs, 4 H, ArCH_2NHCS), 4.25 (bd, *J* 5.0 Hz, 4 H, CONHCH_2Ar), 3.99 (s, 4 H, ArCH_2Ar), 3.87 (bs, 2 H, C*H*CONH), 3.82 (s, 3 H, CO_2CH_3), 1.82-1.21 (m, 16 H, $CH_2CH_2CH_2CH_2$CH), 1.49 (s, 18 H, $C(CH_3)_3$); δ_C(75.5 MHz, $CDCl_3$) 173.6 (C), 167.5 (C), 156.7 (C), 148.5 (C), 140.8 (C), 140.1 (C), 138.7 (C), 130.7 (C), 130.3 (C), 130.0 (C), 129.8 (CH), 129.5 (CH), 128.9 (CH), 128.7 (CH), 128.6 (CH), 127.6 (CH), 127.1 (CH), 79.3 (C), 55.8 (CH), 53.3 (CH_3), 48.3 (CH_2), 44.9 (CH_2), 43.0 (CH_2), 41.8 (CH_2), 32.9 (CH_2), 29.8 (CH_2), 29.5 (CH_3), 24.4 (CH_2). [Found: C, 62.49; H, 6.73; N, 9.08; S, 5.52. $C_{62}H_{76}N_8O_{10}S_2$ requires C, 64.73; H, 6.96; N, 9.44; S, 5.40%].

4-[4-({[1-[(tert-butoxycarbonyl)amino]-5-({[(3-{[({[5-[(tert-butyoxycarbonyl)amino-5-(4-[4-(carboxybenzyl)benzyl]amino)pentyl]amino}carbothioyl)amino]methyl}benzyl)amino] carbothioyl}amino)pentyl]amino}methyl)benzyl]benzoic acid 79

Following Pernia's method,[69] lithium hydroxide (0.24 ml of 1 M aqueous solution) was added to a solution of dimethyl ester **78** (0.2 g, 0.69 mmol) in dioxane (2 ml) and the mixture heated at 45 °C for 32 h. The solvent was removed *in vacuo*, the residue was then dissolved in water and the aqueous layer washed with ethyl acetate. The aqueous layer was then acidified with a 1 M solution of hydrochloric acid until a permanent white precipitate was observed, the aqueous layer was then re-extracted with ethyl acetate and the organics dried ($MgSO_4$) and the filtrate concentrated *in vacuo* to afford the desired product as a solid (0.16 g, 80%); mp decomposed at 234°C; ν_{max}/cm^{-1} 3589.0, 2158.0, 2037.0, 1698.0, 1684.0, 1655.0, 1632.0, 1541.0, 1409.0, 1253.0, 1164.0, 1022.0; δ_H (300 MHz, $CDCl_3$) 8.28 (bt, *J* 4.28 Hz, 2 H, CON*H*CH_2Ar), 7.84 (d, *J* 7.7 Hz, 4 H, Ar*H ortho* to CO_2CH_3), 7.58 (bs, 2 H, CH_2N*H*CS), 7.30 (d, *J* 7.7 Hz, 4 H, Ar*H meta* to CO_2CH_3), 7.16 (s, 12 H, Ar*H*CH_2Ar, Ar*H*CH_2NHCS), 6.88 (bd, *J* 8.6 Hz, 2 H, CHN*H*CO), 4.63 (bs, 4 H, ArCH_2NHCS), 4.23 (bd, *J* 5.0 Hz, 4 H, CONHCH_2Ar), 3.97 (s, 4 H, ArCH_2Ar), 3.97 (bs, 2 H, C*H*CONH), 1.64-1.21 (m, 16 H, $CH_2CH_2CH_2CH_2$CH), 1.42 (s, 18 H, $C(CH_3)_3$). [Found: C, 61.58; H, 6.70; N, 9.04; S, 5.01. $C_{62}H_{76}N_8O_{10}S_2$ requires C, 64.42; H, 6.78; N, 9.66; S, 5.53%].

6.3 Experimental for binding studies

All UV titration experiments were conducted on a Shimadzu UV-1601 UV-visible spectrometer. Guest stock solutions were typically made up using a stock solution of host in dichloromethane, such that addition of aliquots of guest did not alter the concentration of the host under titration and were made such that 5μL of that solution contained 0.2 equivalents of guest with respect to host. The change in absorbance monitored during binding studies was at wavelength 249.5 nm. Binding constants were calculated by fitting the titration data to a 1:1 binding isotherm using *NMRTit HG* software, kindly provided by Prof. C.A. Hunter, University of Sheffield. Where more than one titration experiment was carried out on a substrate the results were averaged for greater accuracy.

*Binding data for N-acetyl L asparagine with macrocycle **59**:*

Solvent:	dichloromethane
Starting volume of host solution	1 ml
Concentration of host solution:	2.6×10^{-5} mol dm^{-3}
Concentration of guest solution:	1.04×10^{-3} mol dm^{-3}
Association constant:	4.60×10^{4} mol^{-1} dm^{3}

Volume added/μL	Abs. @ 249.5nm
0	0.4960
5	0.5404
10	0.5779
15	0.6113
20	0.6454
25	0.6702
35	0.6991
45	0.7233
55	0.7406
65	0.7585
75	0.7717
100	0.7887
125	0.7979
175	0.8203
200	0.8281
225	0.8372
250	0.8439
350	0.8555
400	0.8652
450	0.8673

UNIVERSITY OF SOUTHAMPTON LIBRARY

Binding Curve of mac 59 and NAc L-asparagine

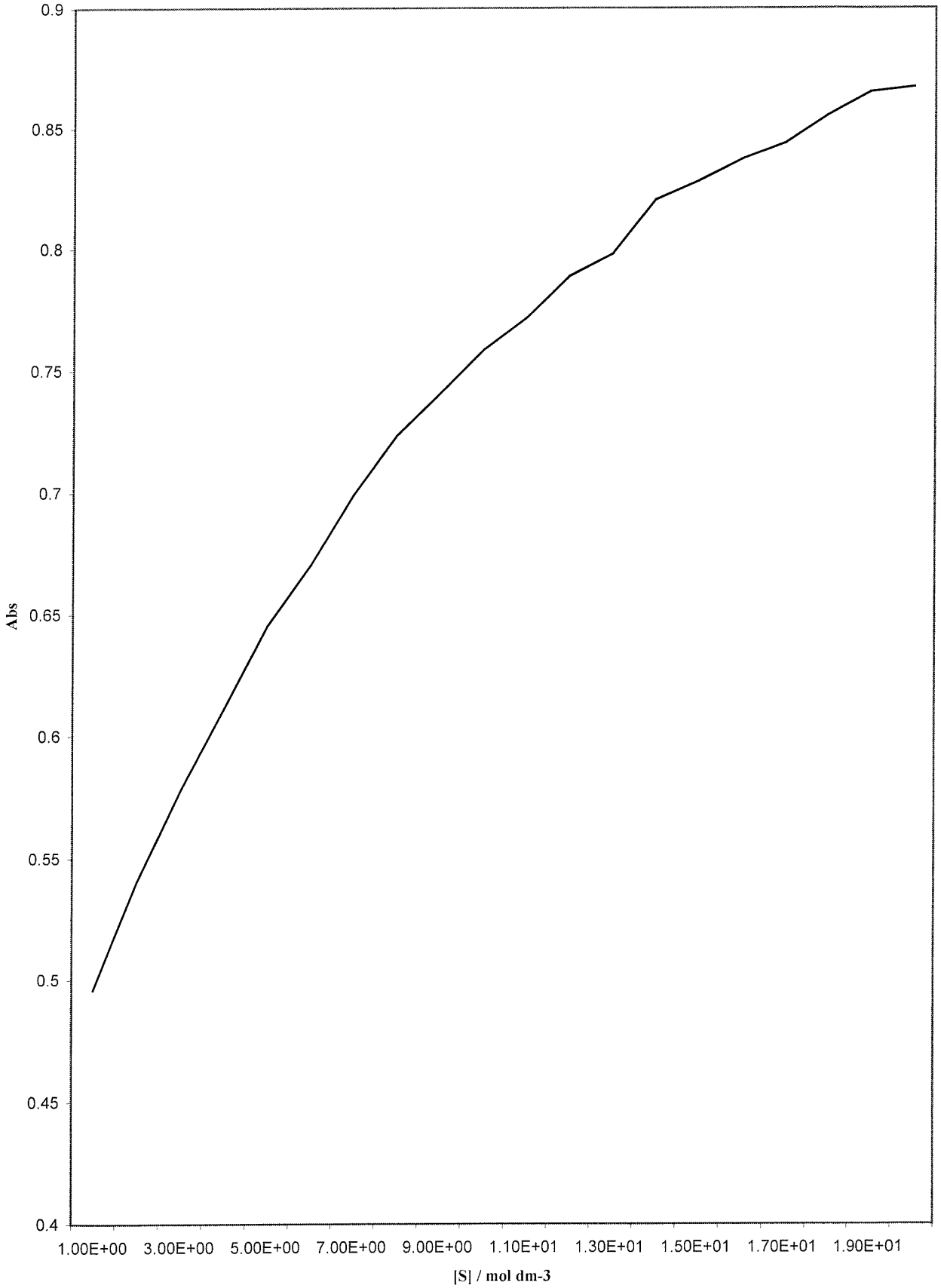

*Binding data for N-acetyl L asparagine with macrocycle **59**:*

Solvent:	dichloromethane
Starting volume of host solution	1 ml
Concentration of host solution:	2.6×10^{-5} mol dm^{-3}
Concentration of guest solution:	1.04×10^{-3} mol dm^{-3}
Association constant:	6.83×10^{4} mol^{-1} dm^{3}

Volume added/μL	Abs. @ 249.5nm
0	0.4703
5	0.5165
10	0.5626
15	0.6007
20	0.6318
25	0.6600
35	0.6910
45	0.7175
55	0.7380
65	0.7551
75	0.7646
100	0.7778
125	0.7853
175	0.8069
200	0.8210
225	0.8245
250	0.8307
350	0.8423
400	0.8483
450	0.8568

Binding Curve of mac 1 + NAc L-Asparagine

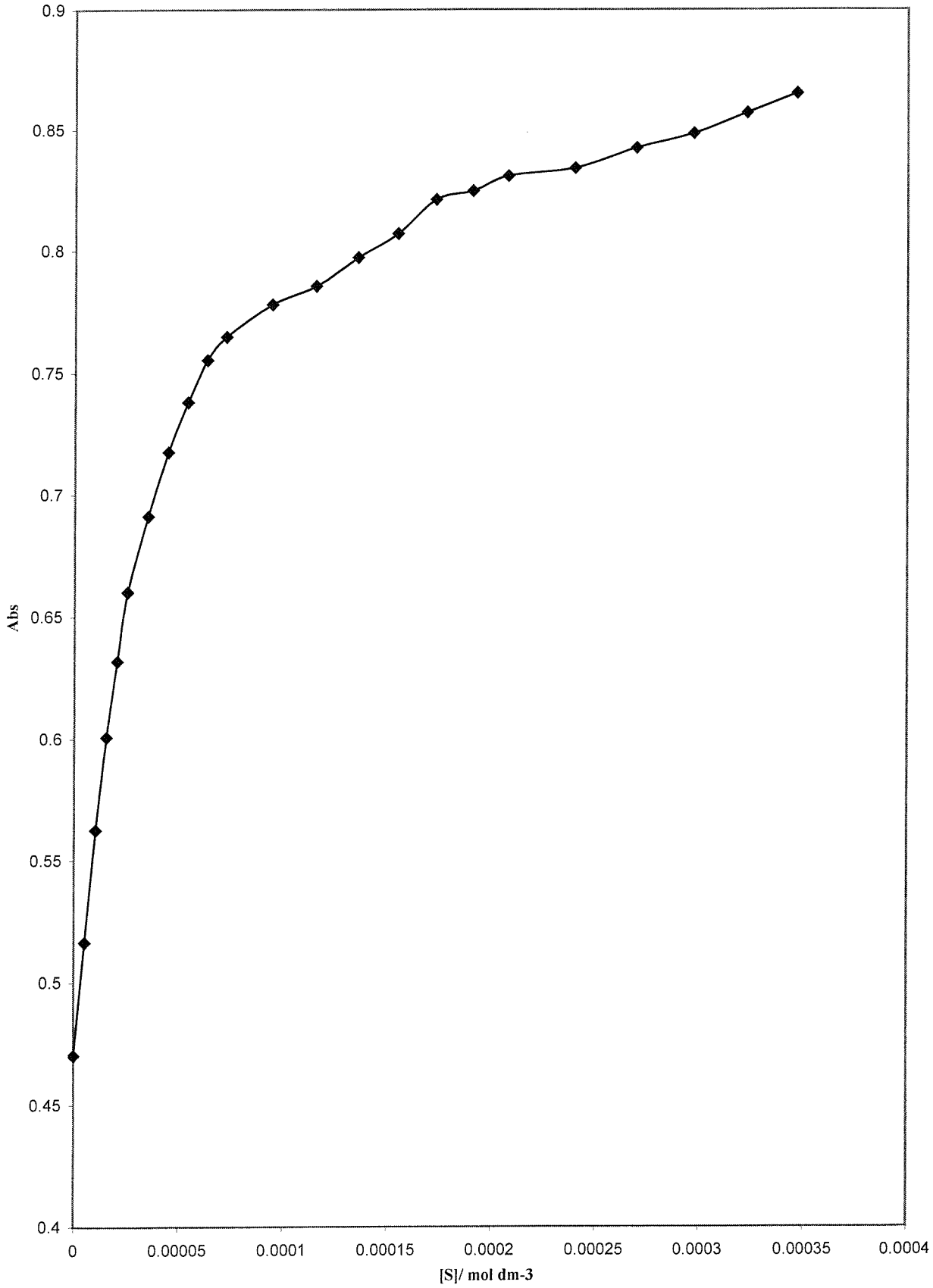

*Binding data for N-acetyl D asparagine with macrocycle **59**:*

Solvent:	dichloromethane
Starting volume of host solution	1 ml
Concentration of host solution:	2.6×10^{-5} mol dm^{-3}
Concentration of guest solution:	1.04×10^{-3} mol dm^{-3}
Association constant:	5.39×10^{4} mol^{-1} dm^{3}

Volume added/μL	Abs. @ 249.5nm
0	0.4816
5	0.5222
10	0.5680
15	0.6050
20	0.6304
25	0.6539
35	0.6740
45	0.6924
55	0.7096
65	0.7249
75	0.7423
125	0.7703
150	0.7789
175	0.7921
200	0.8009
225	0.8080
250	0.8113
350	0.8245
400	0.8304
450	0.8406

Binding curve of mac 1 + NAc D-Asparagine

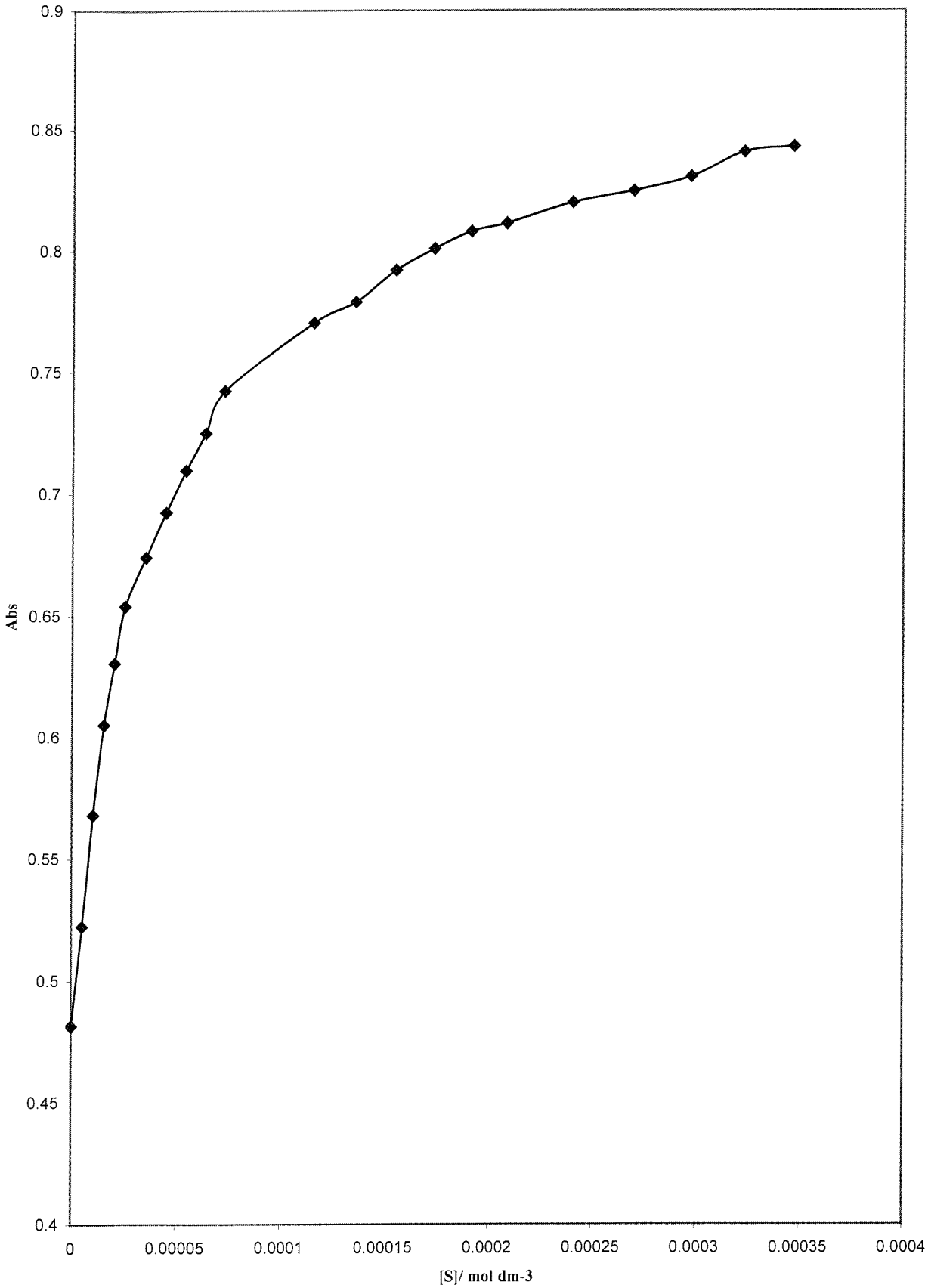

*Binding data for N-acetyl D asparagine with macrocycle **59**:*

Solvent:	dichloromethane
Starting volume of host solution	1 ml
Concentration of host solution:	2.6×10^{-5} mol dm^{-3}
Concentration of guest solution:	1.04×10^{-3} mol dm^{-3}
Association constant:	3.20×10^{4} mol^{-1} dm^{3}

Volume added/μL	Abs. @ 249.5nm
0	0.4226
5	0.4463
10	0.4846
15	0.5168
20	0.5615
25	0.5856
35	0.6113
45	0.6323
55	0.6503
65	0.6702
75	0.6915
100	0.7019
125	0.7205
150	0.7384
200	0.7574
225	0.7645
250	0.7802
350	0.7991
400	0.8113
450	0.8206

Binding Curve of mac 1 + NAc D-Asparagine

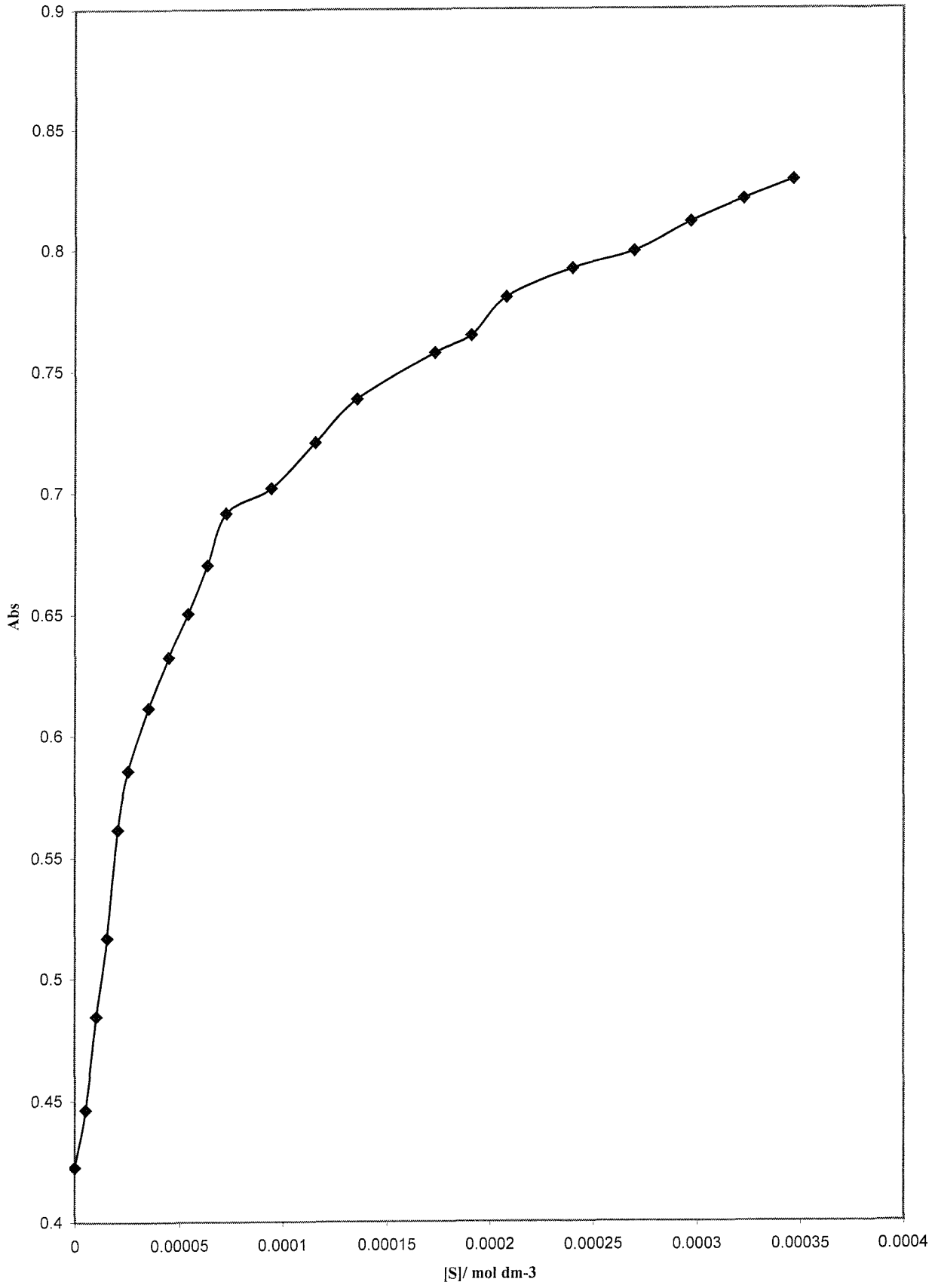

*Binding data for N-acetyl L glutamine with macrocycle **59**:*

Solvent:	dichloromethane
Starting volume of host solution	1 ml
Concentration of host solution:	2.6×10^{-5} mol dm^{-3}
Concentration of guest solution:	1.04×10^{-3} mol dm^{-3}
Association constant:	8.70×10^{3} mol^{-1} dm^{3}

Volume added/μL	Abs. @ 249.5nm
0	0.3735
5	0.3889
10	0.4083
15	0.4200
20	0.4299
25	0.4414
35	0.4568
45	0.4851
55	0.4972
65	0.5100
75	0.5214
100	0.5439
125	0.5575
175	0.5955
200	0.6112
225	0.6222
250	0.6360
350	0.6646
400	0.6736
450	0.6908

Binding Curve of mac 1 + NAc L-glutamine

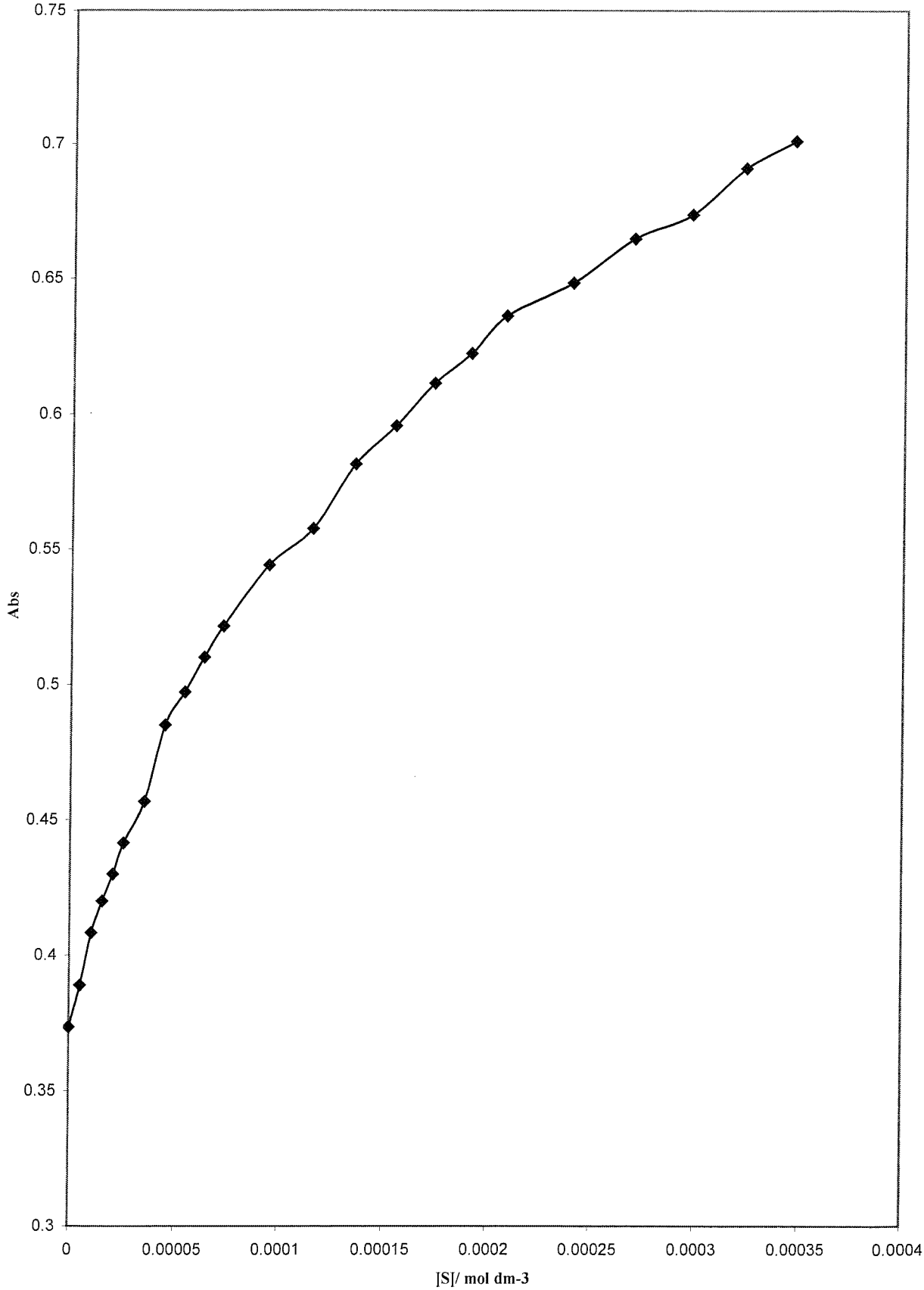

*Binding data for N-acetyl D glutamine with macrocycle **59**:*

Solvent:	dichloromethane
Starting volume of host solution	1 ml
Concentration of host solution:	2.6×10^{-5} mol dm^{-3}
Concentration of guest solution:	1.04×10^{-3} mol dm^{-3}
Association constant:	1.85×10^{4} mol^{-1} dm^{3}

Volume added/μL	Abs. @ 249.5nm
0	0.3915
5	0.4229
10	0.4492
15	0.4731
20	0.4951
25	0.5157
35	0.5363
45	0.5609
55	0.5847
65	0.6013
75	0.6283
100	0.6492
125	0.6604
175	0.6930
200	0.7080
225	0.7208
250	0.7336
350	0.7668
400	0.7819
450	0.7898

Binding Curve of mac 1 + N-Ac D-glutamine

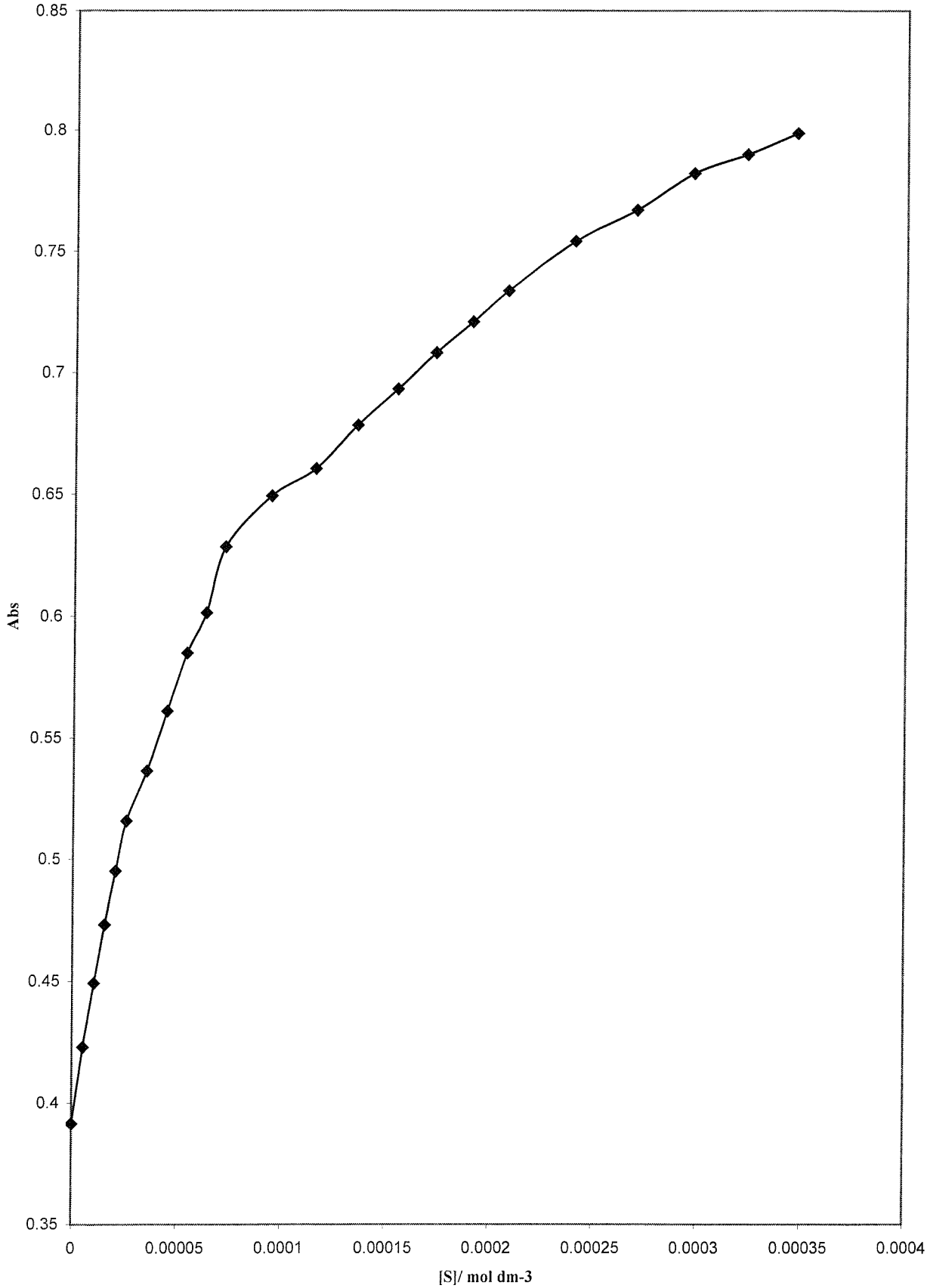

References

References

1. J. M. Lehn, *Angew.Chem. Int. Ed. Eng.*, **1988**, 27, 89
2. K. M. Bharltani, R. P. Bonar-Law, A. P. Davis, B. A. Murray, *J. Chem. Soc. Chem. Commun.*, **1996**, 752
3. C. J. Pedersen, *J. Am. Chem. Soc.*, **1967**, 89, 2495
4. E. Graf, J. M. Lehn, *J. Am. Chem. Soc.*, **1976**, 98, 6403
5. G. Deslongchamps, A. Galan, J. de Mendoza, J. Rebek. Jr, *Angew.Chem. Int. Ed. Eng.*, **1992**, 31, 61
6. J. I. Hong, S. K. Namgoong, A. Bernardi, W. C. Still, *J. Am. Chem. Soc.*, **1991**, 113, 5111
7. M. W. Peczuh, A. D. Hamilton, J. Sanchez-Ouesada, J. de Mendoza, T. Haack, E. Giralt, *J. Am. Chem. Soc.*, **1997**, 119, 9327
8. Z. Stryer, *Biochemistry*, 4th Ed., Reeman, New York, **1995**, 7
9. C. J. Pedersen, *J. Am. Chem. Soc.*, **1967**, 89, 7017
10. E. Graf, J. M. Lehn, *J. Am. Chem. Soc.*, **1975**, 97, 5022
11. T. Steiner, *Chem. Commun.*, **1997**, 727
12. F. A. Cotton, R. L. Luck, *Inorg. Chem.*, **1989**, 28, 3210
13. M. A. Viswarnitra, R. Radhakrishnan, J. Bandekar, G. R. Desiraju, *J. Am. Chem. Soc.*, **1993**, 115, 4868
14. H. S. Rzepa, M. L. Webb, A. M. Z. Slawin, D. J. Williams, *J. Chem. Soc. Chem. Commun.*, **1991**, 765
15. A. Hamilton, *Advances in Supramolecular Chemistry*, Vol. 1, 1
16. P. Dauber, A. Hagler, *Acc. Chem. Res.*, **1980**, 13, 105
17. T. Steiner, *Chem. Commun.*, **1997**, 727
18. C. B. Aakeroy, K. R. Seddon, *Chem. Soc. Rev.*, **1993**, 397
19. a) T. J. Murray, S. C. Zimmerman, *J. Am. Chem. Soc.*, **1992**, 114, 4010
    b) J. Pranata, S. G. Wierschke, W. L. Jorgensen, *J. Am. Chem. Soc.*, **1991**, 113, 2810
20. S. K. Chang, D. van Enges, E. Fan, A. D. Hamilton, *J. Am. Chem. Soc.*, **1991**, 113, 7640
21. C. A. Hunter, J. K. M. Sanders, *J. Am. Chem. Soc.*, **1990**, 112, 5525
22. C. A. Hunter, *Chem. Soc. Rev.*, **1994**, 101

23. a) W. L. Jorgensen, D. L. Severance, *J. Am. Chem. Soc.*, **1990**, 112, 4768
b) G. Karlstrom, P. Linse, A. Wallqvist, N. Jonsson, *J. Am. Chem. Soc.*, **1983**, 105, 3777
24. S. Pkival, S. Geils, C. S. Wilcox, *J. Am. Chem. Soc.*, **1994**, 116, 4487
25. H. Adams, F. J. Carver, C. A. Hunter, J. C. Morales, E. M. Seward, *Angew.Chem. Int. Ed. Eng.*, **1996**, 35, 1542
26. H. Schneider, *Angew.Chem. Int. Ed. Eng.*, **1997**, 36, 1072
27. S. R. la Brenz, J. W. Kelly, *J. Am. Chem. Soc.*, **1995**, 117, 1655
28. D. B. Smithrud, F. Diederich, *J. Am. Chem. Soc.*, **1990**, 112, 339
29. C. Tanford, *The Hydrophobic Effect*, Wiley, New York, **1990**
30. C. Steal, F. Vogtle, *Angew.Chem. Int. Ed. Eng.*, **1992**, 31, 528
31. P. D. Henley, PhD Thesis, University of Southampton, 1998.
32. J. Dunitz, M. Dobler, P. Seiler, R. J. Phizacherly, *Adv. Crystallogr. Sect.B.*, **1974**, 30, 2733
33. A. P. Bisson, C. A. Hunter, J. C. Morales, K. Young, *Chem. Eur. J.*, **1988**, 4, 845
34. A. P. Bisson, C. A. Hunter, *Chem. Commun.*, **1996**, 1723
35. J. P. Mackay, V. Gerhard, D. A. Beuregard, M. S. Westwell, M. S. Searl, D. H. Williams, *J. Am. Chem. Soc.*, **1994**, 116, 4581
36. J. Rebek, B. Askew, D. Nermeth, K. Paris, *J. Am. Chem. Soc.*, **1987**, 109, 2432
37. A. Galan, D. Andreu, A. M. Echavarren, P. Prades, J. de Mendoza, *J. Am. Chem. Soc.*, **1992**, 114, 1511
38. D. Reper, T. Huyton, A. Vagin, G. Dodson, *Proc. Natl. Acad. Sci.U.S.A.*, **2000**, 97, 8921
39. B. Hinzen, P. Seiler, F. Diederich, *Helv. Chim. Acta.*, **1996**, 79, 942
40. T. T. Goodman, M. V. Reddington, J. F. Stoddart, A. E. Kailer, *J. Am. Chem. Soc.*, **1991**, 113, 4335
41. H. Chen, S. Ogo, R. H. Fish, *J. Am. Chem. Soc.*, **1996**, 118, 4993
42. T. Mitzutani, K. Wada, S. Kitagawa, *J. Am. Chem. Soc.*, **1999**, 121, 11425
43. M. Sirish, H. J. Schneider, *J. Chem. Soc. Chem. Commun.*, **1999**, 907
44. A. Hossain, H. J. Schneider, *J. Am. Chem. Soc.*, **1998**, 120, 11208
45. R. Breslow, Z. Yang, R. Ching, G. Trojandt, F. Odobel, *J. Am. Chem. Soc.*, **1998**, 120, 3536

46. K. Kobayashi, M. Tominaga, Y. Asakawa, Y. Aoyama, *Tetrahedron Lett.*, **1993**, 34, 32, 5121
47. C. Schmuk, *Chem. Eur. J.*, **2000**, 6, 4, 709
48. J. D. Kilburn, M. Bonnat, F. Guillier, *J. Org. Chem.*, **1998**, 63, 8696
49. M. Torneiro, W. C. Still, *J. Am. Chem. Soc.*, **1995**, 117, 5887
50. F. Gasparrini, D. Misiti, C. Villani, A. Borchardt, M. T. Burger, W. C. Still, *J. Org. Chem.*, **1995**, 60, 4314
51. L. J. Lawless, A. P. Davis, *J. Chem. Soc. Chem. Commun.*, **1999**, 9
52. T. Mizutani, T. Ema, T. Tomita, Y. Kuroda, H. Ogoshi, *J. Am. Chem. Soc.*, **1994**, 116, 4240
53. Y. Kuroda, Y. Kato, T. Higashioji, J. Hasegawa, S. Kawanami, M. Takahashi, N. Shiraishi, K. Tanabe, H. Ogoshi, *J. Am. Chem. Soc.*, **1995**, 117, 10950
54. Y. Aoyama, A. Yamagishi, M. Asagawa, H. Toi, H. Ogoshi, *J. Am. Chem. Soc.*, **1988**, 110, 4076
55. M. J. Crossley, L. G. Mackay, A. C. Try, *J. Chem. Soc. Chem. Commun.*, **1995**, 1925
56. J. L. Sessler, A. Andrievsky, V. Král, V. Lynch, *J. Am. Chem. Soc.*, **1997**, 119, 9385
57. T. Kawabata, A. Kuroda, E. Nakata, K. Takasu, K. Fuji, *Tetrahedron Lett.*, **1996**, 37, 24, 4153
58. C. Raposo, M. Martin, L. Mussons, M. Crego, J. Anaya, C. Caballero, J. R. Moran, *J. Chem. Soc. Perkin Trans 1*, **1994**, 2113
59. M. Martin, C. Raposo, M. Almavac, M. Crego, C. Caballero, M. Grando, J. R. Moran, *Angew.Chem. Int. Ed. Eng.*, **1996**, 35, 2386
60. H. Tye, E. Eldred, M. Wills, *J. Chem. Soc. Perkin Trans 1*, **1998**, 457
61. J. R. Moran, M. Grego, A. Parteabrogo, C. Naposo, L. Mussons, J. L. Lorez, V. Alcazar, *Tetrahedron Lett.*, **1994**, 35, 1435
62. J. Rebek Jr., B. Askew, P. Ballester, M. Doa, *J. Am. Chem. Soc.*, **1987**, 109, 4119
63. K. S. Jeang, T. Tjivikua, A. Muehldorf, G. Deslongchamps, M. Famulok, J. Rebek Jr., *J. Am. Chem. Soc.*, **1991**, 113, 201
64. A. Echavarren, A. Galan, J. M. Lehn, J. de Mendoza, *J. Am. Chem. Soc.*, **1989**, 111, 4994
65. M. F. Cristofaro, A. R. Chamberlain, *J. Am. Chem. Soc.*, **1994**, 116, 5089

66. H. K. Patel, J. D. Kilburn, G. J. Langley, P. D. Edwards, T. Mitchell, P. Southgate, *Tetrahedron Lett.*, **1994**, 35, 481
67. S. S. Flack, J. D. Kilburn, *Tetrahedron Lett.*, **1995**, 36, 19, 3409
68. G. J. Pernia, J. D. Kilburn, M. Rowley, *J. Chem. Soc. Chem. Commun.*, **1995**, 305
69. G. J. Pernia, J. D. Kilburn, J.W. Essex, R. J. Mortshire-Smith, M. Rowley, *J. Am. Chem. Soc.*, **1996**, 118, 10220
70. R. S. Wareham, J. D. Kilburn, N. H. Rees, D. L. Turner, A. R. Leach, D. S. Holmes, *Tetrahedron Lett.*, **1995**, 36, 3047
71. C. P. Waymark, J. D. Kilburn, I. Gillies, *Tetrahedron Lett.*, **1995**, 36, 3051
72. P. D. Henley, C. P. Waymark, I. Gillies, J. D. Kilburn, *J. Chem. Soc. Perkin Trans 1*, **2000**, 1021
73. P. D. Henley, J. D. Kilburn, *J. Chem. Soc. Chem. Commun.*, **1999**, 1335
74. R. J. Pieters, F. Diederich, *J. Chem. Soc. Chem. Commun.*, **1996**, 2255
75. S. Kohmoto, D. Fukui, T. Nagashima, K. Kishikawa, M. Yamamoto, K. Yamada, *J. Chem. Soc. Chem. Commun.*, **1996**, 1869
76. K. Araki, K. Inada, S. Shinkai, *Angew.Chem. Int. Ed. Eng.*, **1996**, 35, 1, 72
77. S. S. Yoon, W. C. Still, *J. Am. Chem. Soc.*, **1993**, 115, 823
78. S. S. Yoon, W. C. Still, *Tetrahedron Lett.*, **1994**, 35, 2117
79. S. S. Yoon, W. C. Still, *Tetrahedron*, **1995**, 51, 567
80. H. Wennemers, S. S. Yoon, W. C. Still, *J. Org. Chem.*, **1995**, 60, 1108
81. J. Hong, S. K. Namgoong, A. Bernardi, W. C. Still, *J. Am. Chem. Soc.*, **1991**, 113, 5111
82. R. Liu, W. C. Still, *Tetrahedron Lett.*, **1993**, 34, 16, 2573
83. S. S. Yoon, T. M. Georgiadis, W. C. Still, *Tetrahedron Lett.*, **1993**, 34, 42, 6697
84. A. Borchardt, W. C. Still, *J. Am. Chem. Soc.*, **1994**, 116, 7467
85. C. Gennari, P. Nestler, B. Salom, W. C. Still, *Angew.Chem. Int. Ed. Eng.*, **1995**, 34, 16, 1765
86. D. W. P. M. Lowik, M. D. Weingarten, M. Broekema, A. J. Brouwer, W. C. Still, R. M. J. Liskamp, *Angew.Chem. Int. Ed. Eng.*, **1998**, 37, 13, 1846
87. M. Bonnat, M. Bradley, J. D. Kilburn, *Tetrahedron Lett.*, **1996**, 37, 30, 5409
88. T. Fessmann, J. D. Kilburn, *Angew.Chem. Int. Ed. Eng.*, **1999**, 38, 13, 1993
89. R.B. Merrifield, *Angew. Chem.*, **1985**, 97, 10, 801

90. G. J. Pernia, PhD Thesis, University of Southampton, 1996.
91. S. F. Martin, S. A. Williamson, A. P. Gist, K. M. Smith, *J. Org. Chem.*, **1983**, 48, 5170
92. M. Julia, F. Chastrette, *Bull. Soc.Chim.Fr.*, **1962**, 2247
93. A. R. Martin, Y. Yang, *Acta. Chim. Scand.*, **1993**, 47, 221-230
94. N. Miyaura, T. Yanagi, A. Suzuki, *Synth. Commun.*, **1981**, 11, 513
95. H. C. Brown, Y. M. Choi, S. Narasimhan, *Synthesis*, **1981**, 605
96. H. C. Brown, Y. M. Choi, S. Narasimhan, *J. Org. Chem.*, **1982**, 47, 605
97. L. Boymond, M. Rottlander, G. Gahiez, P. Knochel, *Angew.Chem. Int. Ed. Eng.*, **1998**, 12, 1701
98. G. M. Amantharamaih, K. M. Sivanadaiah, *J. Chem. Soc. Perkin Trans 1*, **1977**, 490
99. E. Dyer, T. B. Johnson, *J. Am. Chem. Soc.*, **1974**, 96, 590
100. L. Kisfalaudy, I. Schon, T. Szirtes, O. Ngiki, M. Low, *Tetrahedron Lett.*, **1974**, 15, 1785
101. M. Bodanski, A. Bodanski, *The Practice of Peptide Synthesis*, Springer-Verlag, New York, **1984**, 170
102. J. E. Baldwin, A. Flinn, *Tetrahedron*, **1987**, 28, 36073
103. H. E. Schoemaker, W. H. J. Boester, Q. B. Broxterman, E. C. Ross, B. Kaptein, W. J. J. Van der Tweel, J. Kamphuis, F. P. J. T. Rutjes, *Chimica*, **1997**, 51, 308
104. S. Tripett, D. M. Walker, *J. Chem. Soc.*, **1961**, 1266
105. E. Diekmann, K. Friedrich, J. Lehmann, *Liebigs. Ann. Chem.*, **1989**, 1247
106. A. Lubineau, J. Auge, N. Lubin, *J. Chem. Soc. Perkin Trans 1*, **1990**, 3011
107. U. Schollkopf, W. Hartwig, U. Grath, *Angew.Chem. Int. Ed. Eng.*, **1979**, 18, 862
108. U. Schollkopf, W. Hartwig, K. Posposchil, H. Kehru, *Synthesis*, **1981**, 968
109. M. P. Schneider, M. Goldbach, *J. Am. Chem. Soc.*, **1980**, 102, 590
110. M. A. Brook, T. H. Chan, *Synthesis*, **1983**, 201
111. K. Mori, *Tetrahedron*, **1974**, 30, 3807
112. C. Destabel, J. D. Kilburn, J. Knight, *Tetrahedron*, **1994**, 50, 38, 11267
113. A. I. Meyers *et al*, *J. Am. Chem. Soc.*, **1983**, 105, 5015
114. M. Jacobsen, *J. Am. Chem. Soc.*, **1955**, 77, 2461
115. U. Schollkopf, U. Groth, T. Huhn, B. Porsch, C.Schmeck, *Liebigs. Ann. Chem.*, **1993**, 715

116. V. Jullian, E. Shepherd, T. Gelbrich, M. B. Hursthouse, J. D. Kilburn, *Tetrahedron Lett.*, **2000**, 3963

117. K. E. Koenig, G. M. Lein, P. Stuckler, T. Kaneda, D. J. Cram, *J. Am. Chem. Soc.*, **1979**, 101, 3553

118. C. J. Creswell, A. L. Allred, *J.Phys. Chem.*, **1962**, 66, 1469

119. C. S. Wilcox, *Frontiers In Supramolecular Organic Chemistry And Photochemistry*, ed. H. J. Schneider & H. Durr, VCH, Weinheim, **1991**, 123

120. C. S. Wilcox, J. C. Adrian jr., T. H. Webb, F. J. Zawachi, *J. Am. Chem. Soc.*, **1992**, 114, 10189

121. P. Job, *Ann. Chim. (Paris)*, **1928**, 9, 13

122. K. A. Connors, *Binding Constants, The Measurement of Molecular Complex Stability*, Wiley, New York, **1987**

123. J. H. Hartley, T. D. James, C. J. Ward, *J. Chem. Soc. Perkin Trans 1*, **2000**, 3155

124. P. Krogsgaard-Larsen, J. J. Hansen, *Eds. Excitory Amino Acid Receptors*, Ellis Harwood, Chichester, **1992**

125. E. Fan, S. A. Van Arman, S. Kincaid, A. D. Hamilton, *J. Am. Chem. Soc.*, **1993**, 115, 369

126. V. Jubian, A. Veronese, R. P. Dixon, A. D. Hamilton, *Angew.Chem. Int. Ed. Eng.*, **1995**, 34, 11, 1237

127. K.W. Blake, A.E. Porter, P.G. Sammes, *J. Chem. Soc. Perkin. Trans. 1*, **1972**, 2494

128. a. L.A. LaPlanche, M.T. Rogers, *J. Am. Chem. Soc.*, **1964**, 86, 337; b. T. Drakenberg, S. Forsen, *J. Chem. Soc. Chem. Commun.*, **1971**, 1404; c. W.L.Jorgensen, J. Gao, *J. Am. Chem. Soc.*, **1988**, 110, 4212

129. D. H. Christensen, R.N. Kortzeborn, B. Bak, J.J. Led, *J. Chem. Phys.*, **1970**, 53, 3912; b. D.M. Schnur, Y.H. Yuh, D.R. Dalton, *J. Org. Chem,* **1989**, 54, 3779; c. E.M. Duffy, D.L. Severance, W.L. Jorgensen, *J. Am. Chem. Soc.*, **1992**, 114, 7535

130. J.M. Mellor, A. Wagland, *J. Chem. Soc. Perkin. Trans. 1*, **1989**, 5, 997, 1005

Appendix

Table 1. Crystal data and structure refinement.

Identification code	**00sot016**	
Compound	$C_{41}H_{45}N_7O_5S \cdot 3\ H_2O$	
Empirical formula	$C_{41}H_{51}N_7O_8S$	
Formula weight	801.95	
Temperature	120(2) K	
Wavelength	0.71069 Å	
Crystal system	Monoclinic	
Space group	$P2_1$	
Unit cell dimensions	$a = 9.0659(2)$ Å	$\alpha = 90°$
	$b = 17.6648(3)$ Å	$\beta = 98.6819(7)°$
	$c = 26.1695(6)$ Å	$\gamma = 90°$
Volume	4142.95(15) Å^3	
Z	4	
Density (calculated)	1.286 Mg / m^3	
Absorption coefficient	0.138 mm^{-1}	
F(000)	1704	
Crystal	Plate; colourless	
Crystal size	0.15 × 0.12 × 0.05 mm^3	
θ range for data collection	3.02 – 24.50°	
Index ranges	$-10 \le h \le 10$, $-20 \le k \le 20$, $-30 \le l \le 30$	
Reflections collected	51920	
Independent reflections	13502 [$R_{int} = 0.1397$]	
Completeness to $\theta = 24.50°$	98.8 %	
Max. and min. transmission	0.9931 and 0.9796	
Refinement method	Full-matrix least-squares on F^2	
Data / restraints / parameters	13502 / 1 / 1134	
Goodness-of-fit on F^2	0.993	
Final R indices [$F^2 > 2\sigma(F^2)$]	$R1 = 0.0606$, $wR2 = 0.1223$	
R indices (all data)	$R1 = 0.1047$, $wR2 = 0.1331$	
Absolute structure parameter	0.11(8)	
Extinction coefficient	0.0011(4)	
Largest diff. peak and hole	0.320 and –0.240 e Å^{-3}	

Diffractometer: *Enraf Nonius KappaCCD* area detector (ϕ scans and ω scans to fill *Ewald* sphere). **Data collection and cell refinement**: *Denzo* (Z. Otwinowski & W. Minor, *Methods in Enzymology* (1997) Vol. **276**: *Macromolecular Crystallography*, part A, pp. 307–326; C. W. Carter, Jr. & R. M. Sweet, Eds., Academic Press). **Absorption correction**: *SORTAV* (R. H. Blessing, Acta Cryst. A**51** (1995) 33–37; R. H. Blessing, J. Appl. Cryst. **30** (1997) 421–426). **Program used to solve structure**: *SIR97* (Cascarano et al., Acta Cryst. **A**52 (1996) C-79). **Program used to refine structure**: *SHELXL97* (G. M. Sheldrick (1997), University of Göttingen, Germany).

Further information: http://www.soton.ac.uk/~xservice/strat.htm

Special details:

Table 2. Atomic coordinates [$\times 10^4$], equivalent isotropic displacement parameters [$Å^2 \times 10^3$] and site occupancy factors. U_{eq} is defined as one third of the trace of the orthogonalized U^{ij} tensor.

Atom	*x*	*y*	*z*	U_{eq}	*S.o.f.*
S1	−1948(1)	1560(1)	−4640(1)	37(1)	1
O1	−6239(4)	3537(2)	−7009(1)	46(1)	1
O2	996(3)	4441(2)	−6060(1)	48(1)	1
O3	3607(3)	2951(2)	−3936(1)	32(1)	1
O4	4034(3)	761(2)	−3436(1)	39(1)	1
O5	−5744(3)	703(2)	−7089(1)	40(1)	1
N1	−3837(4)	2649(2)	−4442(1)	38(1)	1
N2	−4436(4)	2934(2)	−7365(1)	33(1)	1
N3	−1551(4)	4344(2)	−6341(2)	40(1)	1
N4	1587(4)	2193(2)	−4087(1)	29(1)	1
N5	−3220(4)	1791(2)	−3796(2)	37(1)	1
N6	3406(4)	1028(2)	−4289(2)	32(1)	1
N7	−4550(4)	1734(2)	−6721(1)	33(1)	1
C1	−3062(5)	2022(3)	−4277(2)	35(1)	1
C2	−3964(5)	2953(3)	−4961(2)	36(1)	1
C3	−5099(5)	2526(3)	−5346(2)	36(1)	1
C4	−5253(5)	2844(3)	−5889(2)	36(1)	1
C5	−6377(5)	2396(3)	−6279(2)	40(1)	1
C6	−5849(5)	2225(3)	−6792(2)	32(1)	1
C7	−5524(5)	2959(3)	−7069(2)	35(1)	1
C8	−3820(5)	3616(3)	−7558(2)	38(1)	1
C9	−2471(5)	3878(2)	−7195(2)	31(1)	1
C10	−2681(5)	4170(3)	−6713(2)	36(1)	1
C11	−1028(5)	3797(3)	−7281(2)	37(1)	1
C12	167(5)	3982(3)	−6909(2)	38(1)	1
C13	−179(5)	4241(3)	−6442(2)	36(1)	1
C14	1188(5)	4021(3)	−5606(2)	34(1)	1
C15	494(5)	3340(3)	−5548(2)	32(1)	1
C16	839(5)	2950(3)	−5090(2)	31(1)	1
C17	1895(4)	3225(2)	−4688(2)	27(1)	1
C18	2556(4)	3920(3)	−4761(2)	31(1)	1
C19	2201(5)	4317(3)	−5209(2)	33(1)	1
C20	2407(5)	2785(2)	−4210(2)	28(1)	1
C21	2145(4)	1693(2)	−3657(2)	27(1)	1
C22	887(4)	1253(2)	−3474(2)	30(1)	1
C23	−102(4)	1729(3)	−3193(2)	33(1)	1
C24	−1452(5)	1302(3)	−3063(2)	36(1)	1
C25	−2597(5)	1117(3)	−3537(2)	37(1)	1
C26	3308(5)	1127(3)	−3789(2)	31(1)	1
C27	4311(5)	447(3)	−4485(2)	37(1)	1
C28	3516(4)	139(2)	−4984(2)	29(1)	1
C29	4077(5)	218(3)	−5448(2)	34(1)	1
C30	3274(5)	−46(3)	−5908(2)	36(1)	1
C31	1918(5)	−391(3)	−5918(2)	32(1)	1
C32	1355(5)	−472(3)	−5458(2)	41(1)	1
C33	2156(5)	−205(3)	−4997(2)	40(1)	1
C35	−443(5)	−232(3)	−6544(2)	36(1)	1
C34	1013(5)	−653(3)	−6411(2)	40(1)	1
C36	−1812(5)	−570(3)	−6528(2)	36(1)	1
C37	−3140(5)	−183(3)	−6643(2)	31(1)	1
C38	−3127(5)	580(3)	−6765(2)	32(1)	1
C39	−1764(5)	935(3)	−6789(2)	32(1)	1
C40	−434(5)	532(3)	−6682(2)	38(1)	1
C41	−4582(5)	1001(3)	−6873(2)	31(1)	1
S1'	−1959(1)	298(1)	−10390(1)	36(1)	1
O1'	−4573(3)	−1147(2)	−7749(1)	43(1)	1
O2'	1999(4)	−2626(2)	−9033(1)	53(1)	1

O3'	3042(3)	−1013(2)	−11092(1)	32(1)	1
O4'	2835(3)	1171(2)	−11569(1)	32(1)	1
O5'	−3561(3)	1568(2)	−7895(1)	34(1)	1
N1'	−4052(4)	−780(2)	−10456(1)	32(1)	1
N2'	−2112(4)	−995(2)	−7772(1)	33(1)	1
N3'	−324(5)	−2461(2)	−8799(2)	40(1)	1
N4'	1028(4)	−326(2)	−10968(1)	28(1)	1
N5'	−4111(4)	−39(2)	−11167(1)	35(1)	1
N6'	2789(4)	904(2)	−10731(1)	29(1)	1
N7'	−2494(4)	473(2)	−8112(1)	32(1)	1
C1'	−3451(4)	−209(2)	−10684(2)	27(1)	1
C2'	−3668(5)	−981(3)	−9907(2)	32(1)	1
C3'	−4502(5)	−503(3)	−9569(2)	32(1)	1
C4'	−3875(5)	−577(3)	−9000(2)	37(1)	1
C5'	−4700(5)	−96(3)	−8649(2)	34(1)	1
C6'	−3833(5)	13(2)	−8103(2)	29(1)	1
C7'	−3515(5)	−771(3)	−7847(2)	29(1)	1
C8'	−1649(5)	−1764(3)	−7597(2)	40(1)	1
C9'	−611(5)	−2074(2)	−7943(2)	29(1)	1
C10'	−1188(5)	−2275(3)	−8446(2)	37(1)	1
C11'	903(5)	−2077(3)	−7810(2)	35(1)	1
C12'	1822(5)	−2267(3)	−8167(2)	35(1)	1
C13'	1131(6)	−2434(2)	−8658(2)	35(1)	1
C14'	1885(5)	−2179(3)	−9467(2)	35(1)	1
C15'	1247(5)	−1462(3)	−9501(2)	33(1)	1
C16'	1257(5)	−1043(3)	−9950(2)	33(1)	1
C17'	1903(4)	−1335(2)	−10360(2)	26(1)	1
C18'	2533(5)	−2052(3)	−10314(2)	32(1)	1
C19'	2476(5)	−2478(3)	−9878(2)	42(1)	1
C20'	2028(5)	−885(2)	−10837(2)	26(1)	1
C21'	1178(4)	186(2)	−11391(2)	27(1)	1
C22'	−313(4)	553(3)	−11593(2)	30(1)	1
C23'	−1507(4)	−5(2)	−11818(2)	30(1)	1
C26'	2363(4)	791(2)	−11233(2)	28(1)	1
C25'	−3739(5)	599(3)	−11487(2)	36(1)	1
C24'	−3032(4)	348(3)	−11950(2)	37(1)	1
C27'	3885(5)	1461(3)	−10513(2)	33(1)	1
C28'	3575(4)	1765(2)	−9998(2)	26(1)	1
C29'	4605(5)	1683(2)	−9558(2)	30(1)	1
C30'	4344(5)	1997(2)	−9094(2)	28(1)	1
C31'	3041(5)	2375(2)	−9053(2)	29(1)	1
C32'	1996(5)	2441(3)	−9495(2)	38(1)	1
C33'	2252(5)	2138(3)	−9963(2)	37(1)	1
C35'	1465(5)	2369(3)	−8352(2)	31(1)	1
C34'	2792(5)	2713(3)	−8538(2)	36(1)	1
C36'	54(5)	2682(3)	−8453(2)	35(1)	1
C37'	−1192(5)	2323(3)	−8333(2)	31(1)	1
C38'	−1069(4)	1621(2)	−8091(2)	26(1)	1
C39'	334(5)	1310(3)	−7958(2)	31(1)	1
C40'	1590(5)	1671(3)	−8089(2)	33(1)	1
C41'	−2463(5)	1224(2)	−8018(2)	26(1)	1
O1W	119(3)	−369(2)	−8438(1)	48(1)	1
O2W	−7358(4)	−416(2)	−7690(1)	52(1)	1
O3W	3970(4)	1511(3)	−12490(1)	67(1)	1
O4W	−4290(4)	2601(2)	−2913(2)	64(1)	1
O5W	−1966(4)	1895(2)	−5853(1)	62(1)	1
O6W	200(20)	618(10)	−9295(6)	104(6)	0.60
O6W'	−570(30)	727(14)	−9184(9)	93(7)	0.40

Table 3. Bond lengths [Å] and angles [°].

S1–C1	1.696(5)
O1–C7	1.234(5)
O2–C14	1.387(5)
O2–C13	1.393(5)
O3–C20	1.244(5)
O4–C26	1.234(5)
O5–C41	1.236(5)
N1–C1	1.348(6)
N1–C2	1.450(6)
N1–H1	0.8800
N2–C7	1.344(5)
N2–C8	1.450(6)
N2–H2	0.8800
N3–C13	1.323(6)
N3–C10	1.339(6)
N4–C20	1.348(5)
N4–C21	1.460(5)
N4–H4	0.8800
N5–C1	1.352(6)
N5–C25	1.443(6)
N5–H5	0.8800
N6–C26	1.335(5)
N6–C27	1.456(6)
N6–H6	0.8800
N7–C41	1.353(6)
N7–C6	1.452(5)
N7–H7	0.8800
C2–C3	1.526(6)
C2–H2A	0.9900
C2–H2B	0.9900
C3–C4	1.514(6)
C3–H3A	0.9900
C3–H3B	0.9900
C4–C5	1.547(6)
C4–H4A	0.9900
C4–H4B	0.9900
C5–C6	1.523(6)
C5–H5A	0.9900
C5–H5B	0.9900
C6–C7	1.535(7)
C6–H6	1.0000
C8–C9	1.504(6)
C8–H8A	0.9900
C8–H8B	0.9900
C9–C11	1.368(6)
C9–C10	1.402(6)
C10–H10	0.9500
C11–C12	1.382(6)
C11–H11	0.9500
C12–C13	1.384(7)
C12–H12	0.9500
C14–C15	1.377(6)
C14–C19	1.382(6)
C15–C16	1.377(6)
C15–H15	0.9500
C16–C17	1.397(6)
C16–H16	0.9500
C17–C18	1.391(6)
C17–C20	1.488(6)
C18–C19	1.362(6)

C18–H18	0.9500
C19–H19	0.9500
C21–C22	1.517(6)
C21–C26	1.529(6)
C21–H21	1.0000
C22–C23	1.500(6)
C22–H22A	0.9900
C22–H22B	0.9900
C23–C24	1.519(6)
C23–H23A	0.9900
C23–H23B	0.9900
C24–C25	1.527(6)
C24–H24A	0.9900
C24–H24B	0.9900
C25–H25A	0.9900
C25–H25B	0.9900
C27–C28	1.495(6)
C27–H27A	0.9900
C27–H27B	0.9900
C28–C33	1.371(6)
C28–C29	1.393(6)
C29–C30	1.390(6)
C29–H29	0.9500
C30–C31	1.369(6)
C30–H30	0.9500
C31–C32	1.383(6)
C31–C34	1.495(6)
C32–C33	1.394(6)
C32–H32	0.9500
C33–H33	0.9500
C35–C36	1.384(6)
C35–C40	1.397(7)
C35–C34	1.509(6)
C34–H34A	0.9900
C34–H34B	0.9900
C36–C37	1.378(6)
C36–H36	0.9500
C37–C38	1.385(6)
C37–H37	0.9500
C38–C39	1.395(6)
C38–C41	1.504(6)
C39–C40	1.393(6)
C39–H39	0.9500
C40–H40	0.9500
S1'–C1'	1.707(4)
O1'–C7'	1.226(5)
O2'–C14'	1.373(5)
O2'–C13'	1.390(5)
O3'–C20'	1.235(5)
O4'–C26'	1.234(5)
O5'–C41'	1.250(5)
N1'–C1'	1.330(5)
N1'–C2'	1.467(5)
N1'–H1'	0.8800
N2'–C7'	1.318(5)
N2'–C8'	1.474(6)
N2'–H2'	0.8800
N3'–C13'	1.316(6)
N3'–C10'	1.338(6)
N4'–C20'	1.348(5)
N4'–C21'	1.452(5)

N4'–H4'	0.8800
N5'–C1'	1.348(5)
N5'–C25'	1.474(6)
N5'–H5'	0.8800
N6'–C26'	1.328(5)
N6'–C27'	1.452(5)
N6'–H6'	0.8800
N7'–C41'	1.349(5)
N7'–C6'	1.464(5)
N7'–H7'	0.8800
C2'–C3'	1.507(6)
C2'–H2'1	0.9900
C2'–H2'2	0.9900
C3'–C4'	1.517(6)
C3'–H3'1	0.9900
C3'–H3'2	0.9900
C4'–C5'	1.526(6)
C4'–H4'1	0.9900
C4'–H4'2	0.9900
C5'–C6'	1.536(6)
C5'–H5'1	0.9900
C5'–H5'2	0.9900
C6'–C7'	1.547(6)
C6'–H6'	1.0000
C8'–C9'	1.504(6)
C8'–H8'1	0.9900
C8'–H8'2	0.9900
C9'–C11'	1.364(6)
C9'–C10'	1.388(6)
C10'–H10'	0.9500
C11'–C12'	1.385(6)
C11'–H11'	0.9500
C12'–C13'	1.373(6)
C12'–H12'	0.9500
C14'–C19'	1.377(6)
C14'–C15'	1.390(6)
C15'–C16'	1.391(6)
C15'–H15'	0.9500
C16'–C17'	1.397(6)
C16'–H16'	0.9500
C17'–C18'	1.388(6)
C17'–C20'	1.498(6)
C18'–C19'	1.375(6)
C18'–H18'	0.9500
C19'–H19'	0.9500
C21'–C22'	1.521(6)
C21'–C26'	1.526(6)
C21'–H21'	1.0000
C22'–C23'	1.516(6)
C22'–H22C	0.9900
C22'–H22D	0.9900
C23'–C24'	1.509(6)
C23'–H23C	0.9900
C23'–H23D	0.9900
C25'–C24'	1.520(6)
C25'–H25C	0.9900
C25'–H25D	0.9900
C24'–H24C	0.9900
C24'–H24D	0.9900
C27'–C28'	1.515(6)
C27'–H27C	0.9900

C27'–H27D	0.9900
C28'–C29'	1.376(6)
C28'–C33'	1.384(6)
C29'–C30'	1.387(6)
C29'–H29'	0.9500
C30'–C31'	1.375(6)
C30'–H30'	0.9500
C31'–C32'	1.385(6)
C31'–C34'	1.523(6)
C32'–C33'	1.388(6)
C32'–H32'	0.9500
C33'–H33'	0.9500
C35'–C36'	1.382(6)
C35'–C40'	1.409(6)
C35'–C34'	1.494(6)
C34'–H34C	0.9900
C34'–H34D	0.9900
C36'–C37'	1.373(6)
C36'–H36'	0.9500
C37'–C38'	1.389(6)
C37'–H37'	0.9500
C38'–C39'	1.381(6)
C38'–C41'	1.482(6)
C39'–C40'	1.392(6)
C39'–H39'	0.9500
C40'–H40'	0.9500
O1W–H1W	0.8596
O1W–H2W	0.8387
O2W–H3W	0.8596
O2W–H4W	0.8386
O3W–H5W	0.8596
O3W–H6W	0.8386
O4W–H7W	0.8596
O4W–H8W	0.8386
O5W–O9W	0.8596
O5W–O10W	0.8386
O6W–H11W	0.8595
O6W–H12W	0.8386
O6W'–H12W	1.2290
O6W'–H12W	0.8596
O6W'–H13W	0.8386

C14–O2–C13	117.5(3)
C1–N1–C2	124.6(4)
C1–N1–H1	117.7
C2–N1–H1	117.7
C7–N2–C8	121.9(4)
C7–N2–H2	119.1
C8–N2–H2	119.1
C13–N3–C10	117.5(4)
C20–N4–C21	120.9(3)
C20–N4–H4	119.6
C21–N4–H4	119.6
C1–N5–C25	126.6(4)
C1–N5–H5	116.7
C25–N5–H5	116.7
C26–N6–C27	124.3(4)
C26–N6–H6	117.9
C27–N6–H6	117.9
C41–N7–C6	123.6(4)
C41–N7–H7	118.2

C6–N7–H7	118.2
N1–C1–N5	115.0(4)
N1–C1–S1	122.8(4)
N5–C1–S1	122.2(4)
N1–C2–C3	112.7(4)
N1–C2–H2A	109.0
C3–C2–H2A	109.0
N1–C2–H2B	109.0
C3–C2–H2B	109.0
H2A–C2–H2B	107.8
C4–C3–C2	113.1(4)
C4–C3–H3A	109.0
C2–C3–H3A	109.0
C4–C3–H3B	109.0
C2–C3–H3B	109.0
H3A–C3–H3B	107.8
C3–C4–C5	112.7(4)
C3–C4–H4A	109.0
C5–C4–H4A	109.0
C3–C4–H4B	109.0
C5–C4–H4B	109.0
H4A–C4–H4B	107.8
C6–C5–C4	114.8(4)
C6–C5–H5A	108.6
C4–C5–H5A	108.6
C6–C5–H5B	108.6
C4–C5–H5B	108.6
H5A–C5–H5B	107.5
N7–C6–C5	111.2(4)
N7–C6–C7	110.8(3)
C5–C6–C7	111.0(4)
N7–C6–H6	107.9
C5–C6–H6	107.9
C7–C6–H6	107.9
O1–C7–N2	123.1(5)
O1–C7–C6	119.8(4)
N2–C7–C6	117.1(4)
N2–C8–C9	110.8(4)
N2–C8–H8A	109.5
C9–C8–H8A	109.5
N2–C8–H8B	109.5
C9–C8–H8B	109.5
H8A–C8–H8B	108.1
C11–C9–C10	116.7(4)
C11–C9–C8	124.8(4)
C10–C9–C8	118.3(4)
N3–C10–C9	123.2(4)
N3–C10–H10	118.4
C9–C10–H10	118.4
C9–C11–C12	121.8(4)
C9–C11–H11	119.1
C12–C11–H11	119.1
C11–C12–C13	116.2(4)
C11–C12–H12	121.9
C13–C12–H12	121.9
N3–C13–C12	124.6(4)
N3–C13–O2	117.5(4)
C12–C13–O2	117.8(4)
C15–C14–C19	120.6(4)
C15–C14–O2	124.2(4)
C19–C14–O2	115.2(4)

C16–C15–C14	119.1(4)
C16–C15–H15	120.4
C14–C15–H15	120.4
C15–C16–C17	121.4(4)
C15–C16–H16	119.3
C17–C16–H16	119.3
C18–C17–C16	117.7(4)
C18–C17–C20	119.3(4)
C16–C17–C20	122.9(4)
C19–C18–C17	121.4(4)
C19–C18–H18	119.3
C17–C18–H18	119.3
C18–C19–C14	119.9(4)
C18–C19–H19	120.1
C14–C19–H19	120.1
O3–C20–N4	120.8(4)
O3–C20–C17	119.7(4)
N4–C20–C17	119.5(4)
N4–C21–C22	111.4(3)
N4–C21–C26	113.1(3)
C22–C21–C26	108.3(3)
N4–C21–H21	108.0
C22–C21–H21	108.0
C26–C21–H21	108.0
C23–C22–C21	113.6(3)
C23–C22–H22A	108.8
C21–C22–H22A	108.8
C23–C22–H22B	108.8
C21–C22–H22B	108.8
H22A–C22–H22B	107.7
C22–C23–C24	113.1(4)
C22–C23–H23A	109.0
C24–C23–H23A	109.0
C22–C23–H23B	109.0
C24–C23–H23B	109.0
H23A–C23–H23B	107.8
C23–C24–C25	113.4(4)
C23–C24–H24A	108.9
C25–C24–H24A	108.9
C23–C24–H24B	108.9
C25–C24–H24B	108.9
H24A–C24–H24B	107.7
N5–C25–C24	111.9(4)
N5–C25–H25A	109.2
C24–C25–H25A	109.2
N5–C25–H25B	109.2
C24–C25–H25B	109.2
H25A–C25–H25B	107.9
O4–C26–N6	123.8(4)
O4–C26–C21	118.8(4)
N6–C26–C21	117.2(4)
N6–C27–C28	110.0(3)
N6–C27–H27A	109.7
C28–C27–H27A	109.7
N6–C27–H27B	109.7
C28–C27–H27B	109.7
H27A–C27–H27B	108.2
C33–C28–C29	117.9(4)
C33–C28–C27	119.7(4)
C29–C28–C27	122.3(4)
C30–C29–C28	120.6(4)

C30–C29–H29	119.7
C28–C29–H29	119.7
C31–C30–C29	121.2(4)
C31–C30–H30	119.4
C29–C30–H30	119.4
C30–C31–C32	118.6(4)
C30–C31–C34	121.9(4)
C32–C31–C34	119.5(4)
C31–C32–C33	120.4(4)
C31–C32–H32	119.8
C33–C32–H32	119.8
C28–C33–C32	121.3(4)
C28–C33–H33	119.3
C32–C33–H33	119.3
C36–C35–C40	117.7(4)
C36–C35–C34	122.5(4)
C40–C35–C34	119.8(4)
C31–C34–C35	113.2(4)
C31–C34–H34A	108.9
C35–C34–H34A	108.9
C31–C34–H34B	108.9
C35–C34–H34B	108.9
H34A–C34–H34B	107.8
C37–C36–C35	122.5(5)
C37–C36–H36	118.8
C35–C36–H36	118.7
C36–C37–C38	119.7(4)
C36–C37–H37	120.1
C38–C37–H37	120.1
C37–C38–C39	119.1(4)
C37–C38–C41	119.1(4)
C39–C38–C41	121.8(4)
C40–C39–C38	120.4(4)
C40–C39–H39	119.8
C38–C39–H39	119.8
C39–C40–C35	120.5(4)
C39–C40–H40	119.8
C35–C40–H40	119.8
O5–C41–N7	121.5(4)
O5–C41–C38	122.5(4)
N7–C41–C38	116.0(4)
C14'–O2'–C13'	117.6(3)
C1'–N1'–C2'	124.7(4)
C1'–N1'–H1'	117.7
C2'–N1'–H1'	117.7
C7'–N2'–C8'	123.1(4)
C7'–N2'–H2'	118.4
C8'–N2'–H2'	118.4
C13'–N3'–C10'	117.7(4)
C20'–N4'–C21'	120.8(3)
C20'–N4'–H4'	119.6
C21'–N4'–H4'	119.6
C1'–N5'–C25'	126.5(4)
C1'–N5'–H5'	116.7
C25'–N5'–H5'	116.7
C26'–N6'–C27'	124.8(4)
C26'–N6'–H6'	117.6
C27'–N6'–H6'	117.6
C41'–N7'–C6'	122.5(4)
C41'–N7'–H7'	118.7
C6'–N7'–H7'	118.7

N1'–C1'–N5'	115.8(4)
N1'–C1'–S1'	123.1(3)
N5'–C1'–S1'	121.0(3)
N1'–C2'–C3'	112.0(3)
N1'–C2'–H2'1	109.2
C3'–C2'–H2'1	109.2
N1'–C2'–H2'2	109.2
C3'–C2'–H2'2	109.2
H2'1–C2'–H2'2	107.9
C2'–C3'–C4'	112.5(3)
C2'–C3'–H3'1	109.1
C4'–C3'–H3'1	109.1
C2'–C3'–H3'2	109.1
C4'–C3'–H3'2	109.1
H3'1–C3'–H3'2	107.8
C3'–C4'–C5'	113.4(4)
C3'–C4'–H4'1	108.9
C5'–C4'–H4'1	108.9
C3'–C4'–H4'2	108.9
C5'–C4'–H4'2	108.9
H4'1–C4'–H4'2	107.7
C4'–C5'–C6'	113.7(3)
C4'–C5'–H5'1	108.8
C6'–C5'–H5'1	108.8
C4'–C5'–H5'2	108.8
C6'–C5'–H5'2	108.8
H5'1–C5'–H5'2	107.7
N7'–C6'–C5'	111.4(3)
N7'–C6'–C7'	113.7(3)
C5'–C6'–C7'	109.1(3)
N7'–C6'–H6'	107.5
C5'–C6'–H6'	107.5
C7'–C6'–H6'	107.5
O1'–C7'–N2'	125.0(4)
O1'–C7'–C6'	118.4(4)
N2'–C7'–C6'	116.5(4)
N2'–C8'–C9'	108.8(4)
N2'–C8'–H8'1	109.9
C9'–C8'–H8'1	109.9
N2'–C8'–H8'2	109.9
C9'–C8'–H8'2	109.9
H8'1–C8'–H8'2	108.3
C11'–C9'–C10'	117.5(4)
C11'–C9'–C8'	123.0(4)
C10'–C9'–C8'	119.0(4)
N3'–C10'–C9'	122.7(4)
N3'–C10'–H10'	118.6
C9'–C10'–H10'	118.6
C9'–C11'–C12'	120.9(4)
C9'–C11'–H11'	119.6
C12'–C11'–H11'	119.6
C13'–C12'–C11'	116.6(4)
C13'–C12'–H12'	121.7
C11'–C12'–H12'	121.7
N3'–C13'–C12'	124.5(4)
N3'–C13'–O2'	116.3(4)
C12'–C13'–O2'	119.1(4)
O2'–C14'–C19'	115.8(4)
O2'–C14'–C15'	123.7(4)
C19'–C14'–C15'	120.4(4)
C14'–C15'–C16'	119.0(4)

C14'–C15'–H15'	120.5
C16'–C15'–H15'	120.5
C15'–C16'–C17'	120.7(4)
C15'–C16'–H16'	119.7
C17'–C16'–H16'	119.7
C18'–C17'–C16'	119.0(4)
C18'–C17'–C20'	118.3(4)
C16'–C17'–C20'	122.5(4)
C19'–C18'–C17'	120.3(4)
C19'–C18'–H18'	119.9
C17'–C18'–H18'	119.9
C18'–C19'–C14'	120.5(4)
C18'–C19'–H19'	119.7
C14'–C19'–H19'	119.7
O3'–C20'–N4'	121.6(4)
O3'–C20'–C17'	120.5(4)
N4'–C20'–C17'	117.9(4)
N4'–C21'–C22'	110.5(3)
N4'–C21'–C26'	111.9(3)
C22'–C21'–C26'	110.4(3)
N4'–C21'–H21'	108.0
C22'–C21'–H21'	107.9
C26'–C21'–H21'	108.0
C23'–C22'–C21'	113.8(4)
C23'–C22'–H22C	108.8
C21'–C22'–H22C	108.8
C23'–C22'–H22D	108.8
C21'–C22'–H22D	108.8
H22C–C22'–H22D	107.7
C24'–C23'–C22'	113.3(4)
C24'–C23'–H23C	108.9
C22'–C23'–H23C	108.9
C24'–C23'–H23D	108.9
C22'–C23'–H23D	108.9
H23C–C23'–H23D	107.7
O4'–C26'–N6'	122.8(4)
O4'–C26'–C21'	119.6(4)
N6'–C26'–C21'	117.4(4)
N5'–C25'–C24'	112.9(4)
N5'–C25'–H25C	109.0
C24'–C25'–H25C	109.0
N5'–C25'–H25D	109.0
C24'–C25'–H25D	109.0
H25C–C25'–H25D	107.8
C23'–C24'–C25'	114.8(4)
C23'–C24'–H24C	108.6
C25'–C24'–H24C	108.6
C23'–C24'–H24D	108.6
C25'–C24'–H24D	108.6
H24C–C24'–H24D	107.5
N6'–C27'–C28'	112.5(3)
N6'–C27'–H27C	109.1
C28'–C27'–H27C	109.1
N6'–C27'–H27D	109.1
C28'–C27'–H27D	109.1
H27C–C27'–H27D	107.8
C29'–C28'–C33'	118.7(4)
C29'–C28'–C27'	120.9(4)
C33'–C28'–C27'	120.4(4)
C28'–C29'–C30'	120.5(4)
C28'–C29'–H29'	119.8

C30'–C29'–H29'	119.8
C31'–C30'–C29'	121.6(4)
C31'–C30'–H30'	119.2
C29'–C30'–H30'	119.2
C30'–C31'–C32'	117.6(4)
C30'–C31'–C34'	120.2(4)
C32'–C31'–C34'	122.2(4)
C31'–C32'–C33'	121.4(4)
C31'–C32'–H32'	119.3
C33'–C32'–H32'	119.3
C28'–C33'–C32'	120.2(4)
C28'–C33'–H33'	119.9
C32'–C33'–H33'	119.9
C36'–C35'–C40'	116.6(4)
C36'–C35'–C34'	122.8(4)
C40'–C35'–C34'	120.4(4)
C35'–C34'–C31'	111.2(4)
C35'–C34'–H34C	109.4
C31'–C34'–H34C	109.4
C35'–C34'–H34D	109.4
C31'–C34'–H34D	109.4
H34C–C34'–H34D	108.0
C37'–C36'–C35'	122.7(4)
C37'–C36'–H36'	118.6
C35'–C36'–H36'	118.6
C36'–C37'–C38'	120.3(4)
C36'–C37'–H37'	119.8
C38'–C37'–H37'	119.8
C39'–C38'–C37'	118.6(4)
C39'–C38'–C41'	123.4(4)
C37'–C38'–C41'	118.0(4)
C38'–C39'–C40'	120.8(4)
C38'–C39'–H39'	119.6
C40'–C39'–H39'	119.6
C39'–C40'–C35'	120.8(4)
C39'–C40'–H40'	119.6
C35'–C40'–H40'	119.6
O5'–C41'–N7'	122.0(4)
O5'–C41'–C38'	122.1(4)
N7'–C41'–C38'	115.8(4)
H1W–O1W–H2W	106.4
H3W–O2W–H4W	106.4
H5W–O3W–H6W	106.4
H7W–O4W–H8W	106.4
O9W–O5W–O10W	106.4
H12W–O6W'–H13W	106.4

Table 4. Anisotropic displacement parameters [Å^2× 10^3]. The anisotropic displacement factor exponent takes the form: $-2\pi^2[h^2a^{*2}U^{11} + \cdots + 2\,h\,k\,a^*\,b^*\,U^{12}]$.

Atom	U^{11}	U^{22}	U^{33}	U^{23}	U^{13}	U^{12}
S1	29(1)	41(1)	40(1)	2(1)	7(1)	−1(1)
O1	45(2)	44(2)	51(2)	0(2)	10(2)	13(2)
O2	47(2)	53(2)	39(2)	12(2)	−6(2)	−17(2)
O3	26(2)	39(2)	29(2)	−3(1)	−2(1)	−4(1)
O4	32(2)	45(2)	37(2)	7(2)	0(2)	2(2)
O5	31(2)	42(2)	43(2)	−3(2)	0(2)	−6(2)
N1	41(2)	48(3)	26(2)	−1(2)	4(2)	3(2)
N2	30(2)	35(2)	36(2)	−2(2)	8(2)	4(2)
N3	33(2)	41(2)	47(3)	−1(2)	9(2)	−8(2)
N4	21(2)	34(2)	30(2)	0(2)	0(2)	−6(2)
N5	34(2)	43(3)	34(2)	−2(2)	3(2)	0(2)
N6	29(2)	29(2)	35(3)	2(2)	1(2)	7(2)
N7	29(2)	32(2)	35(2)	−9(2)	−3(2)	−2(2)
C1	22(3)	40(3)	41(3)	2(2)	0(2)	−6(2)
C2	35(3)	38(3)	35(3)	−1(2)	5(2)	4(2)
C3	30(3)	44(3)	34(3)	−6(2)	6(2)	−1(2)
C4	28(3)	46(3)	37(3)	−1(2)	13(2)	0(2)
C5	35(3)	50(3)	33(3)	−4(2)	2(2)	0(3)
C6	22(3)	38(3)	35(3)	−2(2)	−1(2)	4(2)
C7	21(3)	46(3)	33(3)	−8(2)	−4(2)	1(2)
C8	47(3)	36(3)	31(3)	7(2)	7(2)	11(2)
C9	31(3)	27(3)	34(3)	4(2)	1(2)	6(2)
C10	32(3)	35(3)	42(3)	−5(2)	6(2)	2(2)
C11	42(3)	37(3)	35(3)	7(2)	11(3)	7(2)
C12	23(3)	50(3)	42(3)	7(2)	7(2)	2(2)
C13	41(3)	29(3)	36(3)	13(2)	1(2)	−4(2)
C14	29(3)	42(3)	30(3)	10(2)	6(2)	−3(2)
C15	28(3)	39(3)	28(3)	4(2)	−2(2)	−2(2)
C16	30(3)	31(3)	33(3)	1(2)	8(2)	−3(2)
C17	26(3)	34(3)	21(3)	−2(2)	4(2)	0(2)
C18	23(2)	40(3)	29(3)	−3(2)	2(2)	2(2)
C19	26(3)	35(3)	38(3)	7(2)	4(2)	−4(2)
C20	27(3)	31(3)	27(3)	−11(2)	4(2)	2(2)
C21	27(2)	30(3)	24(2)	2(2)	0(2)	−1(2)
C22	29(3)	28(3)	30(3)	5(2)	1(2)	−8(2)
C23	26(2)	40(3)	32(3)	−5(2)	4(2)	3(2)
C24	33(3)	46(3)	30(3)	6(2)	5(2)	3(2)
C25	34(3)	40(3)	38(3)	12(2)	6(2)	−6(2)
C26	22(3)	35(3)	36(3)	8(2)	5(2)	−8(2)
C27	19(2)	48(3)	45(3)	0(3)	5(2)	2(2)
C28	24(3)	32(3)	32(3)	0(2)	5(2)	3(2)
C29	21(3)	36(3)	46(3)	3(2)	10(2)	4(2)
C30	35(3)	41(3)	33(3)	3(2)	13(2)	3(2)
C31	34(3)	31(3)	31(3)	2(2)	7(2)	9(2)
C32	32(3)	51(3)	39(3)	0(2)	7(2)	−12(3)
C33	30(3)	56(3)	35(3)	4(2)	12(2)	−9(2)
C35	39(3)	44(3)	25(3)	−7(2)	5(2)	5(3)
C34	40(3)	44(3)	34(3)	−2(2)	0(2)	4(2)
C36	42(3)	35(3)	31(3)	3(2)	6(2)	5(3)
C37	31(3)	36(3)	28(3)	−1(2)	10(2)	−8(2)
C38	31(3)	48(3)	16(2)	−5(2)	4(2)	1(2)
C39	32(3)	34(3)	31(3)	−2(2)	3(2)	−8(2)
C40	27(3)	57(4)	29(3)	1(2)	2(2)	−6(3)
C41	31(3)	40(3)	21(3)	5(2)	2(2)	0(2)
S1'	28(1)	44(1)	36(1)	0(1)	2(1)	0(1)
O1'	37(2)	39(2)	53(2)	7(2)	5(2)	−5(2)
O2'	74(3)	54(2)	33(2)	11(2)	17(2)	30(2)
O3'	26(2)	37(2)	34(2)	−2(1)	8(2)	3(1)

O4'	31(2)	38(2)	29(2)	0(2)	7(1)	−5(1)
O5'	33(2)	37(2)	32(2)	3(2)	3(1)	3(2)
N1'	31(2)	33(2)	31(2)	−2(2)	−1(2)	−4(2)
N2'	31(2)	29(2)	39(2)	5(2)	8(2)	−3(2)
N3'	49(3)	29(2)	40(2)	−3(2)	3(2)	7(2)
N4'	29(2)	28(2)	30(2)	−2(2)	7(2)	1(2)
N5'	21(2)	49(3)	34(2)	2(2)	1(2)	−10(2)
N6'	29(2)	28(2)	30(2)	3(2)	4(2)	−10(2)
N7'	33(2)	32(2)	32(2)	1(2)	7(2)	3(2)
C1'	25(2)	31(3)	23(3)	2(2)	2(2)	6(2)
C2'	34(3)	32(3)	31(3)	0(2)	1(2)	6(2)
C3'	30(3)	31(3)	34(3)	−1(2)	−1(2)	2(2)
C4'	44(3)	36(3)	28(3)	7(2)	0(2)	5(2)
C5'	32(3)	38(3)	31(3)	6(2)	3(2)	3(2)
C6'	37(3)	30(3)	21(2)	−2(2)	5(2)	1(2)
C7'	29(3)	37(3)	18(2)	−6(2)	0(2)	−5(2)
C8'	46(3)	31(3)	43(3)	9(2)	11(3)	6(2)
C9'	32(3)	22(2)	33(3)	6(2)	2(2)	8(2)
C10'	25(3)	32(3)	53(4)	5(2)	1(2)	7(2)
C11'	49(3)	30(3)	26(3)	7(2)	6(2)	−4(2)
C12'	30(3)	38(3)	37(3)	10(2)	3(2)	0(2)
C13'	47(3)	29(3)	31(3)	5(2)	9(3)	17(2)
C14'	38(3)	40(3)	26(3)	3(2)	4(2)	14(2)
C15'	39(3)	31(3)	30(3)	−1(2)	7(2)	6(2)
C16'	35(3)	26(3)	38(3)	2(2)	7(2)	6(2)
C17'	19(2)	29(3)	29(3)	−4(2)	1(2)	0(2)
C18'	31(3)	35(3)	30(3)	−3(2)	7(2)	8(2)
C19'	57(3)	35(3)	34(3)	4(2)	8(2)	21(2)
C20'	18(2)	28(3)	32(3)	−9(2)	3(2)	−4(2)
C21'	24(2)	31(3)	26(3)	1(2)	4(2)	−3(2)
C22'	25(3)	37(3)	27(3)	0(2)	−1(2)	−5(2)
C23'	27(3)	40(3)	23(3)	0(2)	3(2)	−2(2)
C26'	23(3)	29(3)	31(3)	2(2)	6(2)	6(2)
C25'	22(3)	52(3)	35(3)	6(2)	5(2)	−4(2)
C24'	22(3)	55(3)	35(3)	2(3)	4(2)	−10(2)
C27'	30(3)	29(3)	39(3)	−4(2)	6(2)	−8(2)
C28'	18(2)	28(3)	31(3)	3(2)	1(2)	−7(2)
C29'	23(3)	29(3)	38(3)	−3(2)	4(2)	−5(2)
C30'	24(3)	26(2)	32(3)	6(2)	−6(2)	−7(2)
C31'	26(3)	32(3)	26(3)	3(2)	−1(2)	−6(2)
C32'	27(3)	47(3)	41(3)	4(2)	2(2)	12(2)
C33'	30(3)	52(3)	25(3)	−1(2)	−11(2)	3(2)
C35'	33(3)	38(3)	21(2)	−9(2)	1(2)	−7(2)
C34'	38(3)	40(3)	29(3)	−5(2)	−5(2)	3(2)
C36'	49(3)	31(3)	23(3)	1(2)	1(2)	3(2)
C37'	25(3)	33(3)	36(3)	−1(2)	5(2)	7(2)
C38'	23(3)	27(3)	28(3)	−4(2)	4(2)	−1(2)
C39'	37(3)	26(3)	32(3)	−1(2)	7(2)	0(2)
C40'	36(3)	37(3)	25(3)	−4(2)	−2(2)	3(2)
C41'	35(3)	26(3)	16(2)	3(2)	−2(2)	4(2)
O1W	37(2)	45(2)	61(2)	−6(2)	5(2)	1(2)
O2W	47(2)	44(2)	64(3)	−10(2)	2(2)	−4(2)
O3W	70(2)	90(3)	39(2)	13(2)	−1(2)	7(2)
O4W	44(2)	58(2)	84(3)	−27(2)	−2(2)	8(2)
O5W	52(2)	83(3)	50(2)	−7(2)	8(2)	7(2)
O6W	193(19)	73(7)	41(9)	−12(6)	−2(8)	12(10)
O6W'	190(30)	67(12)	23(8)	−16(7)	11(11)	−11(13)

Table 5. Hydrogen coordinates [× 10^4] and isotropic displacement parameters [$Å^2$ × 10^3].

Atom	*x*	*y*	*z*	U_{eq}	*S.o.f.*
H1	−4298	2891	−4218	120(30)	1
H2	−4087	2491	−7445	48(15)	1
H4	704	2108	−4269	26(12)	1
H5	−3757	2083	−3622	29(13)	1
H6	2890	1334	−4514	15(10)	1
H7	−3695	1923	−6571	90(20)	1
H2A	−2976	2929	−5078	19(10)	1
H2B	−4261	3492	−4956	26(11)	1
H3A	−4795	1988	−5354	29(11)	1
H3B	−6083	2544	−5226	35(12)	1
H4A	−4264	2838	−6006	15(10)	1
H4B	−5583	3378	−5883	61(16)	1
H5A	−6601	1911	−6117	21(10)	1
H5B	−7319	2687	−6348	29(12)	1
H6	−6672	1954	−7017	18(10)	1
H8A	−4585	4020	−7597	30(11)	1
H8B	−3538	3516	−7903	15(10)	1
H10	−3672	4248	−6648	44	1
H11	−842	3608	−7605	55(15)	1
H12	1170	3934	−6970	45	1
H15	−213	3142	−5820	24(11)	1
H16	349	2484	−5046	12(9)	1
H18	3269	4122	−4492	37	1
H19	2648	4795	−5248	25(11)	1
H21	2625	2014	−3364	33(12)	1
H22A	271	1016	−3777	35	1
H22B	1320	840	−3242	35	1
H23A	−447	2173	−3409	31(12)	1
H23B	487	1918	−2869	38(12)	1
H24A	−1940	1610	−2821	46(13)	1
H24B	−1112	825	−2885	63(16)	1
H25A	−2114	809	−3781	20(11)	1
H25B	−3411	811	−3428	29(11)	1
H27A	4508	32	−4229	51(15)	1
H27B	5281	665	−4540	28(11)	1
H29	5017	455	−5450	14(10)	1
H30	3673	14	−6221	48(14)	1
H32	417	−712	−5457	43(13)	1
H33	1751	−263	−4685	20(10)	1
H34A	799	−1200	−6382	26(11)	1
H34B	1606	−588	−6696	63(16)	1
H36	−1838	−1089	−6434	48(14)	1
H37	−4060	−437	−6638	33(12)	1
H39	−1744	1455	−6880	50(14)	1
H40	487	778	−6702	29(12)	1
H1'	−4728	−1058	−10647	39	1
H2'	−1420	−670	−7830	47(15)	1
H4'	275	−272	−10794	29(12)	1
H5'	−4838	−340	−11305	21(11)	1
H6'	2377	622	−10514	19(11)	1
H7'	−1677	251	−8180	21(11)	1
H2'1	−2582	−913	−9799	39	1
H2'2	−3906	−1521	−9861	39	1
H3'1	−5564	−657	−9622	38	1
H3'2	−4454	34	−9673	38	1
H4'1	−2811	−425	−8948	25(11)	1
H4'2	−3924	−1114	−8897	33(11)	1

H5'1	−5669	−339	−8622	40	1
H5'2	−4910	407	−8811	40	1
H6'	−4497	295	−7897	41(12)	1
H8'1	−2535	−2095	−7611	31(12)	1
H8'2	−1136	−1747	−7235	68(18)	1
H10'	−2241	−2282	−8545	44	1
H11'	1332	−1947	−7468	28(12)	1
H12'	2877	−2281	−8078	23(11)	1
H15'	812	−1262	−9221	38(13)	1
H16'	819	−553	−9978	25(11)	1
H18'	3006	−2250	−10586	30(11)	1
H19'	2847	−2982	−9860	19(10)	1
H21'	1495	−118	−11678	44(13)	1
H22C	−668	832	−11307	28(11)	1
H22D	−164	926	−11863	20(10)	1
H23C	−1219	−232	−12134	29(11)	1
H23D	−1559	−418	−11566	29(11)	1
H25C	−3042	943	−11270	27(11)	1
H25D	−4660	888	−11610	42(13)	1
H24C	−3705	−22	−12152	30(11)	1
H24D	−2954	793	−12174	29(11)	1
H27C	3887	1887	−10759	39	1
H27D	4888	1227	−10466	39	1
H29'	5500	1410	−9572	34(12)	1
H30'	5083	1950	−8797	27(11)	1
H32'	1085	2698	−9477	32(12)	1
H33'	1517	2188	−10261	32(12)	1
H34C	3689	2627	−8278	45(13)	1
H34D	2643	3267	−8577	41(13)	1
H36'	−59	3166	−8613	22(11)	1
H37'	−2143	2556	−8414	22(11)	1
H39'	443	844	−7775	52(14)	1
H40'	2544	1443	−7999	43(14)	1
H1W	975	−403	−8247	72	1
H2W	240	−94	−8689	72	1
H3W	−6666	−752	−7636	78	1
H4W	−7043	−37	−7513	78	1
H5W	4907	1609	−12464	101	1
H6W	3796	1168	−12713	101	1
H7W	−4485	2138	−2848	95	1
H8W	−5115	2822	−2981	95	1
O9W	−2102	1847	−5537	92	1
O10W	−1278	1595	−5895	92	1
H11W	787	993	−9323	156	0.60
H12W	−214	515	−9595	156	0.60
H12W	−758	917	−8898	139	0.40
H13W	−1294	845	−9409	139	0.40

Table 6. Hydrogen bonds [Å and °].

D–H···*A*	*d*(*D*–H)	*d*(H···*A*)	*d*(*D*···*A*)	∠(*DHA*)
N1–H1···O3^{i}	0.88	2.14	2.886(5)	142.0
N2–H2···O5'	0.88	2.11	2.949(5)	159.9
N4–H4···S1	0.88	2.64	3.495(4)	165.0
N5–H5···O4W	0.88	2.19	2.999(6)	153.1
N7–H7···O5W	0.88	2.26	3.020(5)	144.8
N1'–H1'···O3'^{i}	0.88	2.18	2.926(4)	142.7
N2'–H2'···O1W	0.88	2.33	3.067(5)	141.4
N4'–H4'···S1'	0.88	2.62	3.475(4)	163.0
N7'–H7'···O1W	0.88	2.15	3.027(5)	171.8
O1W–H1W···O2W^{ii}	0.86	1.93	2.778(5)	166.6
O1W–H2W···O6W	0.84	2.02	2.851(17)	171.1
O1W–H2W···O6W'	0.84	2.01	2.75(3)	147.8
O2W–H3W···O1'	0.86	2.08	2.861(5)	149.8
O2W–H4W···O5	0.84	1.98	2.796(4)	163.4
O3W–H5W···O4W^{iii}	0.86	2.29	2.820(6)	120.0
O3W–H6W···O4^{iv}	0.84	2.07	2.817(5)	148.6
O4W–H7W···O3W^{v}	0.86	2.11	2.820(6)	139.2
O4W–H8W···O1'^{vi}	0.84	2.68	3.081(5)	110.6
O5W–O9W···S1	0.86	2.39	3.229(4)	166.8
O6W–H12W···S1'	0.84	2.44	3.265(19)	166.4
O6W'–H13W···S1'	0.84	2.72	3.30(2)	127.8

Symmetry transformations used to generate equivalent atoms:
(i) x–1,y,z (ii) x+1,y,z (iii) x+1,y,z–1 (iv) x,y,z–1
(v) x–1,y,z+1 (vi) –x–1,y+1/2,–z–1

Supplementary Material

Table 1. Crystal data and structure refinement.

Identification code	**99jul002**	
Compound	$C_{39}H_{42}N_8O_6S \cdot 2$ MeOH	
Empirical formula	$C_{41}H_{50}N_8O_8S$	
Formula weight	814.95	
Temperature	293(2) K	
Wavelength	0.71073 Å	
Crystal system	Monoclonic	
Space group	$P2_1$	
Unit cell dimensions	$a = 11.0792(2)$ Å	$\alpha = 90°$
	$b = 14.4360(3)$ Å	$\beta = 110.5470(10)°$
	$c = 13.6271(3)$ Å	$\gamma = 90°$
Volume	2040.86(7) Å^3	
Z	2	
Density (calculated)	1.326 Mg / m^3	
Absorption coefficient	0.142 mm^{-1}	
F(000)	864	
Crystal	?; ?	
Crystal size	0.70 × 0.35 × 0.35 mm^3	
θ range for data collection	1.96 – 25.25°	
Index ranges	$-13 \le h \le 13, -17 \le k \le 17, -16 \le l \le 16$	
Reflections collected	70359	
Independent reflections	7395 [$R_{int} = 0.0890$]	
Completeness to $\theta = 25.25°$	99.9 %	
Max. and min. transmission	0.9519 and 0.9070	
Refinement method	Full-matrix least-squares on F^2	
Data / restraints / parameters	7395 / 38 / 612	
Goodness-of-fit on F^2	0.971	
Final R indices [$F^2 > 2\sigma(F^2)$]	$R1 = 0.0423$, $wR2 = 0.1036$	
R indices (all data)	$R1 = 0.0626$, $wR2 = 0.1114$	
Absolute structure parameter	0.07(7)	
Extinction coefficient	0.0053(12)	
Largest diff. peak and hole	0.243 and –0.189 e Å^{-3}	

Diffractometer: *Enraf Nonius KappaCCD* area detector (ϕ scans and ω scans to fill *Ewald* sphere). **Data collection and cell refinement**: *Denzo* (Z. Otwinowski & W. Minor, *Methods in Enzymology* (1997) Vol. **276**: *Macromolecular Crystallography*, part A, pp. 307–326; C. W. Carter, Jr. & R. M. Sweet, Eds., Academic Press). **Absorption correction**: *SORTAV* (R. H. Blessing, Acta Cryst. A**51** (1995) 33–37; R. H. Blessing, J. Appl. Cryst. **30** (1997) 421–426). **Program used to solve structure**: *SHELXS97* (G. M. Sheldrick, Acta Cryst. (1990) A**46** 467–473). **Program used to refine structure**: *SHELXL97* (G. M. Sheldrick (1997), University of Göttingen, Germany).

Table 2. Atomic coordinates [$\times 10^4$], equivalent isotropic displacement parameters [$Å^2 \times 10^3$] and site occupancy factors. U_{eq} is defined as one third of the trace of the orthogonalized U^{ij} tensor.

Atom	*x*	*y*	*z*	U_{eq}	*S.o.f.*
S1	7923(1)	4561(1)	7794(1)	53(1)	1
O1	9387(3)	3427(2)	3793(3)	107(1)	1
O2	14244(2)	4020(2)	7882(1)	60(1)	1
O3	11920(2)	3025(1)	11379(1)	49(1)	1
O4	9461(2)	2034(2)	9649(2)	72(1)	1
O5	4502(2)	1501(2)	5866(2)	66(1)	1
O6	6005(2)	3876(2)	2538(2)	76(1)	1
N1	8662(2)	6302(2)	7704(2)	53(1)	1
N2	10396(2)	4638(2)	3430(2)	52(1)	1
N3	12824(2)	3369(2)	6380(2)	51(1)	1
N4	10188(2)	3744(2)	10245(2)	49(1)	1
N5	7307(2)	6103(2)	8594(2)	48(1)	1
N6	8078(2)	1905(2)	10504(2)	52(1)	1
N7	6365(3)	976(3)	7104(2)	81(1)	1
N8	7450(2)	4395(3)	4013(2)	78(1)	1
C1	7964(2)	5708(2)	8052(2)	41(1)	1
C2	9428(3)	6059(2)	7073(2)	57(1)	1
C3	8658(2)	5984(2)	5930(2)	50(1)	1
C4	9450(3)	5805(2)	5242(2)	56(1)	1
C5	8660(3)	5814(2)	4066(2)	59(1)	1
C6	8268(2)	4889(2)	3554(2)	57(1)	1
C7	9402(3)	4245(2)	3607(2)	58(1)	1
C8	11587(3)	4138(3)	3574(2)	62(1)	1
C9	12419(3)	4091(2)	4714(2)	50(1)	1
C10	12218(3)	3414(2)	5343(2)	53(1)	1
C11	13367(3)	4731(2)	5192(2)	59(1)	1
C12	14000(3)	4704(2)	6245(2)	59(1)	1
C13	13656(2)	4031(2)	6801(2)	48(1)	1
C14	13492(2)	3889(2)	8488(2)	46(1)	1
C15	12171(2)	3993(2)	8113(2)	52(1)	1
C16	11504(2)	3855(2)	8784(2)	47(1)	1
C17	12122(2)	3626(2)	9823(2)	38(1)	1
C18	13452(2)	3546(2)	10187(2)	51(1)	1
C19	14127(2)	3672(2)	9521(2)	55(1)	1
C20	11409(2)	3443(2)	10542(2)	41(1)	1
C21	9278(2)	3345(2)	10676(2)	46(1)	1
C22	8079(2)	3960(2)	10411(2)	48(1)	1
C23	8358(3)	4981(2)	10624(2)	50(1)	1
C24	7162(3)	5583(2)	10277(2)	52(1)	1
C25	6505(2)	5649(2)	9092(2)	50(1)	1
C26	8950(2)	2370(2)	10228(2)	48(1)	1
C27	7602(3)	1006(2)	10042(2)	58(1)	1
C28	6701(3)	1086(2)	8932(2)	51(1)	1
C29	7070(4)	850(3)	8115(3)	77(1)	1
C30	5238(3)	1353(2)	6906(2)	54(1)	1
C31	4729(3)	1603(2)	7659(2)	59(1)	1
C32	5492(3)	1470(2)	8677(2)	60(1)	1
C33	4970(2)	2130(2)	5322(2)	51(1)	1
C34	4506(3)	2063(2)	4237(2)	59(1)	1
C35	4938(2)	2669(2)	3666(2)	56(1)	1
C36	5842(2)	3345(2)	4142(2)	48(1)	1
C37	6239(3)	3431(2)	5226(2)	55(1)	1
C38	5792(3)	2830(2)	5811(2)	56(1)	1
C39	6417(2)	3909(2)	3495(2)	51(1)	1
O7	6473(3)	2229(2)	1707(2)	98(1)	1
C40	7069(4)	1665(3)	2596(4)	94(1)	1
O8	10829(6)	7292(4)	3042(5)	108(3)	0.551(9)
O8'	11269(5)	6535(5)	3503(5)	90(3)	0.449(9)
C41	10305(4)	6520(3)	2405(3)	103(1)	1

Table 3. Bond lengths [Å] and angles [°].

S1–C1	1.689(3)
O1–C7	1.209(4)
O2–C14	1.376(3)
O2–C13	1.386(3)
O3–C20	1.237(3)
O4–C26	1.221(3)
O5–C30	1.381(3)
O5–C33	1.383(3)
O6–C39	1.222(3)
N1–C1	1.348(3)
N1–C2	1.448(3)
N1–H1	0.8600
N2–C7	1.334(4)
N2–C8	1.456(4)
N2–H2	0.8600
N3–C13	1.313(4)
N3–C10	1.336(3)
N4–C20	1.341(3)
N4–C21	1.452(3)
N4–H4	0.8600
N5–C1	1.333(3)
N5–C25	1.451(3)
N5–H5	0.8600
N6–C26	1.334(3)
N6–C27	1.458(4)
N6–H6	0.8600
N7–C30	1.301(4)
N7–C29	1.337(4)
N8–C39	1.317(4)
N8–C6	1.455(3)
N8–H8	0.8600
C2–C3	1.494(4)
C2–H2A	0.9700
C2–H2B	0.9700
C3–C4	1.515(4)
C3–H3A	0.9700
C3–H3B	0.9700
C4–C5	1.533(4)
C4–H4A	0.9700
C4–H4B	0.9700
C5–C6	1.500(5)
C5–H5A	0.9700
C5–H5B	0.9700
C6–C7	1.543(4)
C6–H6A	0.9800
C8–C9	1.504(4)
C8–H8A	0.9700
C8–H8B	0.9700
C9–C10	1.369(4)
C9–C11	1.379(4)
C10–H10	0.9300
C11–C12	1.359(4)
C11–H11	0.9300
C12–C13	1.366(4)
C12–H12	0.9300
C14–C19	1.371(4)
C14–C15	1.379(4)
C15–C16	1.377(4)
C15–H15	0.9300

C16–C17	1.378(3)
C16–H16	0.9300
C17–C18	1.384(3)
C17–C20	1.483(3)
C18–C19	1.377(4)
C18–H18	0.9300
C19–H19	0.9300
C21–C26	1.527(4)
C21–C22	1.531(4)
C21–H21	0.9800
C22–C23	1.513(4)
C22–H22A	0.9700
C22–H22B	0.9700
C23–C24	1.515(4)
C23–H23A	0.9700
C23–H23B	0.9700
C24–C25	1.524(4)
C24–H24A	0.9700
C24–H24B	0.9700
C25–H25A	0.9700
C25–H25B	0.9700
C27–C28	1.496(4)
C27–H27A	0.9700
C27–H27B	0.9700
C28–C29	1.357(4)
C28–C32	1.377(4)
C29–H29	0.9300
C30–C31	1.382(4)
C31–C32	1.361(4)
C31–H31	0.9300
C32–H32	0.9300
C33–C38	1.367(4)
C33–C34	1.388(4)
C34–C35	1.364(4)
C34–H34	0.9300
C35–C36	1.385(4)
C35–H35	0.9300
C36–C37	1.391(4)
C36–C39	1.497(4)
C37–C38	1.382(4)
C37–H37	0.9300
C38–H38	0.9300
O7–C40	1.416(5)
O7–H1O	0.852(3)
C40–H40A	0.961(3)
C40–H40B	1.02(2)
C40–H40C	0.97(2)
O8–C41	1.407(5)
O8–H2O	0.850(3)
O8–H41E	1.21(2)
O8'–C41	1.502(5)
O8'–H2O'	0.850(3)
O8'–H41C	1.41(2)
C41–H41A	0.977(5)
C41–H41B	0.980(5)
C41–H41C	0.981(5)
C41–H41D	0.957(5)
C41–H41E	0.959(4)
C41–H41F	0.956(5)

C14–O2–C13	118.74(17)

C30–O5–C33	117.0(2)
C1–N1–C2	125.7(2)
C1–N1–H1	117.1
C2–N1–H1	117.1
C7–N2–C8	122.1(3)
C7–N2–H2	118.9
C8–N2–H2	118.9
C13–N3–C10	116.2(2)
C20–N4–C21	121.3(2)
C20–N4–H4	119.4
C21–N4–H4	119.4
C1–N5–C25	127.5(2)
C1–N5–H5	116.3
C25–N5–H5	116.3
C26–N6–C27	121.0(2)
C26–N6–H6	119.5
C27–N6–H6	119.5
C30–N7–C29	116.2(3)
C39–N8–C6	125.8(2)
C39–N8–H8	117.1
C6–N8–H8	117.1
N5–C1–N1	114.5(2)
N5–C1–S1	123.7(2)
N1–C1–S1	121.81(18)
N1–C2–C3	113.4(2)
N1–C2–H2A	108.9
C3–C2–H2A	108.9
N1–C2–H2B	108.9
C3–C2–H2B	108.9
H2A–C2–H2B	107.7
C2–C3–C4	114.6(2)
C2–C3–H3A	108.6
C4–C3–H3A	108.6
C2–C3–H3B	108.6
C4–C3–H3B	108.6
H3A–C3–H3B	107.6
C3–C4–C5	113.8(2)
C3–C4–H4A	108.8
C5–C4–H4A	108.8
C3–C4–H4B	108.8
C5–C4–H4B	108.8
H4A–C4–H4B	107.7
C6–C5–C4	116.4(3)
C6–C5–H5A	108.2
C4–C5–H5A	108.2
C6–C5–H5B	108.2
C4–C5–H5B	108.2
H5A–C5–H5B	107.3
N8–C6–C5	111.0(2)
N8–C6–C7	107.7(3)
C5–C6–C7	114.6(2)
N8–C6–H6A	107.7
C5–C6–H6A	107.7
C7–C6–H6A	107.7
O1–C7–N2	121.7(3)
O1–C7–C6	121.8(3)
N2–C7–C6	116.5(3)
N2–C8–C9	111.1(2)
N2–C8–H8A	109.4
C9–C8–H8A	109.4
N2–C8–H8B	109.4

C9–C8–H8B	109.4
H8A–C8–H8B	108.0
C10–C9–C11	116.6(2)
C10–C9–C8	120.2(3)
C11–C9–C8	123.1(3)
N3–C10–C9	124.4(3)
N3–C10–H10	117.8
C9–C10–H10	117.8
C12–C11–C9	120.3(3)
C12–C11–H11	119.8
C9–C11–H11	119.8
C11–C12–C13	117.7(3)
C11–C12–H12	121.1
C13–C12–H12	121.1
N3–C13–C12	124.4(2)
N3–C13–O2	116.9(2)
C12–C13–O2	118.7(2)
C19–C14–O2	116.5(2)
C19–C14–C15	120.1(2)
O2–C14–C15	123.4(2)
C16–C15–C14	119.1(2)
C16–C15–H15	120.5
C14–C15–H15	120.5
C15–C16–C17	121.8(2)
C15–C16–H16	119.1
C17–C16–H16	119.1
C16–C17–C18	118.1(2)
C16–C17–C20	122.2(2)
C18–C17–C20	119.6(2)
C19–C18–C17	120.6(2)
C19–C18–H18	119.7
C17–C18–H18	119.7
C14–C19–C18	120.3(2)
C14–C19–H19	119.8
C18–C19–H19	119.8
O3–C20–N4	121.5(2)
O3–C20–C17	121.3(2)
N4–C20–C17	117.2(2)
N4–C21–C26	107.8(2)
N4–C21–C22	110.1(2)
C26–C21–C22	112.0(2)
N4–C21–H21	109.0
C26–C21–H21	109.0
C22–C21–H21	109.0
C23–C22–C21	114.6(2)
C23–C22–H22A	108.6
C21–C22–H22A	108.6
C23–C22–H22B	108.6
C21–C22–H22B	108.6
H22A–C22–H22B	107.6
C22–C23–C24	113.7(2)
C22–C23–H23A	108.8
C24–C23–H23A	108.8
C22–C23–H23B	108.8
C24–C23–H23B	108.8
H23A–C23–H23B	107.7
C23–C24–C25	114.0(2)
C23–C24–H24A	108.8
C25–C24–H24A	108.8
C23–C24–H24B	108.8
C25–C24–H24B	108.8

H24A–C24–H24B	107.7
N5–C25–C24	112.4(2)
N5–C25–H25A	109.1
C24–C25–H25A	109.1
N5–C25–H25B	109.1
C24–C25–H25B	109.1
H25A–C25–H25B	107.9
O4–C26–N6	121.9(3)
O4–C26–C21	121.7(2)
N6–C26–C21	116.5(2)
N6–C27–C28	112.3(2)
N6–C27–H27A	109.1
C28–C27–H27A	109.1
N6–C27–H27B	109.1
C28–C27–H27B	109.1
H27A–C27–H27B	107.9
C29–C28–C32	116.2(3)
C29–C28–C27	121.6(3)
C32–C28–C27	122.0(3)
N7–C29–C28	125.2(3)
N7–C29–H29	117.4
C28–C29–H29	117.4
N7–C30–O5	117.1(2)
N7–C30–C31	124.6(3)
O5–C30–C31	118.3(3)
C32–C31–C30	116.8(3)
C32–C31–H31	121.6
C30–C31–H31	121.6
C31–C32–C28	121.0(3)
C31–C32–H32	119.5
C28–C32–H32	119.5
C38–C33–O5	122.3(2)
C38–C33–C34	120.3(3)
O5–C33–C34	117.2(2)
C35–C34–C33	119.4(3)
C35–C34–H34	120.3
C33–C34–H34	120.3
C34–C35–C36	121.7(2)
C34–C35–H35	119.2
C36–C35–H35	119.2
C35–C36–C37	117.8(3)
C35–C36–C39	119.7(2)
C37–C36–C39	122.4(2)
C38–C37–C36	120.8(3)
C38–C37–H37	119.6
C36–C37–H37	119.6
C33–C38–C37	119.7(2)
C33–C38–H38	120.2
C37–C38–H38	120.2
O6–C39–N8	121.5(3)
O6–C39–C36	122.0(2)
N8–C39–C36	116.3(2)
C40–O7–H1O	116.3(10)
O7–C40–H40A	114.5(9)
O7–C40–H40B	110.9(15)
H40A–C40–H40B	104.5(18)
O7–C40–H40C	113.7(15)
H40A–C40–H40C	108.6(18)
H40B–C40–H40C	103.8(8)
C41–O8–H2O	118.7(11)
C41–O8–H41E	42.1(3)

H2O–O8–H41E	111(7)
C41–O8'–H2O'	165(4)
C41–O8'–H41C	39.2(3)
H2O'–O8'–H41C	129(2)
O8–C41–O8'	51.6(4)
O8–C41–H41A	113.0(8)
O8'–C41–H41A	145(3)
O8–C41–H41B	112.2(7)
O8'–C41–H41B	109(3)
H41A–C41–H41B	106.1(7)
O8–C41–H41C	113.3(6)
O8'–C41–H41C	65.1(13)
H41A–C41–H41C	106.0(6)
H41B–C41–H41C	105.7(6)
O8–C41–H41D	114(4)
O8'–C41–H41D	108.8(7)
H41A–C41–H41D	43(4)
H41B–C41–H41D	132(3)
H41C–C41–H41D	66(4)
O8–C41–H41E	58.0(13)
O8'–C41–H41E	108.2(7)
H41A–C41–H41E	74(3)
H41B–C41–H41E	84(5)
H41C–C41–H41E	169(4)
H41D–C41–H41E	110.2(7)
O8–C41–H41F	135(4)
O8'–C41–H41F	108.6(7)
H41A–C41–H41F	103(3)
H41B–C41–H41F	28(5)
H41C–C41–H41F	80(4)
H41D–C41–H41F	110.6(7)
H41E–C41–H41F	110.4(7)

Table 4. Anisotropic displacement parameters [$Å^2 \times 10^3$]. The anisotropic displacement factor exponent takes the form: $-2\pi^2[h^2a^{*2}U^{11} + \cdots + 2\,h\,k\,a^*\,b^*\,U^{12}]$.

Atom	U^{11}	U^{22}	U^{33}	U^{23}	U^{13}	U^{12}
S1	64(1)	46(1)	49(1)	−4(1)	18(1)	6(1)
O1	81(2)	71(2)	156(3)	32(2)	28(2)	−16(1)
O2	41(1)	99(2)	43(1)	−2(1)	19(1)	−10(1)
O3	51(1)	54(1)	41(1)	11(1)	15(1)	8(1)
O4	80(1)	72(2)	81(2)	−8(1)	51(1)	3(1)
O5	61(1)	84(2)	51(1)	0(1)	20(1)	−21(1)
O6	82(1)	95(2)	37(1)	6(1)	3(1)	−24(1)
N1	57(1)	57(2)	50(1)	−10(1)	26(1)	−8(1)
N2	57(1)	60(2)	44(1)	5(1)	24(1)	0(1)
N3	60(1)	53(1)	44(1)	2(1)	21(1)	−2(1)
N4	42(1)	56(1)	54(1)	22(1)	23(1)	11(1)
N5	54(1)	41(1)	51(1)	0(1)	23(1)	0(1)
N6	64(1)	51(1)	45(1)	7(1)	26(1)	1(1)
N7	80(2)	108(2)	63(2)	6(2)	35(2)	25(2)
N8	58(1)	141(3)	36(1)	−12(2)	18(1)	−42(2)
C1	38(1)	46(2)	31(1)	−3(1)	3(1)	5(1)
C2	48(2)	73(2)	51(2)	−9(2)	20(1)	−2(2)
C3	47(1)	59(2)	46(2)	4(1)	18(1)	3(1)
C4	48(1)	73(2)	50(2)	−8(1)	18(1)	−4(2)
C5	55(2)	80(2)	47(2)	11(2)	24(1)	9(2)
C6	42(1)	97(2)	31(1)	6(1)	12(1)	−12(1)
C7	60(2)	68(2)	42(2)	1(1)	11(1)	−12(2)
C8	68(2)	81(2)	45(2)	1(2)	28(1)	11(2)
C9	59(2)	56(2)	42(1)	−1(1)	27(1)	9(1)
C10	64(2)	49(2)	46(2)	−8(1)	19(1)	−3(1)
C11	63(2)	65(2)	56(2)	9(2)	32(2)	−6(2)
C12	57(2)	68(2)	58(2)	−6(2)	26(1)	−15(2)
C13	43(1)	63(2)	43(1)	−3(1)	21(1)	3(1)
C14	41(1)	55(2)	43(1)	−1(1)	16(1)	−4(1)
C15	46(1)	73(2)	34(1)	2(1)	12(1)	8(1)
C16	34(1)	63(2)	42(1)	−1(1)	10(1)	1(1)
C17	41(1)	34(1)	41(1)	1(1)	15(1)	2(1)
C18	41(1)	66(2)	39(2)	8(1)	7(1)	3(1)
C19	34(1)	78(2)	50(2)	3(1)	12(1)	−2(1)
C20	45(1)	34(1)	45(2)	2(1)	17(1)	0(1)
C21	44(1)	60(2)	36(1)	12(1)	16(1)	6(1)
C22	46(1)	54(2)	49(2)	9(1)	24(1)	3(1)
C23	50(1)	62(2)	38(1)	2(1)	16(1)	2(1)
C24	61(2)	52(2)	53(2)	1(1)	32(1)	5(1)
C25	38(1)	51(2)	61(2)	3(1)	19(1)	6(1)
C26	48(1)	54(2)	43(1)	8(1)	18(1)	9(1)
C27	81(2)	43(2)	56(2)	8(1)	31(2)	3(2)
C28	66(2)	39(2)	56(2)	2(1)	30(1)	−1(1)
C29	78(2)	96(3)	61(2)	6(2)	31(2)	32(2)
C30	56(2)	59(2)	50(2)	−2(1)	22(1)	−8(1)
C31	51(2)	69(2)	61(2)	−5(2)	23(2)	−7(1)
C32	68(2)	63(2)	59(2)	−9(2)	35(2)	−10(2)
C33	40(1)	69(2)	48(2)	−8(1)	19(1)	−4(1)
C34	46(2)	82(2)	49(2)	−16(2)	16(1)	−16(2)
C35	44(1)	88(2)	34(2)	−14(1)	13(1)	−13(2)
C36	36(1)	65(2)	39(1)	−7(1)	11(1)	1(1)
C37	54(2)	64(2)	44(2)	−12(1)	14(1)	−10(1)
C38	61(2)	69(2)	40(2)	−8(1)	19(1)	−10(2)
C39	43(1)	68(2)	40(2)	−7(1)	11(1)	1(1)
O7	131(2)	94(2)	92(2)	1(2)	66(2)	16(2)
C40	93(3)	99(3)	104(3)	12(3)	55(3)	16(2)
O8	117(4)	72(4)	121(5)	18(3)	25(4)	−33(3)
O8'	68(4)	89(5)	120(6)	16(4)	40(4)	−2(3)
C41	118(3)	108(4)	102(3)	25(3)	63(3)	−11(3)

Table 5. Hydrogen coordinates [$\times 10^4$] and isotropic displacement parameters [$Å^2 \times 10^3$].

Atom	*x*	*y*	*z*	U_{eq}	*S.o.f.*
H1	8651	6875	7872	84(12)	1
H2	10331	5205	3225	76(11)	1
H4	9939	4182	9790	65(9)	1
H5	7366	6696	8655	42(7)	1
H6	7793	2139	10960	62(9)	1
H8	7661	4423	4683	99(13)	1
H2A	9852	5472	7316	54(8)	1
H2B	10092	6524	7173	61(8)	1
H3A	8178	6555	5703	74(10)	1
H3B	8039	5486	5828	64(9)	1
H4A	9869	5208	5424	54(8)	1
H4B	10119	6273	5387	82(11)	1
H5A	7886	6175	3959	84(11)	1
H5B	9158	6133	3708	84(11)	1
H6A	7763	4997	2813	65(9)	1
H8A	12056	4447	3186	78(9)	1
H8B	11385	3515	3298	82(11)	1
H10	11619	2955	5028	53(8)	1
H11	13573	5184	4791	77(10)	1
H12	14645	5130	6576	107(14)	1
H15	11736	4154	7417	52(7)	1
H16	10612	3918	8530	52(7)	1
H18	13892	3406	10888	59(8)	1
H19	15020	3611	9773	81(10)	1
H21	9687	3304	11439	43(7)	1
H22A	7568	3880	9675	76(10)	1
H22B	7563	3749	10813	50(7)	1
H23A	8928	5184	10264	46(7)	1
H23B	8808	5068	11369	60(8)	1
H24A	7396	6201	10557	42(7)	1
H24B	6551	5336	10575	47(7)	1
H25A	6295	5030	8805	32(6)	1
H25B	5705	5990	8933	45(7)	1
H27A	7158	706	10456	65(9)	1
H27B	8327	619	10066	72(10)	1
H29	7878	580	8272	69(9)	1
H31	3904	1849	7480	68(9)	1
H32	5192	1642	9209	70(9)	1
H34	3906	1610	3903	62(8)	1
H35	4617	2628	2939	51(7)	1
H37	6813	3898	5561	37(6)	1
H38	6049	2902	6534	75(10)	1
H1O	6230(50)	2764(16)	1826(12)	148	1
H40A	6501(15)	1450(30)	2940(20)	140	1
H40B	7430(30)	1070(18)	2390(30)	140	1
H40C	7820(20)	1950(30)	3113(15)	140	1
H2O	10560(90)	7420(50)	3540(60)	162	0.551(9)
H2O'	11740(100)	6397(18)	4130(30)	136	0.449(9)
H41A	10180(50)	6625(17)	1668(9)	154	0.551(9)
H41B	9460(30)	6340(30)	2430(40)	154	0.551(9)
H41C	10840(30)	5963(12)	2610(30)	154	0.551(9)
H41D	10740(19)	6360(50)	1934(10)	154	0.449(9)
H41E	9930(50)	7125(16)	2250(20)	154	0.449(9)
H41F	9660(40)	6070(40)	2370(18)	154	0.449(9)

Table 6. Hydrogen bonds [Å and °].

D–H···*A*	*d*(*D*–H)	*d*(H···*A*)	*d*(*D*···*A*)	∠(*DHA*)
N1–H1···O3^{i}	0.86	2.16	2.955(3)	154.2
N5–H5···O3^{i}	0.86	2.08	2.900(3)	158.6
N6–H6···O7^{ii}	0.86	2.06	2.849(4)	152.6
O7–H1O···O6	0.852(3)	1.937(8)	2.760(4)	162.1(19)

Symmetry transformations used to generate equivalent atoms:
(i) −x+2,y+1/2,−z+2 (ii) x,y,z+1